



HAL
open science

Distorted arenes by Scholl cyclizations, towards twisted carbon nanoribbons

Anirban Pradhan

► **To cite this version:**

Anirban Pradhan. Distorted arenes by Scholl cyclizations, towards twisted carbon nanoribbons. Other. Université Sciences et Technologies - Bordeaux I, 2013. English. NNT : 2013BOR14849 . tel-01070635

HAL Id: tel-01070635

<https://theses.hal.science/tel-01070635v1>

Submitted on 2 Oct 2014

HAL is a multi-disciplinary open access archive for the deposit and dissemination of scientific research documents, whether they are published or not. The documents may come from teaching and research institutions in France or abroad, or from public or private research centers.

L'archive ouverte pluridisciplinaire **HAL**, est destinée au dépôt et à la diffusion de documents scientifiques de niveau recherche, publiés ou non, émanant des établissements d'enseignement et de recherche français ou étrangers, des laboratoires publics ou privés.

Le numéro d 'ordre : 4849

THESE

PRESENTEE A

L'UNIVERSITE BORDEAUX 1

ECOLE DOCTORALE DES SCIENCES CHIMIQUES

Anirban PRADHAN

pour obtenir le grade de docteur

Spécialité : Chimie

DISTORTED ARENES BY SCHOLL CYCLIZATIONS, TOWARDS TWISTED CARBON NANORIBBONS.

Directeurs de thèse : Harald BOCK et Fabien DUROLA

Soutenue publiquement le 23 Septembre 2013 devant la commission d'examen formée de :

Prof. Cécile Zakri	Examinatrice, présidente
Prof. Gwénaél Rapenne	Rapporteur
Dr. Jeanne Crassous	Rapportrice
Prof. Dolores Pérez Meirás	Examinatrice
Dr. Fabien Durola	Co-directeur de thèse
Dr. Harald Bock	Co-directeur de thèse

“Dream is not that which you see while sleeping it is something that does not let you sleep.”

- *A. P. J. Abdul Kalam*

Acknowledgments

Sincere thanks to Dr. Harald Bock and Dr. Fabien Durola for their support, for being in my capacity, and for pushing my limits. Thank you Fabien for your continuous support and guidance and lot of help inside and outside the lab.

I would like to acknowledge the financial support of the University of Bordeaux, France during my research (2010-2013), and thanks to Centre de Recherche Paul Pascal (CRPP), for allowing me to work.

I am grateful to the colleagues that I met during these years, for sharing with me their knowledge and good laughs inside and outside the lab. In particular to Julien Kelber, Parantap Sarkar, Guillaume Naulet, Emmanuel Kiyoudi, Aline Ducouso, Pierre Mathey, Daniel Subervie.

Thanks to our collaborators from University of Bologna, Italy: Prof. Massimo Marcaccio, Giovanni Valenti, Prof. Francesco Paolucci for the electrochemical synthesis of our compounds. Thanks to Prof. Jérôme Lacour, Stéphane Grass from University of Geneva, Switzerland for the attempts of separation of the enantiomers of the propeller. Thanks to Dr. Christie Aroulanda from University Paris Sud for the NMR experiments in oriented phases.

Thanks to all the members of M3 group. Thanks to Dr. Pierre Dechambenoit for analyzing the crystal structures by X-ray.

For their technical support, I thank the staff of the cellule chimie in CRPP Wilfrid Neri, Stéphanie Exiga, Frédéric Louërat, Mbolu Rajaoarivelo and Xavier Brilland.

Thanks to my father and mother for their unconditional support and understanding. To my little sister Anindita who lightened my days in spite of being far, far away. Thanks to my uncle Joy Krishna Maity who inspired me in my childhood to study chemistry. I am deeply grateful to my fiancee Sanhita Maity for her understanding, ever-lasting love and support keep me going.

Résumé en français de la thèse de doctorat :

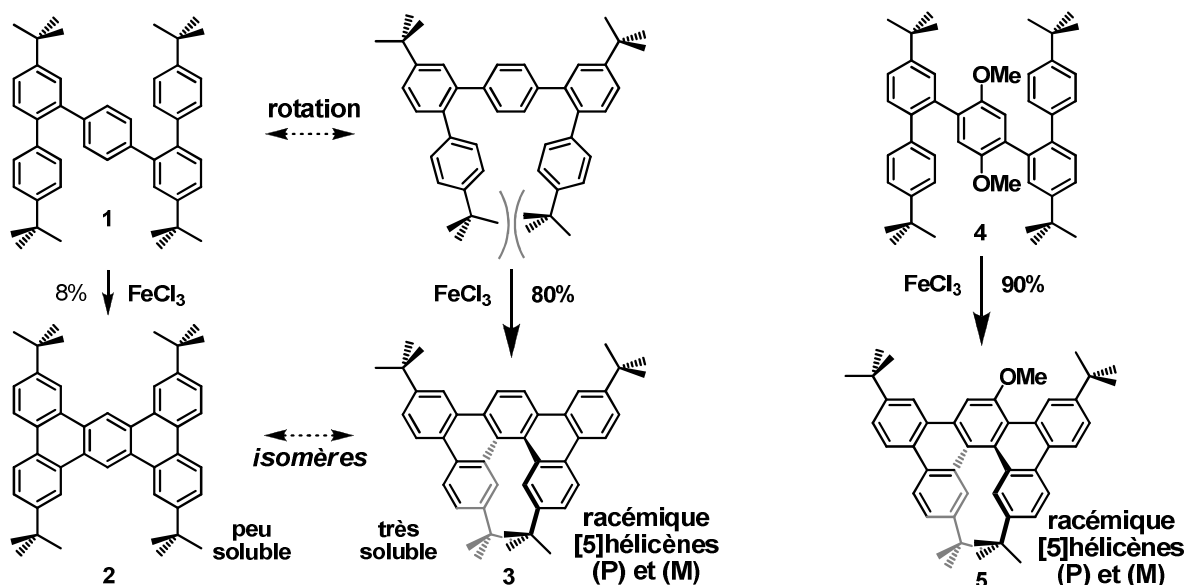
Distorted arenes by Scholl cyclizations, towards twisted carbon nanoribbons

Soutenue par **Anirban Pradhan**, le 23 septembre 2013 au Centre de Recherche Paul Pascal.

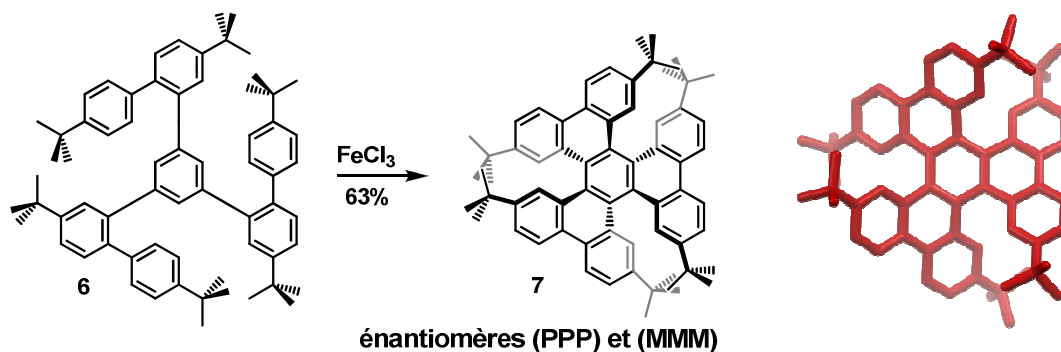
Co-encadrement par Dr Harald Bock et Dr Fabien Durola.

Les nanorubans de carbone présentent aujourd'hui un grand intérêt en tant que segments de graphène aux propriétés électroniques modulables. Alors que des techniques de synthèse destructives *top down* donnent des rubans de très grande taille, d'autres techniques constructives *bottom up*, par synthèse organique, pourraient former des nanorubans bien définis de géométries contrôlées. Dans cette optique, la réaction de Scholl est un outil chimique précieux car elle permet la graphénisation de longs précurseurs flexibles de type polyphénylène.

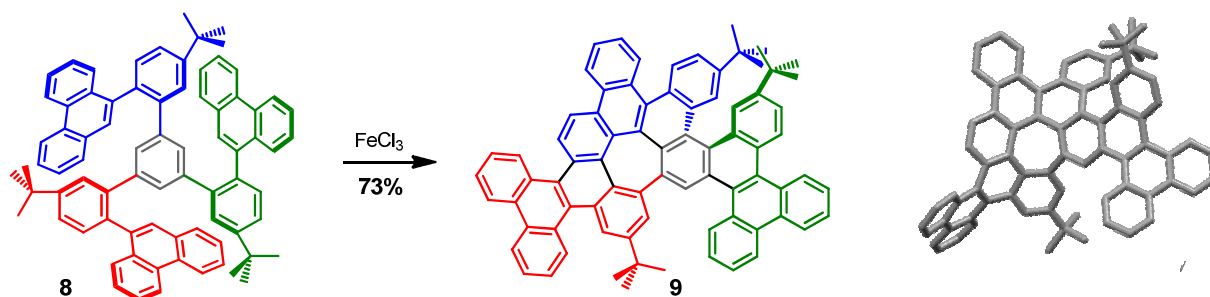
Afin de mieux maîtriser la réaction intramoléculaire de Scholl, bien connue mais néanmoins encore assez incomprise, sa régiosélectivité a été déterminée par l'étude de la réactivité des molécules **1** et **4** qui portent des substituants encombrants et présentent différentes possibilités de cyclisations : en positions *trans* vers un composé plan (**2**), ou en positions *cis* vers des produits de type [5]héliène (**3** et **5** respectivement).



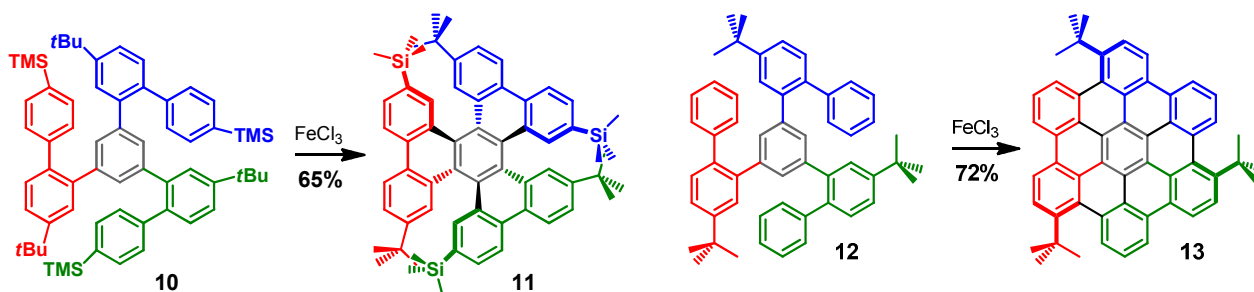
Etonnamment, des structures distordues peuvent être obtenues majoritairement même si des isomères plans moins encombrés sont a priori favorisés. Nous avons ainsi montré que contre toute attente même un encombrement stérique important n'a aucun effet notable sur la régiosélectivité de la réaction de Scholl et que des composés aromatiques polycycliques courbés peuvent être préférentiellement formés. Ainsi, des structures particulièrement tordues, tel que l'hexabenzotriphénylène **7** (HBTP) peuvent être facilement obtenues à partir de précurseurs de type polyphénylène.



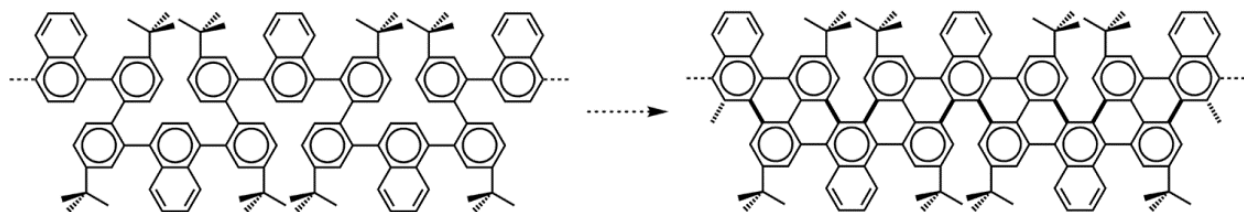
Après avoir découvert cette régiosélectivité inattendue, nous en avons tiré parti pour former des composés de type polyhéliène. Plusieurs tentatives de formation de l'hexaphénanthrotriénylène (HPTP) furent infructueuses à cause de problèmes de réactivité lors des synthèses des précurseurs flexibles correspondants. En mettant au point une stratégie de synthèse versatile fondée sur un précurseur commun, plusieurs substrats flexibles de symétrie C_3 (**8**, **10** et **12**) ont été synthétisés puis soumis à la réaction de Scholl. Des produits de réarrangement (**9**) ont cependant été obtenus au détriment des [6]héliènes attendus.



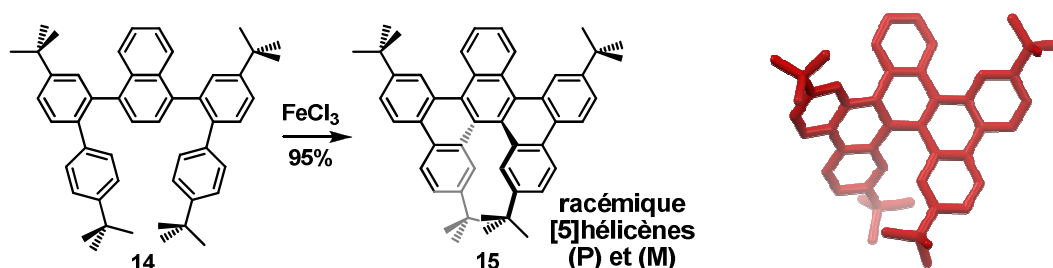
Toutefois, un HBTP (**11**) fonctionnalisé par des groupements TMS a pu être efficacement préparé, montrant la compatibilité de telles fonctions avec la réaction de Scholl. De même, un hexabenzocoronène (HBC) (**13**) a été formé, dont l'exceptionnelle solubilité est due à la distorsion du cœur aromatique sous l'effet des groupements encombrants situés dans les régions baie.



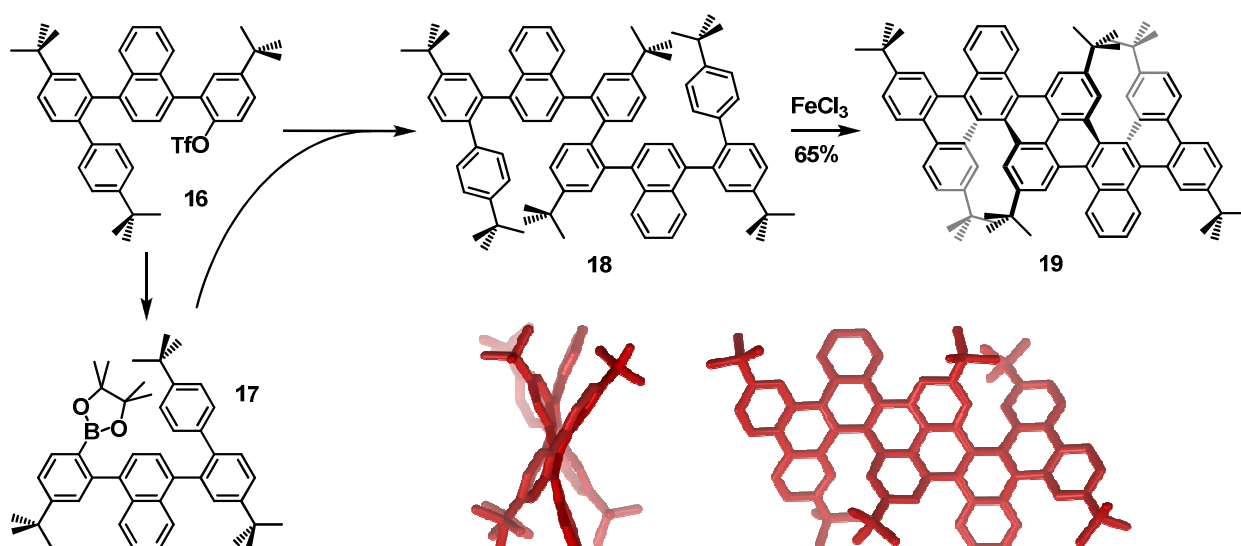
Le fragment [5]héliçène a priori très favorisé a enfin été incorporé dans la formulation de nanorubans de carbone tordus, alors composés d'une succession de ce motif. Dans ce projet, des fragments naphthalène sont utilisés comme brique centrale pour complètement empêcher les cyclisations en positions *trans*



En tant que réaction test, la synthèse du monomère correspondant a été effectuée avec un excellent rendement et le composé résultant (**15**) entièrement caractérisé.

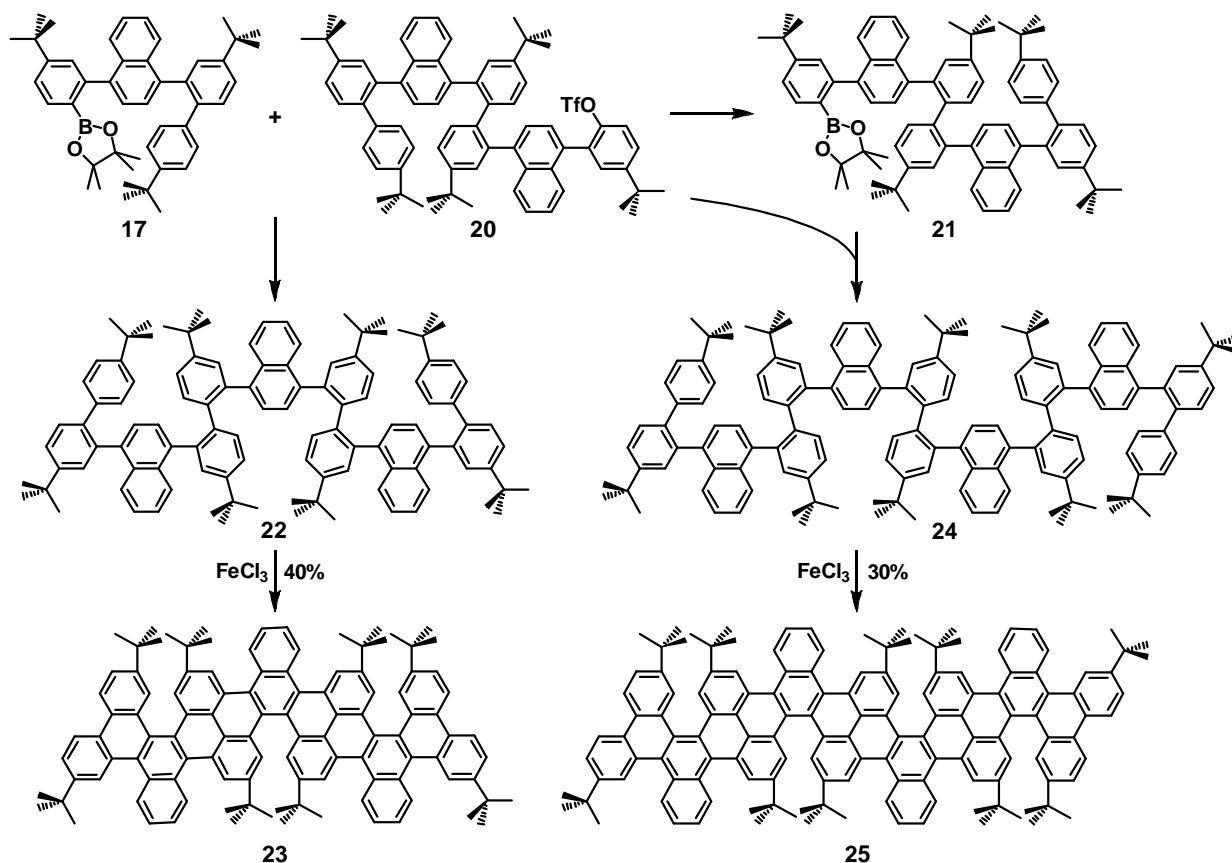


Une stratégie adaptée a été développée pour la synthèse du précurseur flexible (**18**) du dimère. Dans ce cas, la principale difficulté a été de trouver les conditions réactionnelles optimales pour le dernier couplage croisé de type Suzuki entre les intermédiaires **16** et **17**. Le court ruban **19** a néanmoins été obtenu avec un bon rendement, et entièrement caractérisé.



Les structures des monomères et dimères ont été déterminée par diffraction de rayons X sur monocristaux et ont apporté d'intéressantes informations complémentaires quant à leurs configurations.

Une stratégie plus générale a enfin été développée et optimisée pour la synthèse systématique d'oligomères plus longs de nanorubans de carbone tordus. En utilisant cette technique les trimère (**23**) et tétramère (**25**) correspondants ont été synthétisés et caractérisés par spectrométrie de masse.



Les propriétés électrochimiques de ces molécules sont actuellement étudiées, ainsi que leurs propriétés de coordination avec certains métaux de transition. Récemment, des complexes sandwichs de ruthénium, mono- et di-nucléaires, ont été préparés à partir du HBTP **7**, ouvrant ainsi la voie vers des composés aux propriétés intéressantes de valence mixte ou de magnétisme.

Abstract

Carbon nanoribbons are today of great interest as graphene segments with modulable electronic properties. Whilst top down techniques give giant ribbons, bottom-up organic synthesis may lead to exactly designed nanoribbons of controlled geometries. The Scholl reaction is a precious chemical tool for that purpose since it yields efficiently to the graphitization of long and flexible polyphenylene precursors.

Surprisingly, twisted structures may be obtained preferentially even if less crowded isomers are also feasible. It has been shown that, against all expectation, even a strong steric hindrance has no marked effect on regioselectivity and highly twisted polycyclic aromatic hydrocarbons are sometimes preferentially formed, whereas their flat and more symmetrical isomers are only obtained in minority. Highly twisted structures such as hexabenzotriphenylene (HBTP) may then be obtained very easily from flexible poly-phenylene precursors.

After discovering this unexpected regioselectivity, we used it on purpose to form polyhelicenic species. Attempts to prepared hexaphenanthrotriphenylene (HPTP) were unsuccessful due to reactivity issues when synthesizing the corresponding flexible precursor. By using a new versatile strategy leading to an advanced common precursor, several C3-symmetrical flexible substrates have been synthesized and submitted to Scholl reaction. The expected [6]helicenes were not obtained and rearranged products were formed instead, but TMS-bearing HBTP could be prepared, as well as a hexabenzocoronene (HBC) which exceptionnal solubility is due to the distortion of the aromatic core under the effect of bulky tert-butyl substituents in bay regions.

The easily formed [5]-helicene fragment has been incorporated in the design of twisted carbon nanoribbons that would be composed of a succession of such motifs. As a test reaction, the corresponding monomer and dimer have been synthesized with an excellent yield and fully characterized. Their X-ray structures have even been determined, giving interesting informations about their configuration. A more general strategy has then been developed and optimized for the systematic synthesis of longer twisted nanoribbons. Using this technique, the trimer and tetramer have been synthesized and characterized by mass spectrometry.

Table of Contents

Abstract.....	9
Table of Contents.....	11
List of Figures.....	15
Abbreviations.....	23
Chapter I: Carbon rich molecules and macromolecules.....	27
1.1 Graphene and graphene nanoribbons.....	28
1.1a. Introduction.....	28
1.1b. Structure of graphene nanoribbons.....	28
1.1c. Top-down synthesis of graphene nanoribbons from carbon nanotube.....	29
1.2 From polycyclic aromatic hydrocarbons (PAHs) or polycyclic aromatic compounds (PACs) to organic nano-graphenes.....	33
1.2a. About PAHs.....	33
1.2b. Surface-mediated synthesis of porous graphene.....	36
1.2c. Surface-mediated synthesis of nanographene and graphene nanoribbons.....	38
1.2d. Solution synthesis of nanographene.....	40
1.2e. Solution synthesis of graphene nanoribbons.....	41
1.3 Non planar PAHs.....	43
1.3a. Geodesic PAHs.....	43
1.3b. Example of synthesis of geodesic PAHs.....	44
1.3c. Helicenes.....	46
1.3d. Synthesis of helicenes.....	47

1.3d.i. Photocyclization.....	47
1.3d.ii. Diels-Alder reaction.....	48
1.3d.iii. Friedel-Crafts reaction.....	49
1.3d.iv. Palladium(Pd)-Catalyzed cyclizations.....	49
1.3e. Applications of the helicenes Chirality.....	50
1.4 References.....	52
Chapter II: Project: Carbon nanoribbons by Scholl reaction	59
2.1 The Scholl reaction.....	59
2.1a. Definition.....	59
2.1b. Examples of different Scholl reactions.....	60
2.1c. Mechanism of the Scholl reaction.....	62
2.1d. Drawbacks of the Scholl reaction.....	64
2.2 Initial projects.....	65
2.2a. Synthetic Strategy.....	66
2.2b. Test reactions.....	67
2.3 Evolution of the project.....	71
2.3a. Modified project.....	71
2.3b. Test reactions.....	72
2.3c. Attempts of protections.....	75
2.3d. Efficient synthesis hexabenzotriphenylene (HBTP).....	79
2.4 References.....	84
Chapter III: Towards hexa-phenanthro-triphenylene (HPTP)	89

3.1 Introduction.....	89
3.2 Hexa-coupling strategy from hexabromotriphenylene.....	91
3.3 Stepwise strategy from hexahydroxytriphenylene.....	92
3.4 Aryne-based strategy.....	98
3.4a. Principle.....	98
3.4b. First difficulties.....	100
3.4c. Second method.....	101
3.5 References.....	107
Chapter IV: Scholl reaction on C3-symmetrical precursors.....	109
4.1 General strategy for preparing common precursor.....	109
4.2 Phenanthrene based strategy.....	111
4.3 Naphthalene based strategy.....	114
4.4 Scholl reaction on TMS bearing group.....	118
4.5 Synthesis of a soluble hexabenzocoronene.....	122
4.6 References.....	126
Chapter V: Twisted carbon nanoribbons.....	129
5.1 Design of the twisted carbon nanoribbons.....	129
5.2 Test reaction on the monomer, synthesis of ^t Bu ₄ -tribenzopicene.....	132
5.3 Synthesis of the dimer.....	136
5.4 Synthesis of the trimer.....	145
5.5 Synthesis of the tetramer.....	156

5.6 Reference.....	162
Conclusion.....	163
Perspectives.....	165
Experimental section.....	169

List of figures

Figure 1. Different allotropes of carbon.

Figure 2. Edge structures of GNRs. (a) schematics of a zigzag-edged GNR. (b) schematics of a armchair-edged GNR.

Figure 3. Methods for unzipping carbon nanotubes.

Figure 4. a) The proposed chemical mechanism of nanotube unzipping. b) TEM images of MWCNTs (left) and the result of the transformation into an oxidized graphene nanoribbons (right).

Figure 5. Schematic illustration of making GNRs from CNTs.

Figure 6. Examples of different small PAHs (including naphthalene).

Figure 7. Two of the five Kekulé resonance structures of phenanthrene and their corresponding Clar aromatic π -sextets indicated with a circle. The structure with the largest number of aromatic π -sextets is the so-called Clar structure.

Figure 8. Representation of the Clar structures of anthracene and chrysene.

Figure 9. Simple schematic representations of bay region, cove region, fjord region.

Figure 10. a) Structure of CHP and DTPA. b) Structural relationship of the polyphenylene superhoneycomb network (blue lines) and graphene. c) High-resolution STM image of an edge of the porous graphene network based on CHP. d, e) Model and STM simulation of a coordination polymer with Ag atoms and covalent network based on DTPA, respectively.

Figure 11. a) Reaction scheme for conversion of bianthryl monomers to GNRs. b) STM image taken after surface-assisted C-C coupling at 200 °C and DFT-based simulation of the STM image (right) with partly overlaid model of the polymer. c) Overview STM image after cyclodehydrogenation at 400 °C.

Figure 12. Chevron-type GNRs from tetraphenyl-triphenylene monomers.

Figure 13. Examples of some organic syntheses of nanographenes.

Figure 14. Synthesis of fully benzenoid armchair-edge graphene nanoribbons by cyclodehydrogenation with FeCl_3 .

Figure 15. Synthesis of short fully benzenoid zigzag-edge graphene nanoribbons by cyclodehydrogenation with FeCl_3 .

Figure 16. Examples geodesic polyarenes that have been prepared by FVP.

Figure 17. Synthesis of Corannulene by FVP.

Figure 18. Synthesis of buckminsterfullerene C_{60} by FVP.

Figure 19. Synthesis of buckminsterfullerene C_{60} by palladium catalyst.

Figure 20. Examples of different helicenes (a) and (b) Scholz et al. 1967, (c) Newman et al. 1955, (d) Martin et al. 1967.

Figure 21. Helicity of helicenes.

Figure 22. Some 2, 2-disubstituted helicenes prepared by photocyclization.

Figure 23. Helicenes prepared by Diels-Alder methodology.

Figure 24. Helicenes Friedel-Crafts reaction.

Figure 25. Pd-catalysed helicene formation by C-H arylation.

Figure 26. Pd-catalysed helicene formation by [2+2+2] cyclo-addition.

Figure 27. Helicene catalysed asymmetric reaction.

Figure 28. Synthesis of enantiopure Ru(II)-capped helicenes.

Figure 29. Oxidative cyclodehydrogenation reaction.

Figure 30. Scholl reaction using DDQ as an oxidant.

Figure 31. Scholl reaction using $\text{AlCl}_3\text{-SnCl}_4$ as an oxidant.

Figure 32. Scholl reaction using PIFA as an oxidant.

Figure 33. Scholl reaction using MoCl_5 as an oxidant.

Figure 34. Cation radical (or Electron Transfer) mechanism for the Scholl reaction.

Figure 35. Arenium ion (or Proton Transfer) mechanism for the Scholl reaction.

Figure 36. Example of rearrangement during Scholl reaction.

Figure 37. Project of synthesis of thin GNRs by Scholl reaction. (a) Principle from ortho-phenylene chains. (b) Real project.

Figure 38. Retrosynthesis of poly-ortho-phenylene precursors.

Figure 39. Synthesis of test compound **6**.

Figure 40. Scholl reaction of compound **6**.

Figure 41. Synthesis of flexible compound **9**.

Figure 42. Scholl reaction of less hindered compound **10**.

Figure 43. ¹H NMR spectrum of compound **12** displaying the aliphatic signals above (1.3 to 1.6 ppm) and the aromatic signals below (7.5 to 8.9 ppm).

Figure 44. New design of a flexible precursor and its corresponding nanoribbons.

Figure 45. Retro-synthetic fragmentation of zigzag GNR precursor.

Figure 46. Synthesis of tetra-tert-butyl tetrabenzanthracene **17** and highly distorted tetra-tert-butyl dibenzo[5]helicene **18**.

Figure 47. Proposed reaction pathway for the formation of **17** and **18** by a Scholl reaction.

Figure 48. ¹H NMR spectra of (a) planar tetrabenzanthracene **17**, (b) helicenic dibenzopencene **18**.

Figure 49. Regioselectivity of the Scholl reaction on o,p,o-quinquephenyl, reported by Müllen and coworkers.²⁶

Figure 50. First attempt of protection for the Scholl reaction of o,p,o quinquephenyl.

Figure 51. Second attempt of protection for the Scholl reaction of o,p,o-quinquephenyl.

Figure 52. ¹H NMR spectrum of compound **24** displaying the aliphatic signals above (1.7 to 0.9 ppm) and the aromatic signals below (9.6 to 8.9 ppm).

Figure 53. Investigation of the Scholl regioselectivity by Hilt and coworkers.

Figure 54. Free energies for the selectivity determining transition states relative to AX (X=H, F, OMe (underlined values); R = Me).

Figure 55. The four isomers of hexabenzotriphenylene (HBTP).

Figure 56. Synthesis of highly distorted hexa-tert-butyl-hexabenzotriphenylene **28**.

Figure 57. ^1H -NMR spectrum of tBu₆-HBTP **28**.

Figure 58. Crystal structure of tBu₆-HBTP **28** : two different views of a single molecule.

Figure 59. Portion of the crystal structure of **28**·3CH₂Cl₂ illustrating the packing arrangement along the (a,b) plan. Carbon and chlorine atoms are represented by grey and green spheres respectively. Hydrogen atoms are omitted for clarity.

Figure 60. Generations of triphenylene dendrimers series.

Figure 61. Retro-synthetic study for the synthesis of HPTP **30**.

Figure 62. First attempts to form compound **31**.

Figure 63. Retrosynthetic strategy for the stepwise formation of compound **31**.

Figure 64. Synthesis of hexa-triflate compound **33**.

Figure 65. ^1H NMR spectrum of compound **38**. On top are aliphatic signals (2.0 to 0.8 ppm) and below aromatic signals (9.0 to 6.5 ppm).

Figure 66. X-ray structure of hexa-triflate compound **33**.

Figure 67. Failure of the final step for the synthesis of compound **31**.

Figure 68. Generation of benzyne intermediate.

Figure 69. General Pd-catalyzed cyclotrimerization of arynes.

Figure 70. Global mechanism of a Pd-catalyzed cyclotrimerization of arynes.

Figure 71. Retrosynthetic study for the formation of **31** by cyclotrimerization of arynes.

Figure 72. Failing reaction on 3,4-dibromoanisole.

Figure 73. Synthesis of ortho-silylaryltriflate compound **51**.

Figure 74. Failed attempt of cyclotrimerization of compound **42**.

Figure 75. Top ^1H NMR spectrum of compound **53** displaying the peaks of aliphatic (1.6 to 1.1 ppm) and aromatic (7.9 to 6.7 ppm) range. Below ^{13}C NMR spectrum of compound **53** displaying the peaks in aromatic region (159.0 to 115 ppm)

Figure 76. Failed Scholl reaction on biphenylene-based compound **53**.

Figure 77. Formation of trisubstituted substrates for intramolecular Scholl reactions.

Figure 78. Synthesis of common precursor **57**.

Figure 79. Synthesis and Scholl reaction of phenanthrene-based precursor **60**.

Figure 80. Temperature variant ^1H NMR spectrum of compound **59** displaying the peaks in top aliphatic (1.5 to 0.5 ppm) and aromatic (9.0 to 6.0 ppm) range.

Figure 81. (a) Two different views of the crystal structure of the strongly distorted [5]helicene- and hexa[7]circulene-based compound **60**. (b) ORTEP-type view of **60** at 120 K with thermal ellipsoids at 50 % probability level. Hydrogen atoms and $i\text{Pr}_2\text{O}$ solvent molecules are omitted for clarity, only one of the two positions of the disordered t-butyl groups is represented.

Figure 82. Synthesis and Scholl reaction of 2-naphthalene-based precursor **62**.

Figure 83. Structure and Crystal structure of the strongly distorted **63a**.

Figure 84. Synthesis of **65**.

Figure 85. Variable temperature ^1H NMR spectrum of compound **65** displaying the peaks in top aliphatic (1.5 to 1.0 ppm) and aromatic (8.0 to 6.0 ppm) range.

Figure 86. Scholl reaction of compound **65**.

Figure 87. Synthesis and Scholl reaction of TMS-substituted precursor **67**.

Figure 88. (a) Two different views of the crystal structure of triply helicenic TMS-bearing hexabenzotriphenylene **68**. (b) ORTEP-type view of **68** at 120 K with thermal ellipsoids at 50 % probability level. Only one of two molecules present in the asymmetric unit shown. Hydrogen atoms and CH_2Cl_2 solvent molecules are omitted for clarity.

Figure 89. Synthesis and reactivity in Scholl conditions of TMS-bearing pentaphenylene **73**.

Figure 90. Crystal structure of flat oligoarene **74**.

Figure 91. Synthesis and Scholl reaction of TMS-substituted precursor **76**.

Figure 92. Scholl reaction of **76** also gives traces of rearranged compounds **78, 79, 80**.

Figure 93. ORTEP-type view of **79** (left) and **80** (right) as found in **79-80** at 120 K with thermal ellipsoids at 50 % probability level. Carbon, chlorine and oxygen atoms are represented in grey, green and red. Note that these two molecules occupy the same position in the crystal structure with relative occupancies of 0.6/0.4. Only one of the two positions of the disordered t-butyl groups is represented. Hydrogen atoms are omitted for clarity.

Figure 94. Unexpected regioselectivity of the Scholl reaction, leading to distorted arenes.

Figure 95. Design of twisted carbon nanoribbons with compound **18** as a repeat unit.

Figure 96. Twisted carbon nanoribbons.

Figure 97. New design of the twisted GNRs, with protected cyclization positions (one monomer is drawn in blue).

Figure 98. Synthesis of flexible precursor **82**.

Figure 99. ^1H NMR spectrum of compound **82** displaying the peaks in aliphatic (1.4 to 1.1 ppm) and bellow aromatic (7.6 to 6.8 ppm) range.

Figure 100. Schematic presentation of the principle of a square TLC.

Figure 101. Chemical exchange between two conformers of compound **82** on silica.

Figure 102. Synthesis of [5]helicene **83**.

Figure 103. Crystal structure of compound **83** : two different views of a single molecule.

Figure 104. Retro-synthetic strategies for compound **89**.

Figure 105. Syntheses of hindered triflate and bononic ester compounds **87** and **88**.

Figure 106. Synthesis of flexible dimer precursor **89**.

Figure 107. ^1H NMR spectrum of compound **89** ; right: aliphatic (0.8 to 1.6 ppm), left: aromatic (6.0 to 8.0 ppm) range.

Figure 108. Synthesis of the dimer **91** of twisted GNRs.

Figure 109. ^1H NMR spectrum of compound **91**.

Figure 110. The three different stereoisomers of compound **91**.

Figure 111. Crystal structure of **91**: two different views of a single molecule.

Figure 112: Similar curvatures in compound **91** and [8]CPP.

Figure 113. Retro-synthesis of the trimer's flexible precursor **110**.

Figure 114. Synthesis of bifunctional monomers **94** and **95**.

Figure 115. First attempt of synthesis of the trimer precursor **110**.

Figure 116. Second attempt of synthesis of the trimer precursor **110**.

Figure 117. Attempts of hydrolysis of boronic esters **88** and **95**.

Figure 118. Synthesis of methoxy-substituted monomers **101** and **102**.

Figure 119. Synthesis of bis-triflate flexible trimer **105**.

Figure 120. Third attempt of synthesis of the trimer precursor **106**.

Figure 121. Synthesis of the mono-triflate flexible dimer **96**.

Figure 122. Successful fourth attempt of synthesis of flexible trimer precursor **110**.

Figure 123. Formation of the trimer twisted carbon nanoribbon **111**.

Figure 124. Retro-synthetic study of tetramer **117**. Blue way: Homocoupling. Red way: systematic and stepwise approach.

Figure 125. Systematic and stepwise synthesis of flexible oligomers, application to triflate trimer **114**.

Figure 126. Attempt of synthesis of flexible tetramer **115**.

Figure 127. Synthesis of tetramer flexible precursor **115**.

Figure 128. Synthesis of the tetramer of twisted GNRs **117**.

Figure 129. New design of flat nanoribbons.

Figure 130. Synthetic strategy for the formation of bifunctional monomers of flat carbon nanoribbons.

Figure 131. Design of pyrene-based nanoribbons.

Figure 132. Test reaction for the pyrene-based approach to carbon nanoribbons.

Abbreviations

CHP - hexaiodo-cyclohexa-m-phenylene

CNT - Carbon nanotube

COSY - Correlation spectroscopy

CPP - Cyclo-*p*-phenylenes

DBU - 1,8-Diazabicyclo[5.4.0]undec-7-ene

DCM - Dichloromethane

DDQ - 2,3-Dichloro-5,6-dicyano-1,4-benzoquinone

DFT - Density functional theory

DMA - N,N-dimethylacetamide

DMAD - Dimethyl acetylenedicarboxylate

DMSO - Dimethyl sulfoxide

DTPA - Dimethylmethylene-bridged triphenylamine

FD - Field desorption

FET - Field-effect transistor

FI - Field ionization

FVP - flash vacuum pyrolysis

GNRs - Graphene nanoribbons

HBC - Hexabenzocoronene

HBTP - Hexabenzotriphenylene

HPTP - Hexaphenanthrotriphenylene

HRTEM - High-resolution transmission electron microscopy

IUPAC - International union of pure and applied chemistry

JohnPhos - 2-(Dicyclohexylphosphino)biphenyl

LED - Light-emitting diodes

MALDI - Matrix-assisted laser desorption ionization

MS - Mass spectrometry

MWCNT - Multi-walled carbon nanotube

NBS - N-bromosuccinimide

NMR - Nuclear magnetic resonance

NOESY - Nuclear overhauser effect spectroscopy

ORTEP - Oak ridge thermal-ellipsoid plot

PAC - Polycyclic aromatic

PAH - Polycyclic aromatic hydrocarbon

PMMA - Poly(methyl methacrylate)

SPhos - 2-Dicyclohexylphosphino-2',6'-dimethoxybiphenyl

STM - Scanning tunneling microscope

SWCNT - Single-walled carbon nanotube

TEM - Transmission electron microscope

THF - Tetrahydrofuran

TLC - Thin layer chromatography

TMS - Trimethylsilyl

TOF - Time-of-flight mass spectrometry

UV - Ultraviolet

Chapter I: Carbon rich molecules and macromolecules.

Carbon is one of the most abundant elements in nature (4th place in the universe, but only 15th place in earth's crust and 12th place in whole earth).^{1a} For a long time, only three allotropes of carbon were known: amorphous carbon, graphite, and diamond. The crystalline forms (graphite and diamond) vary in physical properties due to their atomic structure.

The reason why carbon assumes many structural forms is that a carbon atom can form distinct types of valence bonds.^{1b}

In sp^2 hybridization, the carbon atoms are arranged hexagonally in honeycomb lattices parallel to each other. In graphite, the sheets are stacked in an ABAB sequence² (**Figure 1a**).

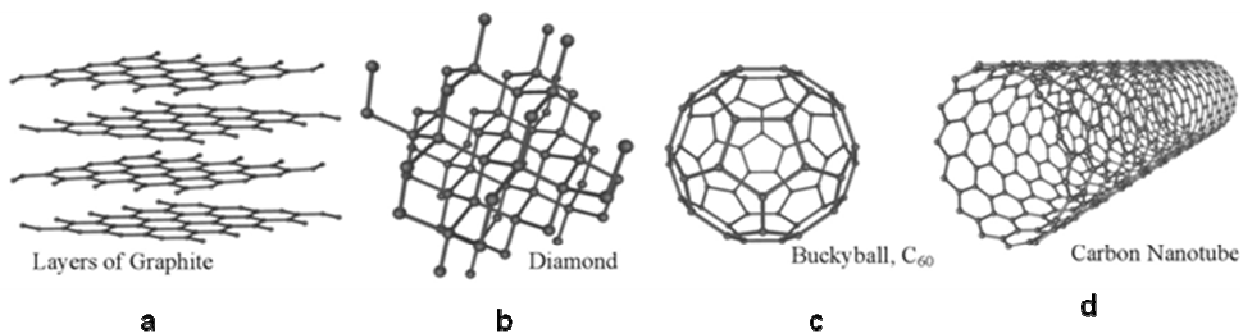


Figure 1. Different allotropes of carbon

This layered configuration makes graphite a dark, soft material, whereas diamond (**Figure 1b**) is transparent and is one of the hardest known materials. In diamond the carbon atoms are bonded tetrahedrally, in this configuration the atoms exhibit sp^3 hybridization.

In 1985 the discovery of C₆₀ (**Figure 1c**) (buckminsterfullerene, a molecule constituted of 60 carbon atoms arranged in a truncated icosahedral structure³) triggered the revolution of carbon nanostructures.⁴ Then, several other carbon nanostructures have been reported, such as single-wall carbon nanotubes⁴ (**Figure 1d**), nano-onions⁵, nanocones⁶ and nanoribbons⁷. More recently, single layers of graphite, called graphene, have been isolated and studied⁸, leading to the physics Nobel Prize in 2010.

1.1 Graphene and graphene nanoribbons.

1.1a. Introduction.

Graphene, a novel allotrope of carbon with a single atomic layer, has unique electronic properties, as first reported by Geim, Novoselov, and co-workers in 2004.⁸ Soon after, great attention was devoted to the exploring of the fundamentals and applications of this unique two-dimensional (2D) material. The single-atom-thick crystal has many novel electronic, physical and chemical properties. These intriguing properties of graphene have inspired exploration of its applications in electronic and photonic devices, sensors and as strong materials.

Graphene nanoribbons (GNRs) are narrow stripes of graphene. GNRs could also be understood as unrolled carbon nanotubes. Theoretical investigation of GNRs could be traced back to 1996, when Nakada et al. first reported the edge effects in narrow GNRs. However, intensive experimental efforts have only started a few years ago, after people realized their potential in future electronics.

1.1b. Structure of graphene nanoribbons.

The presence of open edges is an important feature in GNR lattice structure, which is absent from rolled up carbon nanotubes. The edge structures have significant effects on the properties of GNRs. There are two primary types of edges in GNRs: armchair and zigzag (**Figure 2**). Their crystallographic orientations differ by 30° in graphene. Since the carbon atoms on the edges have unsaturated chemical bonds that increase the total energy of the system, they are usually terminated by certain chemical species in theoretical frameworks. Hydrogen is the most commonly used passivation group in theoretical calculations. Other groups, including hydroxyl group (-OH), carboxyl group (-COOH), amine group (-NH₂), are also used in theoretical calculations. As one may expect, even for GNRs with the same shape, different termination groups may lead to different electronic properties.

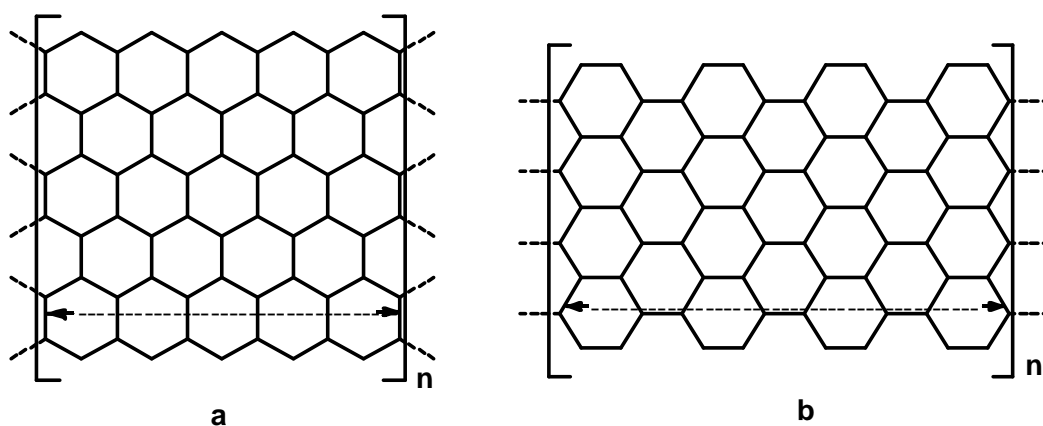


Figure 2. Edge structures of GNRs. (a) scheme of a zigzag-edged GNR. (b) scheme of a armchair-edged GNR.

Very few examples of formation of GNRs from graphene are reported in the literature.⁹ Due to their long geometries, carbon nanotubes are obviously better candidates for the formation of GNRs.

1.1c. Top-down synthesis of graphene nanoribbons from carbon nanotube.

In principle, a single-walled carbon nanotube (SWCNT) can be viewed as a folded or zipped GNR (**Figure 1d**). It is thus natural to seek the reverse process, that is, unzipping SWCNTs to synthesize GNRs. Many attempts have been dedicated to synthesizing GNRs experimentally, including plasma etching,¹⁰ chemical attack,^{11,12} intercalation and exfoliation,^{13,14} (**Figure 3**) but also sonochemical unzipping,^{15,16} laser irradiation,¹⁷ electrochemical unzipping,¹⁸ catalytic cutting under microwave radiation^{19,20} or by transition metal particles (e.g. Co, Ni, or Fe),^{21,22} hydrogen treatment,²³ in situ STM manipulation²⁴ and electrical unwrapping of CNTs.²⁵

In the strong oxidant approach,^{26,27a} a suspension of MWCNTs in sulfuric acid is treated with potassium permanganate under heating (**Figure 4**). The GNRs obtained are well soluble in polar solvents due to a multitude of carboxylic acid and ketone edge groups introduced by the procedure. It may be presumed that in a first step a double bond on the nanotube is opened into a diketone, which creates sterical strain on neighbouring bonds and thus transforms these

into preferred sites for further attack, which again fragilizes the environment, leading eventually to a clean slicing of the tube in longitudinal direction. The nanoribbons obtained display uniform widths inherited from the parent nanotubes, predominantly straight edges and, of course, oxidized defects, which makes them electronically much less homogeneous than graphene sheets.

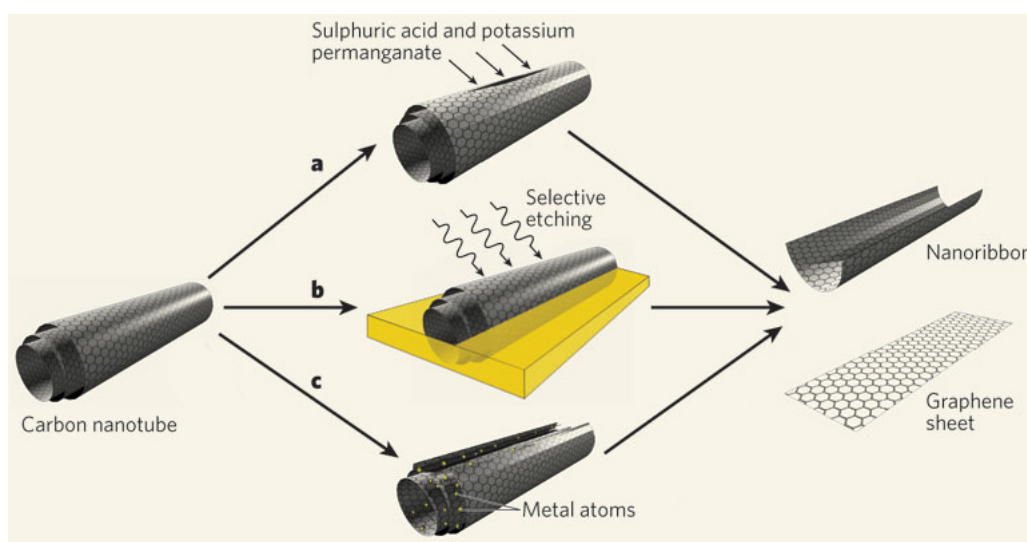


Figure 3. Methods for unzipping carbon nanotubes^{27b}.

Vega-Cantu and co-workers synthesized GNRs by longitudinally unzipping MWCNTs through intercalation of lithium and ammonia followed by exfoliation¹³ (**Figure 3c**). The final products consist of multilayered GNRs, partially opened MWCNTs, and graphene flakes. Although this method is not very promising for high-yield GNR synthesis, it provides a new possibility to realize longitudinal unzipping of CNTs.

Terrones and co-workers and Srivastava and co-workers both exploited transition metal particles (e.g. Co, Ni, or Cu) as chemical scissors to cut MWCNTs,^{21,22} In the cutting procedure, the metal particles serve as catalysts to break H-H and C-C bonds and as solvents for etched C atoms. These processes do not involve any aggressive chemical treatment, and thus smooth graphitic edges can be easily achieved.

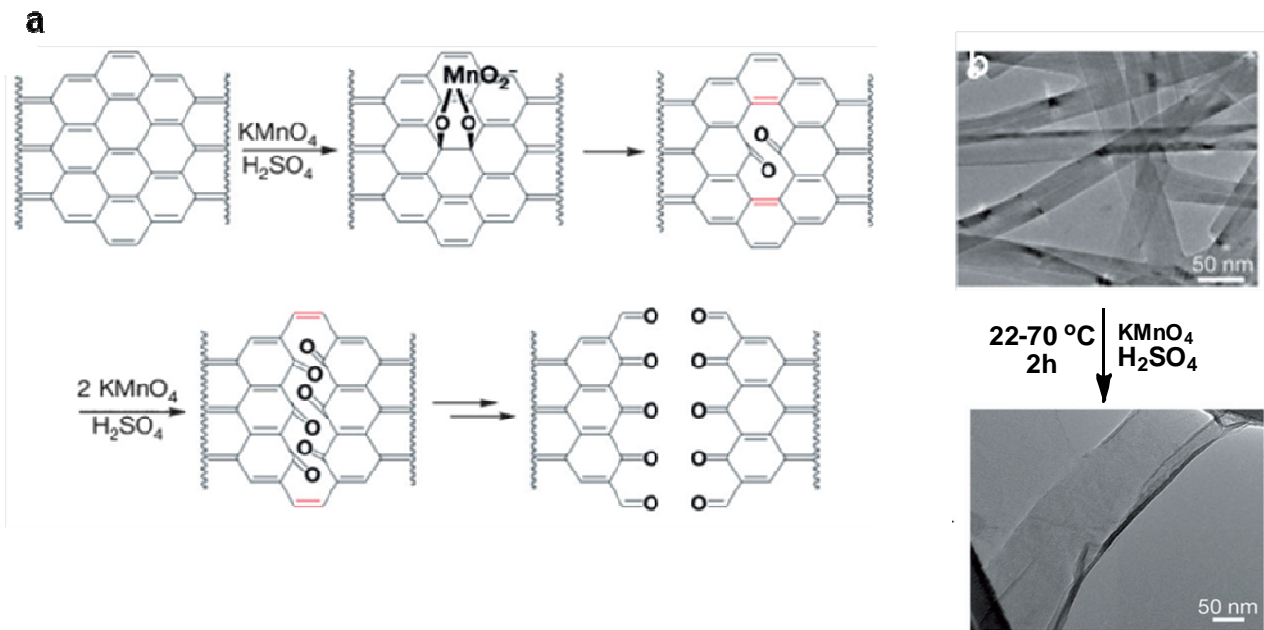


Figure 4. *a) The proposed chemical mechanism of nanotube unzipping. b) TEM images of MWCNTs (top) and the result of the transformation into an oxidized graphene nanoribbons (down).*

In the embedded plasma etching approach,¹⁰ MWCNTs are embedded in a poly(methyl methacrylate) (PMMA) layer, and then the polymer layer is thinned by plasma etching until the uppermost rim of the nanotube is etched away, opening the outermost wall of the MWCNT. Etching may be continued for various periods, allowing to obtain single-, bi- and multilayer GNRs. The remaining PMMA film with embedded GNRs may then be contact deposited on a solid substrate and the polymer removed with solvent vapor (**Figure 5**).

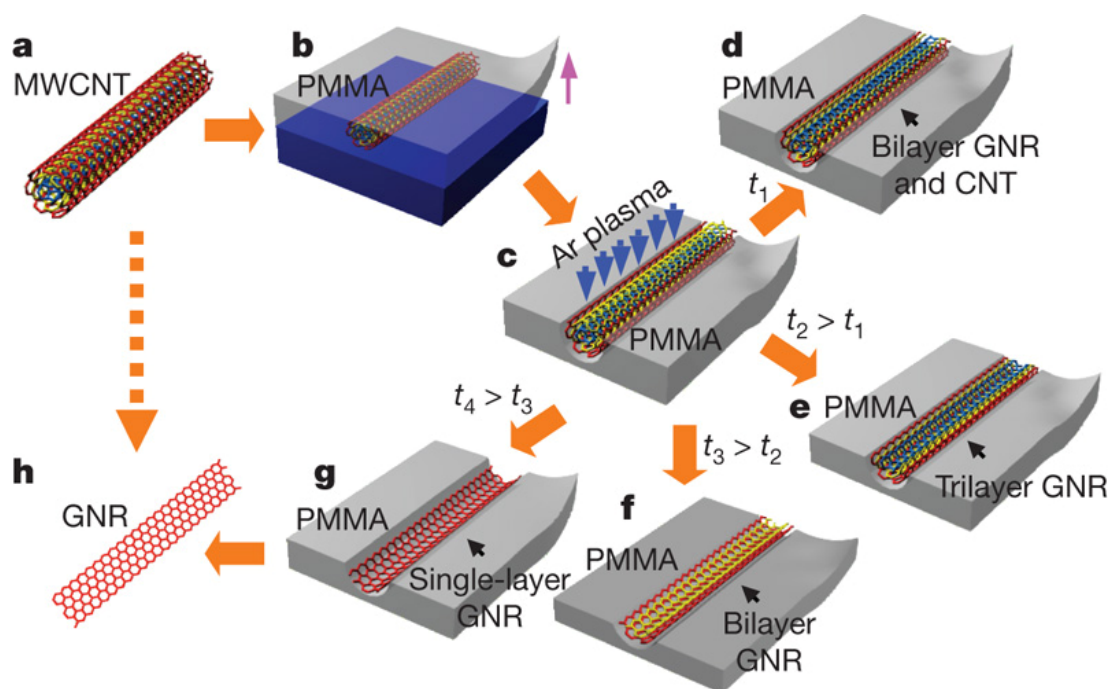


Figure 5. Schematic illustration of making GNRs from CNTs. a) A MWCNT was used as the starting raw material. b) The MWCNT was deposited onto a Si substrate and then coated with a PMMA film. c) The PMMA-MWCNT film was peeled from the Si substrate, turned over, and then exposed to an Ar plasma. d–g) Several possible products were generated after etching for different times: GNRs with CNT cores were obtained after etching for a short time t_1 (d); tri-, bi- and single-layer GNRs were produced after etching for times t_2 , t_3 , and t_4 , respectively ($t_4 > t_3 > t_2 > t_1$; e–g). h) The PMMA was removed to release the GNR^{27c}.

The edges of these ribbons produced by matrix etching are very smooth and, as before, their widths (of the order of 10nm) are quite uniform as consequence of the uniformity of the CNTs used. Field effect transistors made with these ribbons showed charge carrier mobilities only one order of magnitude smaller than those observed with large graphene sheets.

Top-down techniques for GNRs syntheses are very efficient when forming large GNR molecules. Nevertheless there are some major drawbacks in these techniques because of the polydispersity of the obtained GNRs. In contrast, bottom-up organic synthesis approaches have been developed which may serve as an indispensable tool to create structurally defined nanographenes and nanoribbons.

1.2 From polycyclic aromatic hydrocarbons (PAHs) or polycyclic aromatic compounds (PACs) to organic nano-graphenes.

1.2a. About PAHs.

Polycyclic aromatic hydrocarbons (PAHs) are a class of unique compounds that consist of fused conjugated aromatic rings.²⁸ These compounds can be point source (e.g., oil spill) or non-point source (e.g., atmospheric deposition) some of the most widespread organic pollutants. Some of them are known or suspected carcinogens, and are linked to other health problems. They are primarily formed by incomplete combustion of carbon-containing fuels such as wood, coal, diesel, fat, tobacco, or incense.^{29,30} Tar also contains PAHs. Different types of combustion yield different distributions of individual PAHs which can also give rise to isomers. Hence, those produced from coal combustion are in contrast to those yielded by motor-fuel combustion, which differ from those produced by forest fires. Some PAHs occur within crude oil, arising from chemical conversion of natural product molecules, such as steroids, to aromatic hydrocarbons. They are also found in the interstellar medium, in comets, and in meteorites, and are candidate molecules to act as a basis for the earliest forms of life.³¹ As defined by the International Union of Pure and Applied Chemistry (IUPAC), the simplest PAHs are phenanthrene and anthracene but we generally consider that naphthalene belongs to PAHs. PAHs may contain four-, five-, six-, or seven-membered rings, but those with five or six are most common. PAHs comprised only of six-membered rings are called alternant PAHs. PAHs containing up to six fused aromatic rings are often known as “small” PAHs, and those containing more than six aromatic rings are called “large” PAHs. Due to the availability of samples of various small PAHs, the main research on PAHs has been focused on those of up to six rings. Examples of well-known PAHs are shown in figure 5. In graphene, the PAH motif is alternant and extended to large 2D sheets, and represents one of the most intensively investigated class of compounds in synthetic chemistry and materials science. The systematic study of PAHs and their application as materials have spurred scientist for several decades, however, only a few selective synthetic methods have been established so far.

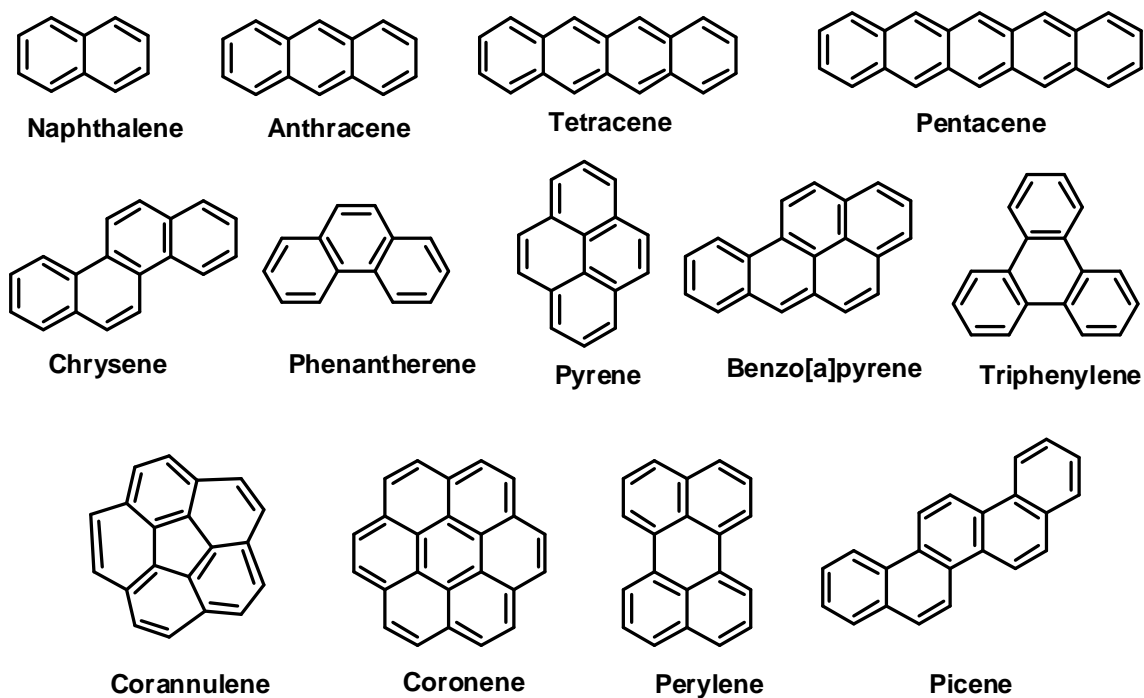


Figure 6. Examples of different small PAHs (including naphthalene).

Fundamental contributions to the directed synthesis and characterization of polycyclic aromatics were pioneered by R. Scholl, E. Clar, and M. Zander, who achieved the synthesis of numerous aromatic compounds under drastic conditions at high temperatures with strong oxidant.³²⁻³⁷ The synthetic breakthrough was achieved as a result of progress of analytical techniques and made the selective synthesis of various PAHs under mild conditions possible.³⁸ One of the intrinsic properties of the PAHs is their aromaticity, which has attracted great interest in theoretic chemistry,³⁹ different theoretical methods have been applied to estimate the electronic properties of graphite based on PAHs with increasing size and varying topologies. As a result of the development of organic semiconductors,⁴⁰ PAHs with unique electronic and optoelectronic properties have received great attention in the scientific community. Large PAHs terminated by hydrogen, alkyl substituents, and functional groups, which endow a facile solution processing, are promising candidates in organic devices such as light-emitting diodes (LEDs), field-effect transistors (FETs), and photo-voltaic cells.^{41,42} Additionally, 2D all-benzenoid graphitic molecules with appropriate substituents are fascinating due to their highly stable columnar mesophases, which are desirable for device processing.⁴¹⁻⁴³ Furthermore, well-defined nanostructures resulting from supramolecular self-

assembly of PAHs, such as nanotubes and nanowires, have a great potential in nanotechnology.⁴⁴⁻⁴⁶

According to Clar's rule, the Kékulé resonance structure with the largest number of disjoint aromatic π -sextets, i.e. benzene-like moieties, is the most important for the characterization of the properties of polycyclic aromatic hydrocarbons (PAHs). Aromatic π -sextets are defined as six π -electrons localized in a single benzene-like ring separated from adjacent rings by formal C-C single bonds. For instance, application of this rule to phenanthrene indicates that the resonance structure 2 (**Figure 7**) is more important than resonance structure 1.

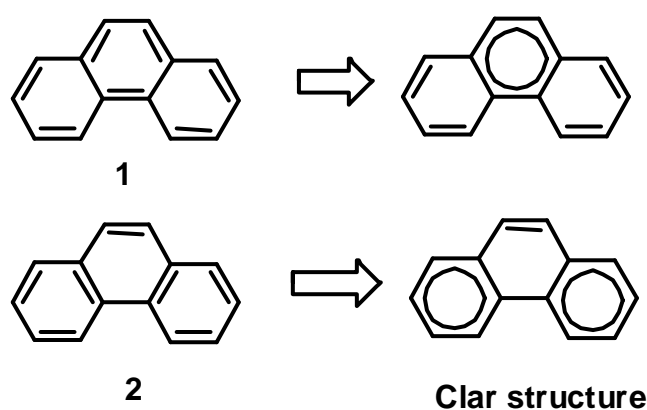


Figure 7. Two of the five Kékulé resonance structures of phenanthrene and their corresponding Clar aromatic π -sextets indicated with a circle. The structure with the largest number of aromatic π -sextets is the so-called Clar structure.

In contrast, in anthracene (**Figure 8a**) the number of sextets is only one and aromaticity spreads out. This difference in number of sextets is reflected in the UV absorbance spectra of these two isomers. Phenanthrene has a highest wavelength absorbance around 290 nm, while anthracene has a highest wavelength bands around 380 nm. Three Clar structures with two sextets are present in chrysene (**Figure 8b**) and by superposition the aromaticity in the outer ring is larger than in the inner rings.

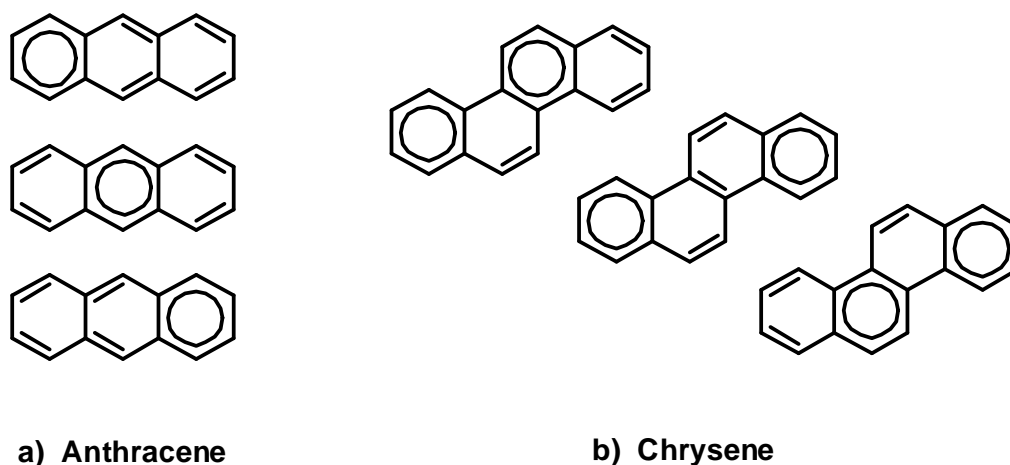


Figure 8. Representation of the Clar structures of anthracene and chrysene.

Depending on their geometry, the concave regions of the periphery of PAHs have different usual names (**Figure 9**). Three fused benzene rings can form a bay region, four can form a fjord region whereas a wider concavity is called cove region.⁴⁷ These positions have different electronic properties and therefore different chemical reactivities.

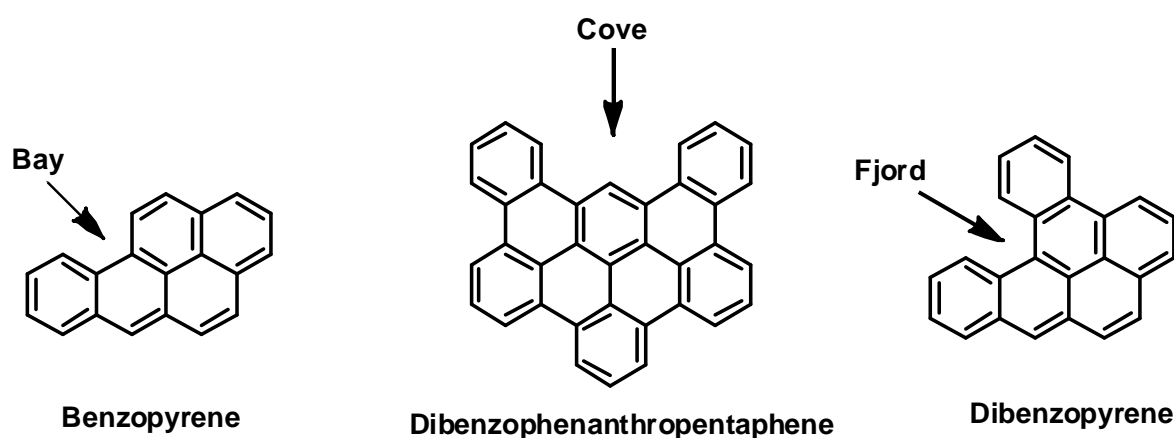


Figure 9. Representations of bay region, cove region and fjord region.

1.2b. Surface-mediated synthesis of porous graphene.

Mullen, and co-workers reported another example of a porous graphene network based on the on surface polymerization of tribromo-substituted dimethylmethylene-bridged triphenylamine (heterotriangulene), DTPA, (**Figure 10 a**) on Ag(111).⁴⁸ A coordination polymer was first formed by treatment of DPTA at 200 °C.

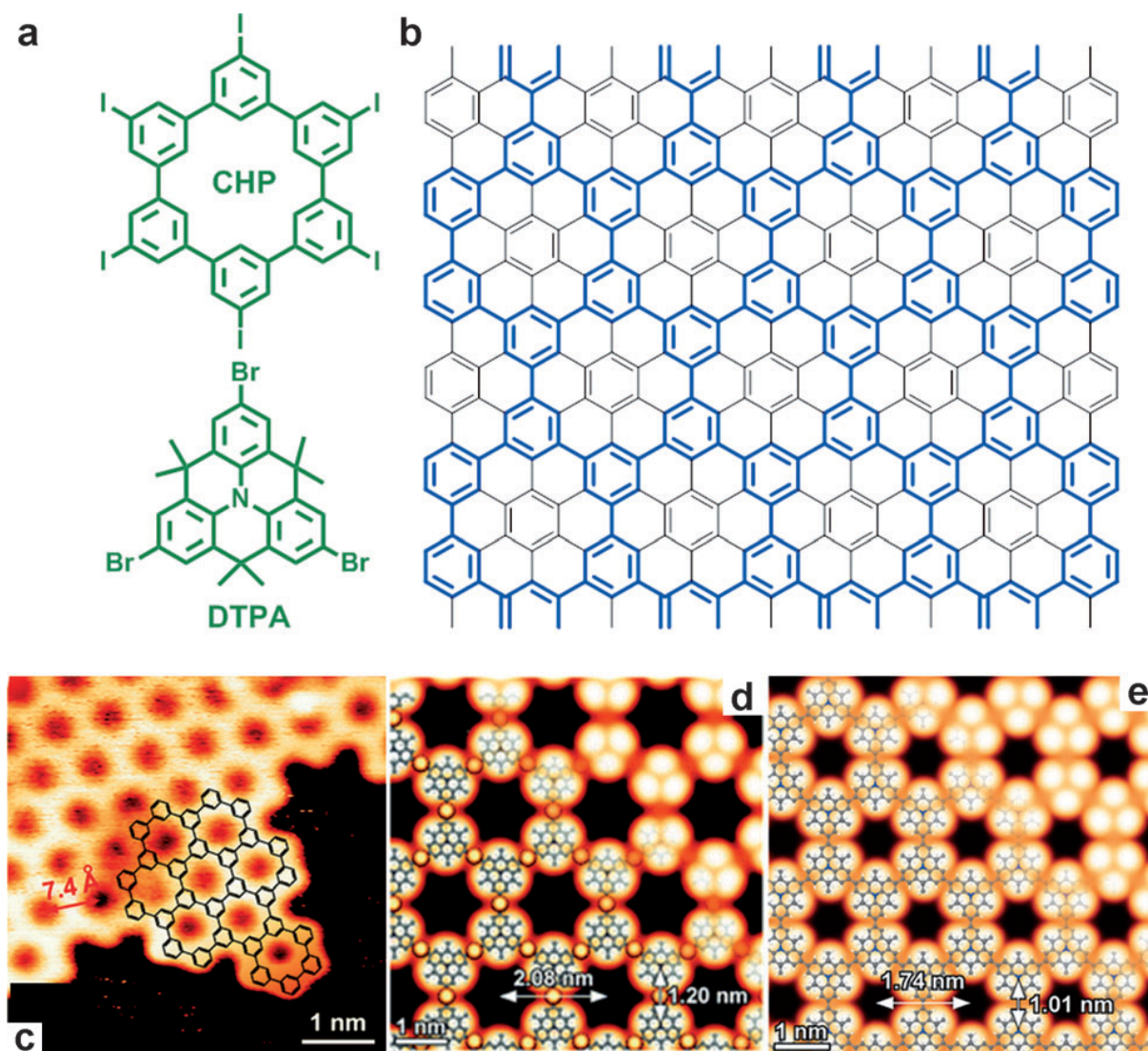


Figure 10. a) Structure of CHP and DTPA. b) Structural relationship of the polyphenylene superhoneycomb network (blue lines) and graphene. c) High-resolution STM image of an edge of the porous graphene network based on CHP. d, e) Model and STM simulation of a coordination polymer with Ag atoms and covalent network based on DTPA, respectively.

As noted before, the top-down methods for graphene synthesis seem to suffer from drawbacks such as uncontrollable sizes and irregular edge structures. This kind of problem can be solved by bottom-up synthesis. Such surface-mediated syntheses, on gold or silver, are very efficient and impressive, mainly because the obtained molecules are very large and don't need to be soluble.

1.2c. Surface-mediated synthesis of graphene nanoribbons.

If the cyclodehydrogenation reactions for graphene synthesis carried out in solution, thus making the solubility of oligophenylene precursors and their compatibility with reaction conditions crucial parameters. In contrast, graphene molecules and graphene nanoribbons with an extended aromatic core always suffer from strong intermolecular π - π stacking and poor solubility in conventional organic solvents, which make solution processing for electronic device applications difficult. The thermal evaporation of either these molecules or ribbons is generally difficult in view of their size. To surmount these obstacles, on-surface covalent synthesis routes would serve as a powerful alternative for the bottom-up creation of graphene structures.

Extended straight and chevron-type GNRs without solubilising substituents have been obtained by the dehydrogenation of polyanthrylene and polyphenylene precursors on gold surfaces at 400 to 440 °C and observed by STM (**Figure 11**).⁴⁹

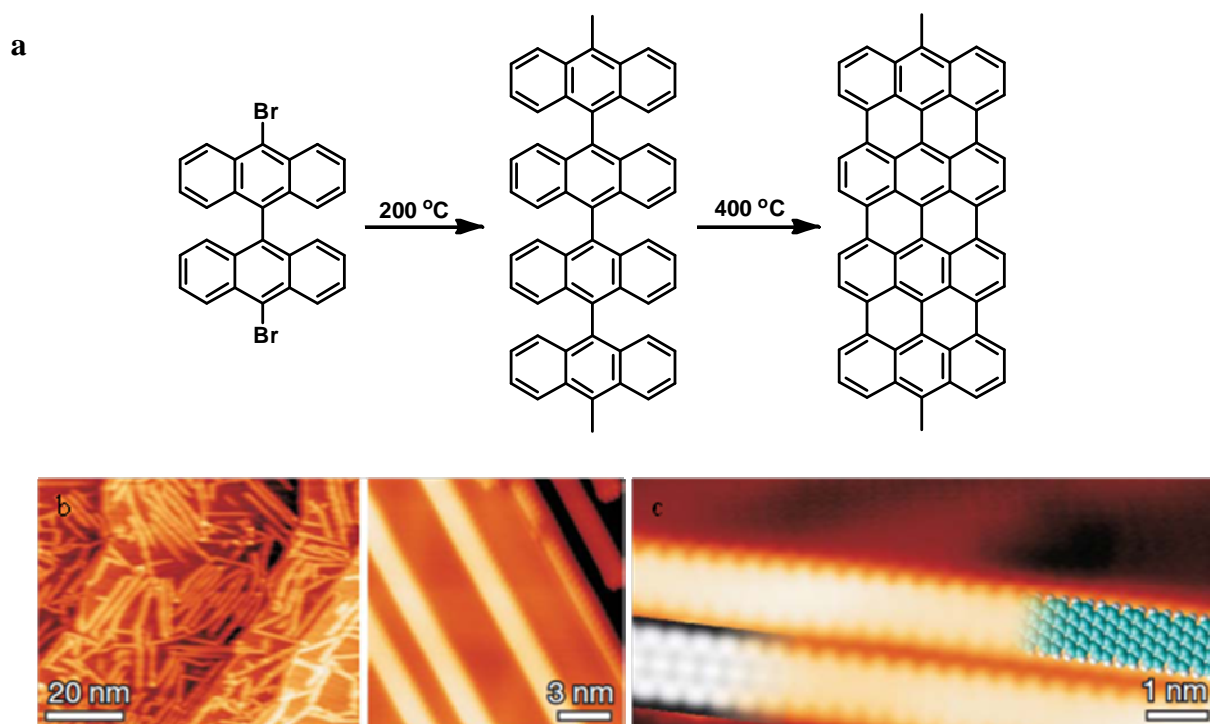


Figure 11. a) Reaction scheme for conversion of bianthryl monomers to GNRs. b) STM image taken after surface-assisted C-C coupling at 200 °C and DFT-based simulation of the STM image (right) with partly overlaid model of the polymer. c) Overview STM image after cyclodehydrogenation at 400 °C.

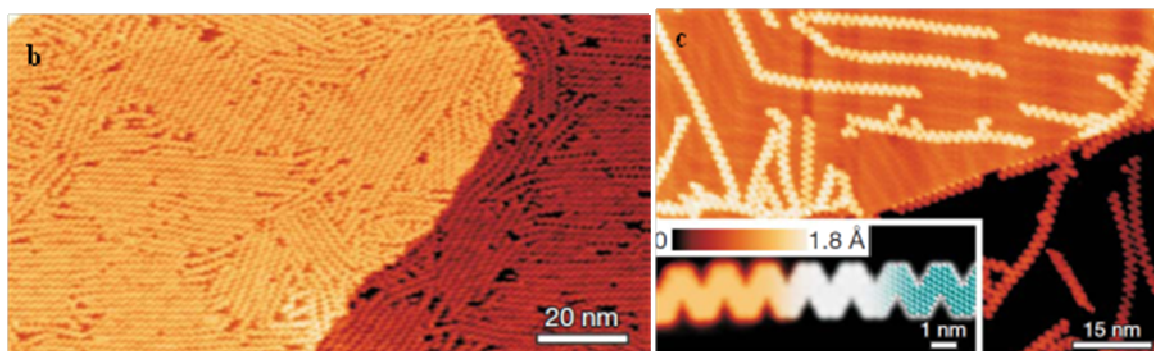
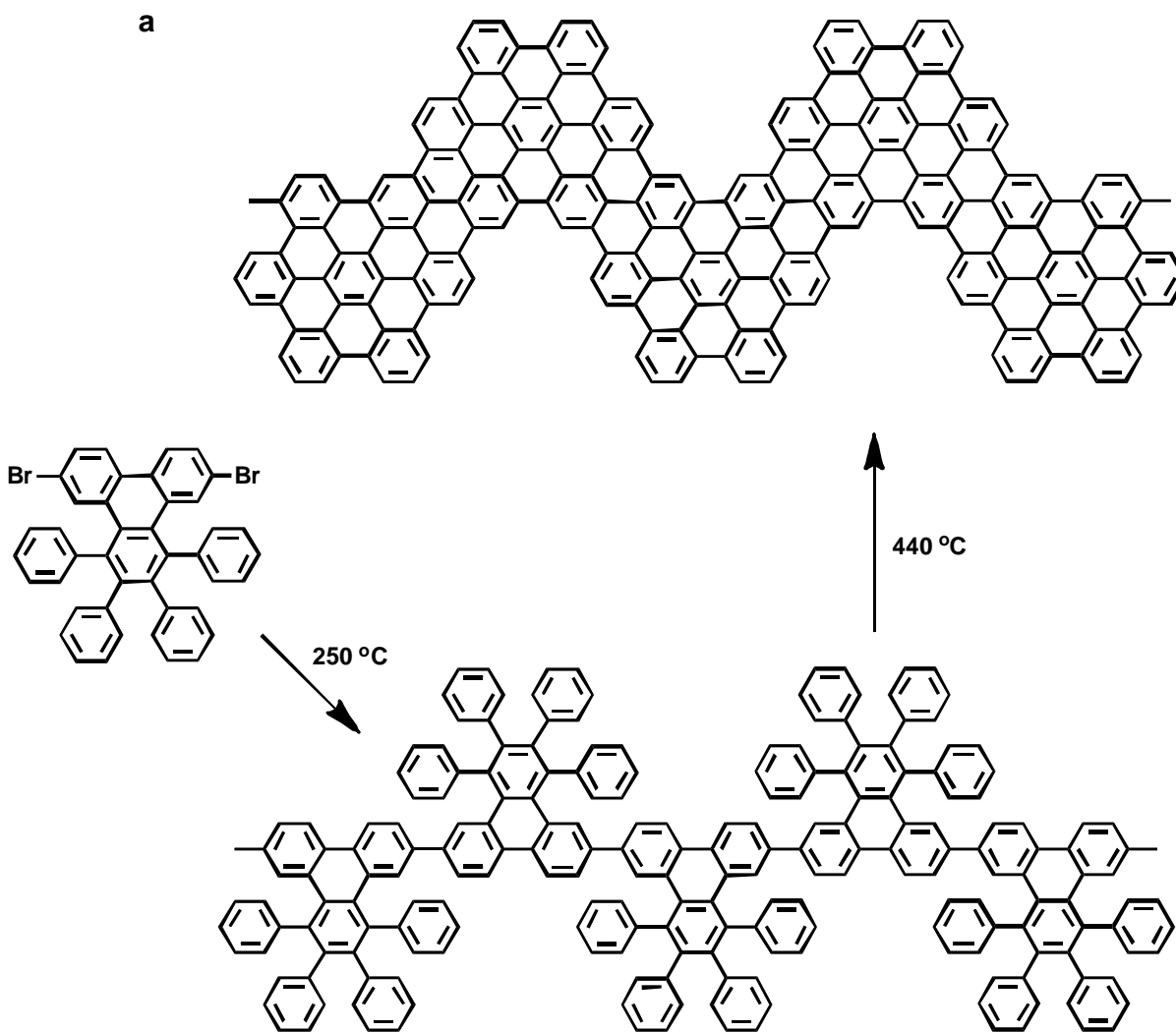


Figure 12. Chevron-type GNRs from tetraphenyl-triphenylene monomers. a) Reaction scheme for conversion of tetraphenyl-triphenylene monomers into chevron-type GNRs. b) Overview STM image of chevron-type GNRs fabricated on a Au(111) surface. c) Schematic model of the junction fabrication process. d) Model (blue C; white H) of the colligated and dehydrogenated molecules forming the threefold junction overlaid on the STM image.

1.2d. Solution synthesis of nanographenes.

Usual organic synthesis techniques, in solution, can be used to form large PAHs but solubility is quickly a limiting factor. For this reason, solubilizing groups such as long alkyl chains are generally functionalizing the edges of the flexible precursors and final rigid compounds. Many examples are reported in the literature and only few examples are discussed in the following section as an illustration.

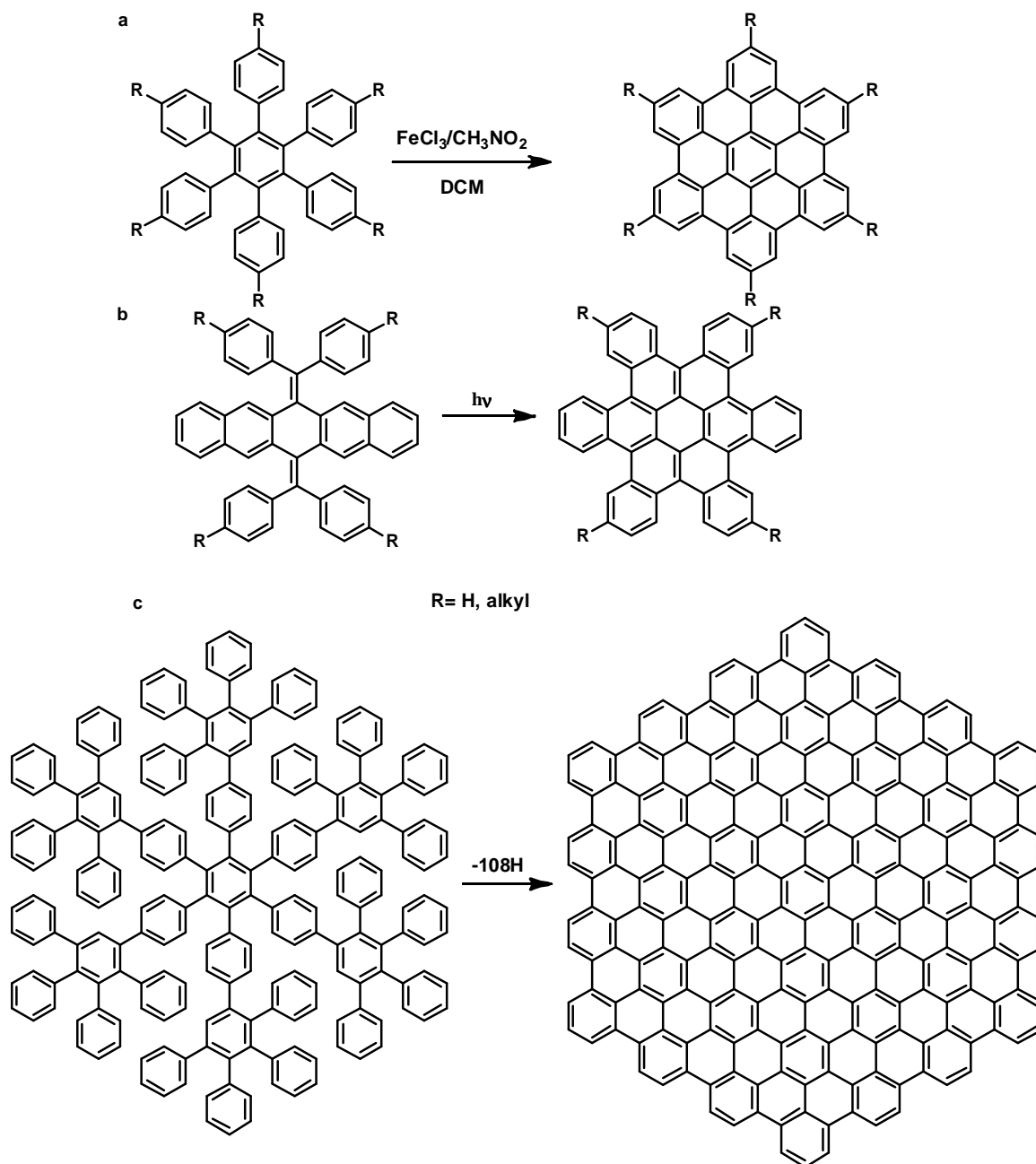


Figure 13. Examples of some organic syntheses of nanographenes.

The Scholl reaction has been developed as a powerful tool to produce various all-benzenoid PAHs^{50,51}. A typical example is the synthesis of hexa-*peri*-hexabenzocoronenes (HBCs) and their derivatives (**Figure 13a**) from substituted hexaphenylbenzene precursors by treatment with iron(III) chloride. Nuckolls and co-workers have developed a novel approach toward a phase-forming, distorted hexa-*cata*-hexabenzocoronene derivative (**Figure 13b**)⁵², whereby the decisive step is accomplished by the photocyclization. According to the definition, graphene molecules with a size between 1 and 5 nm can be considered as small nanographenes. By far, the largest synthesized monodisperse nanographene molecule consists of 222 carbon atoms with a disk diameter of 3.2 nm (**Figure 13c**), while one of the smallest and most frequently investigated nanographene molecules, hexa-*peri*-hexabenzocoronene (HBC), has a size of approximately 1.4 nm (**Figure 13a**).⁵³

1.2e. Solution synthesis of graphene nanoribbons.

Fully benzenoid armchair-edge nanoribbons of tetracene width (4 fused benzene rings in a row) with solubilising alkyl substituents have been obtained by K. Müllen and co-workers,

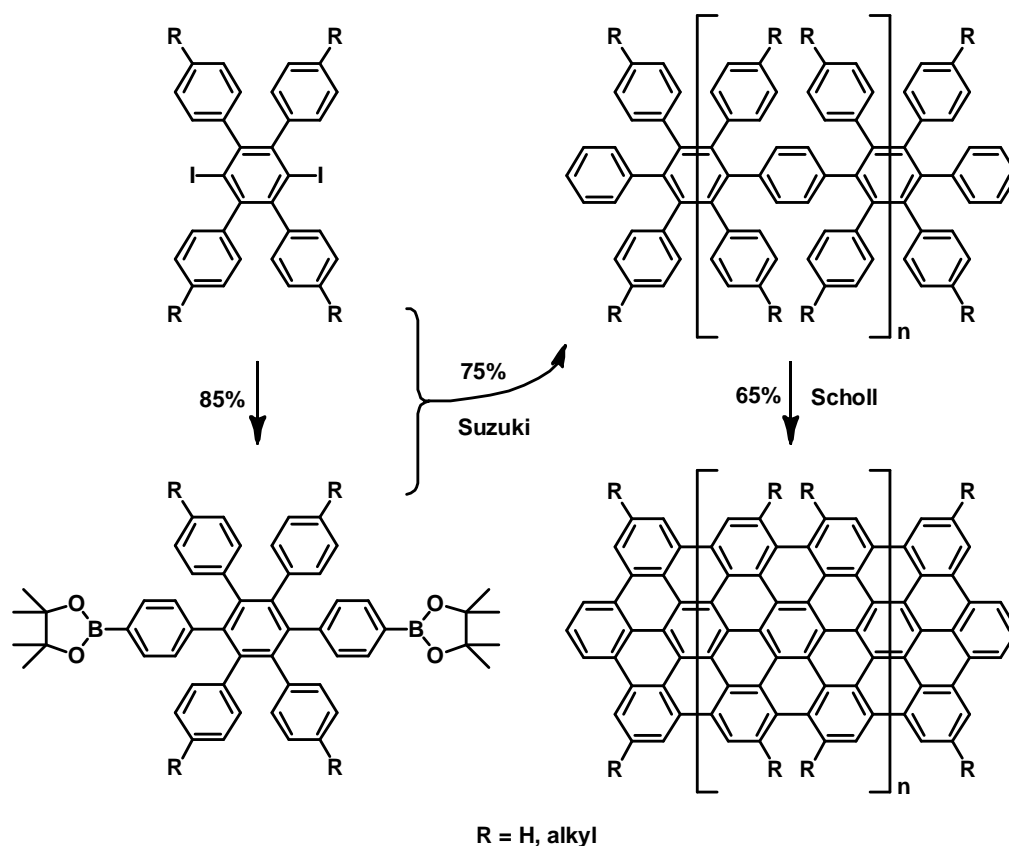


Figure 14. Synthesis of fully benzenoid armchair-edge graphene nanoribbons by cyclodehydrogenation with $FeCl_3$.

using parallel dehydrocyclizations, with ferric chloride, of polyphenylene precursors having a length of around 20 phenylene units (**Figure 14**)⁵⁴ in four steps overall 37% yield.

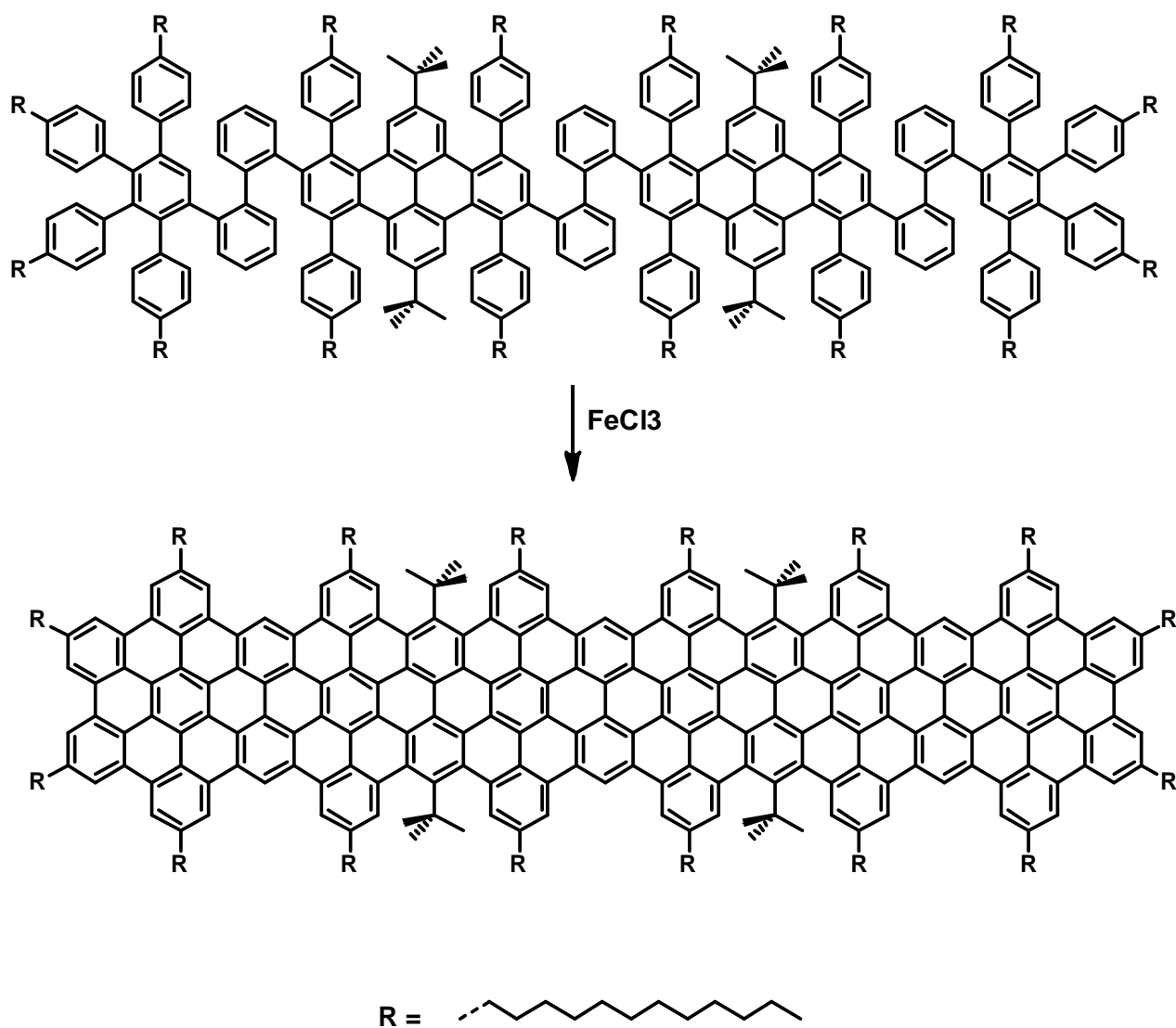


Figure 15. Synthesis of short fully benzenoid zigzag-edge graphene nanoribbons by cyclodehydrogenation with FeCl_3 .

One-dimensional short zigzag-edge graphene nanoribbons were also synthesized by K. Müllen and co-workers, still using intramolecular oxidative cyclodehydrogenation of other soluble branched polyphenylenes (**Figure 15**). While the insolubility of the resulting graphite ribbons precluded standard spectroscopic structure elucidation, their electronic and vibrational

properties were probed by solid-state UVvis, Raman, and infrared spectroscopy and their morphology was studied by high-resolution transmission electron microscopy (HRTEM).

1.3 Non planar PAHs.

1.3a. Geodesic PAHs.

Nanographenes are by definition large PAHs virtually extract from graphene. As a consequence, they are composed of fused benzene rings only and are flat. But some PAHs are not planar and cannot be called nanographenes. Due to their special geometries, their syntheses are mainly done following bottom-up techniques, except for few exceptions such as fullerenes that can be obtained from graphite under hard conditions⁵⁵.

Half-buckminsterfullerene (HB) $C_{30}H_{10}$ is a perfect half of C_{60} when the terminating hydrogen atoms are taken away. The investigation of other geodesic PAHs is fundamental to the understanding of the stability and formation of fullerenes.^{56,57} One of the unique characteristics of geodesic PAHs and fullerenes is their nonplanar distortions, which introduces remarkable strain energies.⁵⁸⁻⁶⁰ For this reason, the formation of these compounds generally needs hard conditions such as Flash-Vacuum Pyrolysis.

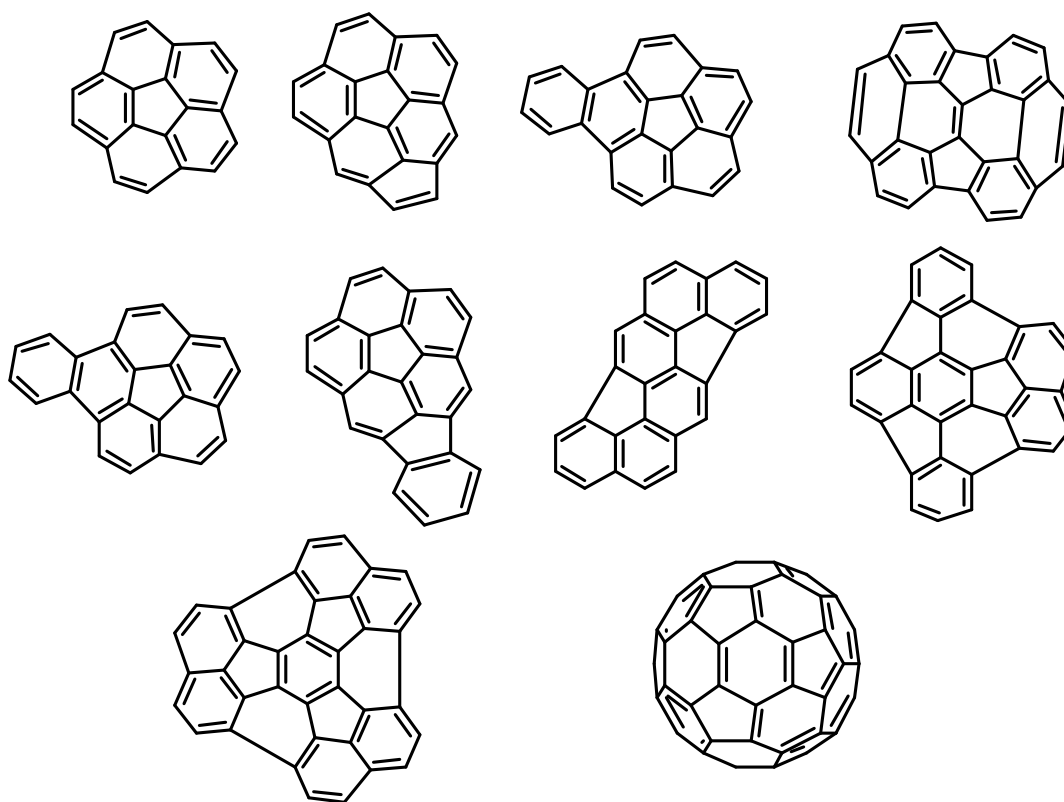


Figure 16. Example of geodesic polyarenes that have been prepared by FVP.

Flash vacuum pyrolysis (FVP) is a method for heating molecules in the gas phase to very high temperatures for a very short time.^{61,62} The hot zone typically consists of a horizontal quartz tube heated by an electric furnace to temperatures in the range of 500-1100 °C. Under vacuum, the sample is sublimed, the vapors pass through a hot zone, and the products are collected in a cold trap.

1.3b. Examples of synthesis of geodesic PAHs.

The synthesis of corannulene illustrated in (**Figure 17**) provided a striking first validation of the strategy that Scott⁶³ and Siegel⁶⁴ had envisioned for preparing geodesic polyarenes by distorting flat PAHs with heat and then “catching” the deformed ring systems by C-C bond forming reactions at the rim.

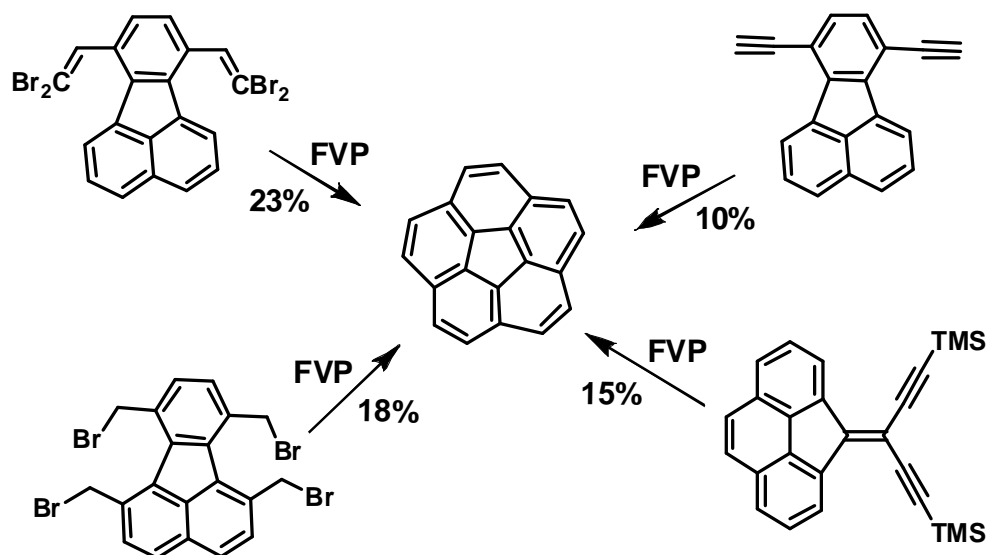


Figure 17. Synthesis of Corannulene by FVP.

The first chemical synthesis of buckminsterfullerene C₆₀, by L. T. Scott, in isolable quantities also relied on FVP to zip up a conventional polyarene and introduce the geodesic curvature (**Figure 18**).^{65,66}

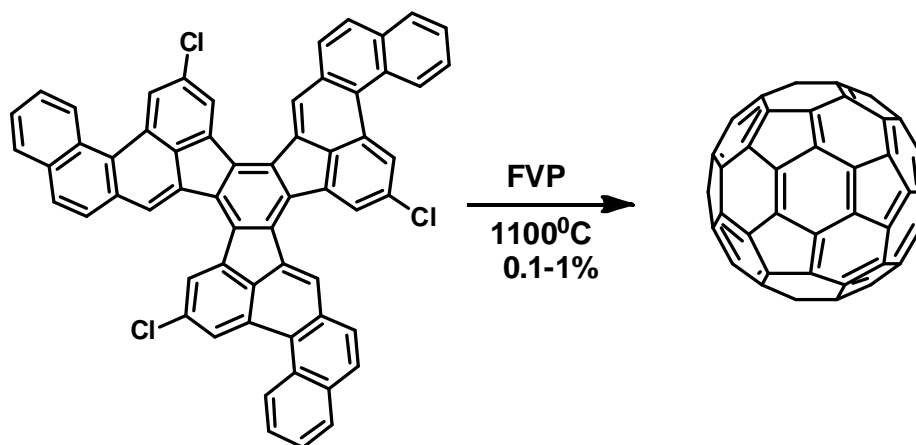


Figure 18. Synthesis of buckminsterfullerene C_{60} by FVP

Another strategy, developed by A. M. Echavarren, relies on a very similar triflate precursor but it involves a microwave promoted reaction (200 W, 10 min) in the presence of $[PdCl_2(PPh_3)_2]$, LiCl and DBU in DMA. It leads to a mixture of products that was analyzed by mass spectrometry (**Figure 19**).

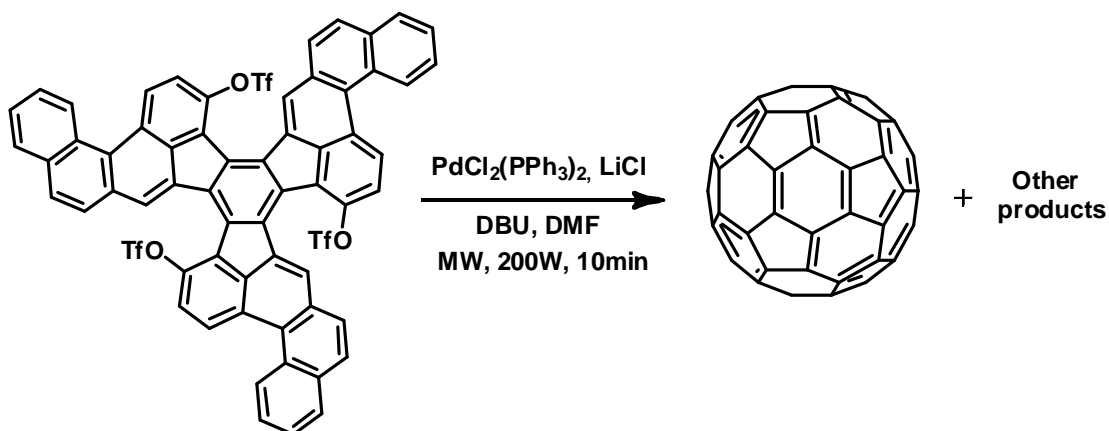


Figure 19. Synthesis of buckminsterfullerene C_{60} by palladium catalyst.

Geodesic PAHs are non planar due to the presence of non hexagonal rings in their structure. Nevertheless, another category of PAHs can present non planarity with only 6-membered rings in their molecular structure.

1.3c. Helicenes.

Helicenes are polycyclic aromatic compounds with non planar screw-shaped skeletons formed by ortho-fused benzene or other aromatic rings.^{67,68} The first helicenes were synthesized by Meisenheimer and Witte in 1903.⁶⁹ During the next few decades, little was discovered about the chemistry of helicenes, except for the synthesis of some helicenes (**Figure 20**).⁷⁰ After Newman and co-workers reported the synthesis and resolution of hexahelicene in the 1950s,⁷¹ however, the study of the chemistry of helicenes really took off. During the following 30 years, Wynberg,⁷² Martin,⁷³ Laarhoven,⁷⁴ and Katz⁷⁵ carried out pioneering studies of the synthesis, spectral properties, and structures of helicenes. In the 1990s, the Diels-Alder synthetic approach after Martin's photochemical methods brought another important breakthrough in the preparation of helicenes on a large scale,⁷⁶ and based on this approach, a large number of helicene derivatives have been synthesized.⁷⁷ Since the late 1990s, more and more new strategies for the synthesis of helicenes with good yields and enantioselectivities have been developed,⁶⁷ especially by utilizing organometallic catalysts.⁷⁸ Moreover, with the help of the theoretical studies using a variety of methods,^{67,79} the properties of helicenes have also become much clearer.

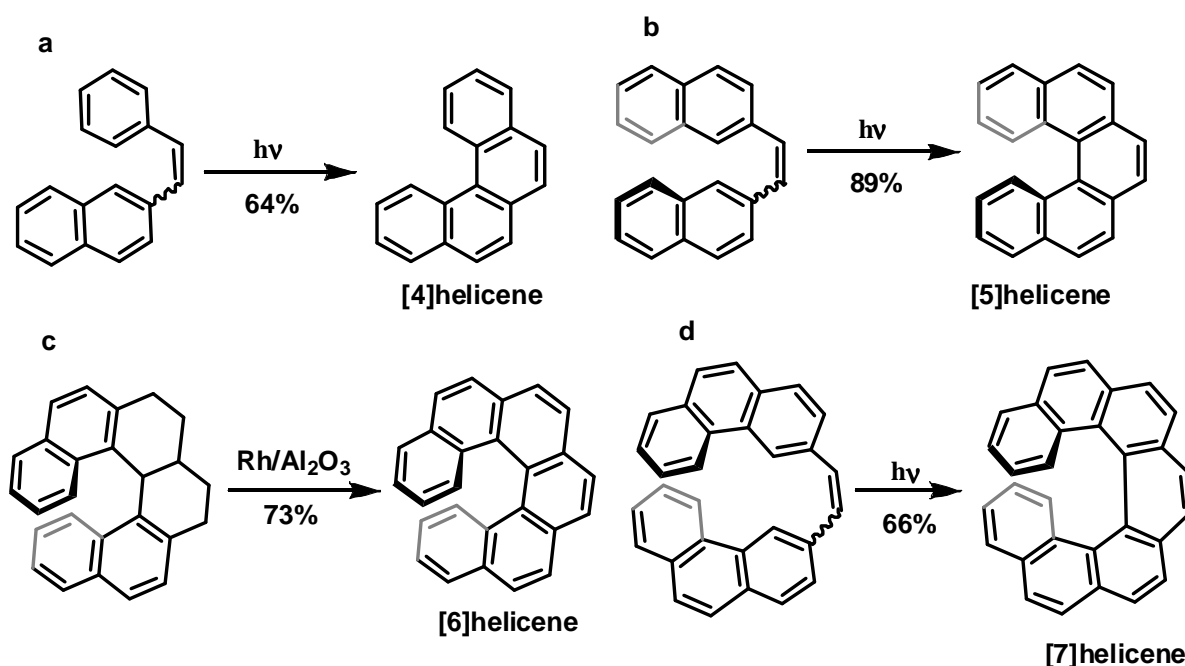


Figure 20. Examples of different helicenes (a) and (b) Scholz et al. 1967, (c) Newman et al. 1955, (d) Martin et al. 1967.

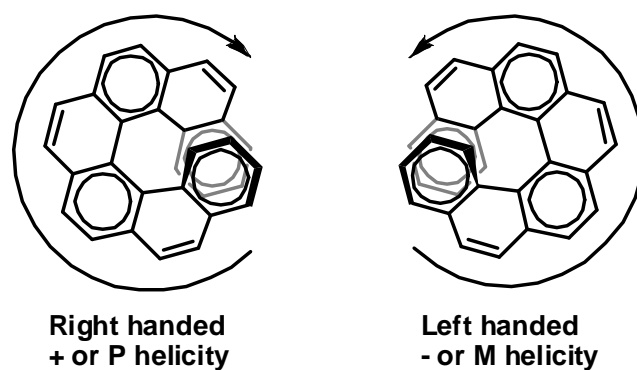


Figure 21. Helicity of helicenes.

This particular geometry of helicenes renders them chiral even though they have no asymmetric carbons or other chiral centers. On the basis of the helicity rule proposed by Cahn, Ingold, and Prelog in 1966, a left-handed helix is designated “minus” and denoted by “M” whereas a right-handed one is designated “plus” and denoted by “P” (**Figure 21**).⁸⁰

1.3d. Synthesis of helicenes.

1.3d.i. Photocyclization.

Photocyclization has become one of the most important methods for the synthesis of many helicene homologues (from [5]- to [14]helicene) and derivatives.

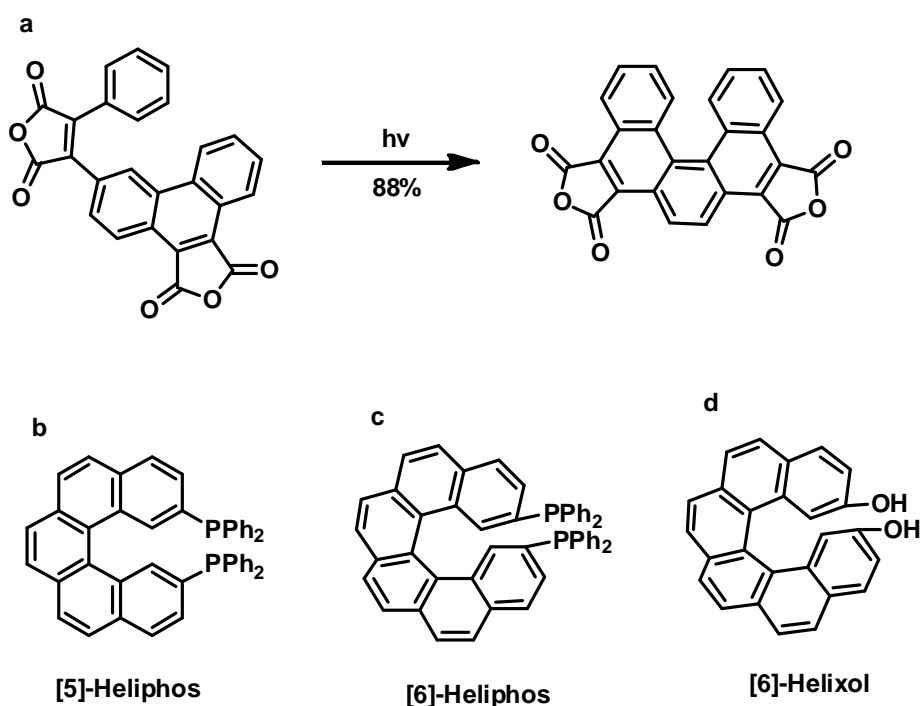


Figure 22. Some 2,2-disubstituted helicenes prepared by photocyclization.

The photoreaction of 1,4-phenylene bis(phenylmaleic anhydride) (**Figure 22a**) afforded photocyclized product in 88% yield; The first helical phosphane ligands heliphos (**Figure 22b, 22c**), which have become important ligands in asymmetric catalysis, were prepared independently by Brunner's group⁸¹ and Reetz's group⁸² in 1997. Four years later, Reetz and Sostmann reported another important ligand helixol (**Figure 22d**).⁸³

1.3d.ii Diels-Alder reaction.

The breakthrough in large-scale preparation of helicenes was made by the pioneering work of Katz and Liu in 1990 utilizing a Diels-Alder methodology.⁷⁷ They obtained [5]helicene with two quinone moieties in reasonable yield and gram scale quantities by the Diels-Alder reaction between p-divinylbenzene and p-benzoquinone. Moreover, the presence of four carbonyl groups in the resulting [5]helicene allows convenient functionalization of the terminal rings (**Figure 23**).⁷⁷

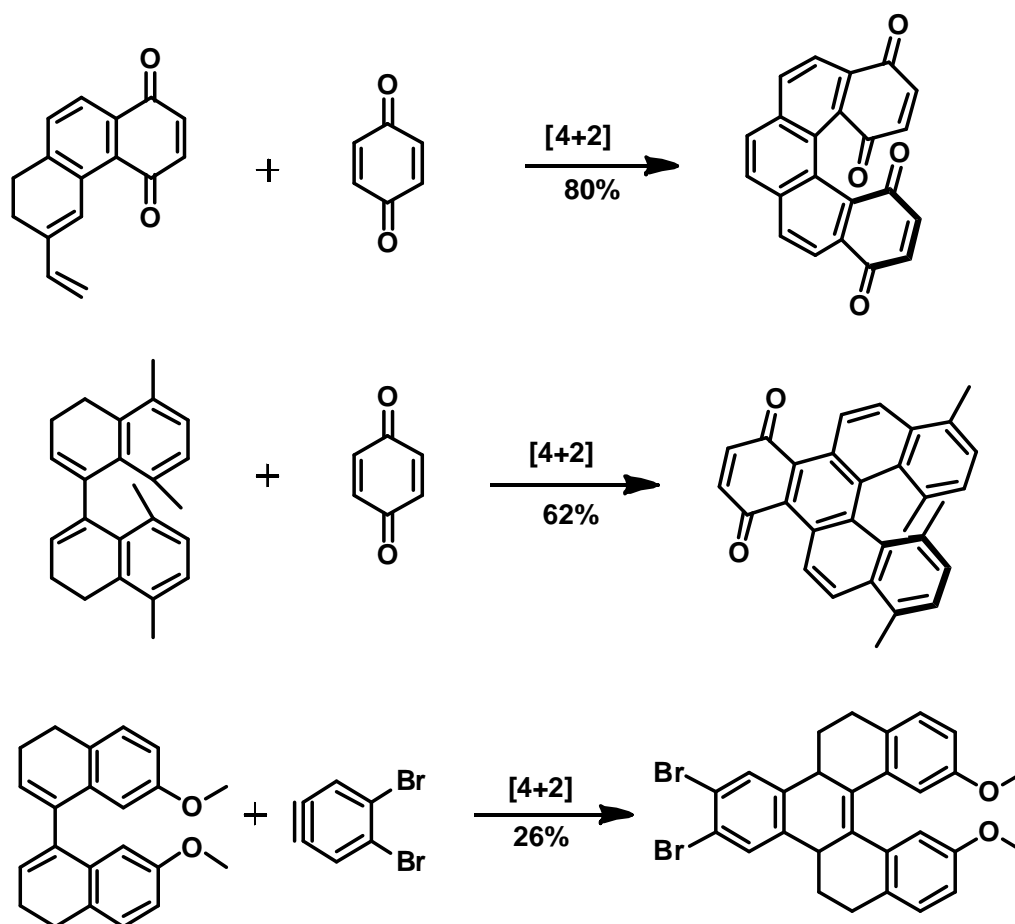


Figure 23. Helicenes prepared by Diels-Alder methodology.

1.3d.iii. Friedel-Crafts reaction.

A Friedel-Crafts-type sequence leading to helicenes was described by Ichikawa and co-workers (**Figure 24**).⁸⁴ The presence of two ortho-methyl groups is important to facilitate the domino cyclization. They not only direct the reaction to form a helical structure but also enhance the nucleophilicity of the aromatic moieties. With the help of magic acid ($\text{FSO}_3\text{H}\cdot\text{SbF}_5$) and Ph_3CBF_4 , double ring closure and dehydrogenation proceeded efficiently, giving (**Figure 24**) 6, 11-dimethyl[6]-helicene in good yield. On the basis of this route, different helicenes can be conveniently synthesized by varying the aryl groups.

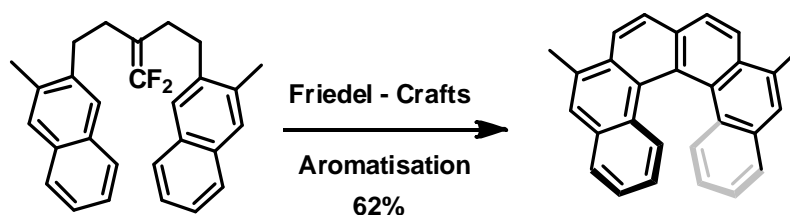


Figure 24. Helicenes Friedel-Crafts reaction.

1.3d.iv. Palladium (Pd)-catalyzed cyclizations.

Several routes for the synthesis of helicenes by Pd-catalyzed coupling reactions have been reported in a review dedicated to helicenes by F. Chen.⁸⁵ A double C-H arylation reaction was employed in the synthesis of [5]- and [6] helicenes in moderate to good yields under the optimized conditions (with Ag_2CO_3 as the additive, $\text{PCy}_3\cdot 3\text{HBF}_4$ as the ligand) (**Figure 25**).

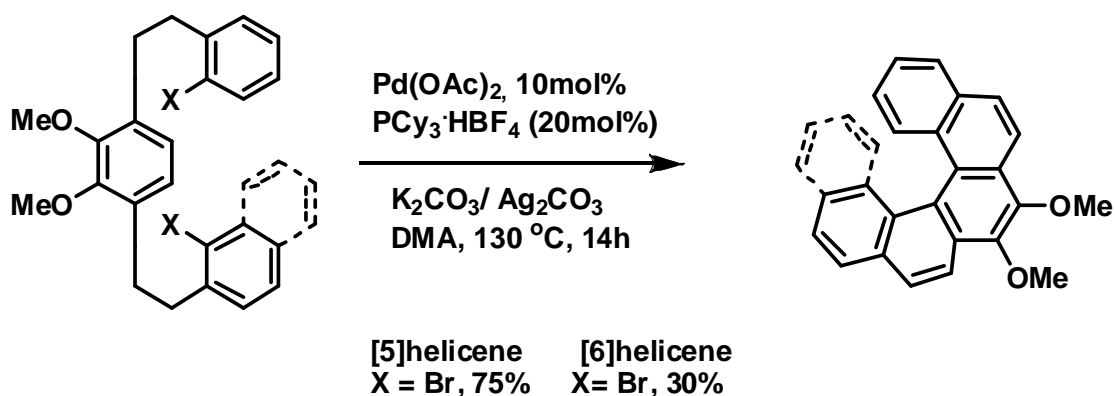


Figure 25. Pd-catalysed helicene formation by C-H arylation.

Pd-catalyzed cyclotrimerization of arynes consists in generating in situ an aryne precursor and make it react with a well adapted catalytic system. It can often be achieved under mild conditions *via* a fluorine-induced elimination from a trimethylsilyl group in *ortho* position to a triflate group onto an aromatic ring. $[2\pi+2\pi+2\pi]$ co-trimerization easily occur in the presence of a Pd(0) catalyst, an aryne and an alkyne⁸⁶. Guitian, Pérez and coworkers have widely explored the efficiency of a simple catalyst,⁸⁷ the lightly coordinated $\text{Pd}_2(\text{dba})_3$, in CH_3CN and in the presence of CsF. One of their most impressive results is the first efficient syntheses of polysubstituted twisted triphenylene (**Figure 26a**) and especially the propeller-shaped hexabenzotriphenylene.⁸⁸

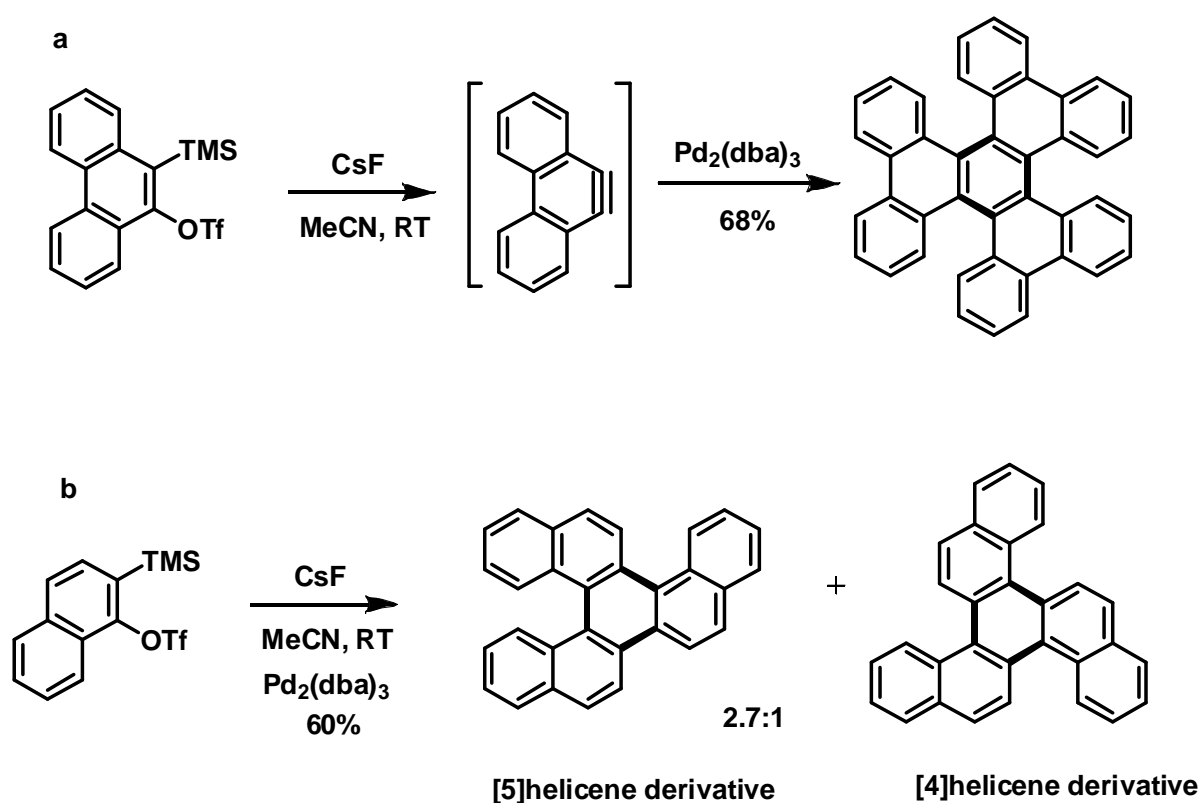


Figure 26. Pd-catalysed helicene formation by $[2+2+2]$ cyclo-addition.

1.3e. Applications of the helicenes chirality.

Since Bredig first reported the preparation of mandelonitrile in <10% ee by utilizing quinine as a catalyst, asymmetric catalysis has continued to develop over nearly 100 years.⁸⁹ Although many different kind of chiral ligands and chiral catalysts have been developed so far, it is surprising that no ligands bearing helical chirality were used in asymmetric catalysis until

1997.⁸² Before that, however, Martin and co-workers utilized substituted [7]helicenes as chiral auxiliaries or chiral reagents in five different diastereoselective reactions, including reduction of α -keto esters,⁹⁰ hydroxyamination⁹¹ and epoxidation⁹² of olefins, synthesis of atrolactic ester,⁹³ and the ene reaction⁹⁴ (**Figure 27**).

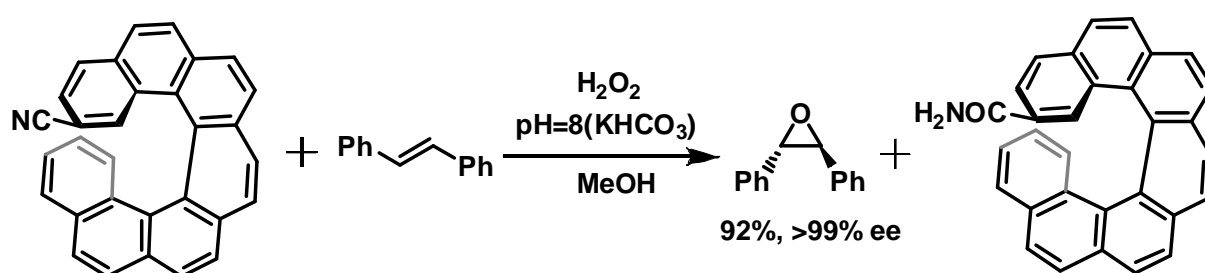


Figure 27. Helicene catalysed asymmetric reaction.

Helicenes have chiroptical properties due to strong metal–ligand electronic interactions. Jeanne Crassous and co-workers have recently developed [6]helicene-based chiroptical switches. In this example (**Figure 28**) the electro-active Ru centers allow the achievement of the first purely [6]helicene-based redox triggered chiroptical switches⁹⁵ (**Figure 28**).

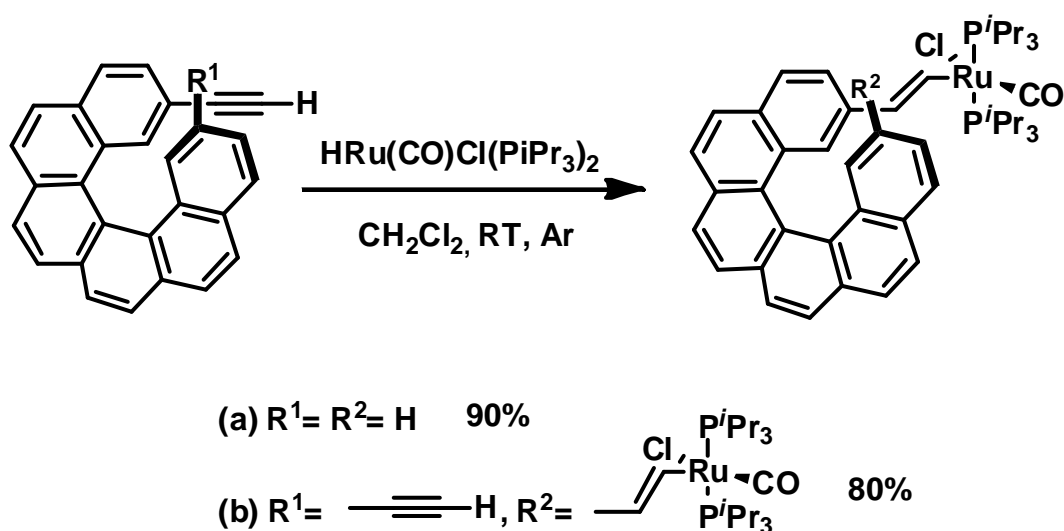


Figure 28. Synthesis of enantiopure Ru(II)-capped helicenes.

1.4 References.

1. (a) <http://en.wikipedia.org/wiki/Carbon> (b) R. Saito, G. Dresselhaus, M. S. Dresselhaus. Physical properties of carbon nanotubes. Imperial college press. London, 1998.
2. A. H. R. Palser, *Phys. Chem. Chem. Phys.* **1999**, *1*, 4459.
3. H. W. Kroto, J. R. Heath, S. C. O'Brien, R. F. Curl, R. E. C. Smalley, *Nature* **1985**, *318*, 162.
4. S. Iijima, *Nature* **1991**, *354*, 56.
5. D. Ugarte, *Nature* **1992**, *359*, 707.
6. A. Krishnan, E. Dujardin, M. M. J. Treacy, J. Hugdahl, S. Lynum, T. W. Ebbesen, *Nature* **1997**, *381*, 454.
7. H. Murayama, T. Maeda, *Nature* **1990**, *345*, 792.
8. K. S. Novoselov, A. K. Geim, S. V. Morozov, D. Jiang, Y. Zhang, S. V. Dubonos, I. V. Grigorieva, A. A. Firsov, *Science* **2004**, *306*, 666.
9. X. Li, X. Wang, L. Zhang, S. Lee, H. Dai, *Science* **2008**, *319*, 1229.
10. L. Jiao, L. Zhang, X. Wang, G. Diankov, H. Dai, *Nature* **2009**, *458*, 877.
11. D. V. Kosynkin, A. L. Higginbotham, A. Sinitskii, J. R. Lomeda, A. Dimiev, B. K. Price, J. M. Tour, *Nature* **2009**, *458*, 872.
12. F. Cataldo, G. Compagnini, G. Patane, O. Ursini, G. Angelini, P. R. Ribic, G. Margaritondo, A. Cricenti, G. Palleschi, F. Valentini, *Carbon* **2010**, *48*, 2596.
13. A. G. Cano-Mrquez, F. J. Rodriguez-Macias, J. Campos-Delgado, C. G. Espinosa-Gonzalez, F. Tristan-Lopez, D. Ramirez-Gonzalez, D. A. Cullen, D. J. Smith, M. Terrones, Y. I. Vega-Cantu, *Nano Lett.* **2009**, *9*, 1527.
14. D. V. Kosynkin, W. Lu, A. Sinitskii, G. Pera, Z. Sun, J. M. Tour, *ACS Nano* **2011**, *5*, 968.
15. L. Jiao, X. Wang, G. Diankov, H. Wang, H. Dai, *Nat. Nanotechnol.* **2010**, *5*, 321.
16. L. Xie, H. Wang, C. Jin, X. Wang, L. Jiao, K. Suenaga, H. Dai, *J. Am. Chem. Soc.* **2011**, *133*, 10394.
17. P. Kumar, L. S. Panchakarla, C. N. R. Rao, *Nanoscale* **2011**, *3*, 2127.
18. D. B. Shinde, J. Debgupta, A. Kushwaha, M. Aslam, V. K. Pillai, *J. Am. Chem. Soc.* **2011**, *133*, 4168.
19. I. Janowska, O. Ersen, T. Jacob, P. Vennegues, D. Begin, M. J. Ledoux, C. P. Huu, *Appl. Catal. A* **2009**, *371*, 22.

20. V. Sridhar, J. H. Jeon, I. K. Oh, *Carbon* **2011**, *49*, 222.
21. A. L. Elas, A. R. B. Mendez, D. M. Rodriguez, V. J. Gonzalez, D. R. Gonzalez, L. Ci, E. M. Sandoval, P. M. Ajayan, H. Terrones, M. Terrones, *Nano Lett.* **2010**, *10*, 366.
22. U. K. Parashar, S. Bhandari, R. K. Srivastava, D. Jariwala, A. Srivastava, *Nanoscale* **2011**, *3*, 3876.
23. A. V. Talyzin, S. Luzan, I. V. Anoshkin, A. G. Nasibulin, H. Jiang, E. I. Kauppinen, V. M. Mikoushkin, V. V. Shnitov, D. E. Marchenko, D. Noreus, *ACS Nano* **2011**, *5*, 5132.
24. M. C. Paiva, W. Xu, M. F. Proenca, R. M. Novais, E. Laegsgaard, F. Besenbacher, *Nano Lett.* **2010**, *10*, 1764.
25. K. Kim, A. Sussman, A. Zettl, *ACS Nano* **2010**, *4*, 1362.
26. D. V. Kosynkin, A. L. Higginbotham, A. Sinitskii, J. R. Lomeda, A. Dimiev, B. K. Price, J. M. Tour, *Nature* **2009**, *458*, 872.
27. (a) A. L. Higginbotham, D. V. Kosynkin, A. Sinitskii, Z. Sun, J. M. Tour, *ACS Nano*, **2010**, *4*, 2059. (b) M. Terrones, *Nature* **2009**, *458*, 845. (c) L. Chen, Y. Hernandez, X. Feng, K. Mullen, *Angew. Chem. Int. Ed.* **2012**, *51*, 2.
28. J. C. Fetzer. *The Chemistry and Analysis of the Large Polycyclic Aromatic Hydrocarbons*, John Wiley, New York, 2000.
29. K. F. Lang, J. Kalowy, H. Buffleb. *Chem. Ber. Recl.* **1964**, *97*, 494.
30. K. F. Lang, J. Kalowy, H. Buffleb. *Chem. Ber. Recl.* **1962**, *95*, 1052.
31. D. J. Cook, S. Schlemmer, N. Balucani, D. R. Wagner, B. Steiner, R. J. Saykally. *Nature* **1996**, *380*, 227.
32. R. Scholl, C. Seer. *Justus Liebigs Ann. Chem.* **1912**, *394*, 111.
33. R. Scholl, C. Seer. *Ber. Dtsch. Chem. Ges.* **1911**, *44*, 1233.
34. E. Clar. *Ber. Dtsch. Chem. Ges.* **1929**, *62*, 1574.
35. E. Clar. *Polycyclic Hydrocarbons*, Vols. 1 and 2, John Wiley, New York, **1964**.
36. E. Clar, M. Zander. *J. Chem. Soc.* **1958**, 1577.
37. M. Zander. *Handbook of Polycyclic Aromatic Hydrocarbons*, Marcel Dekker, New York, **1983**.
38. S. Hagen, H. Hopf. *Top. Curr. Chem.* **1998**, *196*, 44.
39. P. V. R. Schleyer. *Chem. Rev.* **2001**, *101*, 1115.

40. T. A. Skotheim, R. L. Elsenbaumer, J. R. Reynolds (Eds.). *Handbook of Conducting Polymers*, 2nd ed., Marcel Dekker, New York, 1998.
41. M. Watson, A. Fechtenkötter, K. Müllen, *Chem. Rev.* **2001**, *101*, 1267.
42. J. Wu, W. Pisula, K. Müllen, *Chem. Rev.* **2007**, *107*, 718.
43. S. Laschat, A. Baro, N. Steinke, F. Giesselmann, C. Hagele, G. Scalia, R. Judele, E. Kapatsina, S. Sauer, A. Schreivogel, M. Tosoni, *Angew. Chem., Int. Ed.* **2007**, *46*, 4837.
44. J. P. Hill, W. Jin, A. Kosaka, T. Fukushima, H. Ichihara, T. Shimomura, K. Ito, T. Hashizume, N. Ishii, T. Aida, *Science* **2004**, *304*, 1481.
45. Y. Yamamoto, T. Fukushima, Y. Suna, N. Ishii, A. Saeki, S. Seki, S. Tagawa, M. Taniguchi, T. Kawai, T. Aida. *Science* **2006**, *314*, 1761.
46. 19. S. Xiao, J. Tang, T. Beetz, X. Guo, N. Tremblay, T. Siegrist, Y. Zhu, M. Steigerwald, C. Nuckolls *J. Am. Chem. Soc.* **2006**, *128*, 10700.
47. C. Kubel, K. Eckhardt, V. Enkelmann, G. Wegner, K. Mullen, *J. Mater. Chem.* **2000**, *10*, 879.
48. M. Bieri, S. Blankenburg, M. Kivala, C. A. Pignedoli, P. Ruffieux, K. Müllen, R. Fasel, *Chem. Commun.* **2011**, *47*, 10239.
49. J. Cai, P. Ruffieux, R. Jaafar, M. Bieri, T. Braun, S. Blankenburg, M. Muoth, A. P. Seitsonen, M. Saleh, X. Feng, K. Müllen, R. Fasel, *Nature* **2010**, *466*, 470.
50. M. Watson, A. Fechtenkötter, K. Müllen, *Chem. Rev.* **2001**, *101*, 1267.
51. J. Wu, W. Pisula, K. Müllen, *Chem. Rev.* **2007**, *107*, 718.
52. S. X. Xiao, M. Myers, Q. Miao, S. Sanaur, K. L. Pang, M. L. Steigerwald, C. Nuckolls. *Angew. Chem., Int. Ed.* **2005**, *44*, 7390.
53. E. Clar, B. Boggiano, *J. Chem. Soc.* **1957**, 2683.
54. (a) Z. Wang, Z. Tomovic, M. Kastler, R. Pretsch, F. Negri, V. Enkelmann, K. Mullen, *J. Am. Chem. Soc.* **2004**, *126*, 7794. (b) M. Kastler, J. Schmidt, W. Pisula, K. Mullen, *J. Am. Chem. Soc.* **2006**, *128*, 9526.
55. H. W. Kroto, J. R. Heath, S.C. O'Brien, R. F. Curl, R. E. Smalley, *Nature* **1985**, *318*, 162.
56. H. Richter, W. J. Grieco, J. B. Howard, *Combust. Flame* **1999**, *119*, 1.
57. J. Yu, R. Sumathi, W. H. Green, *J. Am. Chem. Soc.* **2004**, *126*, 12685.

58. T. G. Schmalz, W. A. Seitz, D. J. Klein, G. E. Hite, *J. Am. Chem. Soc.* **1988**, *110*, 1113.
59. D. Bakowies, W. J. Thiel, *J. Am. Chem. Soc.* **1991**, *113*, 3704.
60. R. C. Haddon, *Science* **1993**, *261*, 1545.
61. R. F. C. Brown, *Pure Appl. Chem.* **1990**, *62*, 1981.
62. H. McNab, *Aldrichimica Acta* **2004**, *37*, 19.
63. L. T. Scott, M. M. Hashemi, M. S. Bratcher, *J. Am. Chem. Soc.* **1992**, *114*, 1920.
64. A. Borchardt, A. Fuchicello, K. V. Kilway, K. K. Baldrige, J. S. Siegel, *J. Am. Chem. Soc.* **1992**, *114*, 1921.
65. L. T. Scott, M. M. Boorum, B. J. McMahon, S. Hagen, J. Mack, J. Blank, H. Wegner, A. de Meijere, *Science* **2002**, *295*, 1500.
66. L. T. Scott, *Angew. Chem., Int. Ed.* **2004**, *43*, 4994.
67. H. Wynberg, *Acc. Chem. Res.* **1971**, *4*, 65.
68. S. D. Han, D. R. Anderson, A. D. Bond, H. V. Chu, R. L. Disch, D. Holmes, J. M. Schulman,; S. J. Teat, K. P. C. Vollhardt, G. D. Whitener, *Angew. Chem. Int. Ed.* **2002**, *41*, 3227.
69. J. Meisenheimer, K. Witte, *Chem. Ber.* **1903**, *36*, 4153.
70. W. Fuchs, F. Niszel, *Ber. Dtsch. Chem. Ges.* **1927**, *60*, 209.
71. M. S. Newman, W. B. Lutz, D. Lednicer, *J. Am. Chem. Soc.* **1955**, *77*, 3420.
72. M. B. Groen, G. Stulen, G. J. Visser, H. Wynberg, *J. Am. Chem. Soc.* **1970**, *92*, 7218.
73. M. Flammang, J. Nasielsk, R. H. Martin, *Tetrahedron Lett.* **1967**, *8*, 743.
74. A. H. A. Tinnemans, W. H. Laarhoven, S. Sharafiozeri, K. A. Muszkat, *Recl. Trav. Chim. Pays-Bas.* **1975**, *94*, 239.
75. A. Sudhakar, T. J. Katz, *Tetrahedron Lett.* **1986**, *27*, 2231.
76. L. B. Liu, T. J. Katz, *Tetrahedron Lett.* **1990**, *31*, 3983.
77. N. D. Willmore, D. A. Hoic, T. J. Katz, *J. Org. Chem.* **1994**, *59*, 1889.
78. Y. Uozumi, A. Tanahashi, S. Y. Lee, T. Hayashi, *J. Org. Chem.* **1993**, *58*, 1945.
79. (a) H. J. Lindner, *Tetrahedron* **1975**, *31*, 281. (b) O. Katzenelson, J. Edelstein, D. Avnir, *Tetrahedron: Asymmetry* **2000**, *11*, 2695.
80. R. S. Cahn, C. Ingold, V. Prelog, *Angew. Chem., Int. Ed.* **1966**, *5*, 385.
81. A. Terfort, H. Gorls, H. Brunner, *Synthesis* **1997**, 79.
82. M. T. Reetz, E. W. Beuttenmuller, R. Goddard, *Tetrahedron Lett.* **1997**, *38*, 3211.

83. M. T. Reetz, S. Sostmann, *Tetrahedron* **2001**, *57*, 2515.
84. J. Ichikawa, M. Yokota, T. Kudo, S. Umezaki, *Angew. Chem., Int. Ed.* **2008**, *47*, 4870.
85. (a) Y. Shen, C. F. Chen, *Chem. Rev.* **2012**, *112*, 1463. (b) M. Shimizu, I. Nagao, Y. Tomioka, T. Hiyama, *Angew. Chem., Int. Ed.* **2008**, *47*, 8096.
86. M. Gingras, *Chem. Soc. Rev.* **2013**, *42*, 968.
87. (a) J. Caeiro,; D. Pena, A. Cobas, D. Perez, E. Guitian, *Adv. Synth. Catal.* **2006**, *348*, 2466. (b) D. Pena, D. Perez, E. Guitian, L. Castedo, *Org. Lett.* **1999**, *1*, 1555. (c) D. Pena, A. Cobas, D. Perez, E. Guitian, L. Castedo, *Org. Lett.* **2003**, *5*, 1863. (d) C. Romero, D. Pena, D. Perez, E. Guitian, *J. Org. Chem.* **2008**, *73*, 7996.
88. D. Pena, A. Cobas, D. Perez, E. Guitian, L. Castedo, *Org. Lett.*, **2000**, *2*, 1629.
89. G. Bredig, P. Fiske, *Biochem. Z.* **1912**, *46*, 7.
90. B. B. Hassine, M. Gorsane, J. Pecher, R. H. Martin, *Bull. Soc. Chim. Belg.* **1985**, *94*, 597.
91. B. B. Hassine, M. Gorsane, J. Pecher, R. H. Martin, *Bull. Soc. Chim. Belg.* **1985**, *94*, 759.
92. B. B. Hassine, M. Gorsane, F. Geerts-Evrard, J. Pecher, R. H. Martin, D. Castelet, *Bull. Soc. Chim. Belg.* **1986**, *95*, 547.
93. B. B. Hassine, M. Gorsane, J. Pecher, R. H. Martin, *Bull. Soc. Chim. Belg.* **1986**, *95*, 557.
94. B. B. Hassine, M. Gorsane, J. Pecher, R. H. Martin, *Bull. Soc. Chim. Belg.* **1987**, *96*, 801.
95. E. Anger, M. Srebro, N. Vanthuyne, L. Toupet, S. Rigaut, C. Roussel, J. Autschbach, J. Crassous, R. Réau, *J. Am. Chem. Soc.* **2012**, *134*, 15628.

Chapter II: Project - Carbon nanoribbons by Scholl reaction.

Graphene has emerged as a material with interesting low-dimensional physics and potential applications in electronics¹⁻⁴. GNRs, if made into quasi-one-dimensional structures with narrow widths ($\leq \sim 5\text{nm}$) and atomically smooth edges, are predicted to exhibit band gaps useful for room-temperature transistor operations with excellent switching speed and high carrier mobility (potentially even ballistic transport).⁵⁻⁹ Recent theoretical work predicted that quantum confinement and edge effects make narrow graphene nanoribbons (width $w \leq \sim 5\text{nm}$) into semiconductors,^{5,6} which differs from single-walled carbon nanotubes (SWCNTs) that contain $\sim 1/3$ metallic species.

Lithographic patterning of graphene sheets has yielded GNRs down to widths of $\sim 20\text{nm}$ thus far⁹ but there are difficulties in obtaining smooth edges (for example, with roughness $< \sim 5\text{ nm}$) and reaching true nanometer-scale ribbon width. Chemical approaches and self-assembly processes may produce graphene structures with desired shape and dimensions for fundamental and practical applications.

As explained before, the top-down methods for graphene synthesis seem to suffer from drawbacks such as uncontrollable sizes and irregular edge structures. In contrast, bottom up organic synthesis approaches may serve to create structurally defined graphenes.

In the previous section we observed that in such approaches, the last step is always a rigidification of a flexible precursor. For this purpose, one specific reaction is very often used: The intramolecular oxidative cyclodehydrogenation of adjacent benzene rings with Lewis acids, i.e. the intramolecular Scholl reaction.

2.1 The Scholl reaction.

2.1a. Definition.

The Scholl reaction¹⁰ is a coupling (C-C bond formation) reaction between two arene compounds and has been extensively used for intramolecular oxidative cyclodehydrogenation of various polybenzenoid hydrocarbons (**Figure 29**).

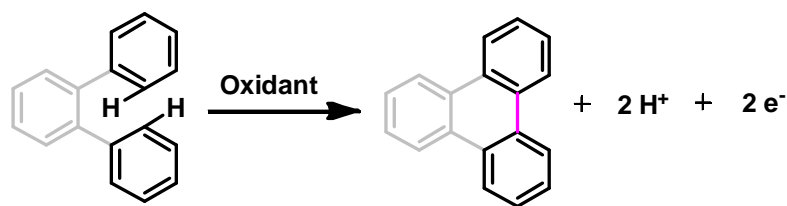


Figure 29. Oxidative cyclodehydrogenation reaction.

This reaction has been especially efficient for the oxidative cyclodehydrogenation of a variety of (substituted) hexaarylbenzenes and *ortho*-terphenyls to produce the corresponding planar polycyclic aromatic hydrocarbons (PAHs), i.e., hexa-*peri*-hexabenzocoronenes (HBCs) and triphenylenes, respectively.¹¹

2.1b. Examples of different Scholl reactions.

The Scholl reaction can be accomplished by using various oxidants. FeCl₃ in nitromethane is the most commonly used oxidant but many other examples can be found in the literature. For instance, hexa-*tert*-butyl-hexa-*peri*-hexabenzocorene has been formed by R. Rathore in 2009 using DDQ in MeSO₃H¹² (**Figure 30**).

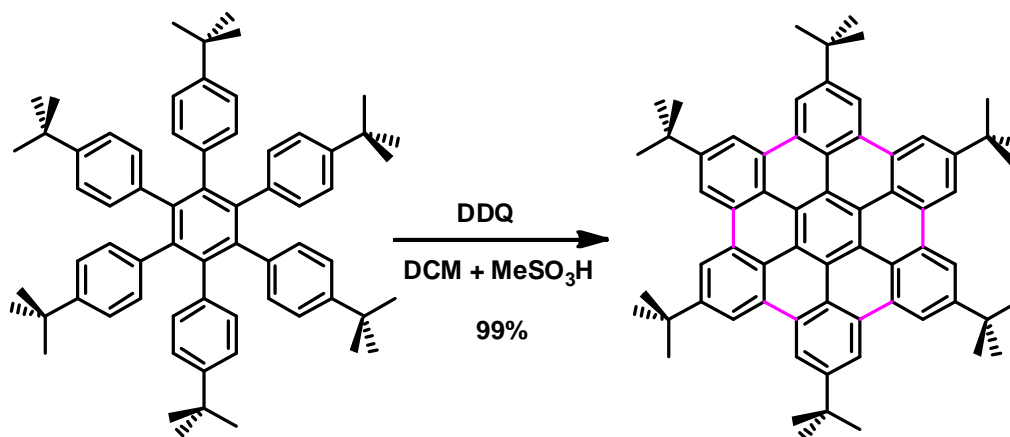


Figure 30. Scholl reaction using DDQ as an oxidant.

In 1971, J. A. Campbell has reported a Scholl reaction using AlCl₃ and SnCl₄ in CF₃CO₂H to form dibenzopyrene from 1-phenylbenz(a)anthracene¹³ (**Figure 31**).

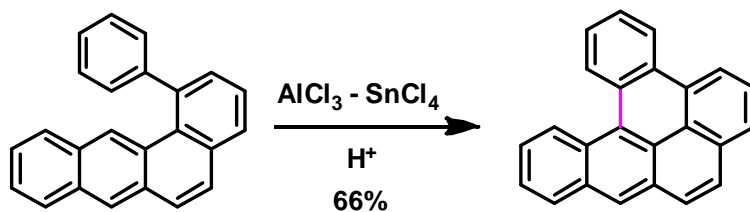


Figure 31. Scholl reaction using $\text{AlCl}_3\text{-SnCl}_4$ as an oxidant.

In 2007, B. T. King has described a triphenylene synthesis involving a Scholl reaction with $\text{C}_6\text{H}_5\text{I}(\text{O}_2\text{CCF}_3)_2$ (“PIFA”) and $\text{BF}_3\text{-OEt}_2$ in DCM (**Figure 32**). Nevertheless, a recurring problem is the oligomerization of the product which can be prevented by tert-butyl substituents.^{14a}

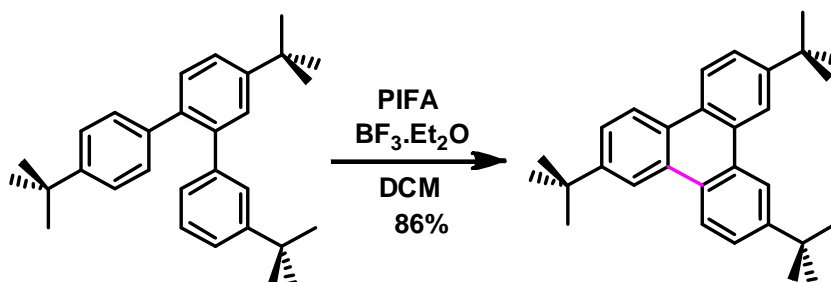


Figure 32. Scholl reaction using PIFA as an oxidant.

Activating groups such as methoxy improve yield and selectivity and in such cases, a soft oxidant such as MoCl_5 ¹⁷ can be used, as reported by B. T. King in 2007 (**Figure 33**).^{14a}

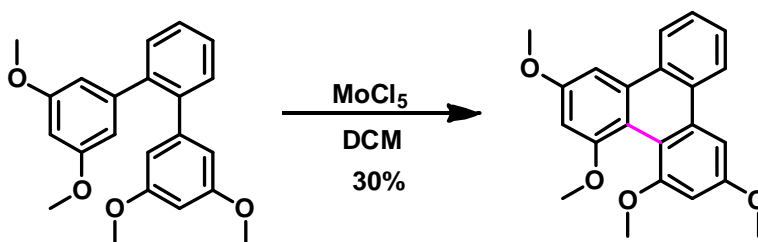


Figure 33. Scholl reaction using MoCl_5 as an oxidant.

An exhaustive list would be very long but some interesting other reacting systems are triethyloxonium hexachloroantimonate ($\text{Et}_3\text{O}^+ \text{SbCl}_6^-$),¹⁵ SbCl_5 ,¹⁶ $\text{Tl}(\text{O}_2\text{CCF}_3)_3$. Moreover, the Scholl reaction can also be effected by electrochemical oxidation.¹⁸

2.1c. Mechanism of the Scholl reaction.

The reaction depicted in Figure 29 is the simplest intramolecular Scholl reaction and will be used as a model to describe its mechanism. Interestingly, its nature is still very controversial and two different models are in opposition.

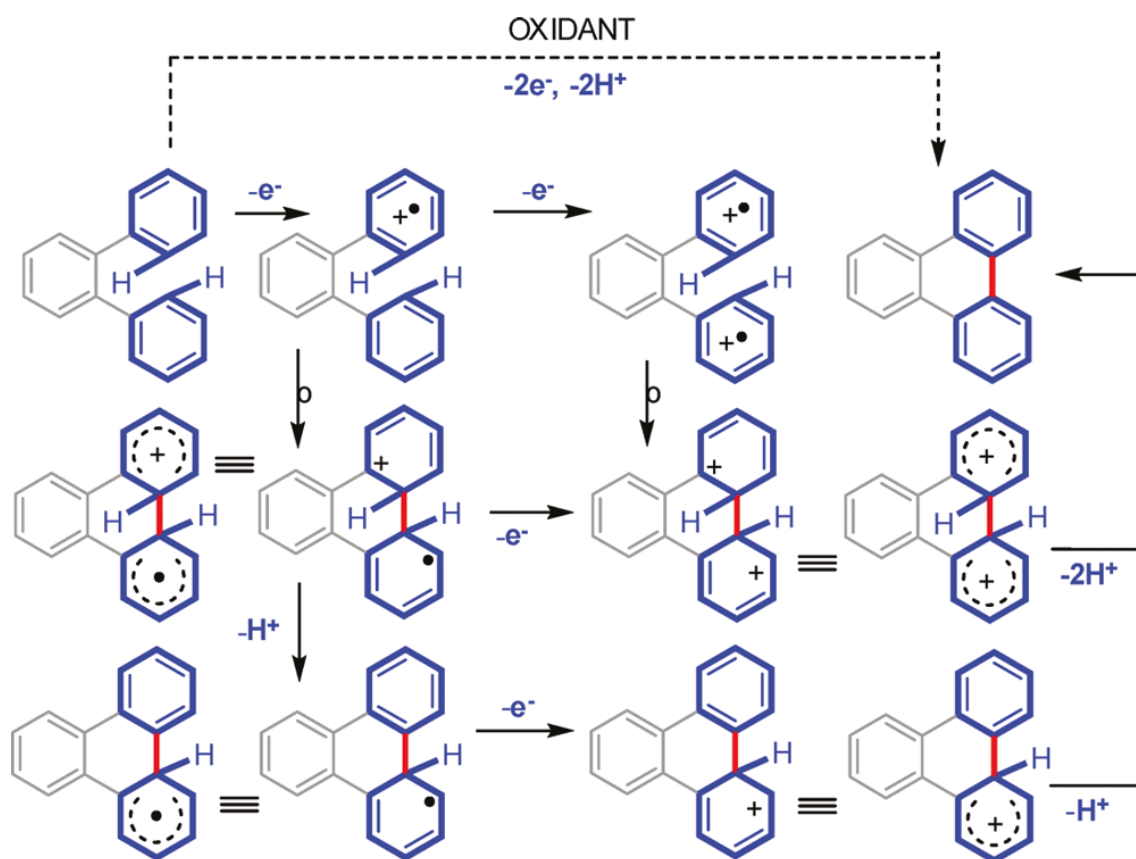


Figure 34. Cation radical (or electron transfer) mechanism for the Scholl reaction.

The involvement of cation radical intermediates (formed by one electron oxidation) in biaryl synthesis has been carefully probed by Parker and co-workers.¹⁹ A detailed mechanism of oxidative biaryl synthesis involving cation radical intermediates is presented in (Figure 34). A recent series of papers by King and co-workers^{20,21} have advocated that Scholl reaction occurs via diamagnetic arenium ion intermediates (see Figure 35) owing to the presence of

adventitious acids in various oxidizing systems²³⁻²⁵ utilized for Scholl reaction. It is further suggested by King and coworkers²⁰ that these reactions are accelerated as they proceed because of the formation of 2 equivalents of acid per C-C bond formation. Interestingly, however, no evidence has been forthcoming for such a time-dependent acceleration which, if true, can be taken advantage of by added acids (**Figure 35**).

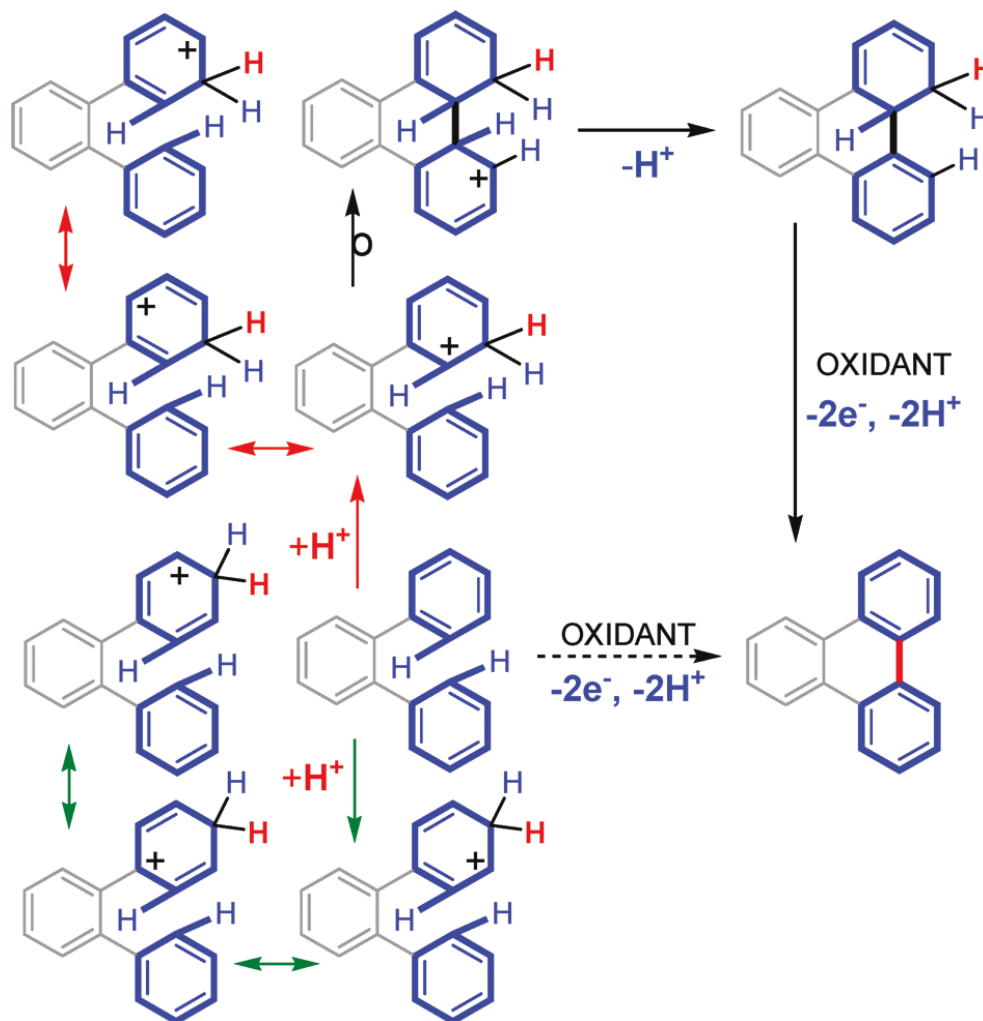


Figure 35. Arenium ion (or proton transfer) mechanism for the Scholl reaction.

The arenium-ion mechanism, depicted in (**Figure 35**), demands that C-C bond formation be accomplished only if the protonation occurs at a least preferred site, i.e., meta to an electron-releasing phenyl substituent (i.e., red arrow in **Figure 35**) and finally producing a non aromatic cyclohexadiene derivative. Furthermore, the mechanism of aromatization of the

cyclohexadiene derivative is overlooked in these studies^{20,21} and supposedly is rapid and proceeds via an ECEC mechanism.^{18,19} It is further noted that no experimental evidence is available from these studies for the time-dependent acceleration of the Scholl reaction or the acid-catalyzed formation of the non aromatic cyclohexadiene derivatives.^{20,21}

2.1d. Drawbacks of the Scholl reaction.

Many oxidants used in intramolecular Scholl reactions are metal chlorides. This generally involves creation of hydrochloric acid during the reaction, which can easily react, in the conditions present, with the polycyclic aromatic compounds, leading to unwanted chlorinated products. For this reason, it is often necessary to constantly degas the solution during the reaction, to eliminate HCl from the reacting mixture.

In addition, intramolecular Scholl reactions suffer from unpredictable rearrangements on some substrates, as described by King and coworkers (**Figure 36**)^{14b}.

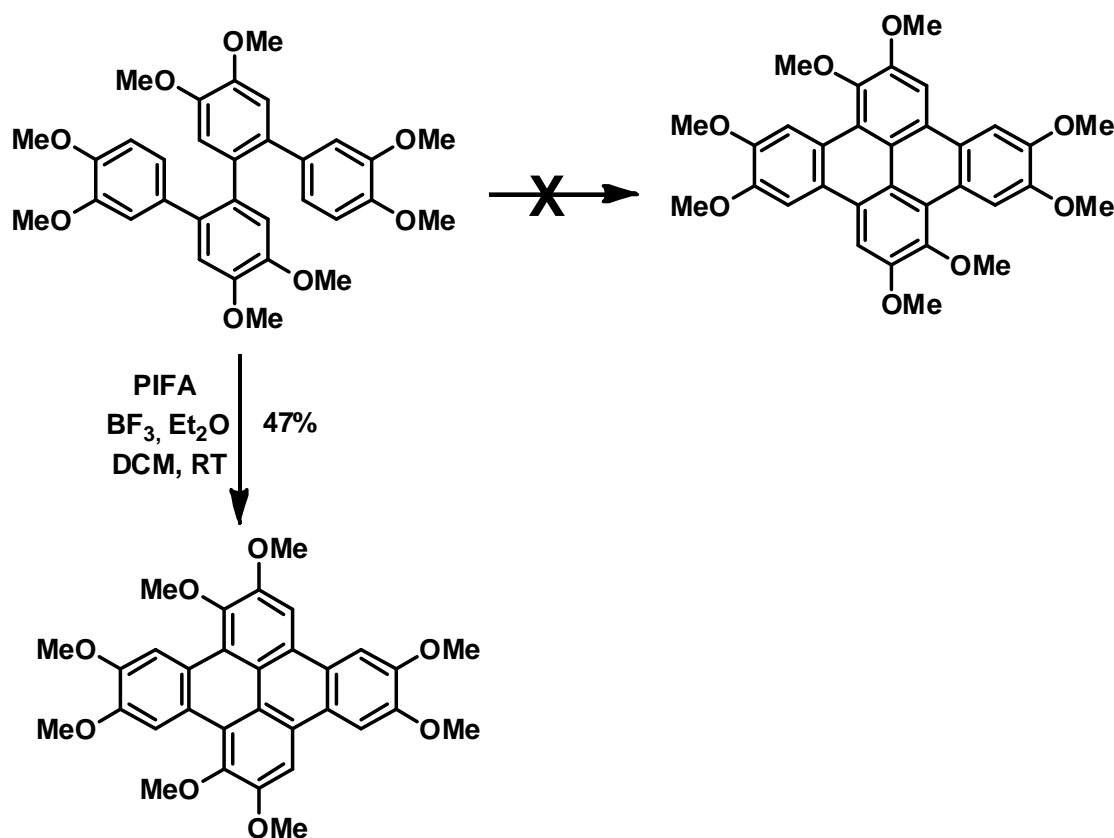


Figure 36. Example of rearrangement during Scholl reaction.

2.2. Initial Projects.

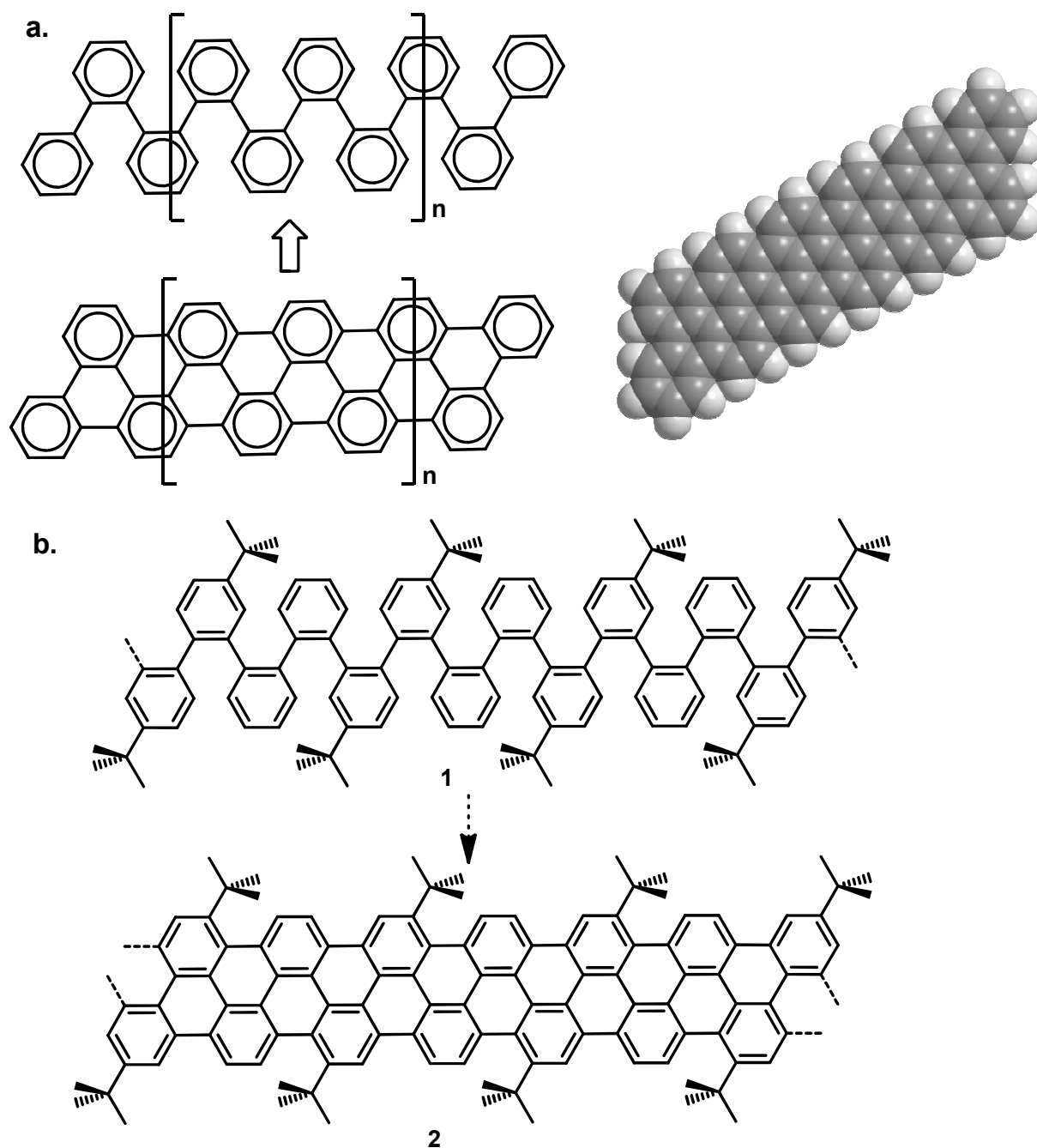


Figure 37. Project of synthesis of thin GNRs by Scholl reaction.

(a) Principle from ortho-phenylene chains. (b) Initial project.

The initial project of my PhD at the Centre de Recherche Paul Pascal was to develop the organic synthesis of thin, flat and well defined graphene nanoribbons. For this purpose, we first focused on poly-ortho-phenylene chains as flexible precursors, which had then to be rigidified, or graphitized, by intramolecular Scholl reaction (**Figure 37a**). In order to keep

these molecules soluble, it was obvious that solubilizing groups would be necessary and we decided to introduce tert-butyl groups on several edge positions (**Figure 37b**). The interest of tert-butyl compared to other alkyl chains is that some de-tert-butylation reactions exist and would finally allow us to obtain fully aromatic nanoribbons.

2.2a. Synthetic strategy.

As *ortho*-phenylene oligomers are the flexible precursors of the final Scholl reaction, we first envisioned the following retro synthesis (**Figure 38**). The *ortho*-phenylene oligomers **1** should be obtained by multiple coupling reactions from two different disubstituted biphenyl compounds, one also bearing solubilizing tert-butyl groups. These two biphenyl molecules should be prepared by bromination, and boronation for one of them, of the corresponding unsubstituted biphenyl compounds (**Figure 38**).

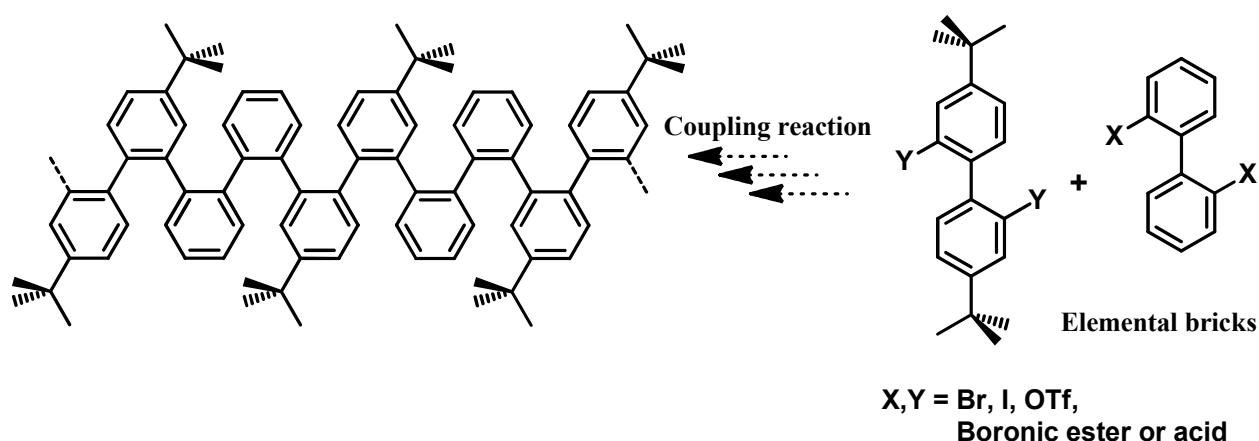


Figure 38. Retrosynthesis of poly-*ortho*-phenylene precursors.

Before synthesizing large and complicated *ortho*-phenylene oligomers, we needed a clear idea of how to carry on the Scholl-reaction on smaller units of these *ortho*-phenylene oligomers. Therefore, our first objective was the synthesis of smaller flexible test molecules, followed by a close study of their Scholl reaction.

2.2b. Tests reactions.

First, 4,4'-di-tert-butylbiphenyl **3** was brominated by a very simple but new procedure, in the presence of bromine in chloroform at 70°C without any catalyst, to give 2-bromo-4,4'-di-tert-butylbiphenyl **4** in good yield. The bromo substituent is then replaced by a boronic acid function, following a classical procedure involving an organolithium intermediate, and giving compound **5a**. This latter reacts with 2-bromo-4,4'-di-tert-butylbiphenyl **4**, in classical conditions for Suzuki cross-coupling reactions with Pd(PPh₃)₄ as a catalyst, and gives the expected hydrocarbon **6** in excellent yield (95%) (**Figure 39**).

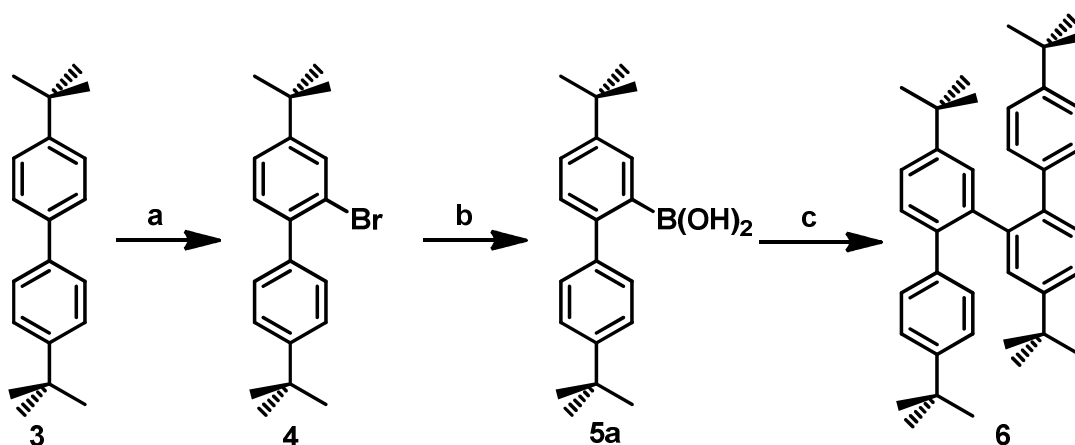


Figure 39. Synthesis of test compound **6**.

(a) Br₂, chloroform, 70°C, 16h, 69%. (b) BuLi, THF, -78°C, 15min, then B(OMe)₃, THF, -78°C to RT, 1h, 1(M) HCl, 75%, c) Pd(PPh₃)₄, Na₂CO₃, PhMe + H₂O + EtOH, 90°C, 48h, 95%.

Finally, precursor **6** was submitted to Scholl reaction conditions (**Figure 40**) by dissolution first in dry and degassed dichloromethane and then slow addition of a FeCl₃ solution in nitromethane, under strong bubbling of argon to remove HCl from the mixture. Then, the reaction is quenched with an alcohol (methanol or ethanol) and the crude products is analyzed by thin layer chromatography (TLC) to show several very close spots, none of them being frankly dominant. As a result it was very difficult to separate them by column chromatography. It appeared to us that during the short time of the Scholl reaction chlorination happens.

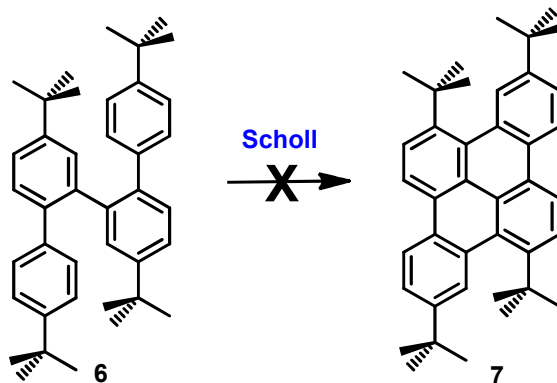


Figure 40. Scholl reaction of compound **6**.

Several attempts to obtain the graphitized compound **7** from the Scholl precursor **6** were done by applying different reaction conditions. Always in the presence of strong argon bubbling, we changed the temperature of the reaction mixture from room temperature (RT) to 0 °C. We also changed the reaction time from 30 minutes to 3 hours, but unfortunately a complex mixture was always obtained.

Our conclusion was that the presence of very close sterically hindering t-butyl groups on the small *ortho*-phenylene unit **6** may lower its reactivity in Scholl conditions. We then decided to try this reaction on another test molecule, a less hindered isomer of the former one.

This time, 4,4'-di-tert-butylbiphenyl **3** (**Figure 41**) was twice brominated in the presence of bromine and iron powder as a catalyst in CCl₄ at room temperature, to give 2, 2'-dibromo-4,4'-di-tert-butylbiphenyl **8** in good yield. Then 2,2'-dibromo-4,4'-di-tert-butylbiphenyl **8** reacts with 4-tert-butylphenylboronic acid **9**, in classical conditions for Suzuki cross-coupling reactions with Pd(PPh₃)₄ as a catalyst, and gives the hydrocarbon **10** in excellent yield (80%).

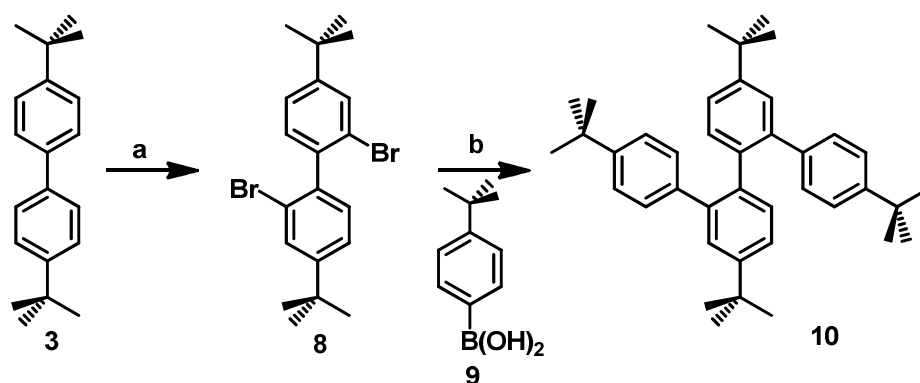


Figure 41. Synthesis of flexible compound 10.

(a) Fe, Br₂, chloroform, 70°C, 16h, 75%. (b) Pd(PPh₃)₄, Na₂CO₃, PhMe + H₂O + EtOH, 90°C, 48h, 80%.

Then the precursor 10 is exposed to various Scholl reaction conditions, by dissolution first in dry and degassed dichloromethane followed by slow addition of a FeCl₃ solution in nitromethane, under strong bubbling of argon. At room temperature, after quenching with an alcohol (methanol), the crude product is analyzed by TLC to show several very close spots corresponding to chlorinated compounds. Nevertheless, when the reaction was carried out at 0°C after 30 minutes one main spot appears on TLC.

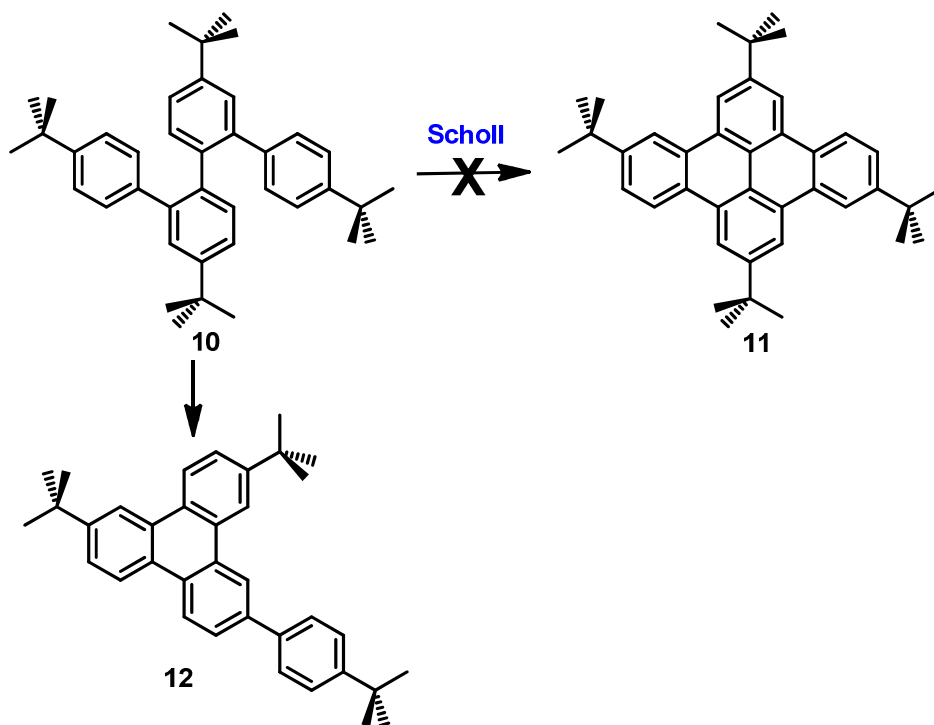


Figure 42. Scholl reaction of less hindered compound 10.

Unfortunately, after purification by column chromatography, the expected product was not formed but instead some unpredicted rearrangement was observed (**Figure 42**). This rearranged compound was the major product, obtained reproducibly in 75% yield, and has been easily identified by $^1\text{H-NMR}$ (**Figure 43**). Only one C-C bond was formed, instead of two, and one t-butyl group was removed, which was further confirmed by mass spectrometry.

On the $^1\text{H-NMR}$ spectrum (**Figure 43**) only three different signals of t-butyl group can be observed in the aliphatic region, which indicates that the molecule is asymmetrical and that one t-butyl group was removed in compound **12**. In addition, two large doublets indicate the presence of one unreacted 4-t-butyl phenyl group.

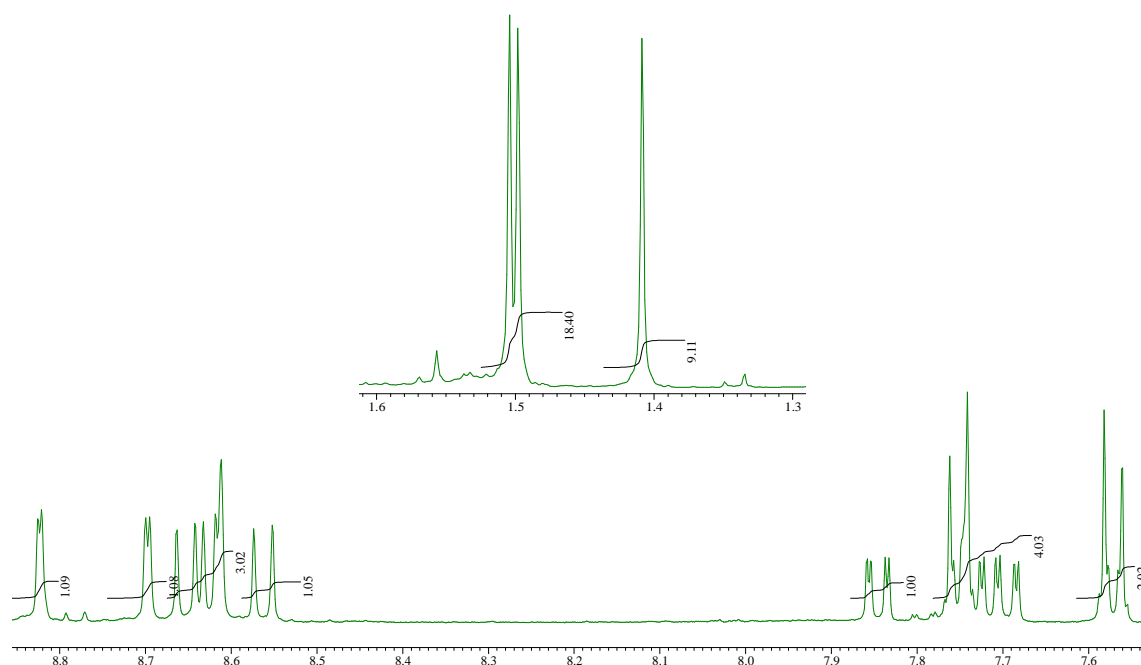


Figure 43. ^1H NMR spectrum of compound **12** displaying the aliphatic signals above (1.3 to 1.6 ppm) and the aromatic signals below (7.5 to 8.9 ppm).

Our conclusion was then that poly-*ortho*-phenylene chains may not be well suitable for the Scholl reaction conditions to give graphene nanoribbons. A new design of the flexible precursor seemed to be necessary.

2.3 Evolution of the project.

In order to make the flexible poly-phenylene precursor less sterically hindered, we designed a new motif having one spacing para-phenylene unit between the ortho-disubstituted biphenyl units (**Figure 44**). This time, the edge geometry of the corresponding nanoribbons has a zigzag geometry and incorporates cove regions, with solubilizing tert-butyl substituents on external positions.

2.3a Modified project.

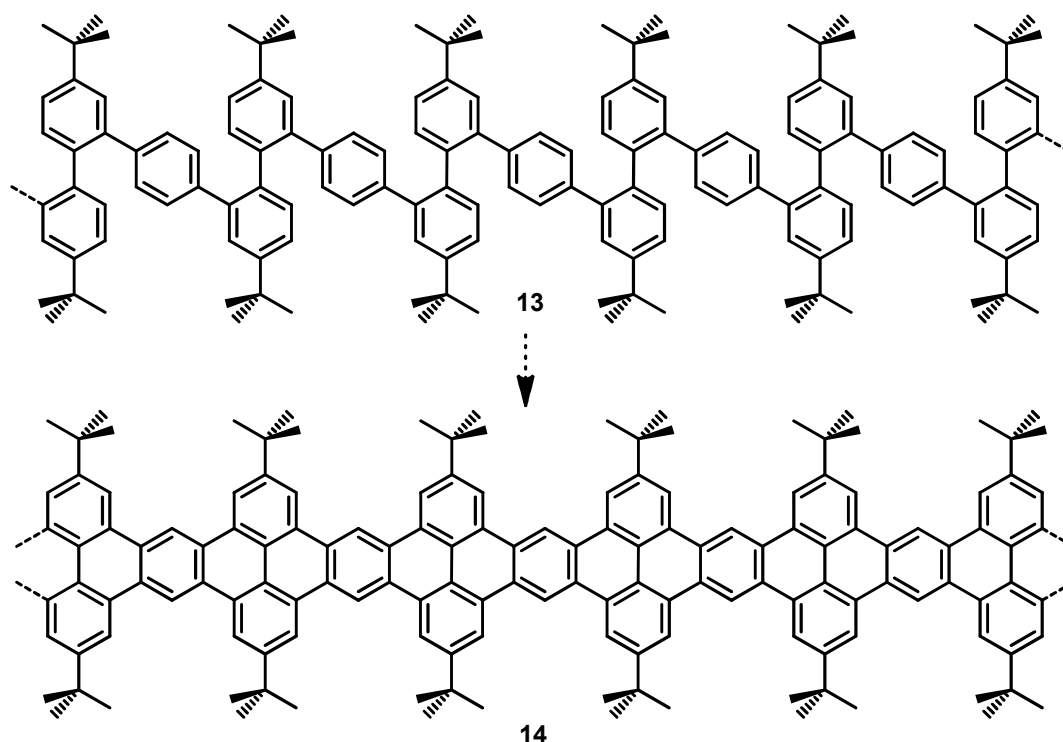


Figure 44. New design of a flexible precursor and its corresponding nanoribbons.

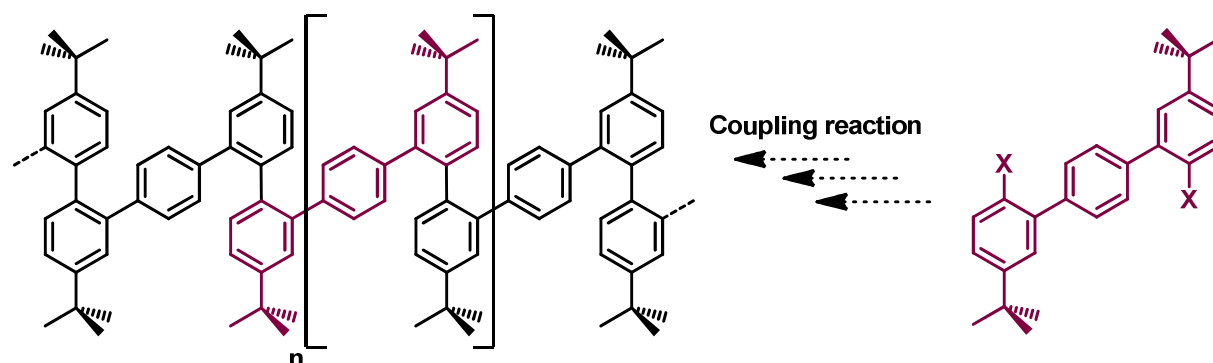


Figure 45. Retro-synthetic fragmentation of zigzag GNR precursor.

Another advantage of that strategy is that it involves only one type of substituted para-terphenyl unit (**Figure 45**). Again, the retro-synthesis consists in using coupling reactions of aryl compounds to form the desired disubstituted terphenyl monomer.

2.3b Test reactions.

Again, it was preferable to confirm this new strategy by a test reaction on the simplest motif of this new ribbon. In order to form this tetrabenzanthracene core by sterically forcing a transoid double cyclisation, we have synthesized the tetra-substituted zig-zag quinquephenyl **16**, where bulky *tert*-butyl groups generate a strong steric hindrance when the molecule is in cisoid conformation (**Figure 46**).

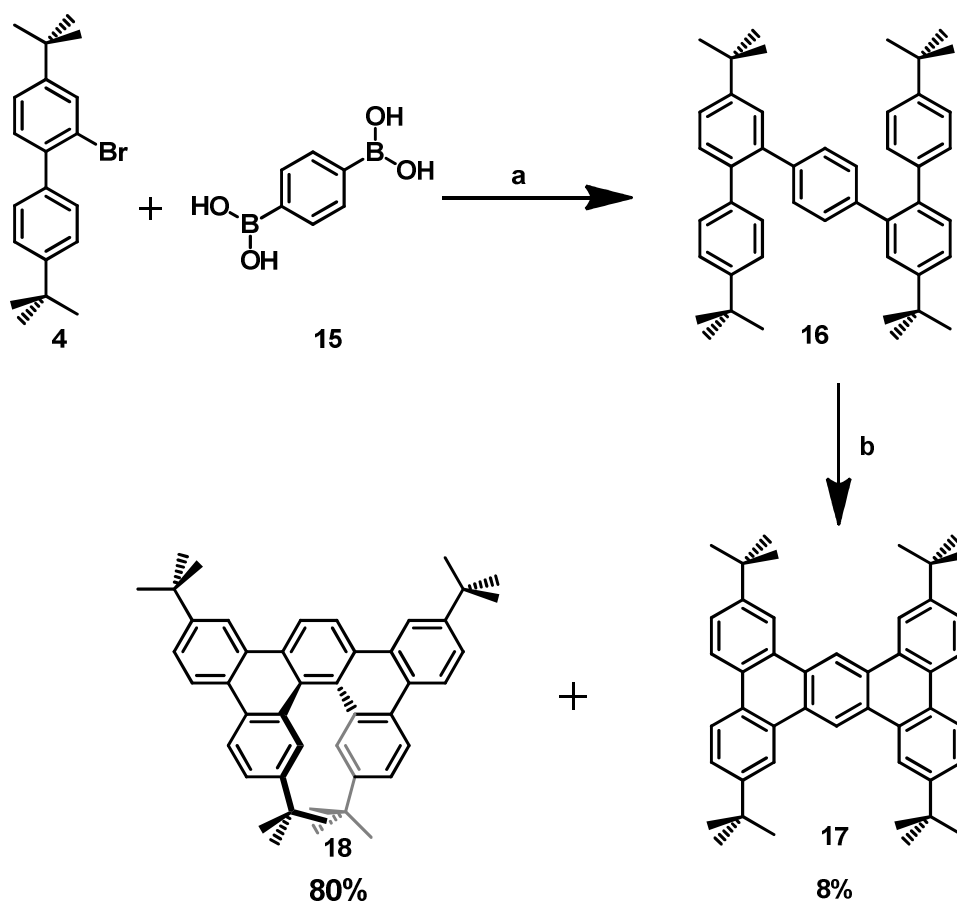


Figure 46. Synthesis of tetra-*tert*-butyl tetrabenzanthracene **17** and highly distorted tetra-*tert*-butyl dibenzo[5]helicene **18**: (a) $\text{Pd}(\text{PPh}_3)_4$, Na_2CO_3 , $\text{PhMe} + \text{H}_2\text{O} + \text{EtOH}$, 90°C , 48h, 80%. (b) FeCl_3 , $\text{MeNO}_2 + \text{CH}_2\text{Cl}_2$, Ar bubbling, room T, 1h, EtOH , 80% for **18**, 8% for **17**.

We were puzzled to find that this considerable steric hindrance seems to have only a weak, if at all, influence on the regioselectivity of this particular Scholl reaction since tetrabenzanthracene **17** is surprisingly formed with only 8% yield, whereas the sterically disfavored dibenzopicene (or dibenzo[5]helicene) **18** is obtained with 80% yield.

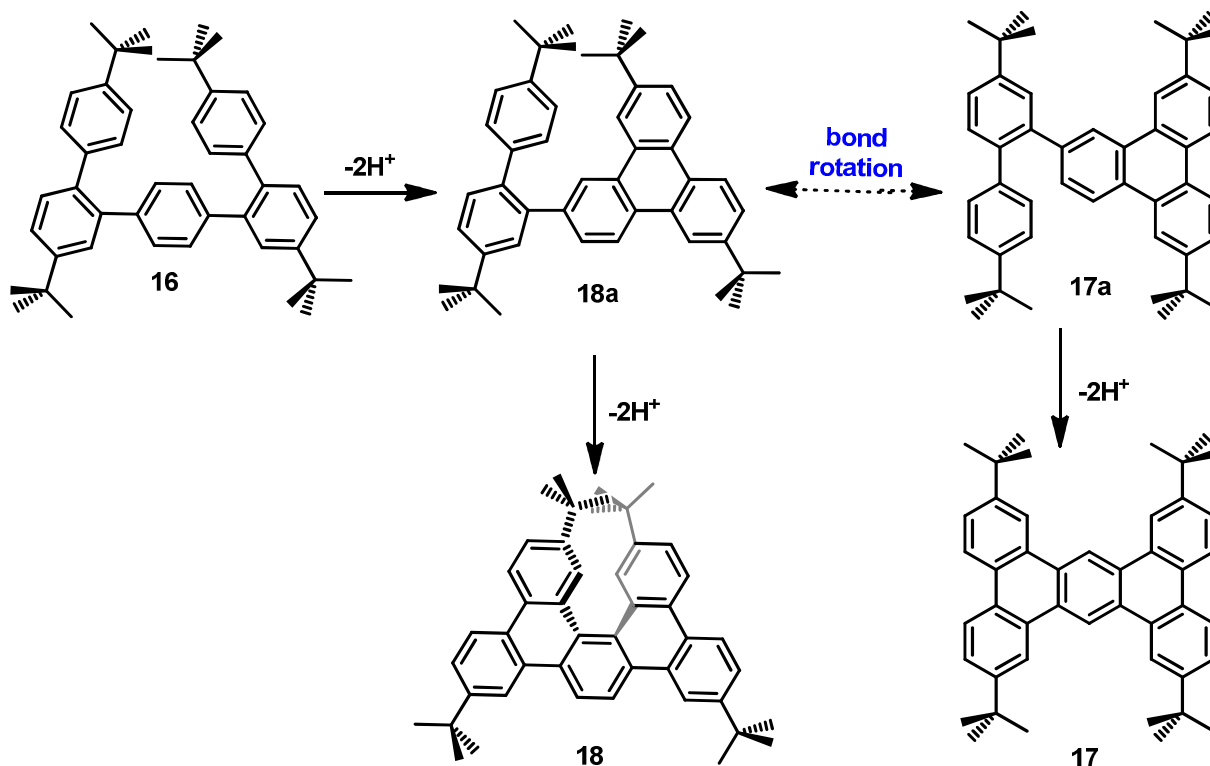


Figure 47. Proposed reaction pathway for the formation of **17** and **18** by a Scholl reaction.

The formation of the congested compound **18** (**Figure 47**) can be rationalized by a first ring closure leading to a partially closed intermediate, which has two opposite conformations **18a** and **17a**. Surprisingly, the most sterically hindered conformer **18a** is more likely than **17a** to undergo one more oxidative ring closure to form the [5]helicene **18** instead of its planar isomer **17**.

This result has been asserted without any ambiguity by 1H -NMR since **17** is more symmetrical than **18**, and because a significant shielding effect (shift of 0.4 ppm) can be

observed on the protons of the two *tert*-butyl groups at the helicene bay entrance of **18** and proves that these substituents are facing an aromatic ring (**Figure 48**).

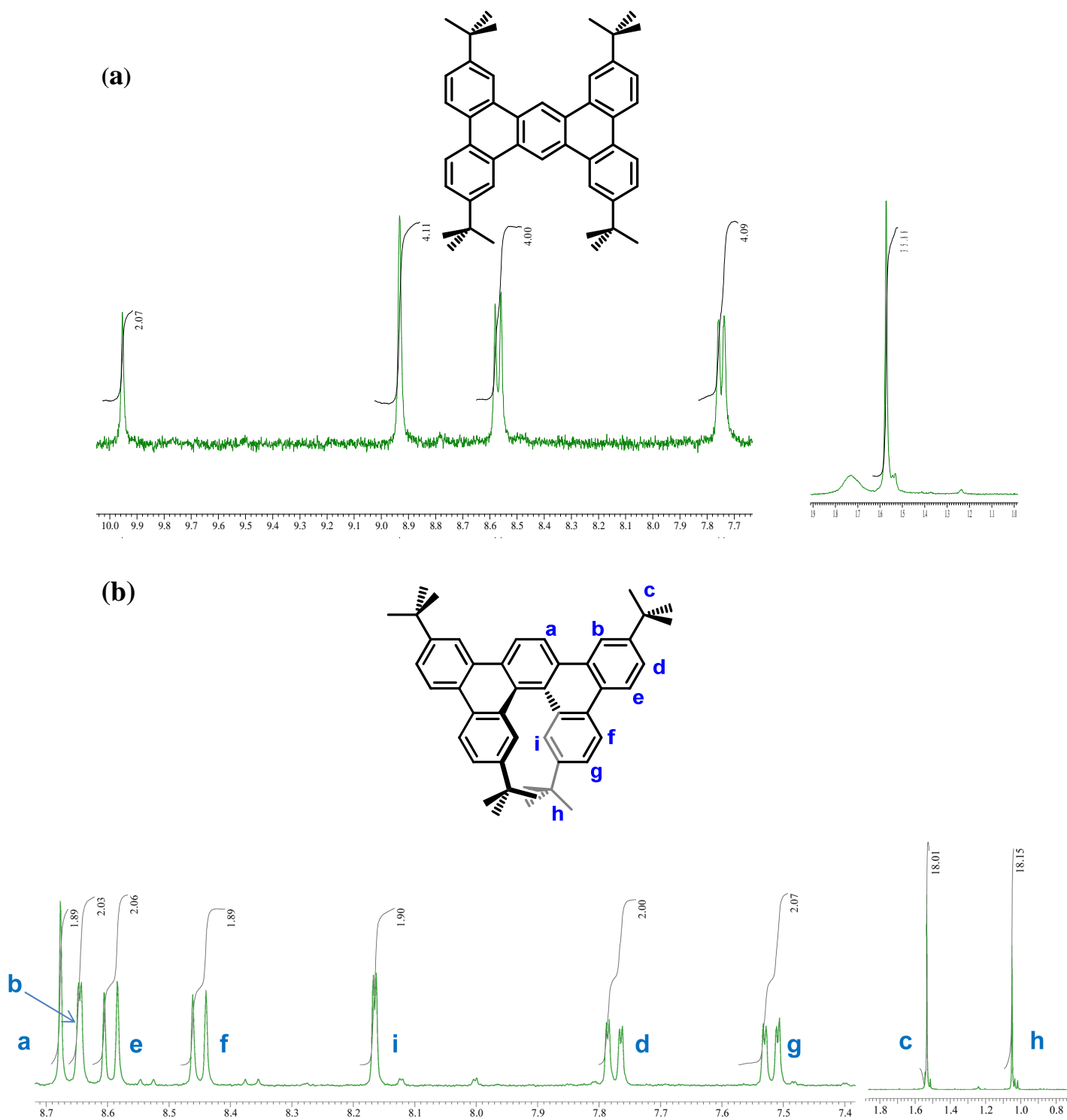


Figure 48. ^1H NMR spectra of (a) planar tetrabenzanthracene **17**, (b) helicenic dibenzopicene

18.

74

It appears that the reactivity and regioselectivity of intramolecular Scholl reactions remain only partially predictable. Shortly after we could observe this result, a similar selectivity has been reported by Müllen²⁶ (**Figure 49**). In that case, the structure of the penta-phenylene chain is identical but the substituents don't induce steric hindrance in any conformation. Very similarly, in spite of a slightly higher steric hindrance, the intramolecular Scholl condensation of compound "A" was reported to lead exclusively to the more condensed tribenzoperylene "C" instead of the equally benzenoid tetrabenzanthracene "B".

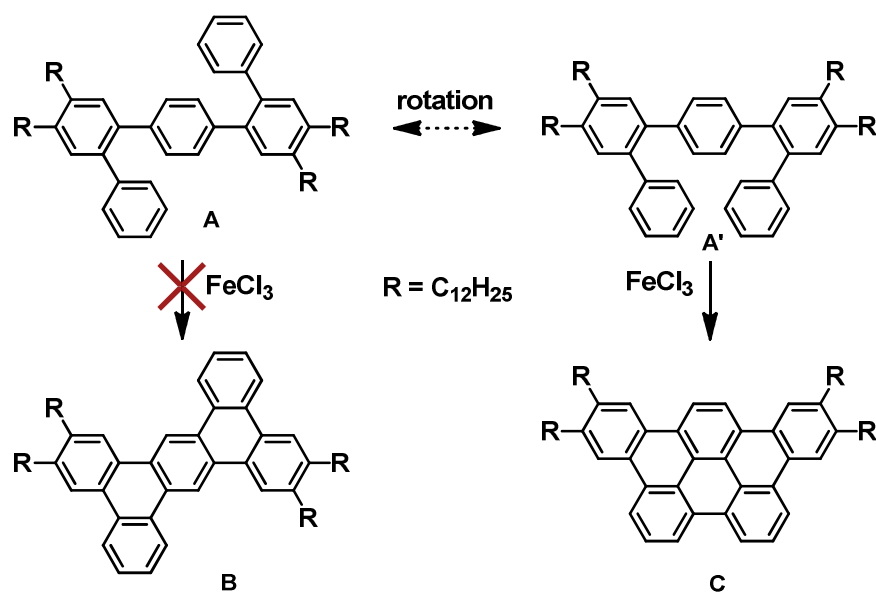


Figure 49. Regioselectivity of the Scholl reaction on *o,p,o*-quinquephenyl, reported by Müllen and coworkers.²⁶

According to the authors, this experimentally found regioselectivity remains unexplained.

2.3c Attempts of protections.

To avoid the formation of such unexpectedly favored products, we decided to protect two of the four cyclization positions on the central benzene ring. A first test was done with methyl groups using first dibromo-dimethylbenzene **19** to form the protected Scholl substrate **20** (**Figure 50**). Unfortunately, after the partial analysis of the Scholl reaction's main product **21** we could observe that methyl groups have indeed induced a transoid graphitization but benzylic protons are too reactive in these conditions and one of the methyl substituents has probably been chlorinated (**Figure 50**).

This result leads to an interesting conclusion that the alkyl groups on the central arene moiety are non-innocent substituents while the tert-butyl groups on the extremities of the molecule remain unchanged.

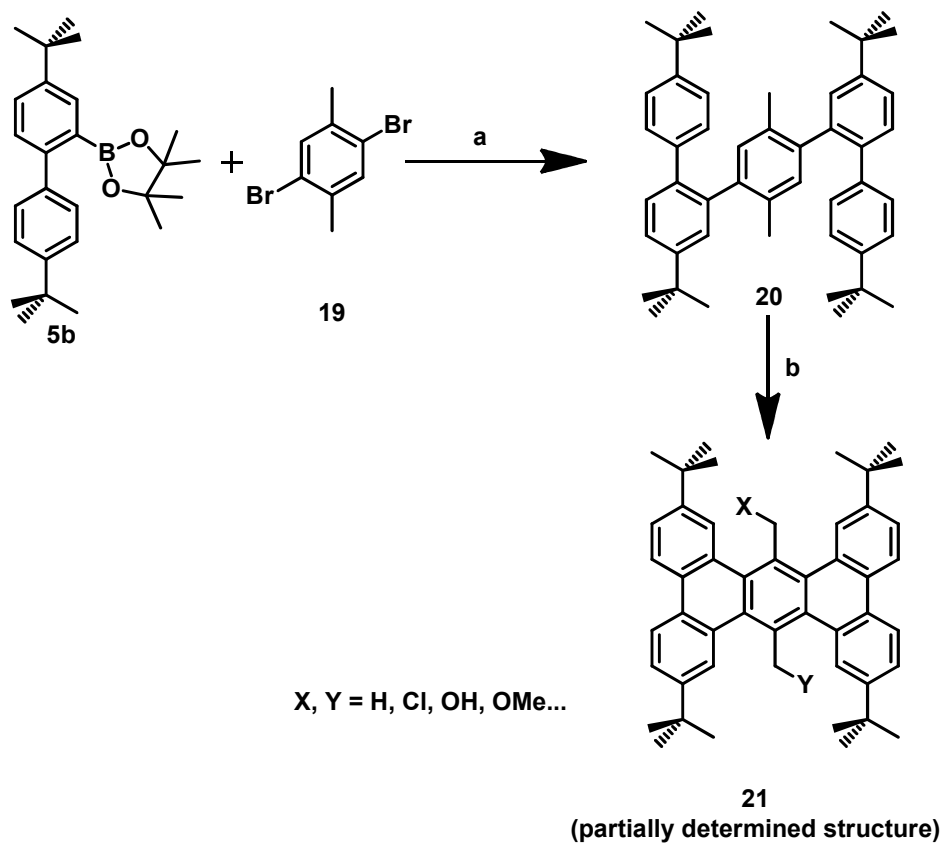


Figure 50. First attempt of protection for the Scholl reaction of *o,p,o*-quinquephenyl.

(a) $\text{Pd}(\text{PPh}_3)_4$, Na_2CO_3 , $\text{PhMe} + \text{H}_2\text{O} + \text{EtOH}$, 90°C , 48h, 84%. (b) FeCl_3 , $\text{MeNO}_2 + \text{CH}_2\text{Cl}_2$, Ar bubbling, RT, 1h, EtOH.

As a second attempt of protection, the exact same strategy was used with methoxy groups instead of methyl groups. Dibromo-dimethoxybenzene **22** was submitted to a double Suzuki cross-coupling reaction with two equivalents of boronic ester **5b** to give the protected quinquephenyl **23** (Figure 51). But disappointingly, after complete analysis of the only product of Scholl reaction **24** we observed that in spite of the protection, the regioselectivity has been maintained by removal of one of the pretended protecting groups and formation again of a [5]helicene-based compound.

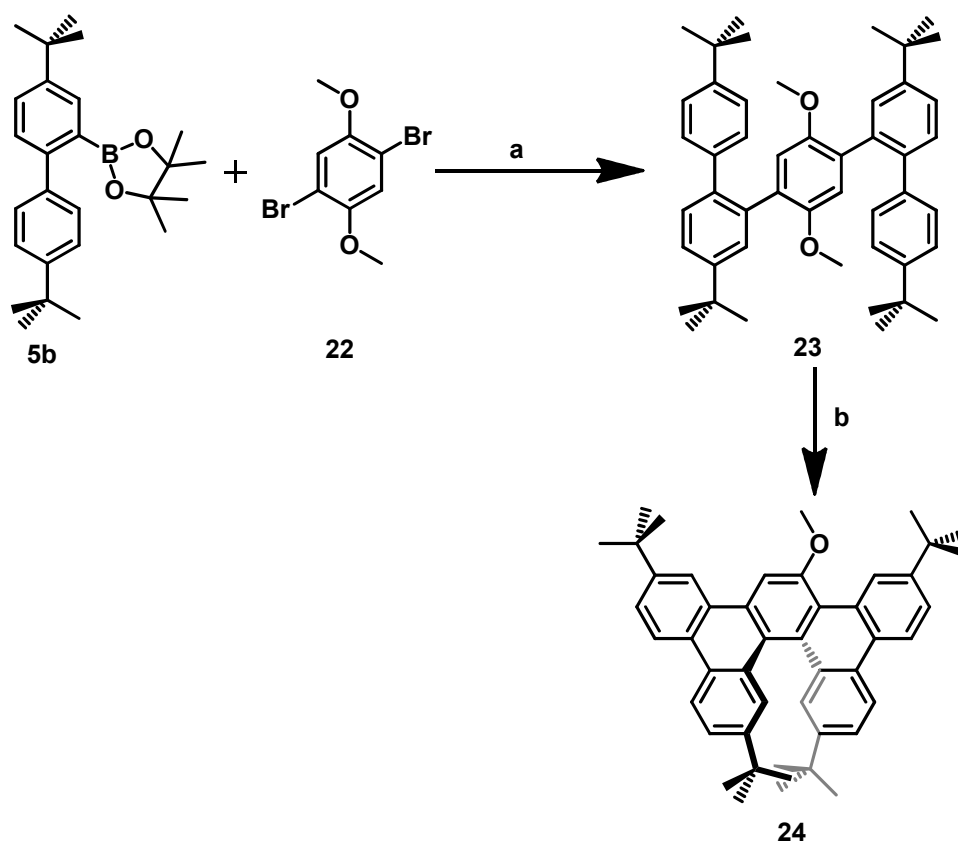


Figure 51. Second attempt of protection for the Scholl reaction of *o,p,o*-quinquephenyl.

(a) $\text{Pd}(\text{PPh}_3)_4$, Na_2CO_3 , $\text{PhMe} + \text{H}_2\text{O} + \text{EtOH}$, 90°C , 24h , 82%. (b) FeCl_3 , $\text{MeNO}_2 + \text{CH}_2\text{Cl}_2$, Ar bubbling, RT, 1h, EtOH, 89%.

The helicenic compound **24** has been analyzed without any ambiguity by $^1\text{H-NMR}$, NOESY and MS. Its $^1\text{H-NMR}$ spectrum is very similar (with some doubled signals) to the one of compound **18**, where the remaining methoxy group is replaced by a hydrogen (**Figure 52**).

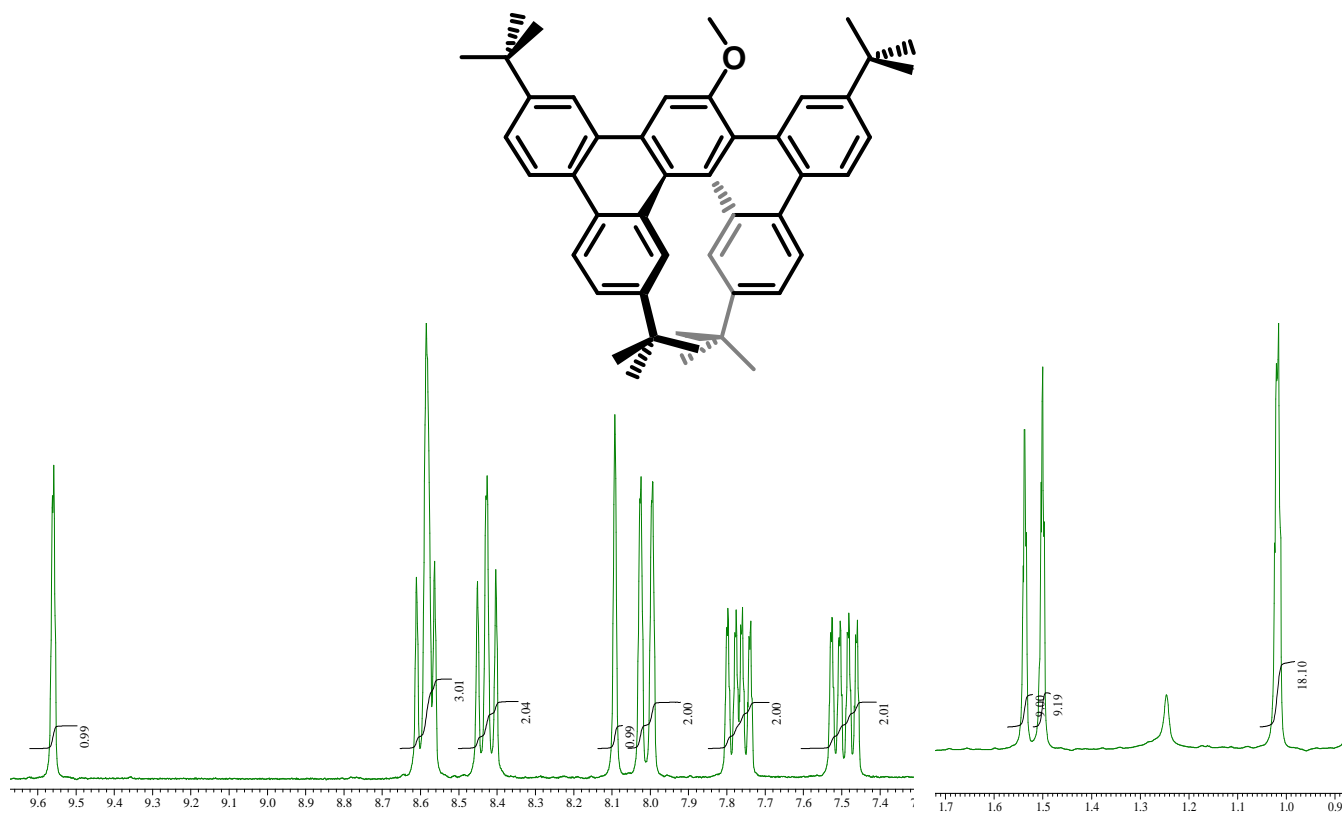


Figure 52. ^1H NMR spectrum of compound **24** displaying the aliphatic signals right (1.7 to 0.9 ppm) and the aromatic signals left (9.6 to 8.9 ppm).

Shortly after, similar investigations were carried out by Hilt and coworkers.²⁹ They tried to protect the quinquephenyl molecules already described by Müllen with methoxy groups and

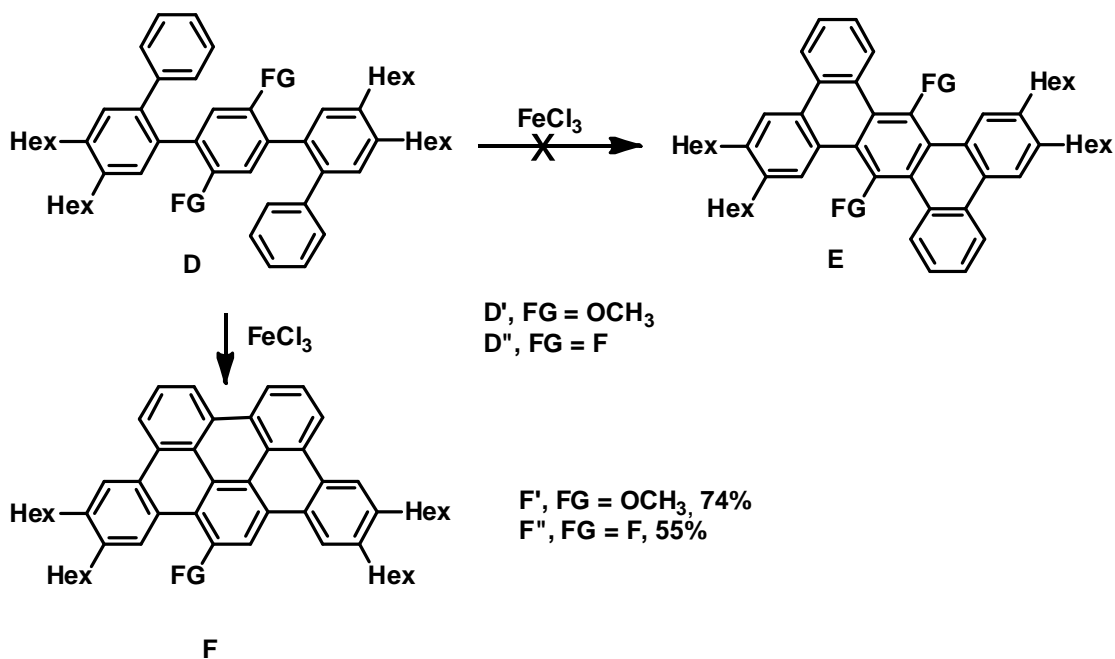


Figure 53. Investigation of the Scholl regioselectivity by Hilt and coworkers.

then could observe the same phenomenon, i.e. the perseverance of the regioselectivity with elimination of one protecting group (**Figure 53**). The same result was obtained when fluorine atoms were used instead of methoxy fragments. In addition, they showed that changing the Scholl oxidant has no marked effect on the final result, except on the yield. They finally conducted theoretical studies on this particular reactivity, assuming a radical cation mechanism and using quantum-chemical calculations at the DFT level to estimate the relative energies of the different transition states when one C-C bond is already made and for the two opposite pathways (**Figure 54**). It indicates that the barriers towards the experimentally observed product $D1_X$ (via radical cation $C1_X$) are indeed favored in the case of all substituents “X”.

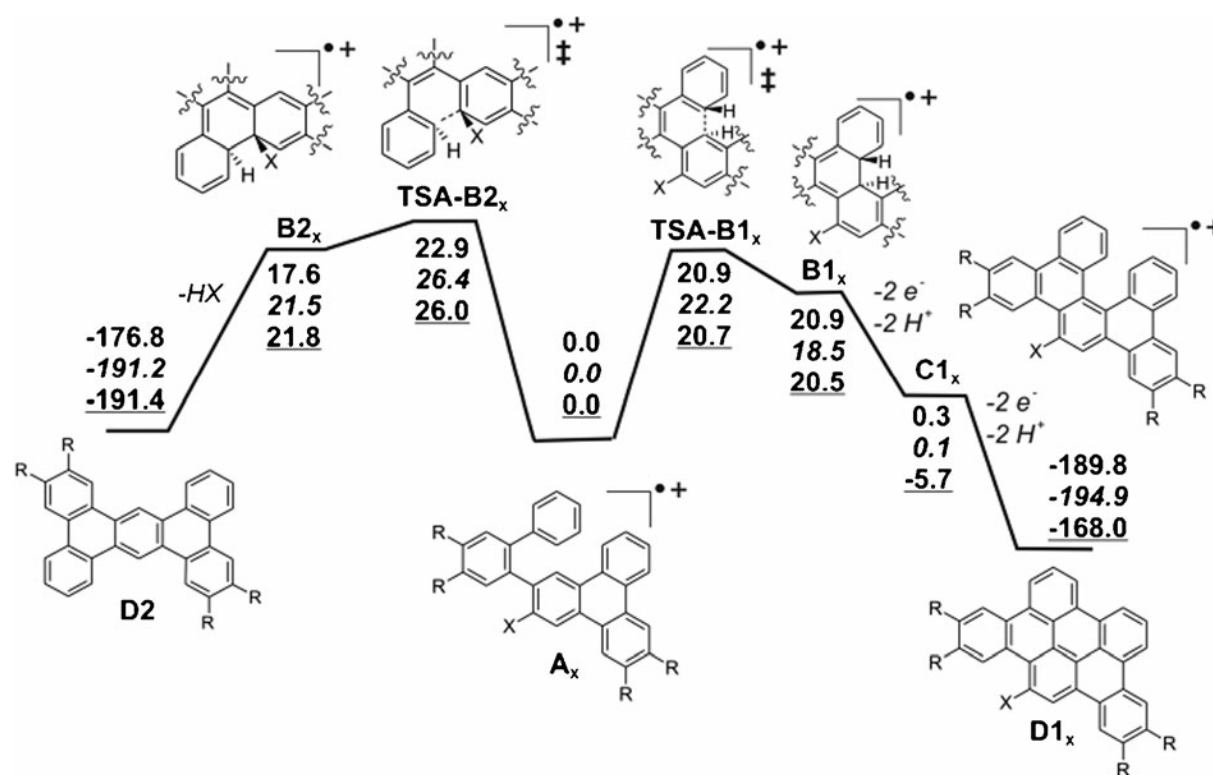


Figure 54. Free energies for the selectivity determining transition states relative to AX ($X=H, F, OMe$ (underlined values); $R = Me$).

2.3d Efficient synthesis of hexabenzotriphenylene (HBTP).

After observing this strong regioselectivity, and facing the evidence that we would not be able to avoid it, we decided to take advantage of it and to explore this new path of access to highly distorted polycyclic aromatic cores. We have first turned our attention to molecules incorporating several helicene parts and more particularly to hexabenzotriphenylene (HBTP)

25, which is the smallest molecule that includes three [5]helicene units. Due to its triple helicity, HBTP presents four diastereoisomers (**Figure 55**).^{30b} When the three helicene fragments have the same configuration, (+) or (-), the HBTP has a D_3 symmetry, and these two enantiomers are propeller-shaped molecules. When one helicene is different from the two others, the two HBTP enantiomers have a C_2 symmetry.

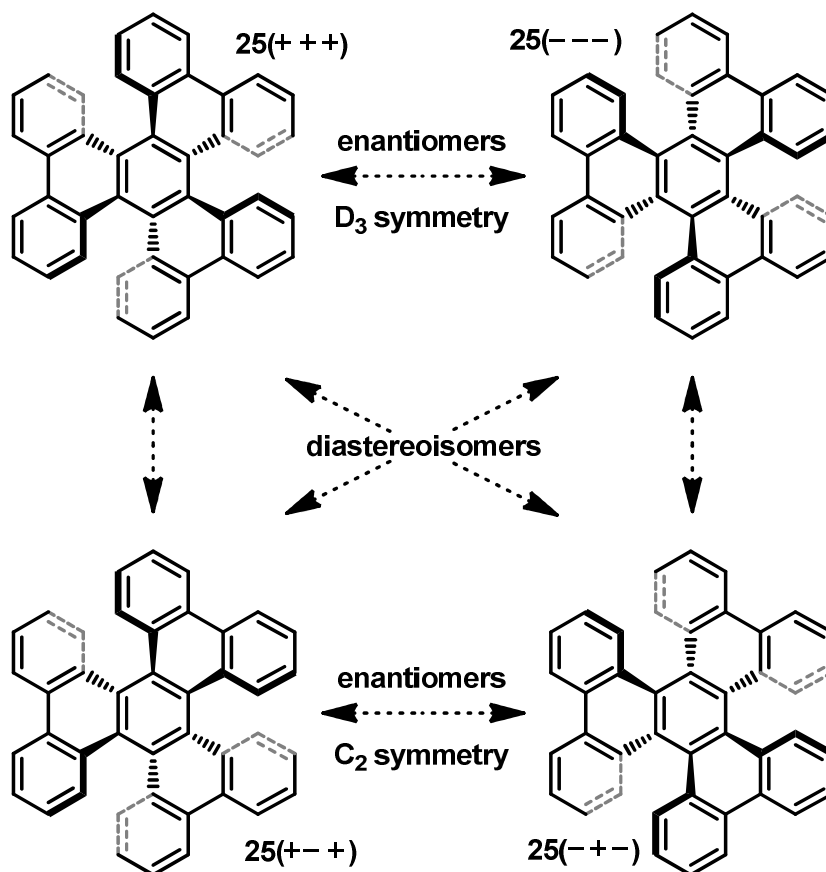


Figure 55. The four isomers of hexabenzotriphenylene (HBTP).

The synthesis of unsubstituted HBTP has already been described;³⁰ an efficient way follows a completely different strategy based on a Pd-catalyzed cyclotrimerization of a polycyclic aryne.^{30c} Substituted HBTPs have not yet been reported, and partial Scholl reactions on hexaphenylbenzene-based species have never led to HBTP.^{27, 31}

By taking advantage of the discovered non-sensitivity to steric hindrance of the Scholl reaction, hexa-*tert*-butyl-hexabenzotriphenylene (*t*Bu₆-HBTP) **28** (**Figure 56**) is quickly and easily obtained after a four-step synthesis from commercially available products. Then synthesis of 2-(4,4'-di-*tert*-butylbiphenyl-2-yl)-4,4,5,5-tetramethyl-1,3,2-dioxaborolane **5b** from commercially available starting material 4,4'-di-*tert*-butylbiphenyl **3** has already been described. Then 2-(4,4'-di-*tert*-butylbiphenyl-2-yl)-4,4,5,5-tetramethyl-1,3,2-dioxaborolane **5b** reacts three times on 1,3,5-tribromobenzene **26**, in classical conditions for Suzuki cross-coupling reactions with Pd(PPh₃)₄ as catalyst, and gives the hydrocarbon compound **27** in very good yield (76%), despite the triple reaction.

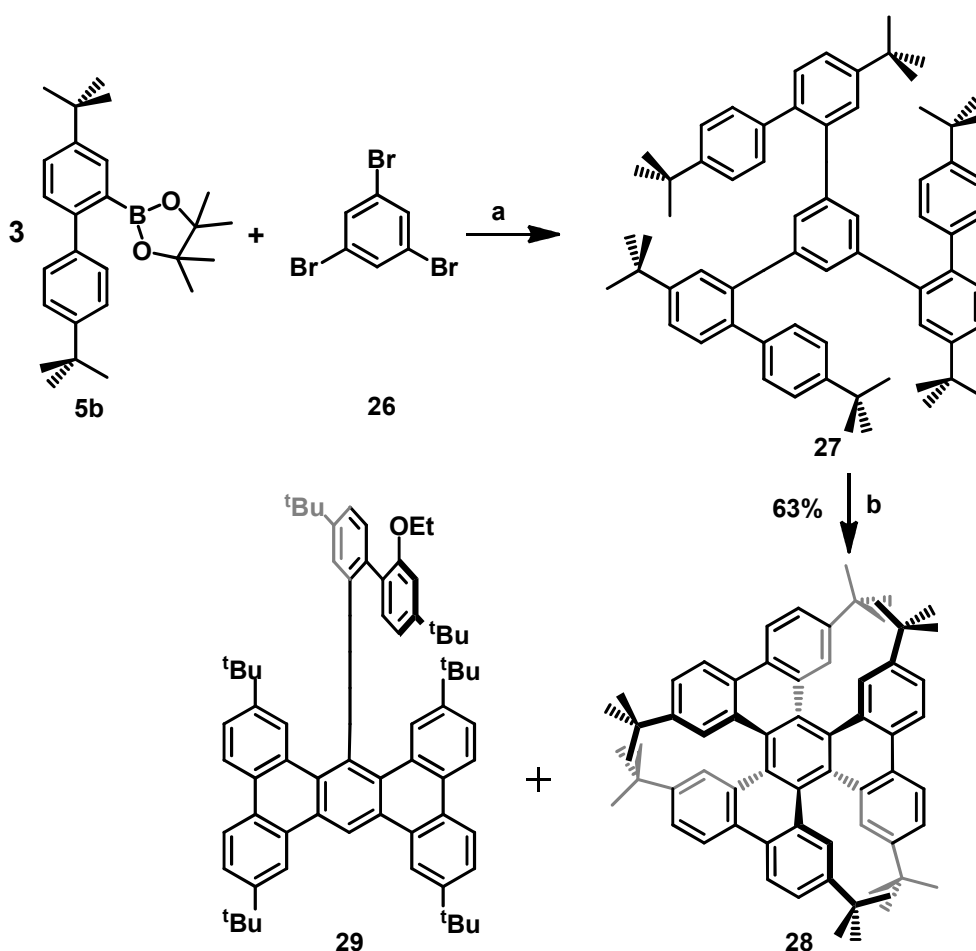


Figure 56. Synthesis of highly distorted hexa-*tert*-butyl-hexabenzotriphenylene **28**.

(a) Pd(PPh₃)₄, Na₂CO₃, PhMe + H₂O + EtOH, 90°C, 48h, 76%. (b) FeCl₃, MeNO₂ + CH₂Cl₂, Ar bubbling, room T, 1h, EtOH, 63% for **28**, 25% for **29**.

Finally, precursor **27** is submitted to well-established Scholl reaction conditions, by dissolution first in dry and degassed dichloromethane and then slow addition of a FeCl₃ solution in nitromethane, under strong bubbling of argon to remove HCl from the mixture. After one hour, the reaction is quenched with an alcohol (methanol or ethanol) and the crude product is purified by chromatography on column. Two very closely migrating products were isolated and identified. The major product is a racemic mixture of pure three-bladed propeller-shaped *t*Bu₆-HBTP **28**, obtained in 63% yield.

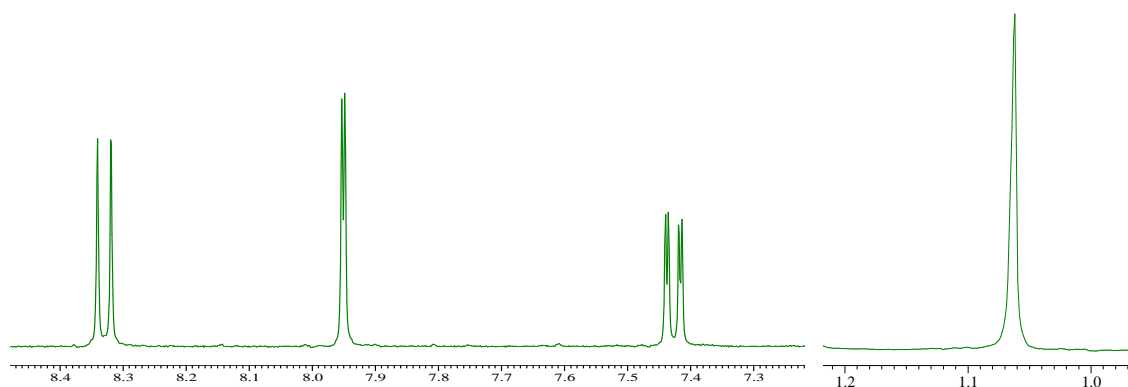


Figure 57. ¹H NMR spectrum of *t*Bu₆-HBTP **28**.

Its high D₃ symmetry makes it easy to identify from its ¹H-NMR spectrum of only 4 signals (**Figure 57**). C₂ symmetric isomers of **28** have not been observed. The global yield, over 4 steps, for the formation of **28** is 25%. The minor product **29**, obtained with a yield of 25% on the last step, is a tetrabenzanthracene resulting from a transoid second dehydrocyclisation, which has statistically 1 chance out of 3 to occur. This structure has been determined by 2D ¹H-NMR (COSY and NOESY) analysis. This side product is surprisingly substituted by an alkoxy group during the quenching of the reaction with an alcohol. The origin of this substituent has been confirmed by changing the nature of the quenching alcohol, which leads to a different alkoxy group on **29**.

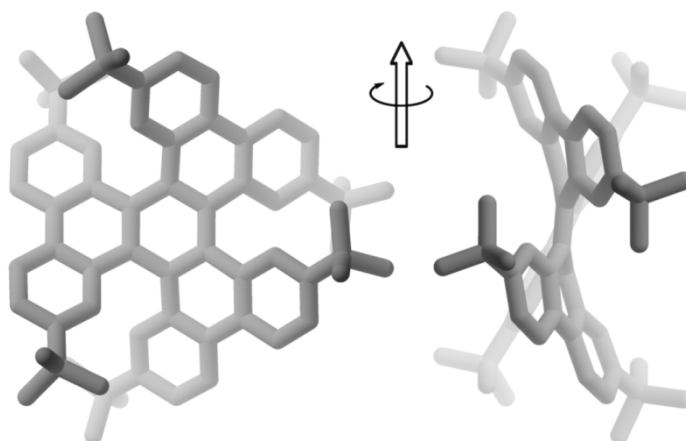


Figure 58. Crystal structure of *t*Bu₆-HBTP **28** : two different views of a single molecule.

In spite of its very good solubility in many solvents, single crystals of *t*Bu₆-HBTP **28** could be obtained as large yellow needles by slow diffusion of methanol into a dichloromethane solution. Analysis by X-ray diffraction of these crystals has been possible and evidenced the distortion of the *t*Bu₆-HBTP molecules **28** in the solid state (**Figure 58**).

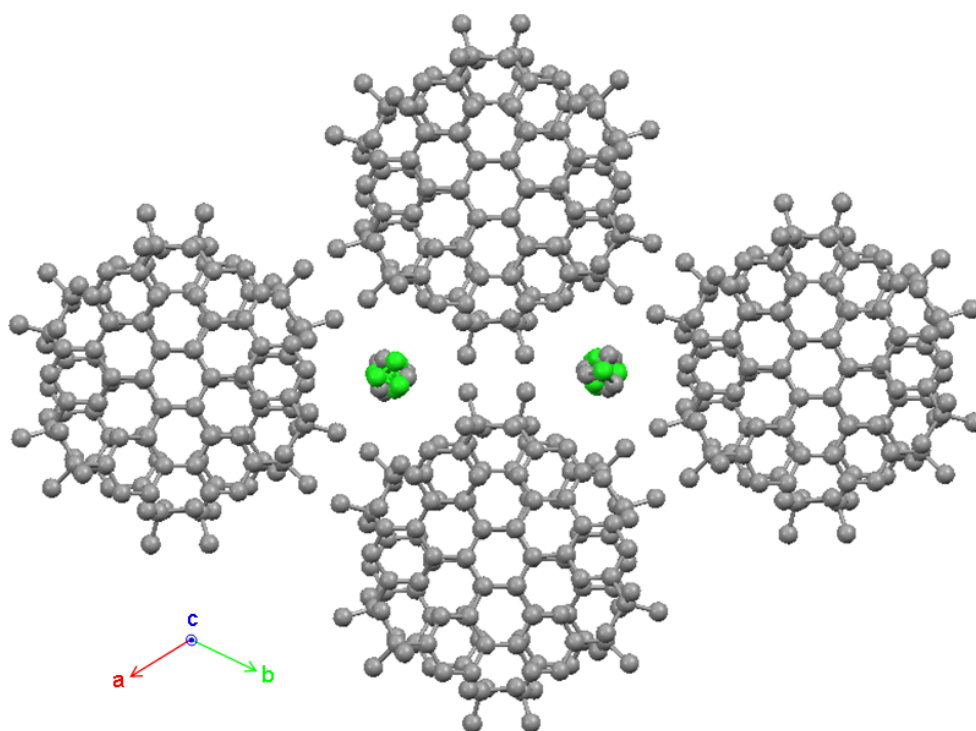


Figure 59. Portion of the crystal structure of **28-3CH₂Cl₂** illustrating the packing arrangement along the (a,b) plan. Carbon and chlorine atoms are represented by grey and green spheres respectively. Hydrogen atoms are omitted for clarity.

In single crystals of **28** + 3 CH₂Cl₂ the compound crystallizes in the centrosymmetric P-3c1 space group and is composed of a racemic mixture of the two enantiomers. The structure of the molecule is similar to the one reported for HBTP, with additional *tert*-butyl groups. The centre of the molecule is on a three-fold crystallographic axis. Each mean plane formed by the blade is tilted by an angle of 47° with respect to each other. Surprisingly, in spite of the bulky *tert*-butyl groups, this tilt angle is very similar to the one found in unsubstituted HBTP (49°-50°).^{15a} The bond distances are consistent with six peripheral aromatic rings (C-C distances between 1.368(4) and 1.414(4) Å and dihedral angles C-C-C-C less than 1.6°) connected to a distorted central benzene ring (C-C distances of 1.403(5) and 1.439(5) Å and dihedral angles up to 19.2°) by quite long C-C bonds consistent with single bonds (1.471(3) Å). The three resulting 6-membered rings are twisted with C-C-C-C dihedral angles of up to 31.3°.

2.4 References:

1. A. K. Geim, K. S. Novoselov, *Nature Materials* **2007**, *6*, 183.
2. K. S. Novoselov, A. K. Geim, S. V. Morozov, D. Jiang, Y. Zhang, S. V. Dubonos, I. V. Grigorieva, A. A. Firsov, *Science* **2004**, *306*, 666.
3. Y. Zhang, Y. W. Tan, H. L. Stormer, P. Kim, *Nature* **2005**, *438*, 201.
4. C. Berger, Z. Song, X. Li, X. Wu, N. Brown, C. Naud, D. Mayou, T. Li, J. Hass, A. N. Marchenkov, E. H. Conrad, P. N. First, W. A. Hee, *Science* **2006**, *312*, 1191.
5. Y. W. Son, M. L. Cohen, S. G. Louie, *Phys. Rev. Lett.* **2006**, *97*, 216803.
6. V. Barone, O. Hod, G. E. Scuseria, *Nano Lett.* **2006**, *6*, 2748.
7. D. A. Areshkin, D. Gunlycke, C. T. White, *Nano Lett.* **2007**, *7*, 204.
8. K. Nakada, M. Fujita, *Phys. Rev. B* **1996**, *54*, 17954.
9. M. Y. Han, B. O. Zylmaz, Y. Zhang, P. Kim, *Phys. Rev. Lett.* **2007**, *98*, 2068.
10. (a) R. Scholl, J. Mansfeld, *Ber. Dtsch. Chem. Ges.* **1910**, *43*, 1734. (b) P. Kovacic, M. B. Jones, *Chem. Rev.* **1987**, *87*, 357.
11. (a) A. J. Berresheim, M. Muller, K. Mullen, *Chem. Rev.* **1999**, *99*, 1747. (b) M. D. Watson, A. Fechtenkotter, K. Mullen, *Chem. Rev.* **2001**, *101*, 1267.
12. (a) L. Zhai, R. Shukla, R. Rathore, *Org. Lett.* **2009**, *15*, 3474. (b) T. Herwig, V. Enkelmann, O. Schmelz, K. Müllen, *Chem. Eur. J.* **2000**, *6*, 1834.
13. F. A. Vingiello, J. Yanez, J. A. Campbell, *J. Org. Chem.* **1971**, *36*, 2053.

14. (a) B. T. King, J. Kroulík, C. R. Robertson, P. Rempala, C. L. Hilton, J. D. Korinek, L. M. Gortari, *J. Org. Chem.* **2007**, *72*, 2279. (b) J. L. Ormsby, T. D. Black, C. L. Hilton, Bharat, B. T. King, *Tetrahedron* **2008**, *64*, 11370.
15. R. Rathore, A. S. Kumar, S. V. Lindeman, J. K. Kochi, *J. Org. Chem.* **1998**, *63*, 5847.
16. (a) J. S. Yang, T. M. Swager, *J. Am. Chem. Soc.* **1998**, *120*, 5321. (b) S. Yamaguchi, T. M. Swager, *J. Am. Chem. Soc.* **2001**, *123*, 12087. (c) A. Rose, J. D. Tovar, S. Yamaguchi, E. E. Nesterov, Z. Zhu, T. M. Swager, *Philos. Trans. R. Soc. London, Ser. A* **2007**, *365*, 1589.
17. (a) B. Kramer, R. Frohlich, S. R. Waldvogel, *Eur. J. Org. Chem.* **2003**, *354*, 3549. (b) S. R. Waldvogel, E. Aits, C. Holst, R. Frohlich, *Chem. Commun.* **2002**, 1278. (c) P. Kovacic, R. M. Lange, *J. Org. Chem.* **1963**, *28*, 968.
18. (a) A. Ronlan, O. Hammerich, V. D. Parker, *J. Am. Chem. Soc.* **1973**, *95*, 7132. (b) A. Ronlan, V. D. Parker, *J. Org. Chem.* **1974**, *39*, 1014. (c) R. Rathore, J. K. Kochi, *J. Org. Chem.* **1995**, *60*, 7479.
19. O. Hammerich, V. D. Parker, *Adv. Phys. Org. Chem.* **1984**, *20*, 55.
20. P. Rempala, J. Kroulik, B.T. King, *J. Am. Chem. Soc.* **2004**, *126*, 15002.
21. (a) P. Rempala, J. Kroulik, B. T. King, *J. Org. Chem.* **2006**, *71*, 5067. (b) B. T. King, J. Kroulik, C. R. Robertson, P. Rempala, C. L. Hilton, J. D. Korinek, L. M. Gortari, *J. Org. Chem.* **2007**, *72*, 2279. (c) X. Dou, X. Y. Yang, G. J. Bodwell, M. Wagner, V. Enkelmann, K. Mullen, *Org. Lett.* **2007**, *9*, 2485.
22. (a) A. A. O. Sarhan, C. Bolm, *Chem. Soc. Rev.* **2009**, *38*, 2730. (b) N. Boden, R. J. Bushby, G. Headdock, O. R. Lozman, A. Wood, *Liq. Cryst.* **2001**, *28*, 139. (c) N. Boden, R. J. Bushby, A. N. Cammidge, S. Duckworth, G. J. Headdock, *Mater. Chem.* **1997**, *7*, 601. (d) V. Percec, J. H. Wang, S. J. Okita, *Polym. Sci., Polym. Chem.* **1991**, *29*, 1789.
23. (a) C. D. Simpson, G. Mattersteig, K. Martin, L. Gherghel, R. E. Bauer, H. J. Rader, K. Muellen, *J. Am. Chem. Soc.* **2004**, *126*, 3139. (b) C. Kubel, K. Eckhardt, V. Enkelmann, G. Wegner, K. Mullen, *J. Mater. Chem.* **2000**, *10*, 879.
24. A. McKillop, A. G. Turrell, D. W. Young, E. C. Taylor, *J. Am. Chem. Soc.* **1980**, *102*, 6504.
25. J. B. Aylward, *J. Chem. Soc. B* **1967**, 1268.
26. L. Dössel, L. Gherghel, X. Feng, K. Müllen, *Angew. Chem. Int. Ed.* **2011**, *50*, 2540.

27. X. Feng, J. Wu, V. Enkelmann, K. Müllen, *Org. Lett.* **2006**, *8*, 1145.
28. a) X. Dou, X. Yang, G. J. Bodwell, M. Wagner, V. Enkelmann, K. Müllen, *Org. Lett.* **2007**, *9*, 2485; b) J. L. Ormsby, T. D. Black, C. L. Hilton, Bharat, B. T. King, *Tetrahedron* **2008**, *64*, 11370.
29. M. Danz, R. Tonner, G. Hilt, *Chem. Commun.* **2012**, *48*, 377.
30. a) N. P. Hacker, F. W. Mcomie, J. Meunier-Piret, M. Van Meerssche, *J. Chem. Soc., Perkin Trans.* **1982**, *1*, 19; b) L. Barnett, D. M. Ho, K. K. Baldrige, R. A. Pascal Jr., *J. Am. Chem. Soc.* **1999**, *121*, 727; c) D. Peña, D. Pérez, E. Guitian, L. Castedo, *Org. Lett.* **1999**, *1*, 1555.
31. Y. Lu, J. S. Moore, *Tetrahedron. Lett.* **2009**, *50*, 4071.

Chapter III: Towards hexa-phenanthro-triphenylene (HPTP).

3.1. Introduction.

Hexabenzotriphenylene HBTP could be considered as the second generation dendrimer of the triphenylene series. In fact, it is virtually obtained by the fusion of two distinct benzo groups on each external benzene ring of the triphenylene molecule, which is itself the result of such a triple fusion from benzene (**Figure 60**). The next element of this series would be the TriPhenanthroTriphenylene, where each of the six outer benzene rings of the HBTP is fused with two distinct benzo groups. The resulting molecule, exceptionally crowded due to the presence of three [5]helicene and three [7]helicene units, has never been synthesized but its configuration has been predicted theoretically¹, at the PM3 (Parametric model number 3) level due to its great size (C₉₀H₄₈).

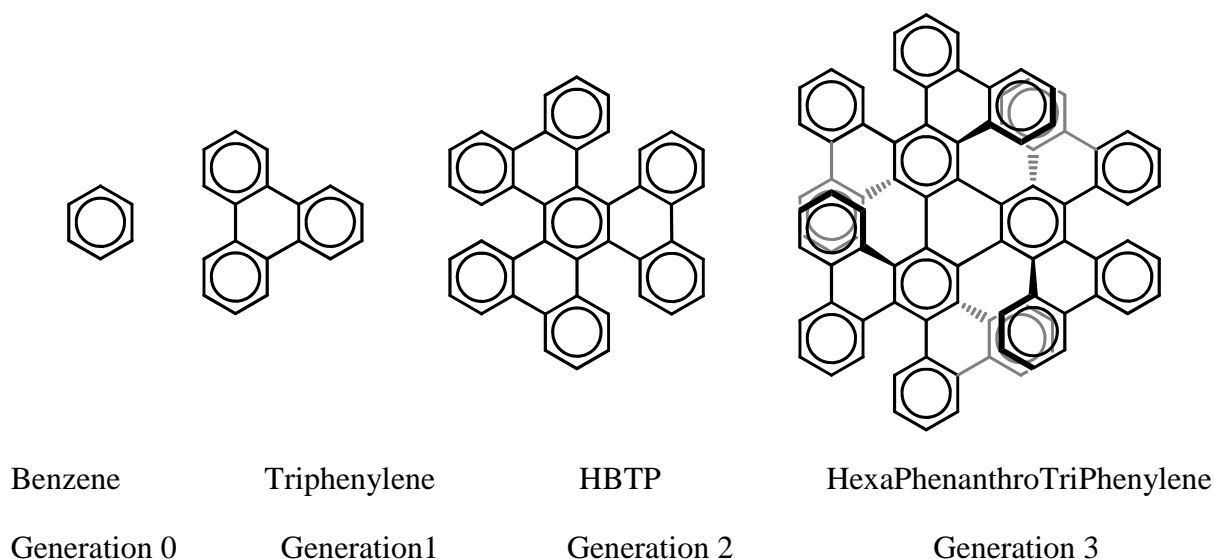


Figure 60. Generations in the triphenylene dendrimer series.

Given our newly acquired insights into the Scholl reaction and the facility of the synthetic technique we just developed for the formation of HBTP, we naturally decided to apply this technique to the synthesis of a tBu-substituted HPTP, which is a much more challenging molecule.

The first step of the retro-synthetic study is to determine the structure of the flexible precursor which will be submitted to intramolecular Scholl cyclizations to hopefully give the desired compound. In the case of the targeted HPTP **30**, which is substituted by several tert-butyl groups to avoid complete graphitization and to mimic the previous HBTP synthesis, we decided that on the flexible precursor **31** biphenyl units should be first linked to a central triphenylene unit on less hindering external positions (**Figure 61**). Then two possible pathways are reasonable for the formation of **31**. The most obvious one (in blue on **Figure 61**) consists in hexa-coupling reactions on a hexasubstituted triphenylene. The second one (in red on **Figure 61**) consists in forming the central triphenylene by a cyclotrimerization of three identical aryne-like compounds.

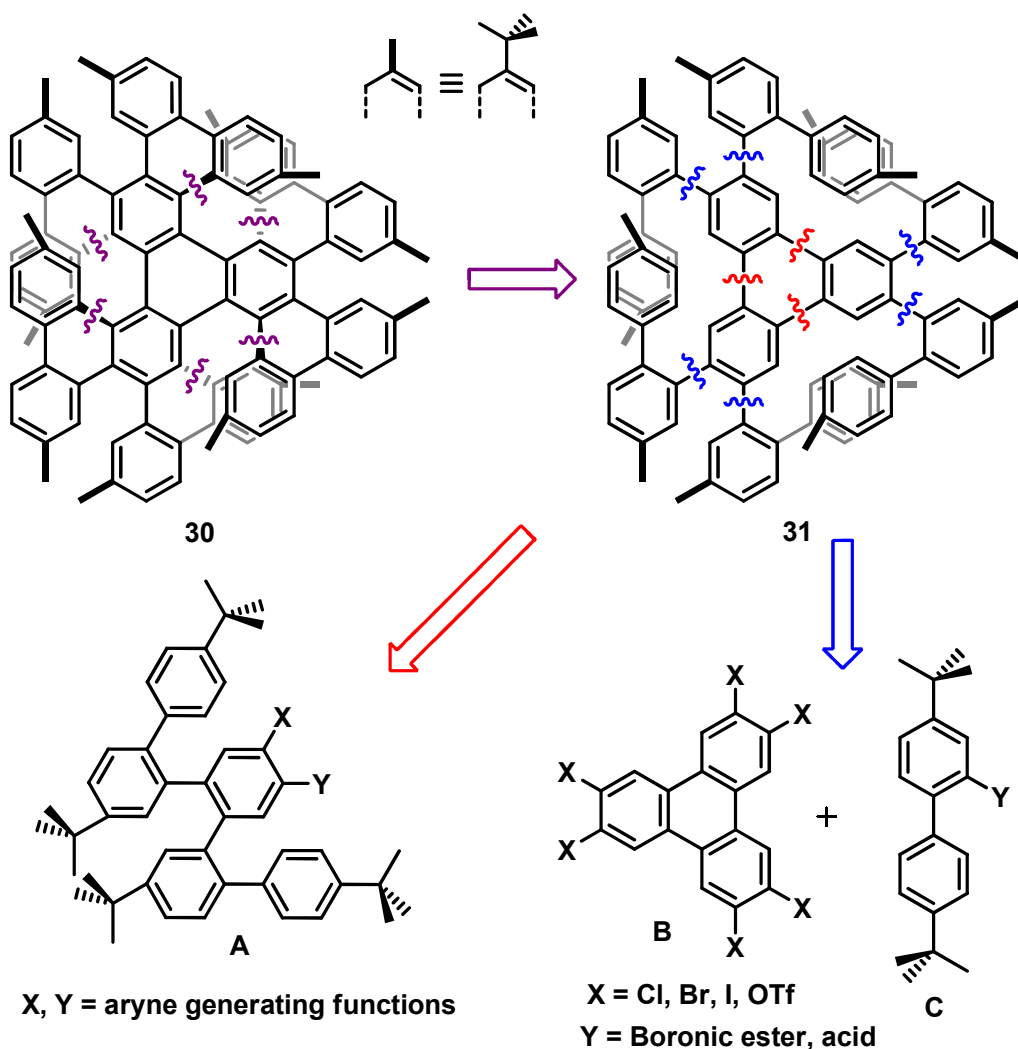


Figure 61. Retro-synthetic study for the synthesis of HPTP **30**.

3.2 Hexa-coupling strategy from hexabromotriphenylene.

Given the only few steps of synthesis and since we already knew how to form the boronic acid **5a**, we logically decided to first explore the strategy relying on the hexa-Suzuki coupling reaction on commercially available hexabromotriphenylene **32**. Unfortunately, in addition to the very poor solubility of the latter, several difficulties occurred, probably because of the strong steric hindrance felt by the last coupling reactions. In fact, several catalytic systems were used (**Table 1**) but each attempt gave a complicated and unpurifiable mixture containing partially reacted molecules and even dehalogenated compounds.

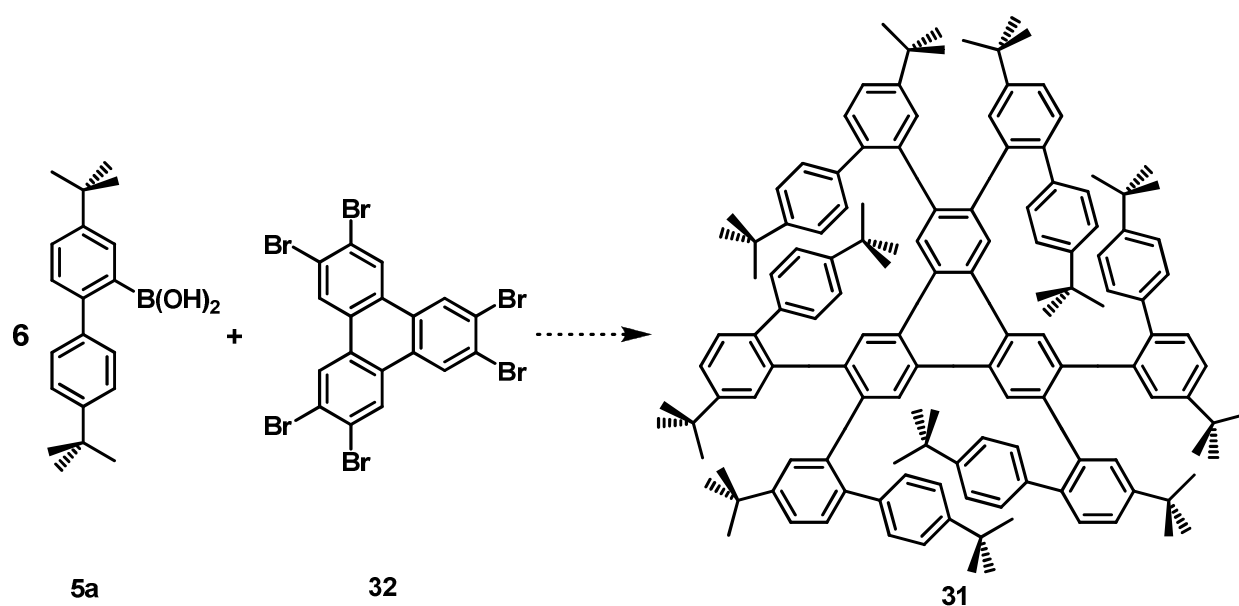


Figure 62. First attempts to form compound 31.

Table 1. Different reaction conditions tried for the synthesis of compound 31.

Attempt	Catalyst	Base	Sovents	Conditions
1	Pd(PPh ₃) ₄	Na ₂ CO ₃	PhMe/H ₂ O/EtOH	90°C, 96h
2	Pd(OAc) ₂ , SPhos	LiOH	THF/H ₂ O	70°C, 120h
3	Pd(PPh ₃) ₄	1(M) NaOH	THF	70°C, 96h
4	Pd ₂ (dba) ₃ , SPhos	K ₃ PO ₄	PhMe/H ₂ O	90°C, 96h

Considering all these problems, and especially because of the impossibility to isolate the expected compound **31** from a mixture containing other apolar hydrocarbons coming from unwanted dehalogenation reactions, we decided to give up this one-step strategy and focus on a longer but more controllable approach.

3.3 Stepwise strategy from hexahydroxytriphenylene.

Our first concern was to solve the problem of the bad solubility of the hexabromotriphenylene **32**. For that purpose, we decided to use solubilizing triflate groups instead of bromo substituents. Nevertheless, the synthesis of hexa(triflyl)triphenylene **35** is not described in the literature but according to our experience we were confident in being able to form it from commercially available hexahydroxytriphenylene **36**. In addition, boronic acid **5a** being too hindering to successfully react six times on the same molecule, we also decided to proceed stepwise and to use only substituted phenyl rings (**Figure 63**). Again, methoxy, hydroxyl and triflate groups are used as substituents, not to help the solubility, but to make the targeted molecules more polar and thus easier to purify by chromatography. This strategy still relies on a first sixfold Suzuki cross-coupling reaction, but with a less hindering methoxy-substituted phenylboronic acid. Then the six methoxy groups will have to be deprotected and changed into triflate substituents. Finally, a second six fold Suzuki cross-coupling reaction will have to be done to replace every triflate by a tert-butylphenyl fragment.

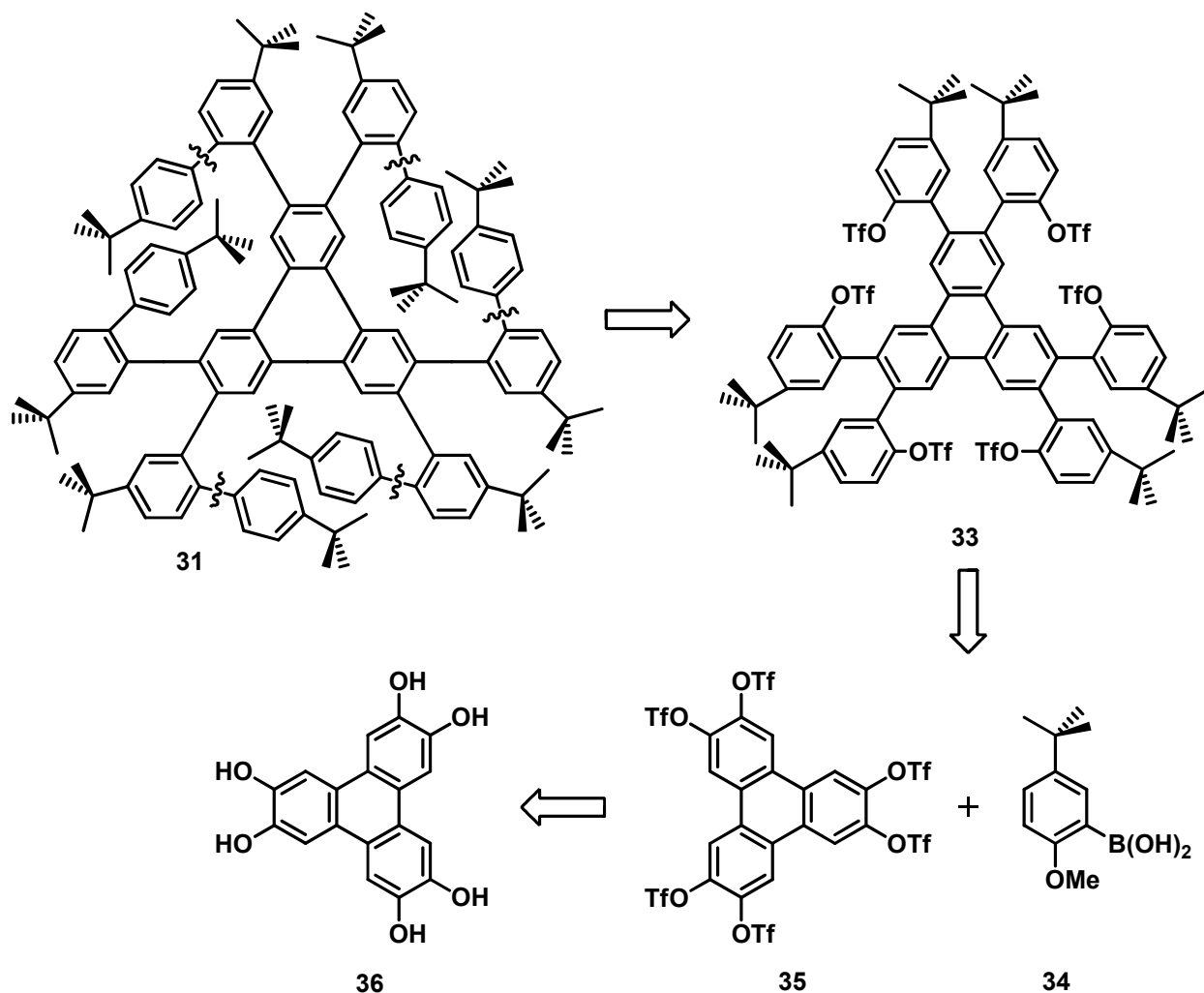


Figure 63. Retrosynthetic strategy for the stepwise formation of compound 31.

As expected, the commercially available starting material 2,3,6,7,10,11-hexahydroxytriphenylene **36** was successfully transformed into 2,3,6,7,10,11-hexa(triflyl)triphenylene **35** under usual triflation conditions in the presence of triflic anhydride in anhydrous pyridine (**Figure 64**), with an excellent yield (85%) given the six reactions. In parallel the methoxy-substituted boronic acid **34** was easily formed from the corresponding brominated compound under usual conditions (details in experimental section). Hexa(triflyl)triphenylene **35** is then submitted to the first six fold Suzuki cross-coupling reaction with 6 equivalents of boronic acid **34**. For this purpose, we used specific reaction conditions developed by Buchwald and coworkers² involving Pd(OAc)₂ and the very efficient SPhos (2-Dicyclohexylphosphino-2',6'-dimethoxybiphenyl) ligand as a catalytic system, in the presence of K₃PO₄ as a base in a mixture of THF and water.

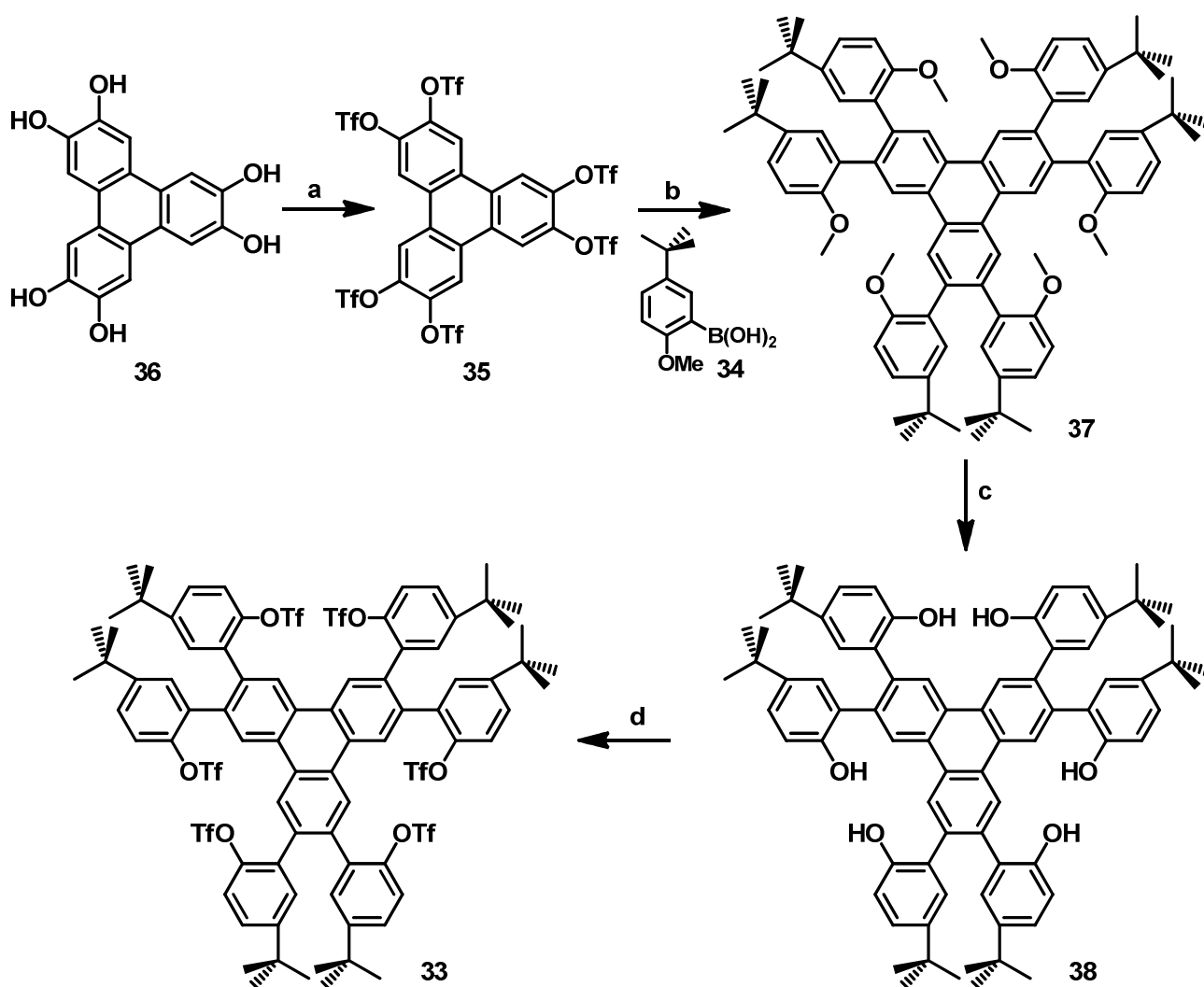


Figure 64. Synthesis of hexa-triflate compound 33

(a) Tf_2O , pyridine in CH_2Cl_2 , RT, 16h, 85%. (b) $Pd(OAc)_2$, $SPhos$, K_3PO_4 in THF/H_2O , $67^\circ C$, 48h, 75%. (c) BBr_3 in CH_2Cl_2 , RT, 16h, 99%. (d) Tf_2O , pyridine in CH_2Cl_2 , RT, 16h, 95%.

The result was beyond our expectations since the desired six-times coupled compound **37** has been obtained with an excellent yield of 75% and was easily purified by chromatography due to the presence of polar functions. Then the six methoxy groups were quantitatively deprotected in usual conditions using BBr_3 and the hexaphenol intermediate **38** was then submitted to usual triflation conditions to give the expected hexa-triflate compound **33** with still an excellent yield (95%).

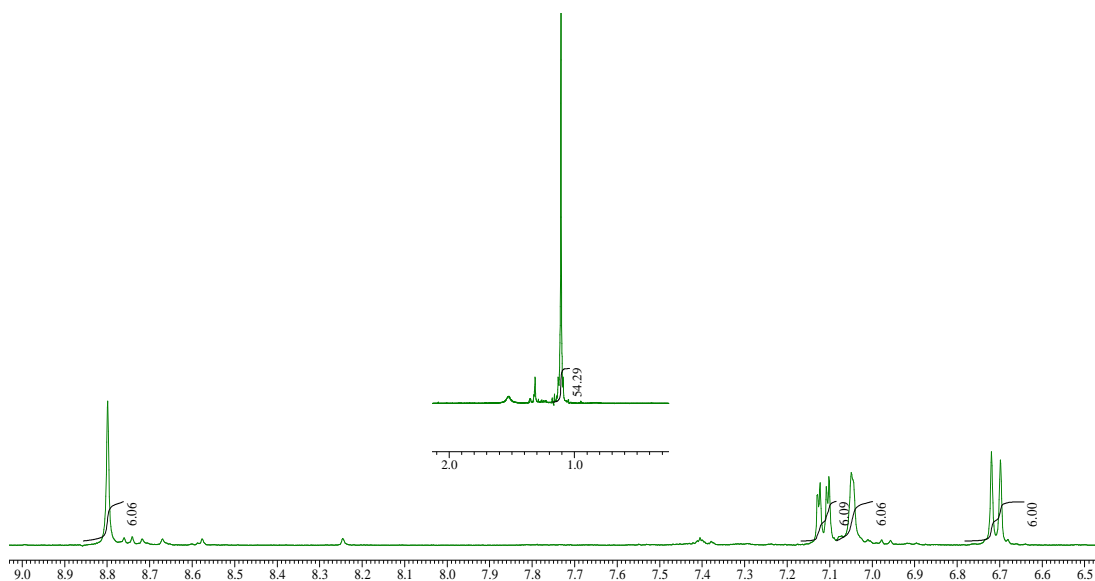


Figure 65. ^1H NMR spectrum of compound **38**, On top are aliphatic signals (2.0 to 0.8 ppm) and below aromatic signals (9.0 to 6.5 ppm).

Due to its high symmetry, compound **38** has been easily characterized by ^1H -NMR, as shown in (**Figure 65**). In fact, only one aliphatic singlet (tert-butyl groups) has been observed and the aromatic region is also very simply interpreted with only one singlet (triphenylene) and the three usual signals (doublet, thin doublet, double doublet) of *o,p*-trisubstituted phenyl rings.

In addition, we were lucky enough to obtain analyzable single crystals of compound **33** and the X-ray analysis (**Figure 66**) undoubtedly confirmed the structure of molecule **33**. Interestingly, the orientation of the phenyl rings is disordered in this X-ray structure, which is confirmed by the complicated ^1H NMR showing several stable conformers.

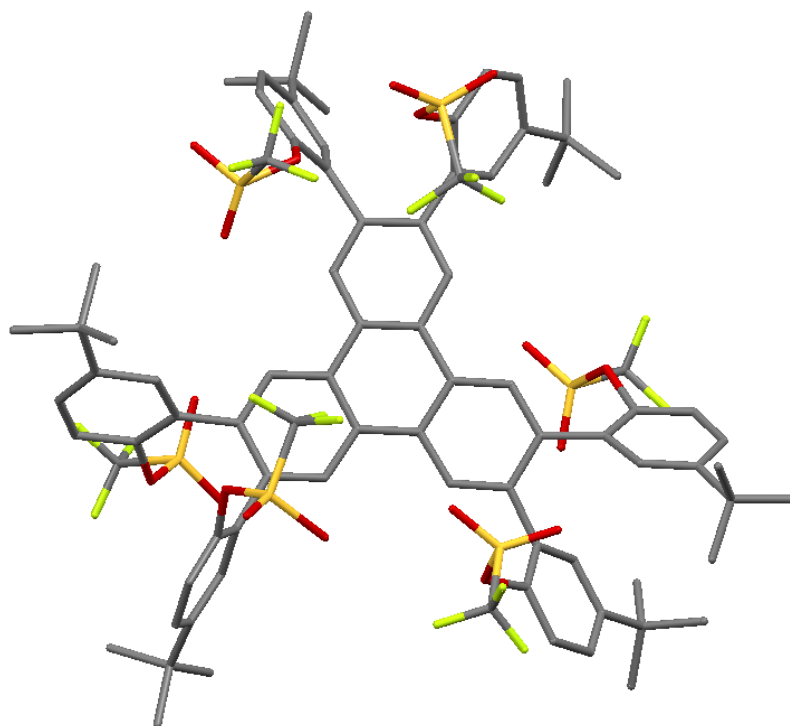


Figure 66. X-ray structure of hexa-triflate compound **33**.

The final step for the formation of the flexible Scholl precursor is another six fold Suzuki cross-coupling reaction to change every triflate groups of compound **33** into para-tert-butylphenyl fragments (**Figure 67**). For this purpose, the same catalytic system and the same conditions than the previous hexa-coupling reaction were used, in presence of the commercially available para-tert-butylphenylboronic acid. Unfortunately, we were very surprised to realize that in this case not any coupling was observed and the starting compound **33** was almost completely recovered. Other reaction conditions were tried with the same catalyst (**Table 2**), varying the solvent and using a boronic ester, but none of them gave any positive result, even after several days.

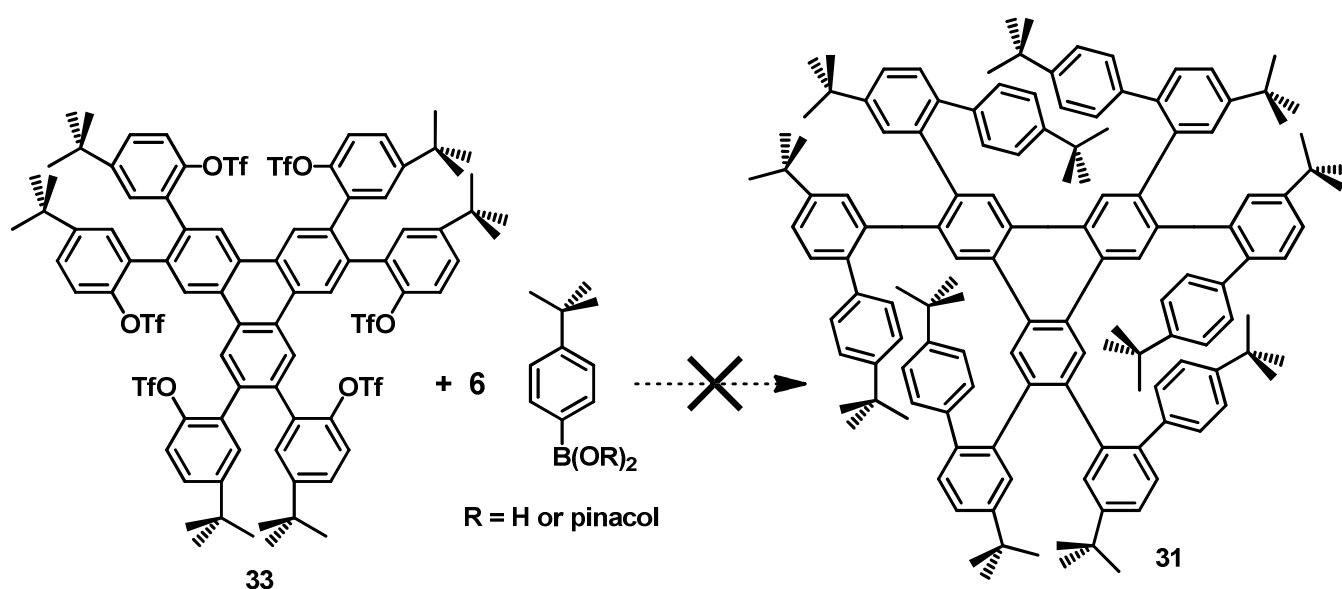


Figure 67. Failure of the final step for the synthesis of compound **31**.

Table 2. Different reaction conditions tried for the synthesis of compound **31** from hexatrienyl triflate compound **33**.

Attempt	Catalysts	Base	33+ Reactants	Sovent	Conditions
1	Pd(OAc) ₂ , SPhos	K ₃ PO ₄	4-tert-Butylphenylboronic acid	THF/H ₂ O	70°C, 96h
2	Pd(OAc) ₂ , SPhos	K ₃ PO ₄	4-tert-Butylphenylboronic acid	THF	70°C, 120h
3	Pd(OAc) ₂ , SPhos	K ₃ PO ₄	4-tert-Butylphenylboronic pinacol ester	THF/H ₂ O	70°C, 96h

Facing this very disappointing result, and assuming that a too important steric hindrance will always be problematic for multiple Suzuki cross-coupling reactions, we decided to give-up these triphenylene-based strategies and to focus instead on a cyclotrimerization-based approach.

3.4 Aryne-based strategy.

3.3a Principle.

Arynes, i.e. aromatic rings having two adjacent radicals, are extremely reactive species that must be generated in situ.³ Common methods employed for the generation of *ortho*-arynes, are based either on the generation of aryl anions by treatment of a strong bases *ortho* to a leaving group⁴ or by treatment of *ortho*-dihalogenobenzene in the presence of metals like Mg, Li⁵ or *n*-BuLi⁶ to promote metal-halogen exchange followed by α,β -elimination. Another methodology is based on the thermal or photochemical decomposition of zwitterionic species⁷ or oxidation of 1-aminobenzotriazol derivatives via nitrene species that undergo decomposition leading to benzyne (**D'**). Although these methods are useful for the generation of benzyne, their tolerance to certain functional groups is limited. In 1983, Kobayashi described a mild and versatile method for the in situ preparation of benzyne (**D'**) through the fluoride-induced 1,2- elimination of *ortho*-silylaryltriflates "**D**" (**Figure 68**).⁸

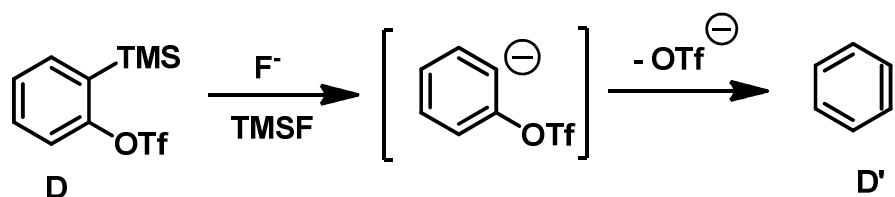


Figure 68. Generation of benzyne intermediate.

In 1998, Guitián and co-workers reported the trimerization reaction of *ortho*-silylaryltriflates in the presence of palladium(0) catalysts for the synthesis of triphenylene derivatives (**Figure 69**).⁹ The best results, with yields between 70% and 30%, were obtained in the presence of 10 mol% of [Pd(PPh₃)₄], CsF or *n*-Bu₄NF as fluoride sources, in CH₃CN at room temperature¹⁰.

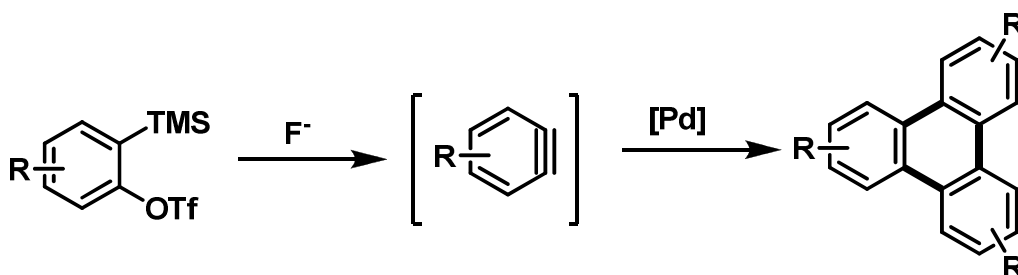


Figure 69. General Pd-catalyzed cyclotrimerization of arynes.

The mechanism proposed for the cyclotrimerization of arynes shown in (**Figure 70**) is similar to the mechanism for [2+2+2]-cycloadditions of alkynes.¹¹

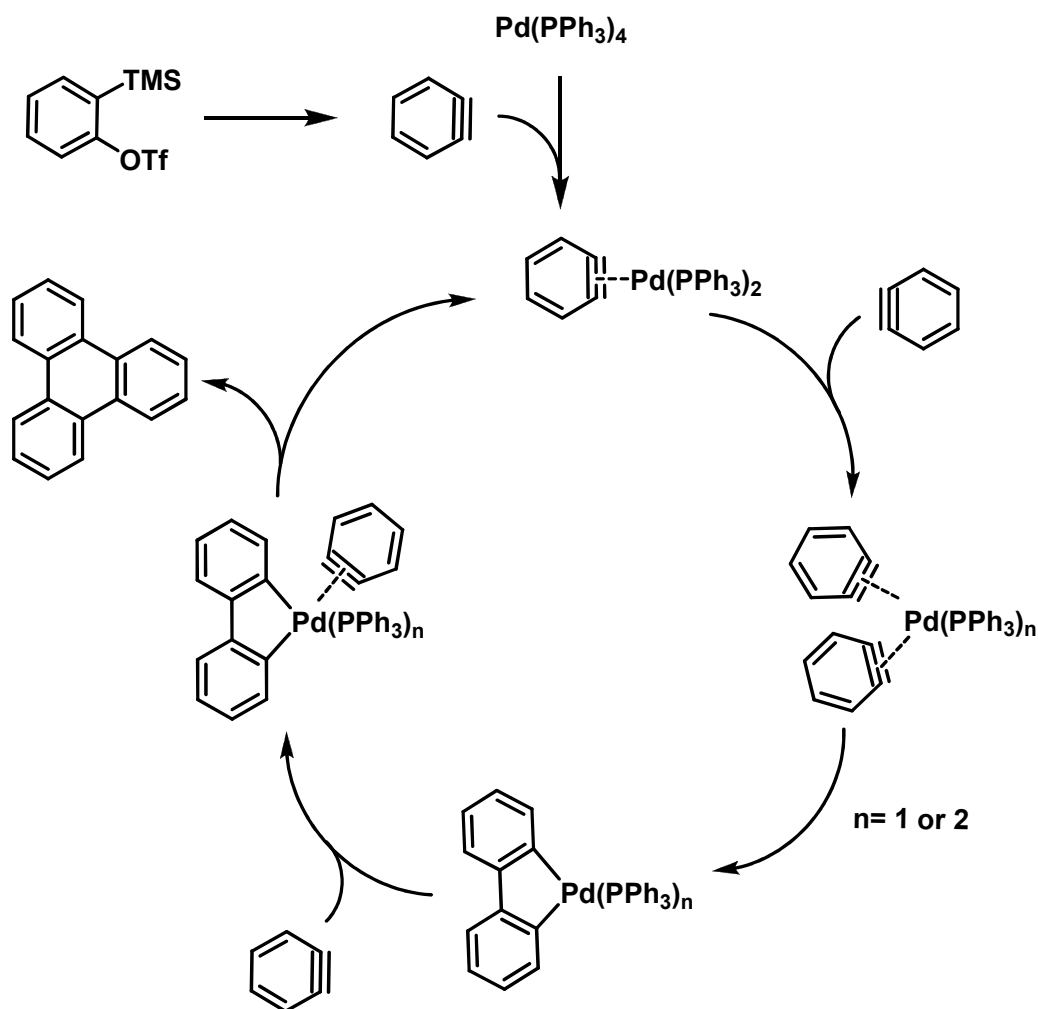


Figure 70. Global mechanism of a Pd-catalyzed cyclotrimerization of arynes.

In order to apply this cyclotrimerization technique to the synthesis of the flexible Scholl precursor **31**, which is a hexa-substituted triphenylene, the retrosynthetic study consists in designing the structure and the synthesis of the aryne-based compound (**Figure 71**). Being inspired by the previous work of Guitián and coworkers,¹⁰ the structure of the aryne-generating *ortho*-silylaryl triflate compound was obvious and its synthesis was logical from

the corresponding phenol, following the usual series of steps (alpha-bromination, double silylation, deprotection and triflation) described in the literature. Concerning the phenol compound, it should be obtained by usual Suzuki cross coupling reactions between 3,4-dibromoanisole **41** and boronic acid **5a**, followed by a deprotection of the methoxy group.

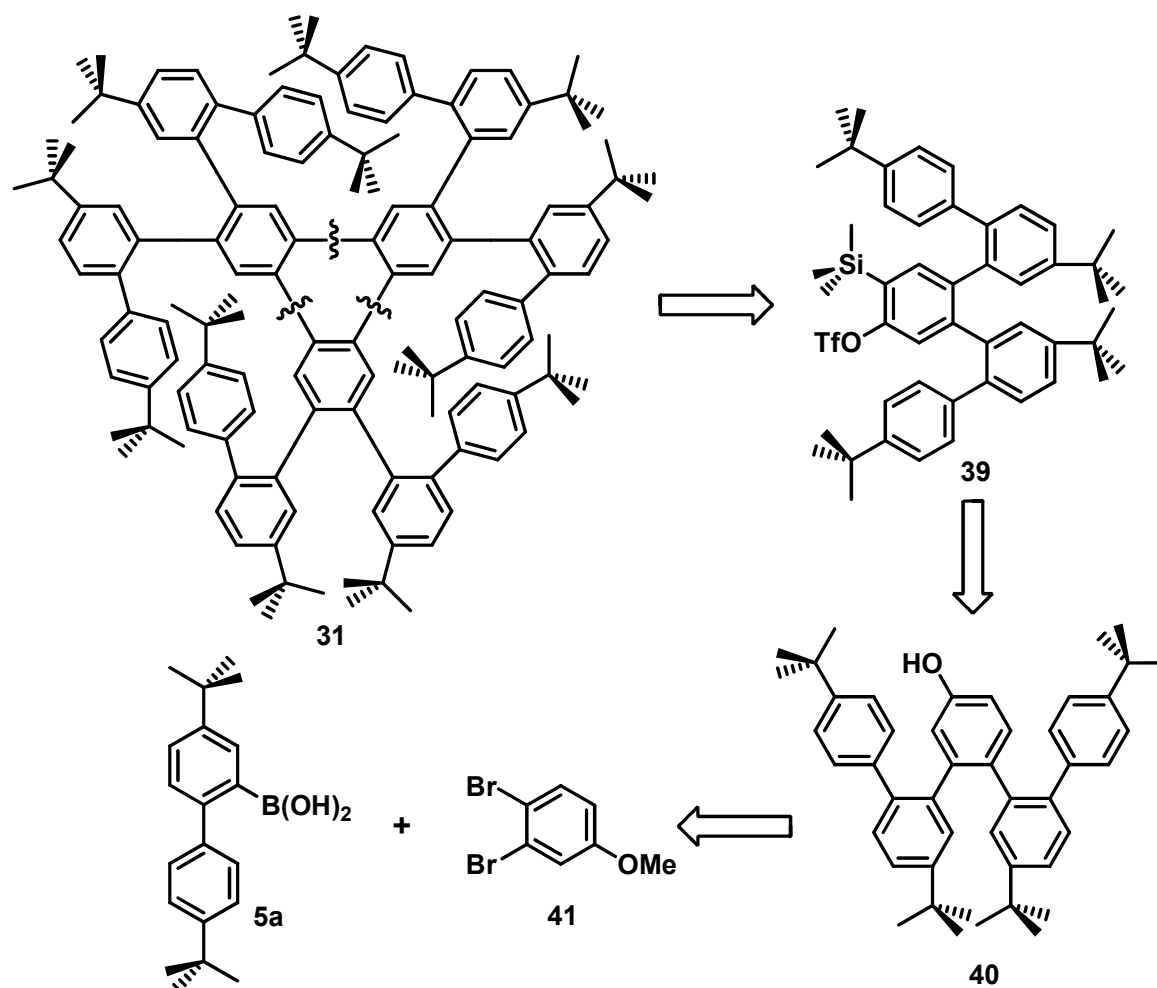


Figure 71. Retrosynthetic study for the formation of **31** by cyclotrimerization of arynes.

3.4b First difficulties.

3,4-dibromoanisole **41** was quantitatively prepared from commercially available 3,4-dibromophenol **42** by simple methylation with methyl iodide and K_2CO_3 as a base (**Figure 72**). Unfortunately, the next step was already problematic since we did not succeed in making

a double Suzuki cross-coupling reaction on the 3,4-dibromoanisole **41** with the boronic acid **5a**, even after several days of reaction. We assumed that the double coupling on two ortho positions is again highly disfavored, even on a very simple molecule.

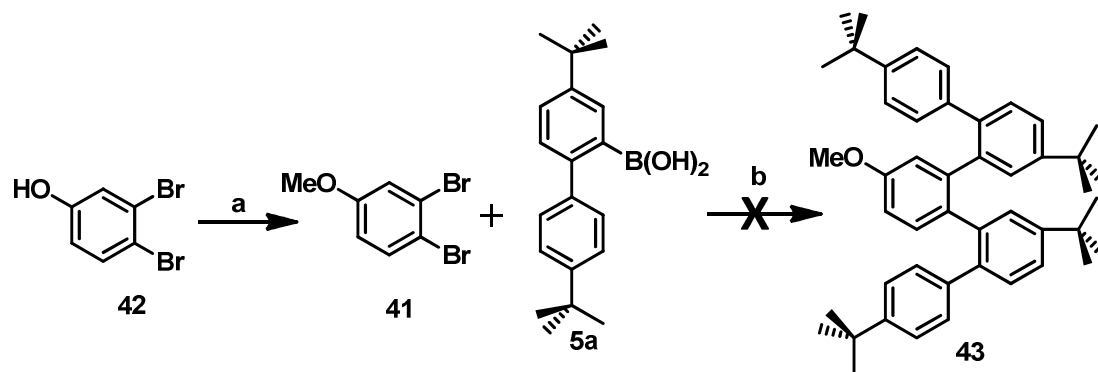


Figure 72. Failing reaction on 3,4-dibromoanisole.

(a) K_2CO_3 , MeI in Acetone, 58°C, 16h, 100%. (b) Na_2CO_3 , $Pd(PPh_3)_4$ in PhMe/ H_2O / $EtOH$, 90°C, 48h.

3.4c Second method.

Facing this early difficulty, we decided to make a compromise and to follow a very similar procedure on less hindered 2,4-dibromoanisole **45** instead of 3,4-dibromoanisole **41**, hoping that such a change would not affect too much the yield of the trimerization step.

2,4-dibromoanisole **45** was also quantitatively prepared from commercially available 3,4-dibromophenol **44** by simple methylation with methyl iodide and K_2CO_3 as a base (**Figure 73**). Then it efficiently reacts with boronic acid **5a**, in classical conditions for Suzuki cross-coupling reactions with $Pd(PPh_3)_4$ as a catalyst, and gives the expected compound **46** (80%).

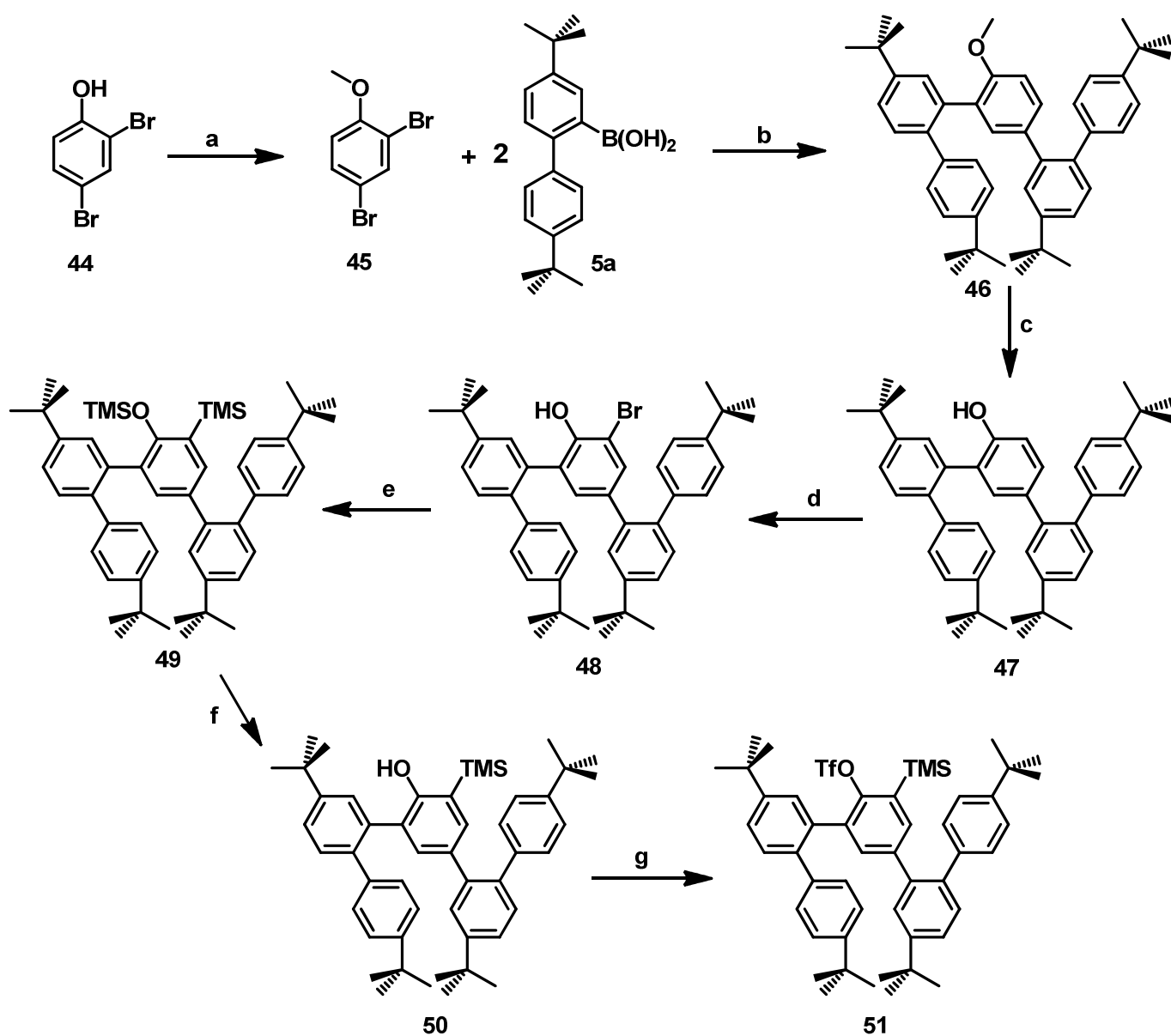


Figure 73. Synthesis of *ortho*-silylaryltriflate compound **51**.

(a) K_2CO_3 , MeI in Acetone, $58^\circ C$, 16h, 100%. (b) Na_2CO_3 , $Pd(PPh_3)_4$ in PhMe/ H_2O /EtOH, $90^\circ C$, 48h, 80%. (c) BBr_3 in CH_2Cl_2 , RT, 16h, 94%. (d) NBS, *i*-Pr₂-NH in CH_2Cl_2 , RT, 1h, 84%. (e) BuLi, THF, $-78^\circ C$, 15min, then TMSCl, 10min, RT again BuLi, $-78^\circ C$, 15min, then TMSCl, $-78^\circ C$ to room T, 3h, 80%. (f) 1(M) NaOH, THF, RT, 16h, 99%. (g) BuLi, THF, $-90^\circ C$, 15min, then Tf_2O , $-78^\circ C$ to room T, 3h, 80%.

Its methoxy group is then deprotected by action of BBr_3 , leading quantitatively to the phenolic intermediate **47**. Selective *ortho*-bromination was then achieved in very good yield (84%) by reaction of **48** with *N*-bromosuccinimide (NBS) in the presence of a catalytic amount of diisopropylamine. Sequential treatment of the resulting brominated compound **48** with *n*-BuLi and TMSCl (2 equivalents) in one pot afforded the doubly silylated (one on the oxygen, the other on the carbon) compound **49** in good yield (80%). The trimethylsilyl ether on **49** was then quantitatively and selectively deprotected by action of a 1M NaOH solution to afford the phenolic compound **50**, which then reacts with *n*-BuLi and Tf_2O to give the expected *ortho*-silylaryltriflate compound **51** in 80% yield, and a very satisfying overall yield (40%) for this 7- step sequence.

In order to proceed to the final cyclotrimerization and thus form the new Scholl precursor **52**, *ortho*-silylaryltriflate compound **51** has been treated with CsF in the presence of $\text{Pd}_2(\text{dba})_3$ as a catalyst in a refluxing mixture of acetonitrile and dichloromethane during four days. After work-up and purification, one single product has been isolated with a good yield (65%) and analyzed by $^1\text{H-NMR}$, giving a clear spectrum, consistent with the expected compound **53**. Unfortunately, analysis by mass spectrometry revealed to us that instead of the expected trimer, only a dimer was formed (**Figure 74a**), which $^1\text{H-NMR}$ spectrum (**Figure 75**) is logically similar. This disappointing result has been confirmed by $^{13}\text{C-NMR}$, where we could observe signals around 159 ppm, witnessing the presence of a 4-membered ring containing biphenylene unit (**Figure 75**).

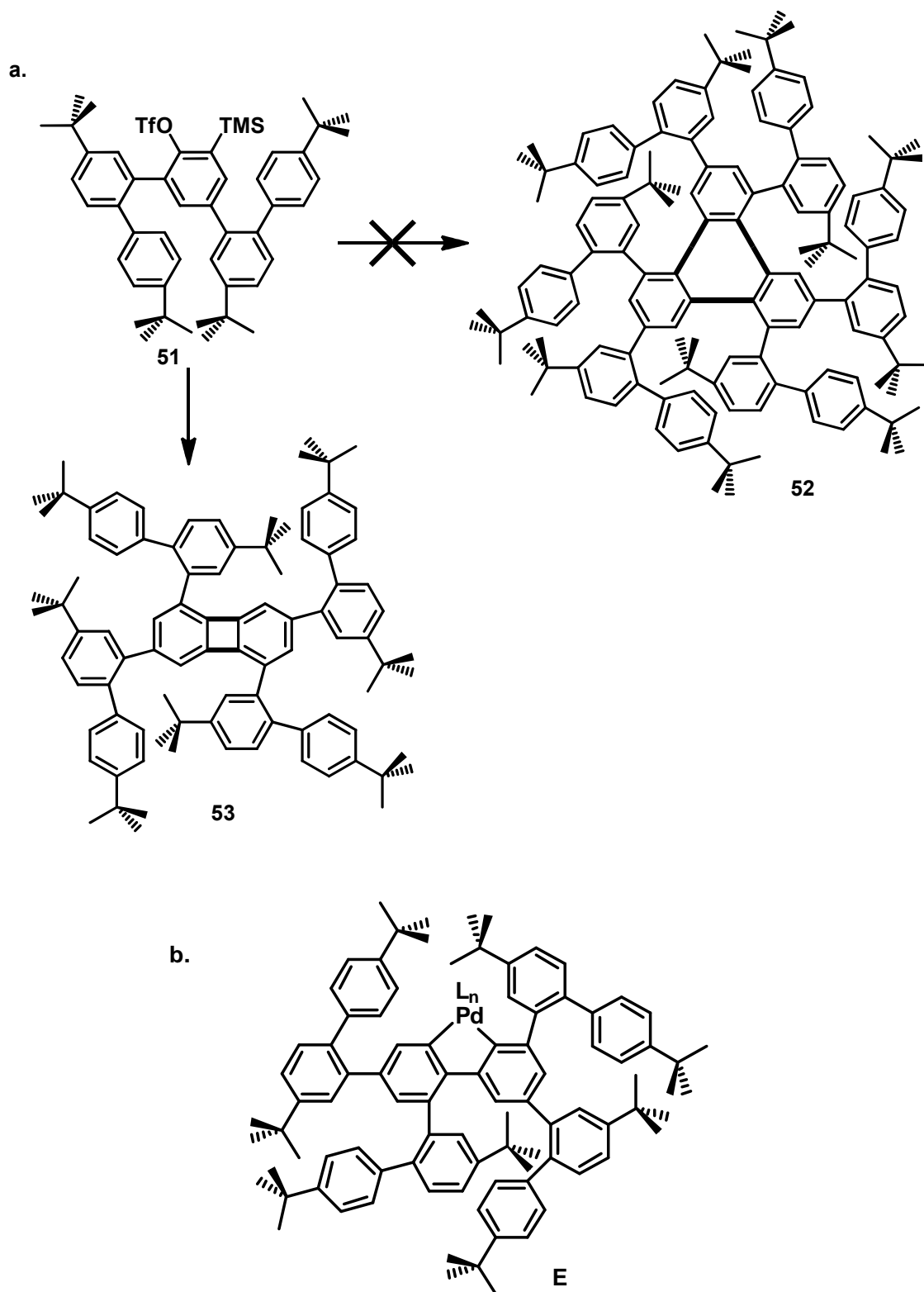


Figure 74. Failed attempt of cyclotrimerization of compound 42.

(a) CsF , $Pd_2(dba)_3$ in $MeCN/DCM$, $40^\circ C$, 96h, 65%. (b) Reaction intermediate “E”

This unexpected reactivity could be explained by considering the cyclic Pd complex **E** (**Figure 74b**). This highly hindered intermediate in the catalytic cycle of the trimerization probably does not allow the third aryne to get close enough to the catalytic center to react as expected. Instead of this, the Pd complex certainly undergoes a reductive elimination to expel the Pd and thus form a biphenylene compound, i.e. a dimer instead of a trimer.

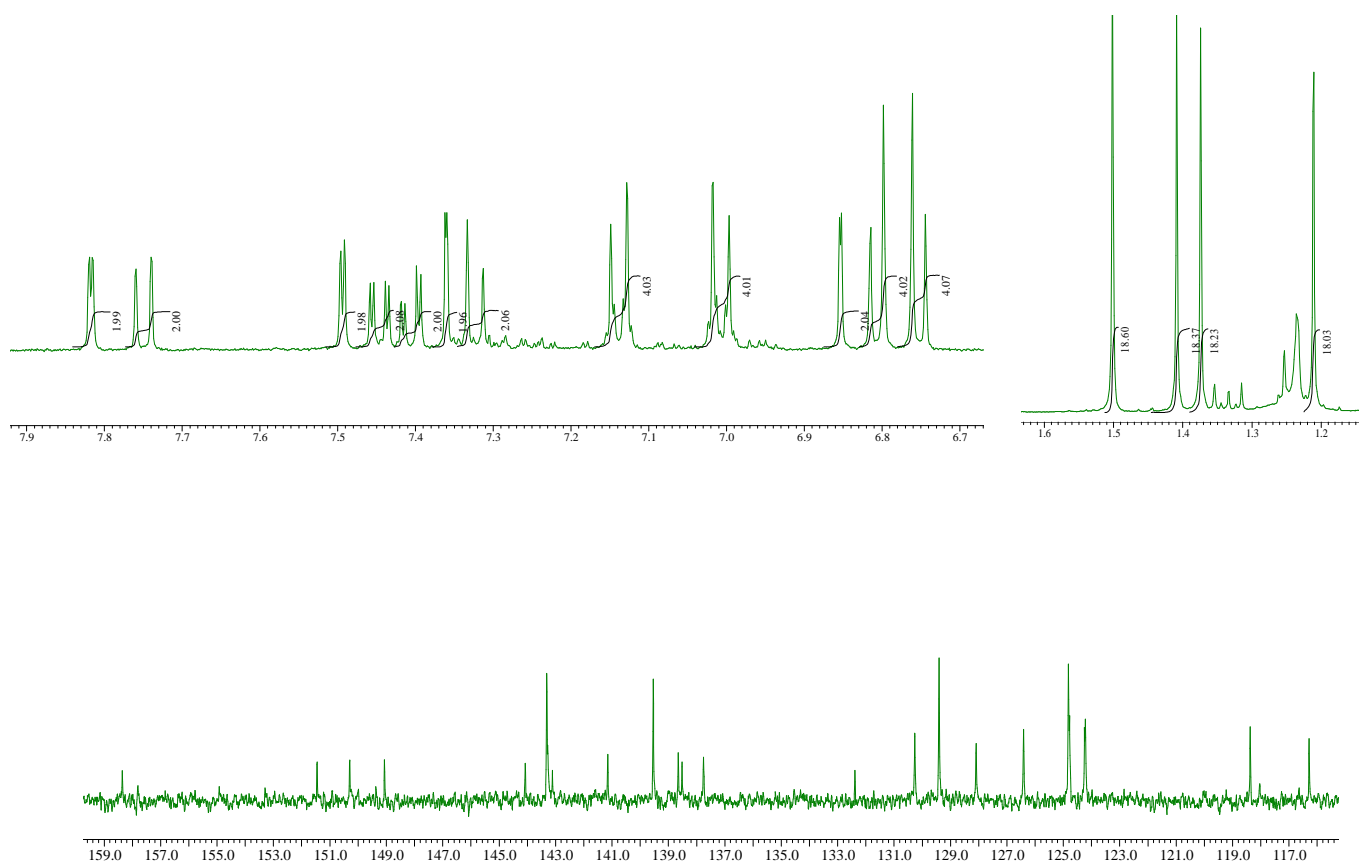


Figure 75. Top ¹H NMR spectrum of compound **53** displaying the peaks of aliphatic (1.6 to 1.1 ppm) and aromatic (7.9 to 6.7 ppm) range. Below ¹³C NMR spectrum of compound **53** displaying the peaks in aromatic region (159.0 to 115 ppm).

Nevertheless, even if not expected, compound **53** was still an interesting flexible precursor for Scholl reaction. It was therefore submitted to usual Scholl reaction conditions, by dissolution first in dry and degassed dichloromethane and then slow addition of a FeCl₃ solution in nitromethane, under strong bubbling of argon. Finally, the reaction was quenched with an alcohol (methanol) and the crude product was analyzed by TLC, unfortunately showing many

very closely migrating spots. This made us conclude that biphenylene compounds may not be stable under Scholl reaction conditions.

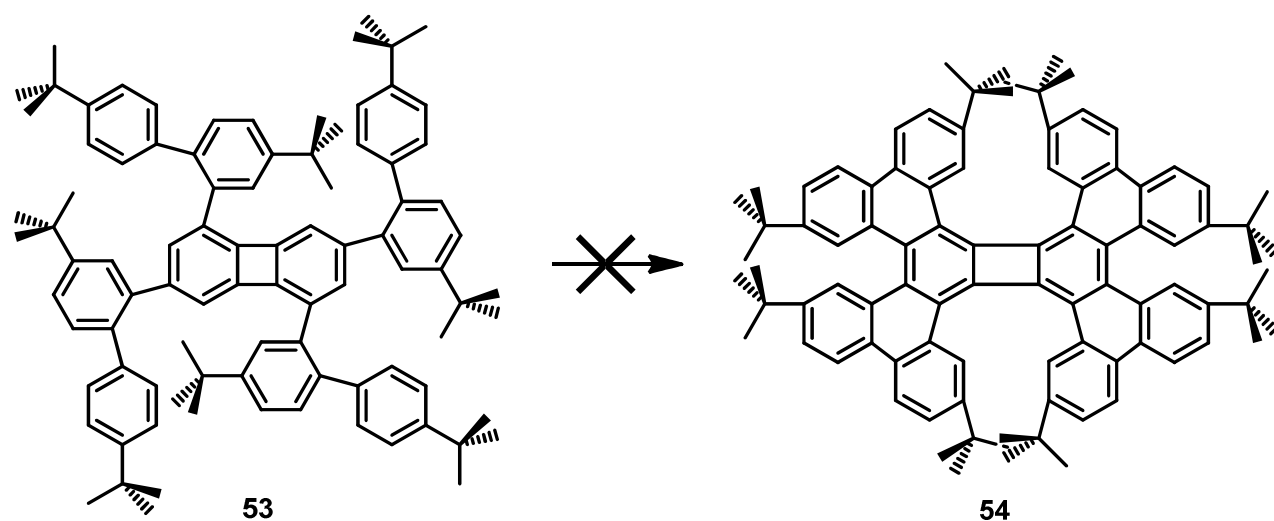


Figure 76. Failed Scholl reaction on biphenylene-based compound **53**.

We finally stopped our investigations on the synthesis of the HPTP at that point. Nevertheless, one remaining strategy could still be reasonable, even if representing a lot of work. In fact, a stepwise synthesis could easily be imagined for the formation of the first targeted *ortho*-silylaryltriflate compound (from 3,4-dibromoanisole **41**), which is a lot less hindering than its isomer **51**, and therefore would still have a chance to undergo cyclotrimerization to give the HPTP precursor **31**.

Before spending a lot of time and energy on this long synthesis, we first decided to investigate better the Scholl reaction, on simpler precursors, to check if the formation of higher order than [5]helicenes is possible by this technique.

3.5 References.

1. L. Barnett, D. M. Ho, K. K. Baldrige, R. A. Pascal *J. Am. Chem. Soc.* **1999**, *121*, 727.
2. S. D. Walker, T. E. Barder, J. R. Martinelli, S. L. Buchwald, *Angew. Chem. Int. Ed.* **2004**, *43*, 1871.
3. H. H. Wenk, M. Winkler, E. Sander, *Angew. Chem. Int. Ed.* **2003**, *42*, 502,
4. P. Caubère, *Chem. Rev.* **1993**, *93*, 2317.
5. G. Wittig, *Org. Synth.* **1959**, *39*, 75.
6. H. Gilman, R. D. Gorsich, *J. Am. Chem. Soc.* **1956**, *78*, 2217.
7. P. C. Buxton, M. Fensome, H. Heaney, K. G. Manson, *Tetrahedron* **1995**, *51*, 2959.
8. Y. Himeshima, T. Sonada, H. Kobayashi, *Chem. Lett.* **1983**, 1211.
9. (a) D. Peña, S. Escudero, D. Pérez, E. Guitián, *Angew. Chem. Int. Ed.* **1998**, *37*, 2659.
(b) C. Romero, D. Peña, D. Pérez, E. Guitián, *Chem. Eur. J.* **2006**, *12*, 5677.
10. D. Pérez, D. Peña, E. Guitián, *Eur. J. Org. Chem.* **2013**, 5981.
11. V. Gandon, C. Aubert, M. Malacria, *Chem. Commun.* **2006**, 2209.

Chapter IV: Investigation of the Scholl reaction on C₃-symmetrical precursors.

We attempted to synthesize multiple [7]helicenes by Scholl reaction but faced big challenges making the flexible precursor. We therefore tried to make some multiple [6]helicenes from simpler molecular precursors.

4.1. General strategy for preparing common precursor.

A quick and simple synthetic strategy towards the highly distorted propeller-shaped hexa-*tert*-butyl-hexabenzotriphenylene (^tBu₆-HBTP) **28**, from the flexible precursor **27** obtained by trisubstitution of tribromobenzene **26** (Figure 56) with three biphenylic blades (Figure 77), has already been described as proof of the efficiency of the Scholl reaction to form multiple helicenic compounds¹.

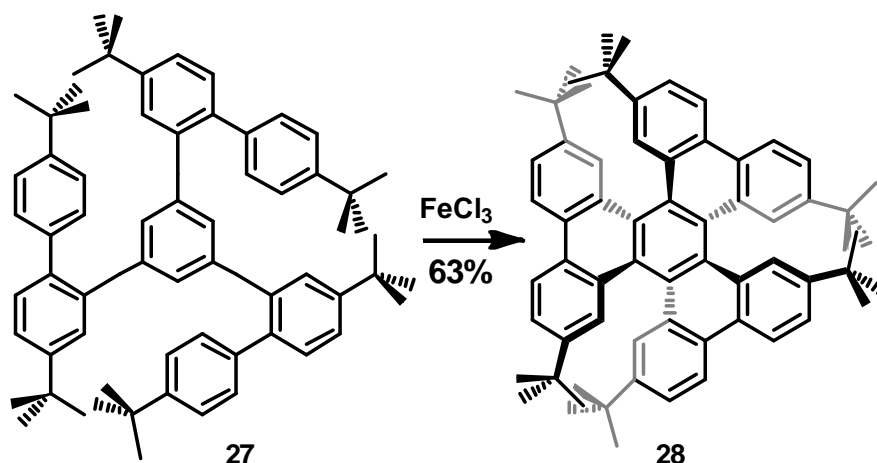


Figure 77. Formation of trisubstituted substrates for intramolecular Scholl reactions.

We have then developed a systematic and versatile strategy to synthesize a family of such flexible C₃-symmetrical substrates for subsequent Scholl treatment. This new method involves more steps than in the case of **28** but gives access to several series of compounds from a single common trifunctionalized precursor **57** by only changing the nature of the arylboronic acid added in the last step.

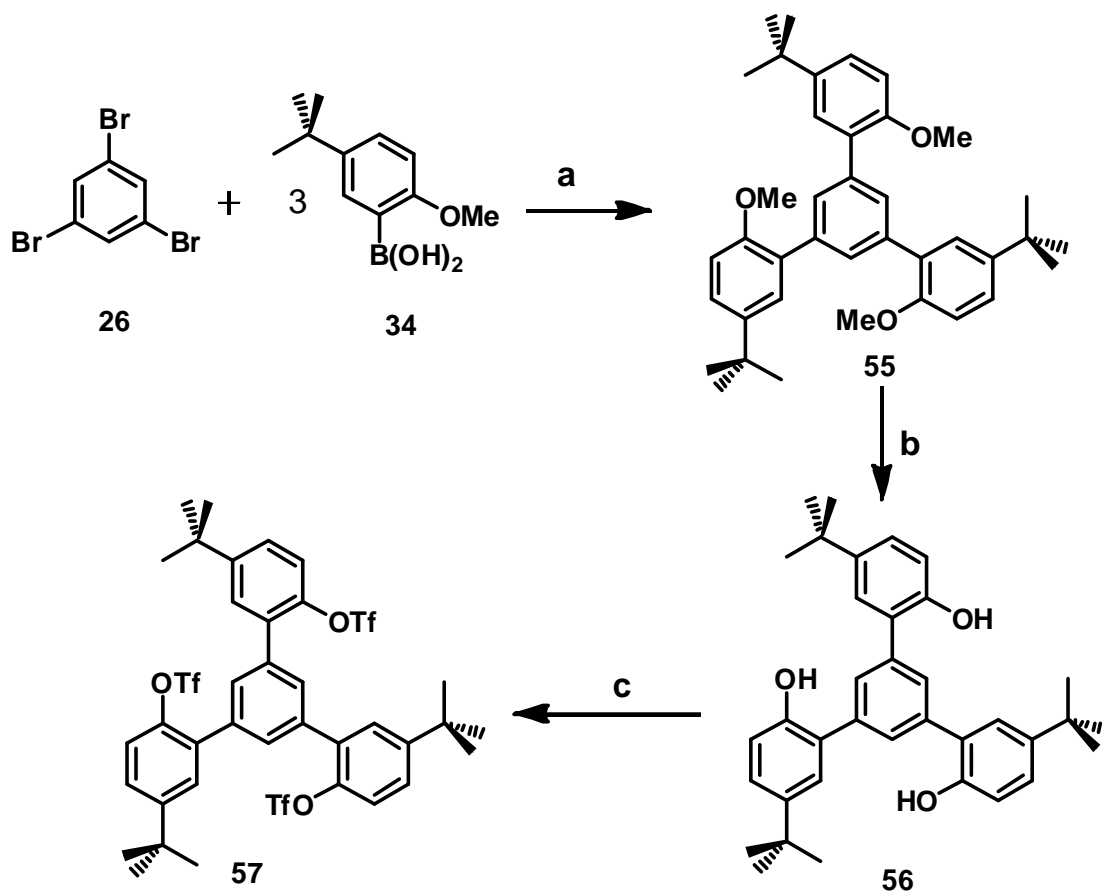


Figure 78. Synthesis of common precursor **57**. (a) Na_2CO_3 , $\text{Pd}(\text{PPh}_3)_4$ in $\text{PhMe}/\text{H}_2\text{O}/\text{EtOH}$, 90°C , 48h, 95%. (b) BBr_3 in CH_2Cl_2 , RT, 16h, 99%. (c) Tf_2O , pyridine in CH_2Cl_2 , RT, 16h, 96%.

The formation of the common precursor **57** (**Figure 78**) relies on a trisubstitution of *sym*-tribromobenzene **26**, by a very efficient (95% yield) Suzuki cross-coupling reaction in classical conditions. This time **26** is not reacted with a complete blade (boronic ester **5b**), but with the shorter methoxy substituted arylboronic acid **34**, which was synthesized in two steps following existing procedures². The three methoxy groups of the resulting compound **55** are then deprotected by action of BBr_3 , leading quantitatively to the triphenolic intermediate **56**. The phenol functions are then transformed into triflate groups in excellent yield to give the common precursor **57**.

Due to the important steric hindrance of the reacting sites on this substrate **57**, optimized catalytic conditions had to be established for the last trisubstitution step by Suzuki cross-coupling reaction. A very satisfying catalytic system, developed by Buchwald's group³, is based on $\text{Pd}(\text{OAc})_2$, SPhos (2-Dicyclohexylphosphino-2',6'-dimethoxybiphenyl) as ligand and

K_3PO_4 as base in a mixture of THF and water. Commercially available arylboronic acids were then used to give trisubstituted flexible Scholl substrates in excellent yields (between 92% and 98%).

4.2. Phenanthrene based strategy.

The triple Suzuki reaction between 9-phenanthracenylboronic acid **58** and tris-triflate **57** affords the flexible but sterically very congested compound **59** (Figure 79).

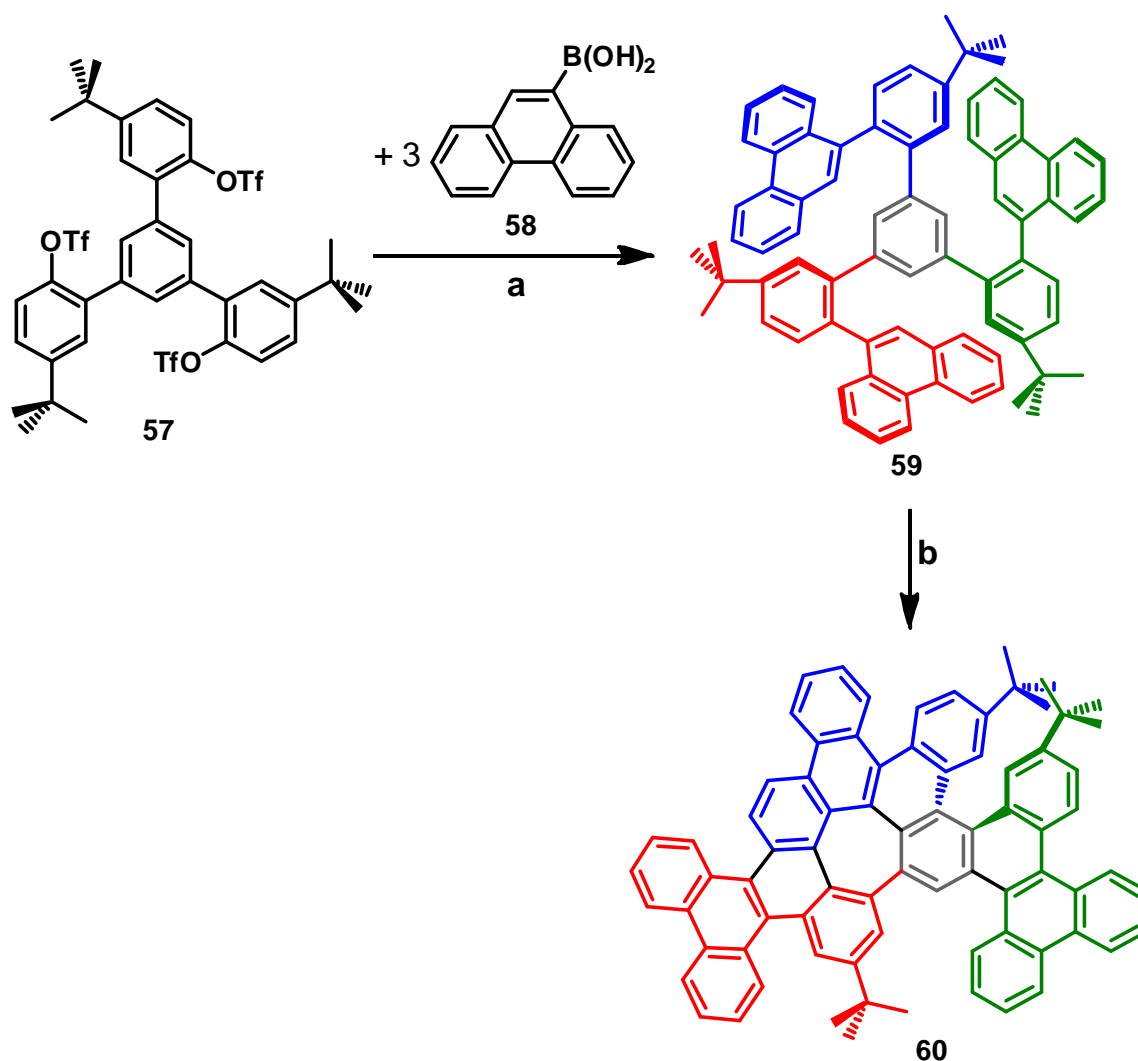


Figure 79. Synthesis and Scholl reaction of phenanthrene-based precursor **59**.

(a) $Pd(OAc)_2$, *SPhos*, K_3PO_4 in THF/ H_2O , $67^\circ C$, 48h, 95%. (b) $FeCl_3$ in $MeNO_2/CH_2Cl_2$, RT, 1.5h, 73%.

This molecule, if represented in 2D, shows several overlaps of carbons and has two stable conformers at room temperature, as indicated by a variable temperature ^1H NMR (**Figure 80**) study with coalescence reached around 125°C in DMSO-d_6 .

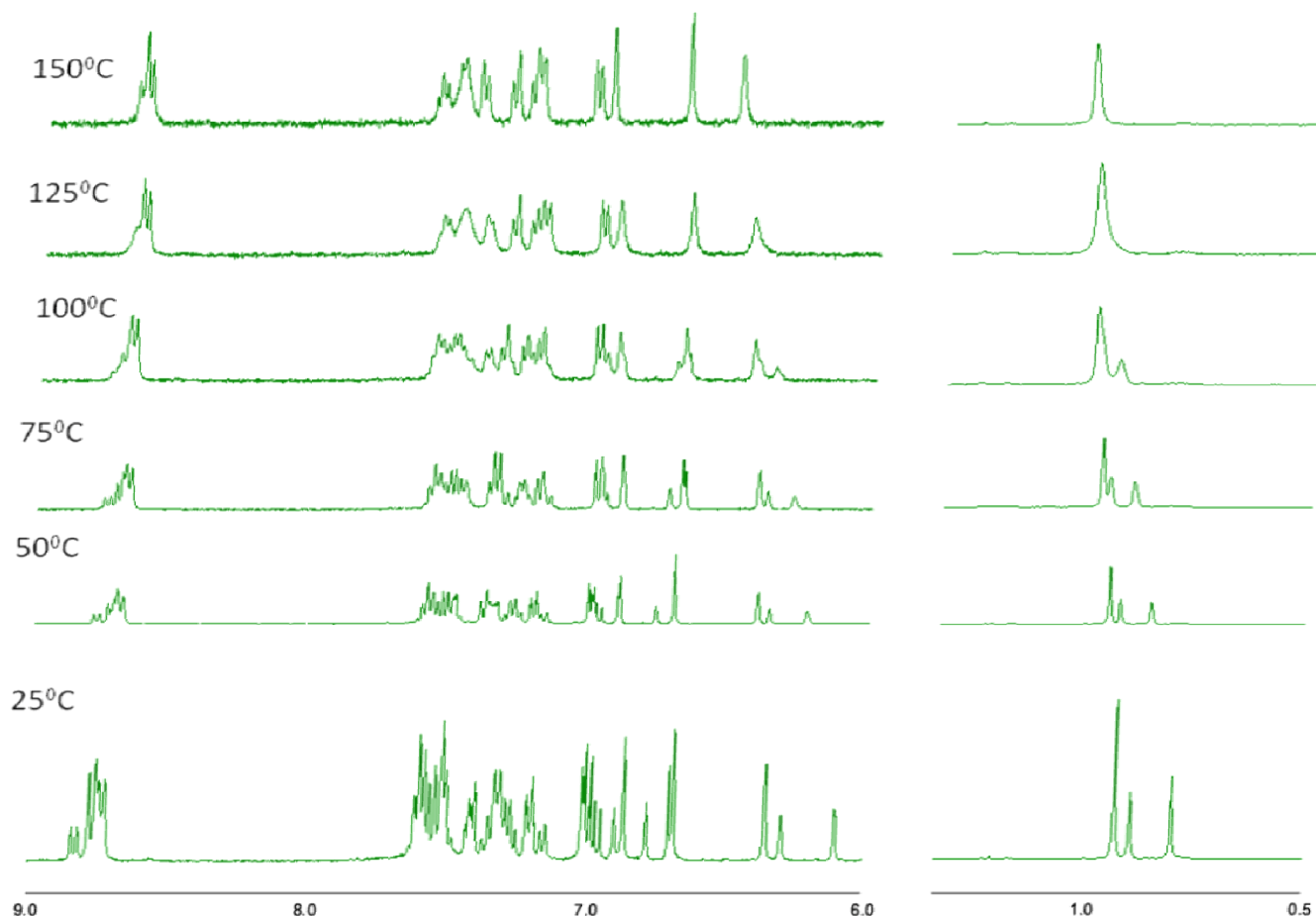


Figure 80. Temperature variant ^1H NMR spectrum of compound **59** displaying the peaks in top aliphatic (1.5 to 0.5 ppm) and aromatic (9.0 to 6.0 ppm) range.

The Scholl reaction on this substrate **59** was predicted to form 3 new C-C bonds, between the central benzene ring and position 10 of each phenanthrene part, to give a symmetrical triple [6]helicene. Nevertheless, we were surprised to reproducibly obtain, after purification, an asymmetrical major product **60** (**Figure 79**) whose formula, (unambiguously confirmed by mass spectrometry), indicates that 8 hydrogen atoms had been removed, implying the creation

of four instead of three C-C bonds. Fortunately, we were able to crystallize this compound by slow diffusion of diisopropyl ether in CCl_4 , and the analysis by X-ray diffraction on single crystals revealed the unexpected structure of oligoarene **60** (Figure 81).

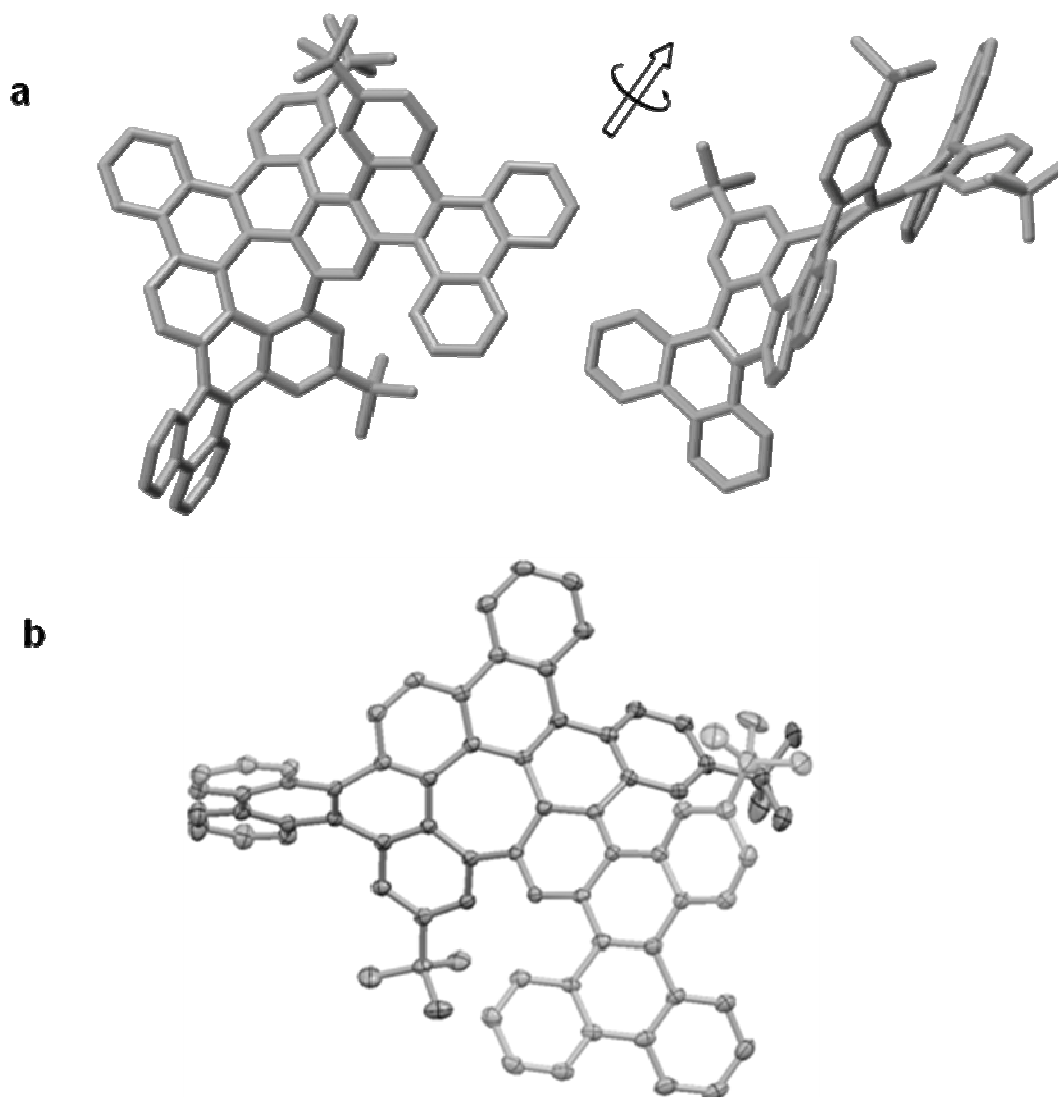


Figure 81. (a) Two different views of the crystal structure of the strongly distorted [5]helicene- and hexa[7]circulene-based compound **60**. (b) ORTEP-type view of **60** at 120 K with thermal ellipsoids at 50 % probability level. Hydrogen atoms and $i\text{Pr}_2\text{O}$ solvent molecules are omitted for clarity, only one of the two positions of the disordered *t*-butyl groups is represented.

The latter is highly distorted due to two different structural ingredients: a) one [5]helicene, whereas [6]helicenes were expected; and b) one 7-membered ring that is part of a hexa[7]circulene fragment. This final structure can be explained by two successive rearrangements during the Scholl process. One blade (blue on **Figure 79**) cyclizes as expected on the central benzene ring, with the second blade (green on **Figure 79**) migrating to an adjacent yet hindered carbon and also cyclizing on the central benzene ring to form a [5]helicene. The phenanthrene part of the third blade (red on **Figure 79**) then migrates to an adjacent carbon on the benzene part of the blade to allow its previous position to cyclize onto another phenanthrene (blue) to form the 7-membered ring. Finally a fourth cyclization occurs between two phenanthrene parts (red and blue). This reproducible and very efficient, yet absolutely unpredicted, outcome tells us that a highly twisted [5]helicenic fragment (between blue and green blades) bearing 2 *tert*-butyl groups on hindered positions, is apparently very favored by the Scholl reaction. This is because it benefits from regioselectivity (Chapter-II, **Figure 46**) but even rearrangements might have occurred to prevent its formation. The 7-membered ring formation by Scholl reaction is also noteworthy since known examples of such heptagonal structures are exceedingly rare, either with only sp^2 -hybridized carbons⁴ or even including one tetrahedral apex⁵.

4.3 Naphthalene based strategy.

When 2-naphthylboronic acid **61** is used to form another flexible substrate **62** (**Figure 82**), two adjacent carbons are free on the 2-naphthyl group. Therefore each blade can theoretically cyclize on the central benzene ring in two different ways. Nevertheless a unique compound **63** is isolated (90% yield) after Scholl treatment. This product has the same greenish color as compound **60**, a very similar ¹H NMR spectrum with several identical peaks, and the mass spectrum also indicates that 4 C-C bonds were formed. For these reasons we hypothesize that the structure of **63** is comparable to the one of **60**. Unfortunately, we are not able to crystallize **63** and thus cannot give any clear evidence of its structure.

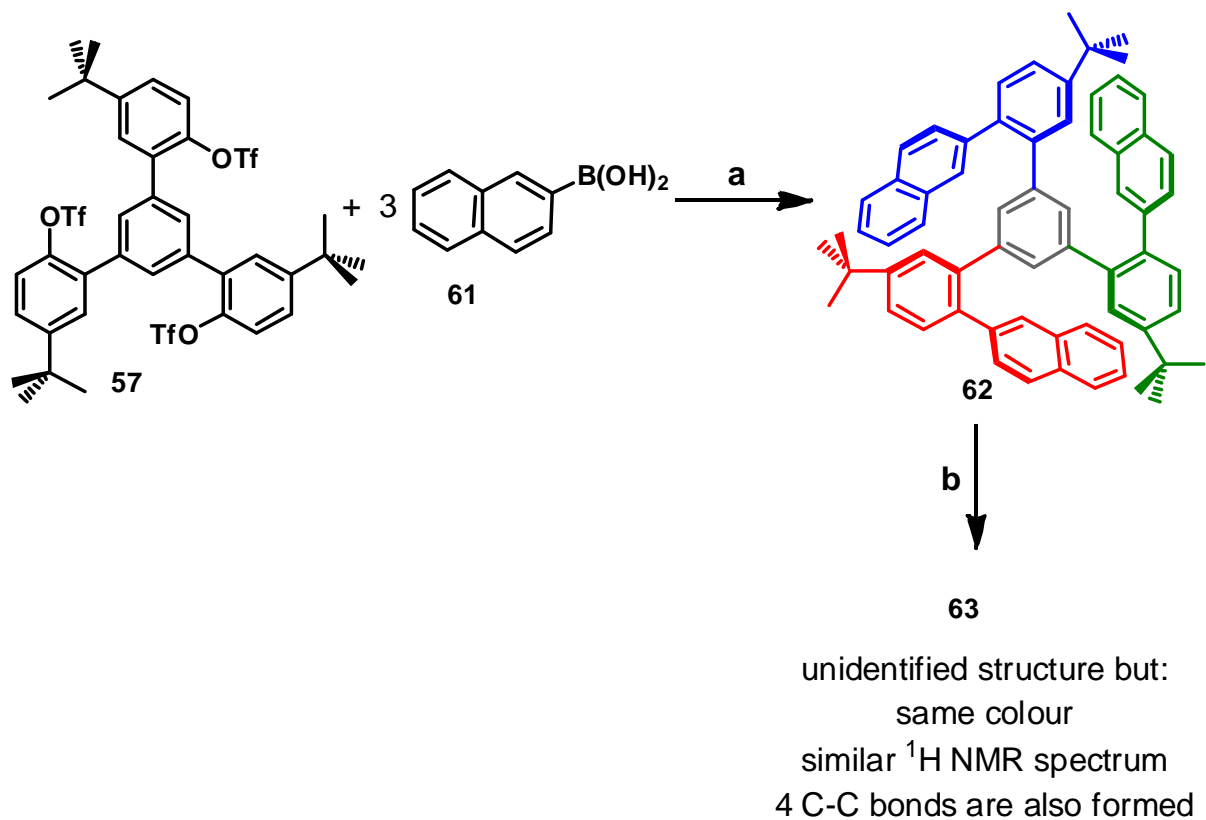


Figure 82. Synthesis and Scholl reaction of 2-naphthalene-based precursor **62**.

(a) $\text{Pd}(\text{OAc})_2$, *SPhos*, K_3PO_4 in $\text{THF}/\text{H}_2\text{O}$, 67°C , 48h, 92%. (b) FeCl_3 in $\text{MeNO}_2/\text{CH}_2\text{Cl}_2$, RT, 1.5h, 90%.

By storing crystallization tubes of **63** for three months in a mixture of DCM and methanol, without protecting it from light, we finally obtain crystals of a surprising rearranged, spiro, methoxy and halogenated compound **63a** (Figure 83). Nevertheless, we are not able to pretend that this molecule is a degradation product of **63**, it could as well be an impurity of the Scholl reaction on precursor **62**.

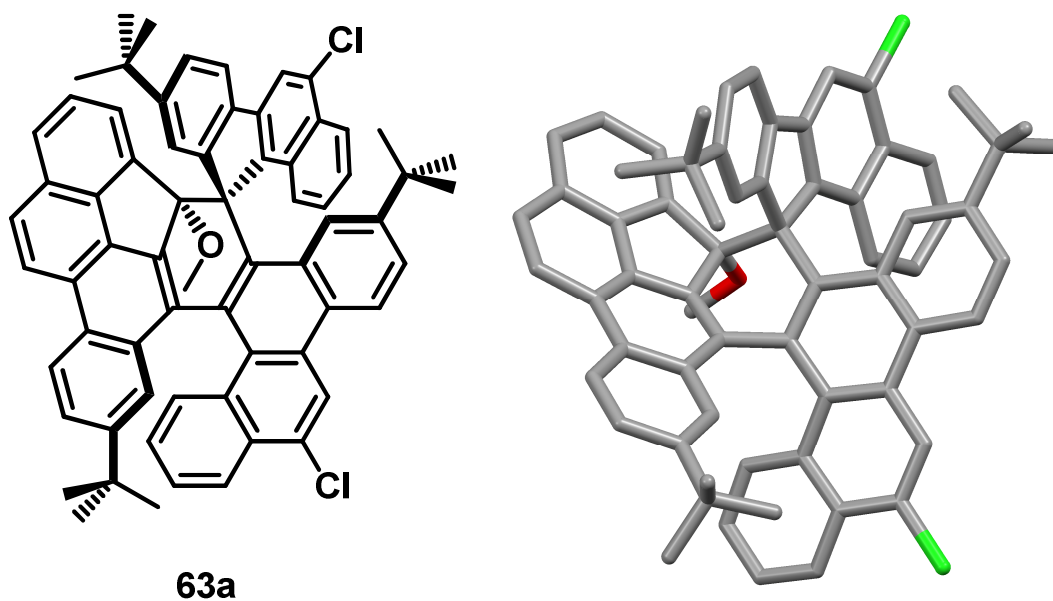


Figure 83. Structure and crystal structure of the strongly distorted **63a**.

The 1-naphthylboronic acid **64** has also been used to form another flexible substrate **65** (**Figure 84**). Here only one adjacent carbon is free on the 1-naphthyl group for cyclizations, but complete cyclizations, leading to a non-helicenic PAH are possible.

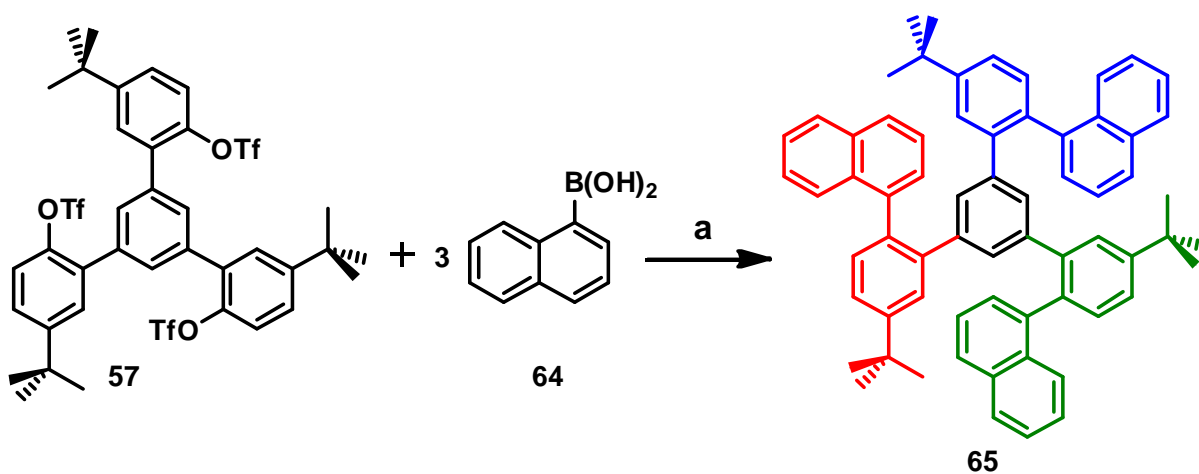


Figure 84. Synthesis of **65**, $\text{Pd}(\text{OAc})_2$, *SPhos*, K_3PO_4 in $\text{THF}/\text{H}_2\text{O}$, 67°C , 48h, 90%.

Compound **65** still has two stable conformers at room temperature as indicated by a variable temperature ^1H NMR (**Figure 85**) study with coalescence reached around 125°C in DMSO-d_6 .

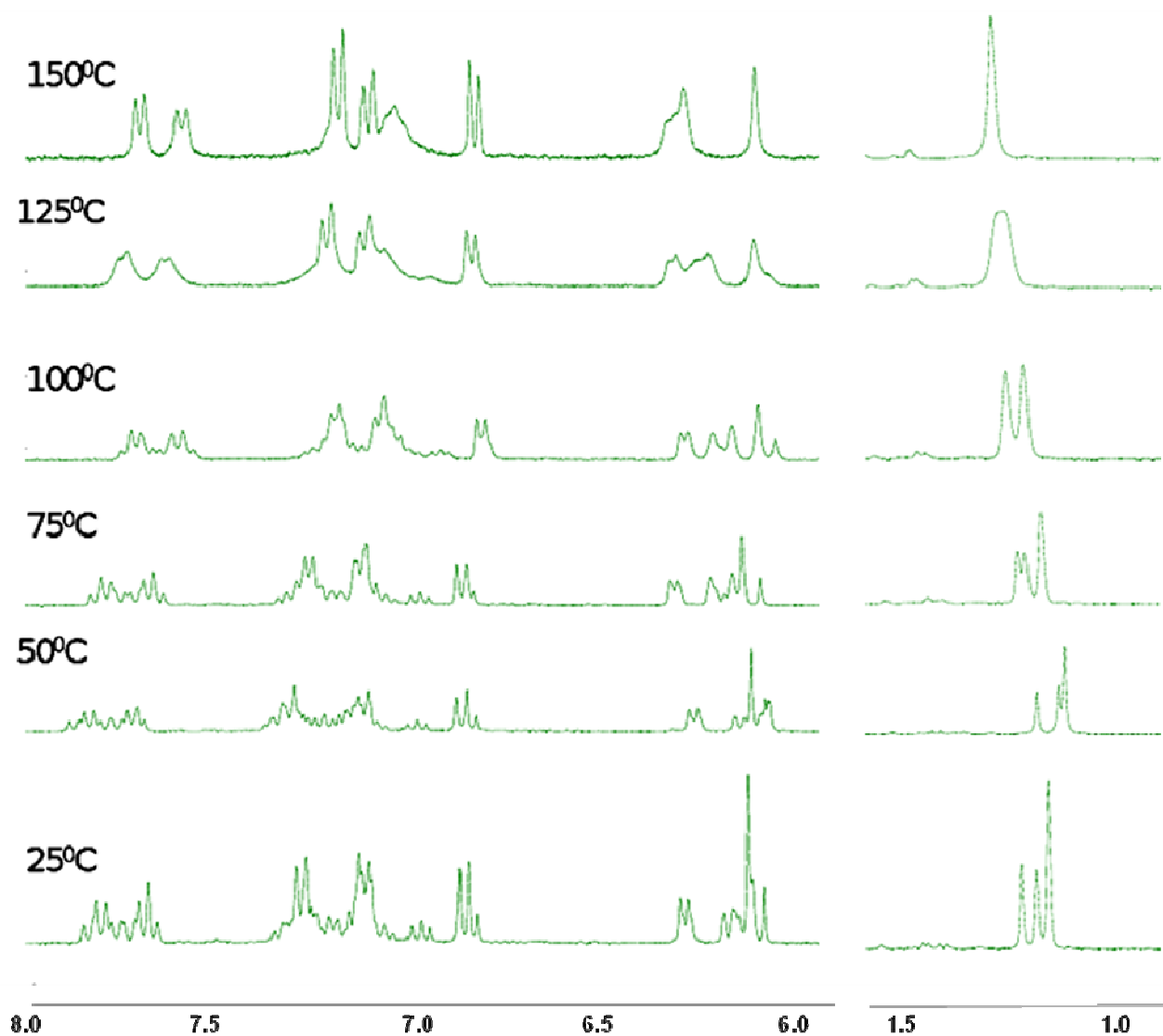


Figure 85. Variable temperature ^1H NMR spectrum of compound **65** displaying the peaks in top aliphatic (1.5 to 1.0 ppm) and aromatic (8.0 to 6.0 ppm) range.

The Scholl reaction of compound **65** was predicted to form 3 to 6 new C-C bonds (**Figure 86**), first between the central benzene ring and position 2 of each naphthalene part, and maybe then between the position 3 of each naphthalene and the phenyl ring of its adjacent blade. Unfortunately after several Scholl reactions in usual conditions but varying the reaction time,

very complex mixtures were obtained and not any major product was clearly identified, making us think that some rearrangements occurred again.

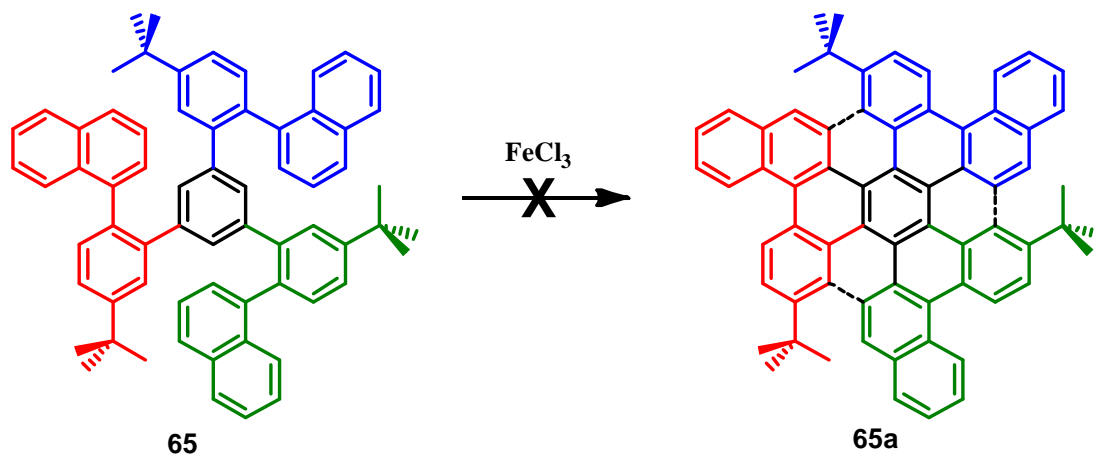


Figure 86. Scholl reaction of compound **65**. $FeCl_3$ in $MeNO_2/CH_2Cl_2$, RT, 1.5h (Complex mixture).

Intramolecular rearrangements when trying to form [6]helicenes by Scholl reaction have already been reported⁶ and our results unfortunately confirm that this reaction may not be suitable to make helicenes with more than five benzene rings in the helix.

4.4 Scholl reaction on TMS bearing precursors.

Given the surprising rearrangements observed during the Scholl reaction of precursors **59** and probably compounds **62** and **65**, we were intrigued to find out whether such reactions also occurred, but with no visible consequences, when cyclizing the fully symmetrical propeller-shaped *t*-Bu₆-HBTP **28**. In order to dissymmetrize its flexible precursor **27** without changing the global shape of the molecule, we coupled 4-(trimethylsilyl)phenylboronic acid **66** on tris-triflate compound **57** to obtain the flexible substrate **67**. Substrate **67** differs from **27** only by the replacement of three carbons by three silicon atoms. The Scholl reaction of this TMS-substituted compound **67** leads as expected (with a comparable yield) to another propeller-shaped HBTP **68**, still bearing six tetrahedral substituents (**Figure 87**).

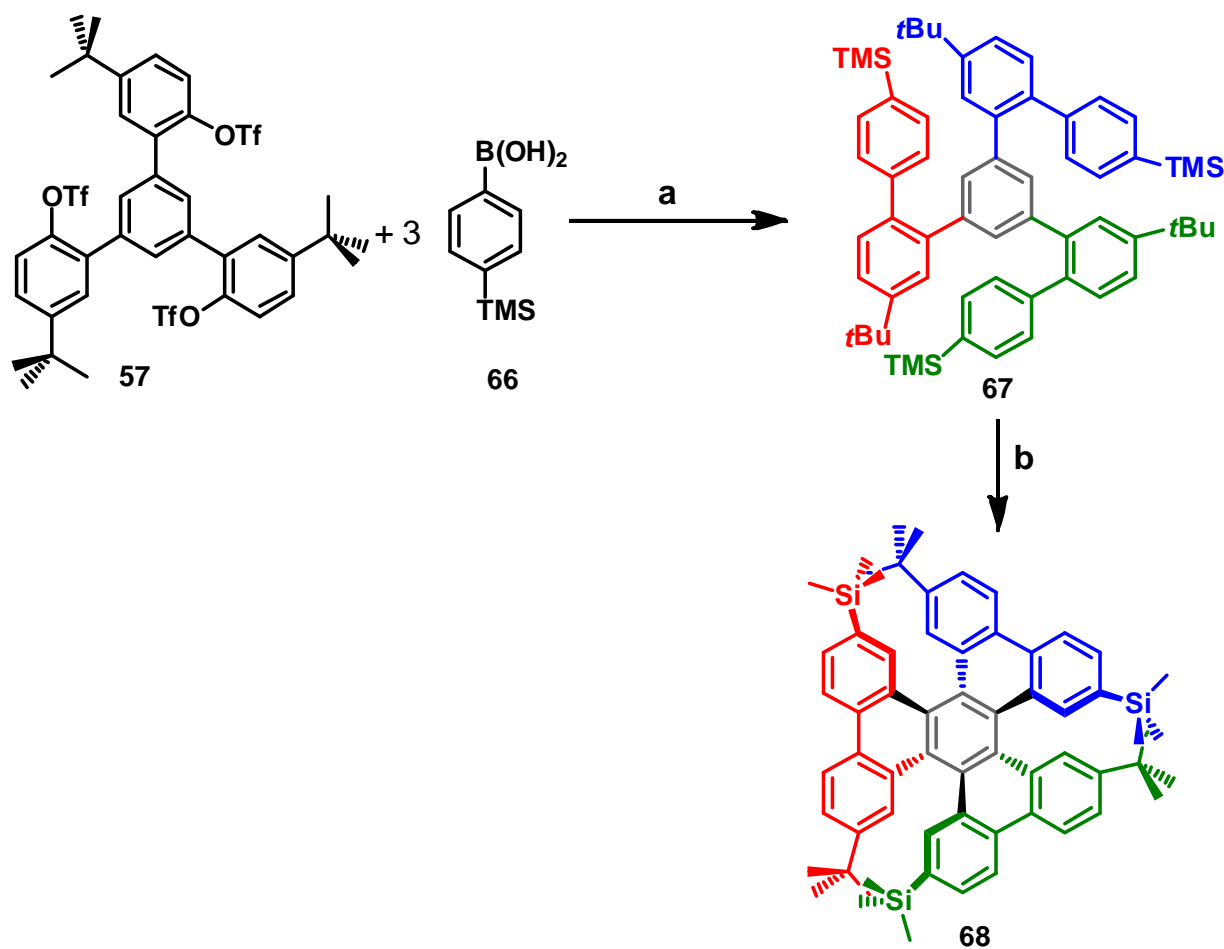


Figure 87. Synthesis and Scholl reaction of TMS-substituted precursor **67**. (a) $\text{Pd}(\text{OAc})_2$, *SPhos*, K_3PO_4 in $\text{THF}/\text{H}_2\text{O}$, 67°C , 48h, 96%. (b) FeCl_3 in $\text{MeNO}_2/\text{CH}_2\text{Cl}_2$, RT, 1.5h, 65%.

This new oligoarene **68** has been crystallized as a racemic mixture, and analyzed by single crystal X-ray diffraction. The propeller shape of **68** has thus been confirmed (**Figure 88**) but the TMS and *t*-Bu groups are indistinguishable in the crystal structure because of orientational disorder of the molecules in the unit cell (quaternary C from *t*-Bu and quaternary Si from TMS show 50/50 occupancy). Nevertheless, the extreme simplicity of the ^1H NMR spectrum of **68** (only 6 aromatic and 2 aliphatic signals) can only be assigned to a highly symmetrical molecule, i. e. a C_3 symmetrical product, showing that no rearrangement occurred during the Scholl reaction.

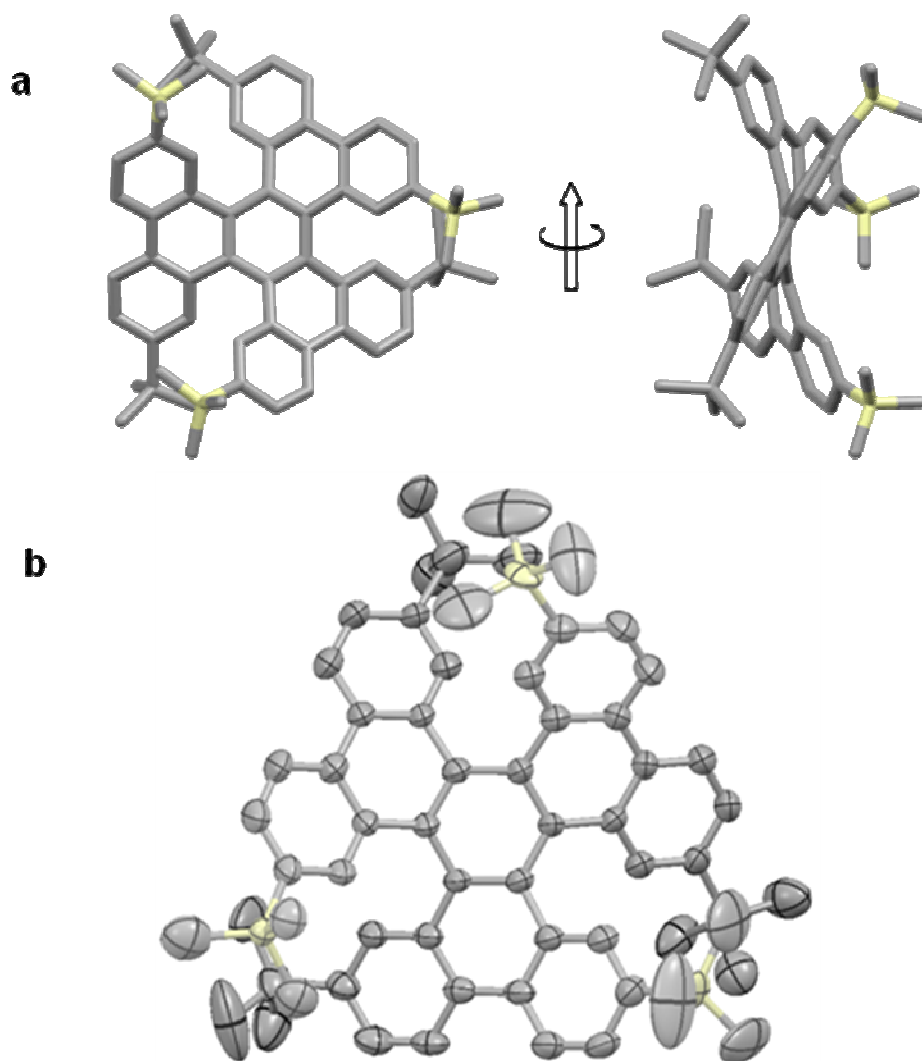


Figure 88. (a) Two different views of the crystal structure of triply helicenic TMS-bearing hexabenzotriphenylene **68**. (b) ORTEP-type view of **68** at 120 K with thermal ellipsoids at 50 % probability level. Only one of two molecules present in the asymmetric unit shown. Hydrogen atoms and CH_2Cl_2 solvent molecules are omitted for clarity.

The compatibility with TMS groups of this Scholl reaction is also noteworthy as no other examples are known within the literature.

To investigate this compatibility more and to check if TMS-substituted substrates obey to the same reactivity rules as their *tert*-butylated counterparts, we synthesized pentaphenylene **73** (**Figure 89**) following a similar strategy used for tri-substituted substrates **57**.

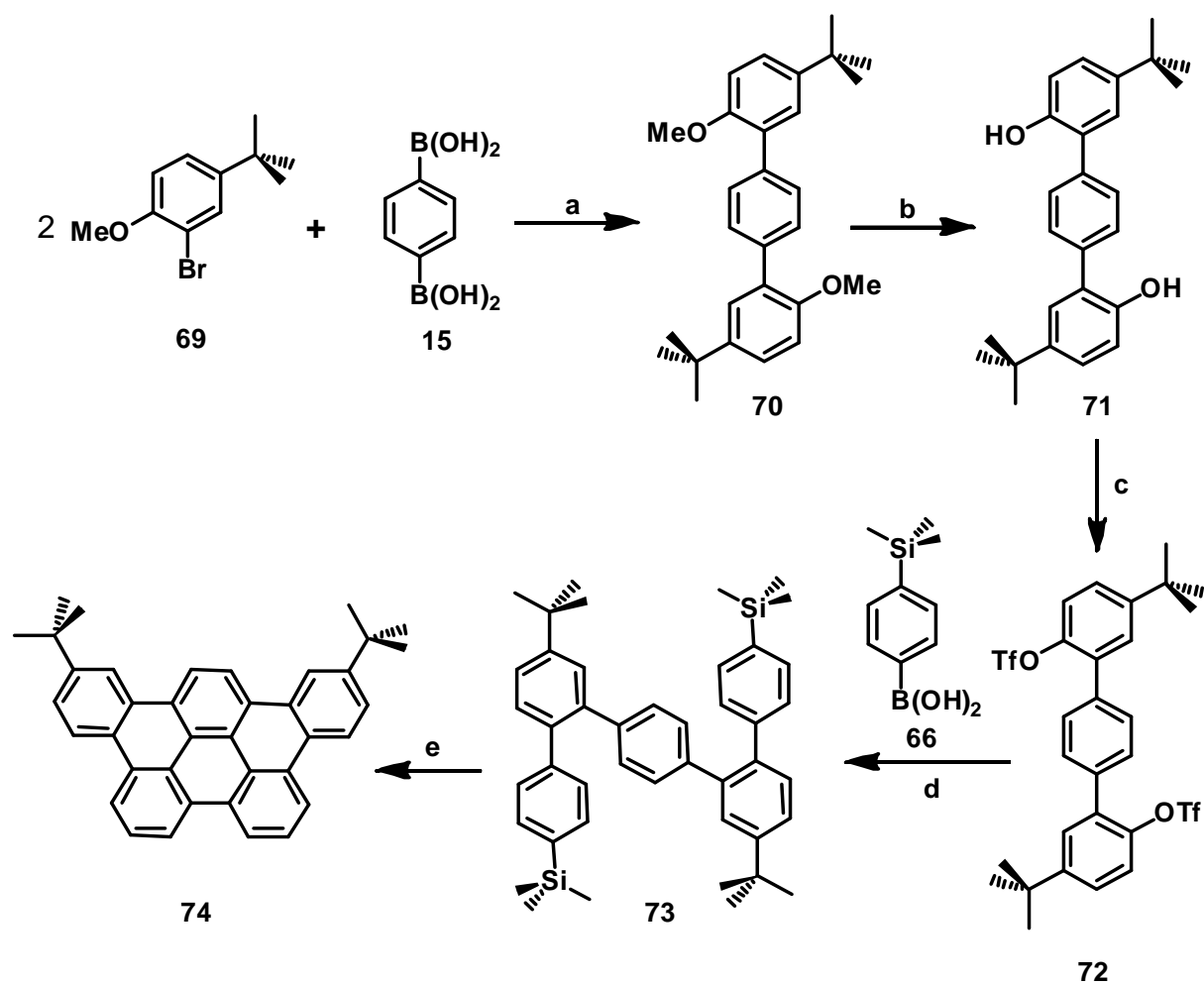


Figure 89. Synthesis and reactivity in Scholl conditions of TMS-bearing pentaphenylene **73**.
 (a) Na_2CO_3 , $\text{Pd}(\text{PPh}_3)_4$ in $\text{PhMe}/\text{H}_2\text{O}/\text{EtOH}$, 90°C , 48h, 90%. (b) BBr_3 in CH_2Cl_2 , RT, 16h, 99%. (c) Tf_2O , pyridine in CH_2Cl_2 , RT, 16h, 95%. (d) $\text{Pd}(\text{OAc})_2$, *SPhos*, K_3PO_4 in $\text{THF}/\text{H}_2\text{O}$, 67°C , 48h, 90%. (e) FeCl_3 in $\text{MeNO}_2/\text{CH}_2\text{Cl}_2$, RT, 1.5h, 91%.

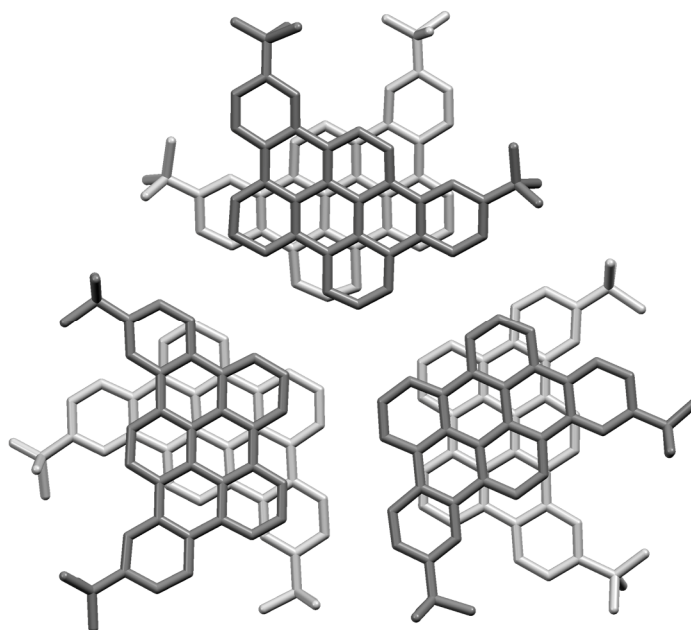


Figure 90. Crystal structure of flat oligoarene **74**.

Contrary to pentaphenylene **16** which mainly leads to [5]helicene **18** by Scholl reaction (**Figure 46**), the silylated version **73**, under the same conditions, very quickly loses its two TMS groups and fully cyclizes to give the flat oligoarene **74** (**Figure 89**), whose structure was perfectly determined by NMR, mass spectrometry and even single crystal X-ray crystallography (**Figure 90**). The compatibility of TMS groups with the Scholl reaction cannot be generalized since they may also be expelled in favor of certain bond formations.

4.5 Synthesis of a soluble hexabenzocoronene.

Scholl cyclizations of 1,3,5-tris(2-biphenyl)ylbenzene species have already been studied by Müllen's group⁷ but were only successful in the case of unsubstituted flexible precursors, or with iodides on non-hindering positions. When these deactivating iodides are located on hindering positions, the reaction remains incomplete.

The triple Suzuki cross-coupling reaction of tris-triflate **57** with simple phenylboronic acid **75** gives the flexible precursor **76**, with only three *tert*-butyl substituents located on hindered positions. Submitted to Scholl reaction conditions, this molecule fully cyclizes by forming six C-C bonds, in a good yield (72%) to give 1,7,13-tri-*tert*-butylhexabenzocoronene **77** (**Figure 91**). This hexabenzocoronene, triply substituted by very bulky groups in bay regions has been

unambiguously characterized by mass spectrometry, ^1H and ^{13}C -NMR. Unfortunately we were not able to grow crystals suitable for X-ray analysis to determine the solid state structure. In fact, this undoubtedly distorted oligoarene shows unusually high solubilities in many organic solvents compared to other flat hexabenzocoronenes.

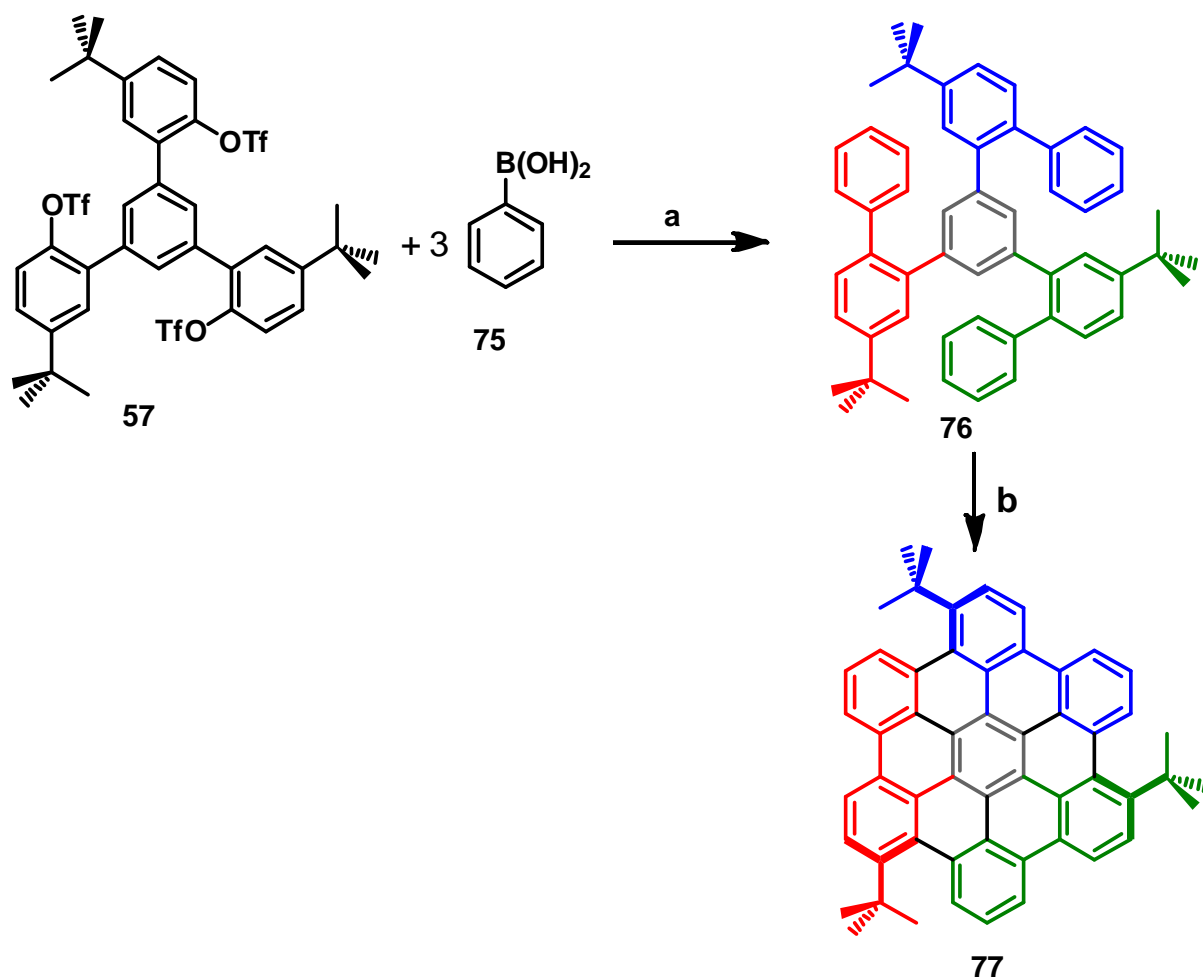


Figure 91. Synthesis and Scholl reaction of TMS-substituted precursor 76.

(a) $\text{Pd}(\text{OAc})_2$, *SPhos*, K_3PO_4 in $\text{THF}/\text{H}_2\text{O}$, 67°C , 48h, 98%. (b) FeCl_3 in $\text{MeNO}_2/\text{CH}_2\text{Cl}_2$, RT, 1.5h, 72%.

When attempting to crystallize hexabenzocoronene **77**, we could obtain a few single crystals from a crystallization tube containing an impure fraction of **78** (about 10% impurities). Disappointingly, X-ray analysis revealed that these crystals were only composed of unexpected rearranged products **79** and **80** (**Figure 93**), co-crystallizing together (in a 3:2 ratio). In this case, again, one blade migrates onto an adjacent carbon of the central benzene ring to form the usual [5]helicene. In addition the *t*-Bu group on the fully cyclized third blade is removed and replaced by a chlorine (**80**) or two opposite hydroxyl groups (**79**) (**Figure 92**). Such a loss of a *t*-Bu group on the symmetrical main product **78** and the presence of **79** and **80** has also been observed by mass spectrometry.

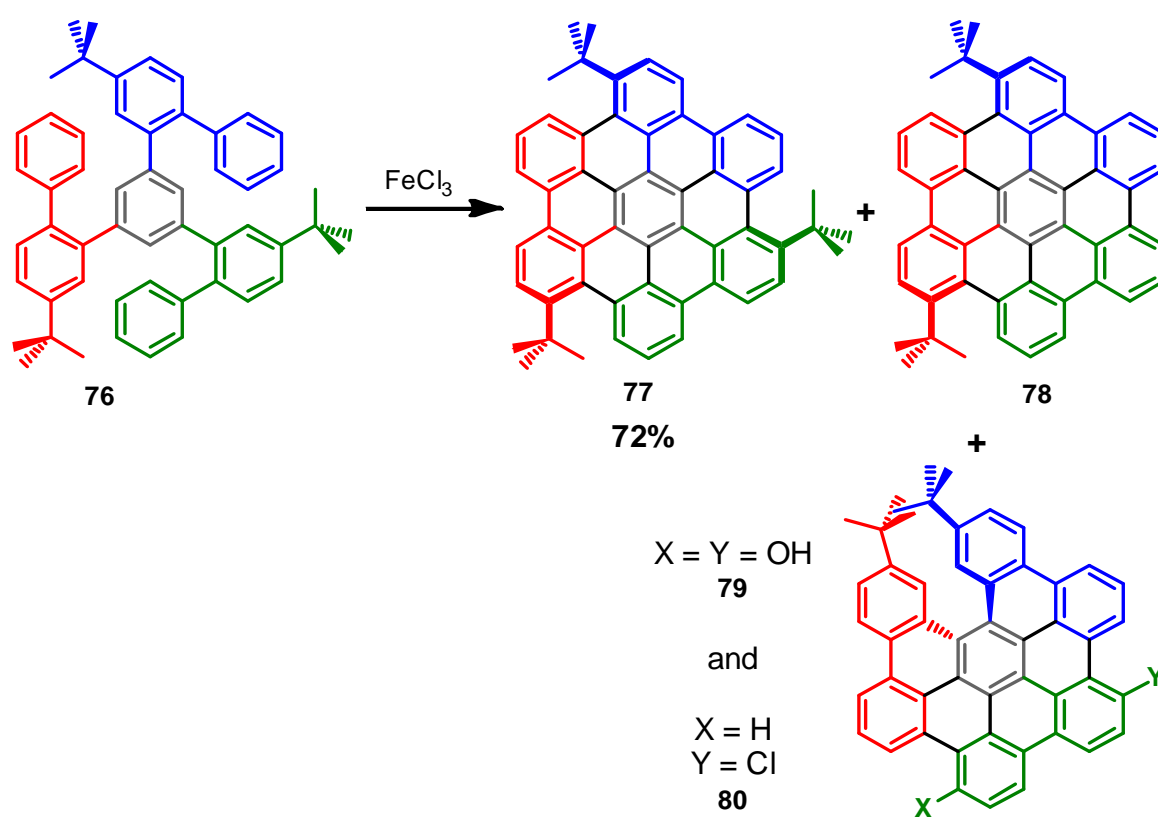


Figure 92. Scholl reaction of **76** also gives traces of rearranged compounds **78**, **79**, **80**.

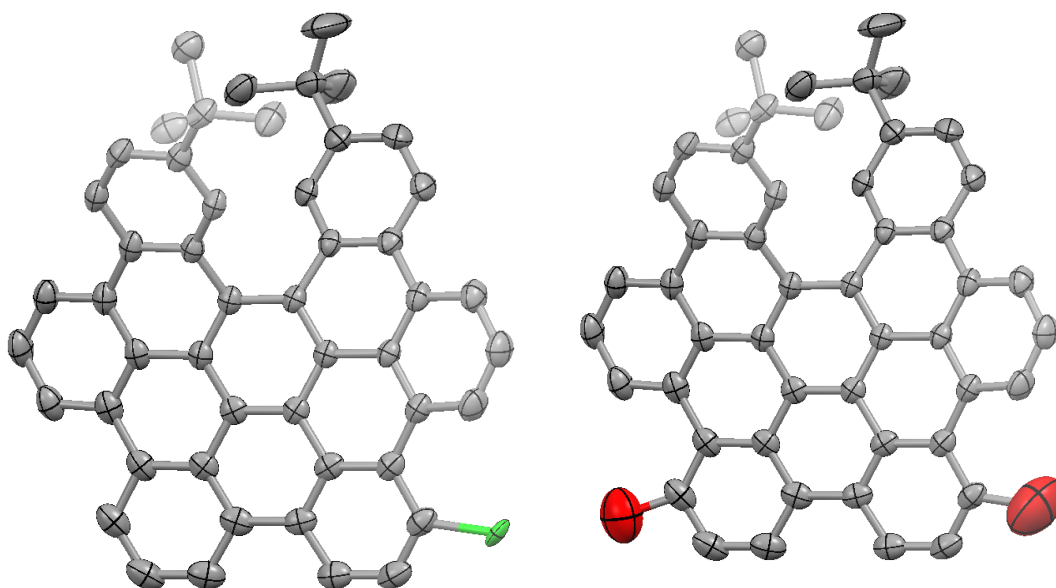


Figure 93. ORTEP-type view of **79** (left) and **80** (right) as found in **79-80** at 120 K with thermal ellipsoids at 50 % probability level. Carbon, chlorine and oxygen atoms are represented in grey, green and red. Note that these two molecules occupy the same position in the crystal structure with relative occupancies of 0.6/0.4. Only one of the two positions of the disordered *t*-butyl groups is represented. Hydrogen atoms are omitted for clarity.

We developed a versatile synthetic technique for the formation of a family of flexible yet strongly crowded C_3 -symmetrical poly-aromatic chains as substrates for graphitization by intramolecular Scholl reaction. We found that the formation of [6]helicenes appears precluded with this approach because of surprising rearrangements leading to hexa[7]circulene species. Nevertheless, under the same conditions, strongly congested [5]helicenes with bulky groups on hindered positions seem to be highly favored even when a labile TMS group replaces one of the two *t*-Bu substituents. Finally, a distorted and soluble bay-substituted hexabenzocoronene can efficiently be synthesized by Scholl reaction on a tris(biphenyl)ylbenzene precursor bearing three activating *t*-Bu groups on congesting positions.

4.6 References.

1. A. Pradhan, P. Dechambenoit, H. Bock, F. Durola, *Angew. Chem. Int. Ed.* **2011**, *50*, 12582.
2. (a) J. A. Bryant, R. C. Helgeson, C. B. Knobler, M. P. deGrandpre, D. J. Cram, *J. Org. Chem.* **1990**, *55*, 4622. (b) M. Turlington, A. M. DeBerardinis, L. Pu, *Org. Lett.* **2009**, *11*, 2441.
3. S. D. Walker, T. E. Barder, J. R. Martinelli, S. L. Buchwald, *Angew. Chem. Int. Ed.* **2004**, *43*, 1871.
4. (a) J. H. Dopper, D. Oudman, H. Wynberg, *J. Org. Chem.* **1975**, *40*, 3398. (b) P. Sarkar, P. Dechambenoit, F. Durola, H. Bock, *Asian J. Org. Chem.* **2012**, *1*, 366.
5. E. Ullah Mughal, D. Kuck, *Chem. Commun.* **2012**, *48*, 8880
6. M. Müller, V. S. Iyer, C. Kübel, V. Enkelmann, K. Müllen, *Angew. Chem. Int. Ed.* **1997**, *36*, 1607.
7. X. Feng, J. Wu, V. Enkelmann, K. Müllen, *Org. Lett.* **2006**, *8*, 1145.

Chapter V: Twisted Carbon Nanoribbons.

The initial project of my PhD thesis was the organic synthesis of soluble GNRs (**Figure 44**). For that purpose we did several test reactions (**Figures 46 and 94**) but we surprisingly observed some unexpected regioselectivity of the Scholl reaction. We then planned to take advantage of this unusual reactivity and to explore this new path of access to highly distorted polycyclic aromatic cores. We have turned our attention to molecules incorporating several helicene parts and successfully prepared hexabenzotriphenylene (HBTP) **28**, which is the smallest aromatic core that includes three [5]helicene units. After that we tried to use this regioselectivity to synthesize higher ordered helicenes but instead we observed some rearrangements (**Figure 79**), making us think that higher order helicene formations seem impossible with this strategy.

Nevertheless, we did not give up our initial goal and we then planned to focus on the synthesis of helicene-incorporating carbon nanoribbons, that is to say twisted GNRs.

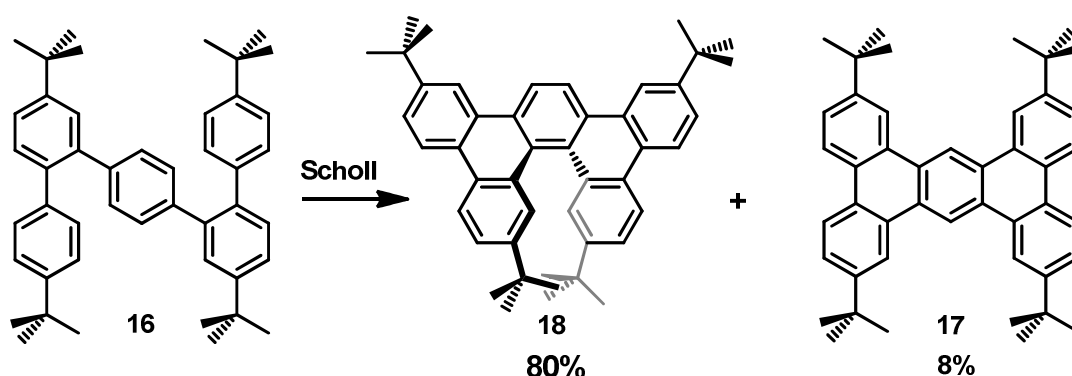


Figure 94. Unexpected regioselectivity of the Scholl reaction, leading to distorted arenes.

5.1. Design of the twisted carbon nanoribbons.

The simplest [5]helicene motif accessible by such a Scholl reaction is the dibenzo-picene **18** (**Figure 95**). On this compound, some additional functionalization can be imagined on the two lateral biphenyl fragments. In fact, by a mind view, if several **18** units are fused together, having in common one biphenyl part with each adjacent unit, this would lead to a linear chain of fully conjugated upside down [5]helicenes. (**Figure 95**).

Two lateral positions for additional functionalizations:

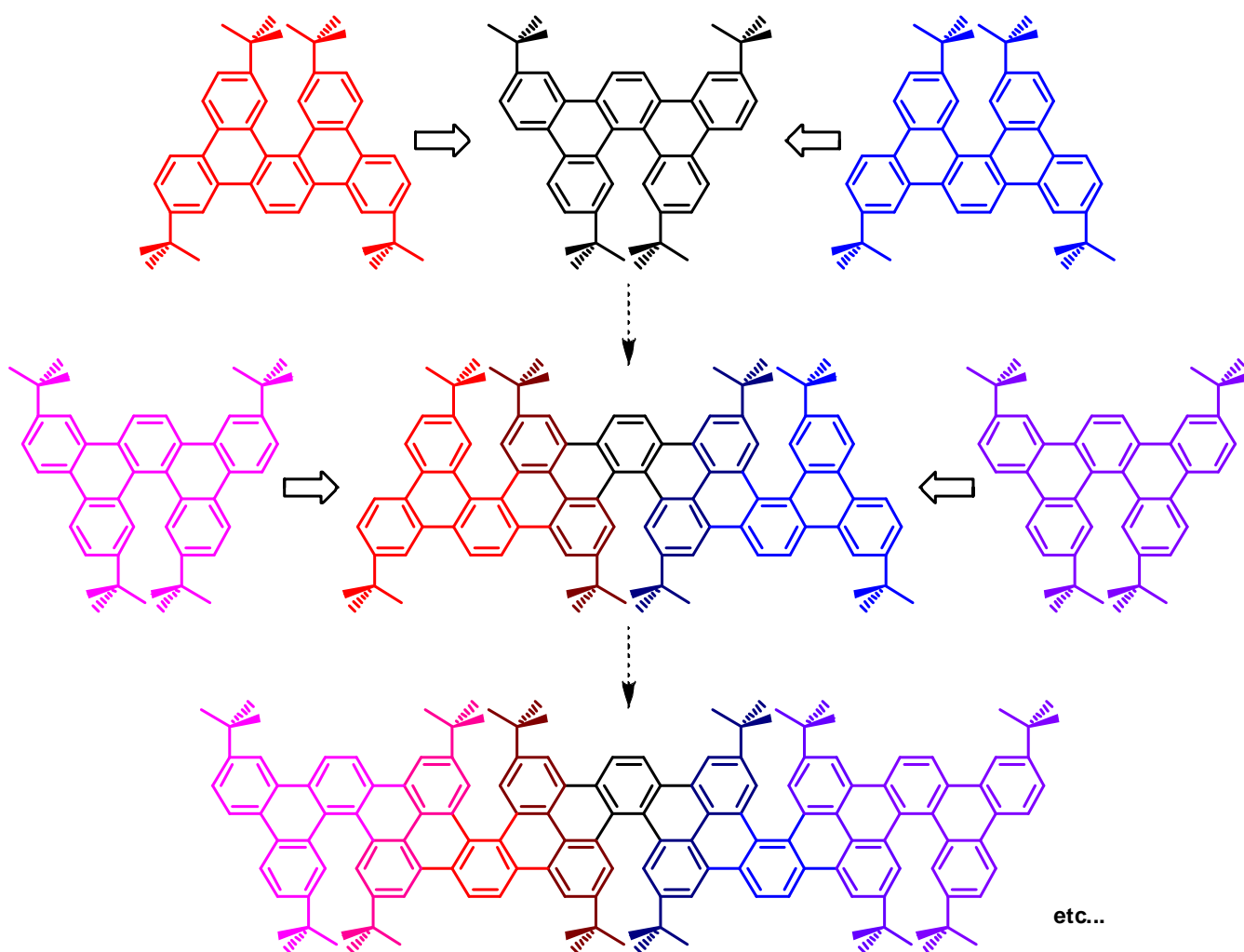
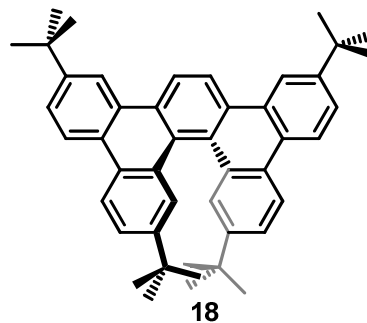


Figure 95. Design of twisted carbon nanoribbons with compound **18** as a repeat unit.

The first part of the retrosynthetic study is to determine which C-C bonds should be formed by Scholl reaction during the last step. In this case, by considering the previous results on

dibenzopicene **18**, it is obvious that on each helicene unit of a ribbon the same central bonds should be formed (**Figure 96**). It is now interesting to consider the corresponding flexible precursors and realize that they are in fact oligomers with a linear di-tert-butyl-triphenyl unit as a monomer (in blue on **Figure 96**).

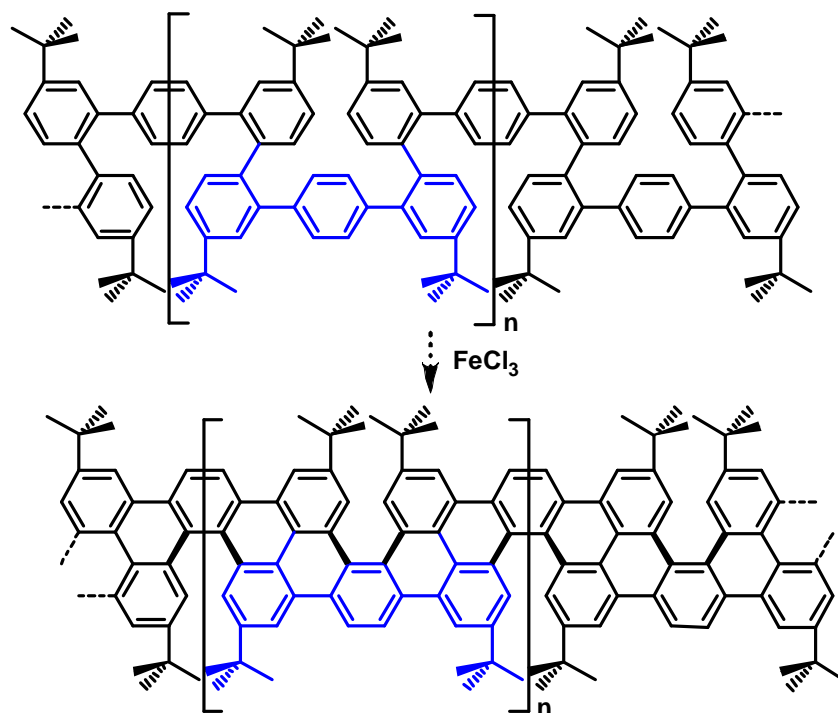


Figure 96. Twisted carbon nanoribbons.

We could observe during the Scholl reaction of the penta-phenylene compound **16** that the transoid double cyclization, giving the flat tetrabenzanthracene **17**, is still possible with a low yield of 8% (**Figure 94**). Nevertheless, this transoid reaction will become much more problematic on the flexible oligomers to make homogeneous twisted carbon nanoribbons. For this reason, we decided to change the structure of the monomer and to replace the central para-phenylene fragment by a 1,4-naphthylene, where two adjacent positions are now protected, leaving only one possibility for the double cyclization reaction (**Figure 97**).

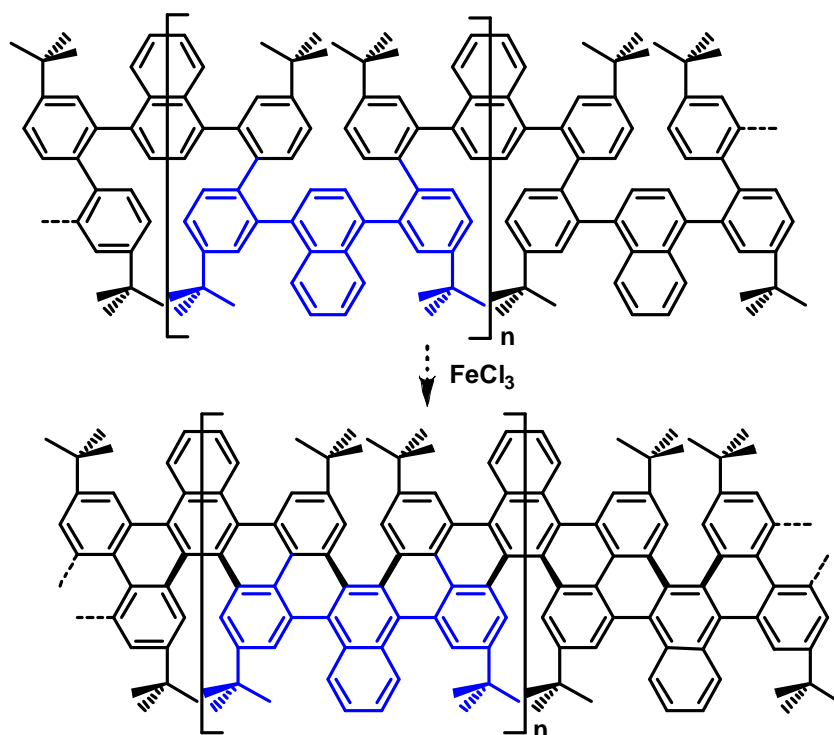


Figure 97. New design of the twisted GNRs, with protected cyclization positions (one monomer is drawn in blue).

5.2. Test reaction on the monomer, synthesis of ^tBu₄-tribenzopicene.

In order to be sure that the naphthalene does not change the reactivity, compared to the benzene fragment, during the Scholl reaction, it was necessary to do a test reaction on the precursor (**82**) of the “shortest twisted carbon nanoribbon”, that is to say a flexible chain composed of one monomer functionalized with two para-tert-butylphenyl groups as ending fragments.

The Suzuki coupling of commercially available 1,4-dibromo-naphthalene **81** with previously synthesized boronic ester **5b** under classical conditions with Pd(PPh₃)₄ as a catalyst gave compound **82** after 2 days in 90% yield (**Figure 98**). Interestingly, after only 16 hours with these classical Suzuki conditions, the reaction only produces the asymmetrical mono reacted compound **84** (**Figure 105**).

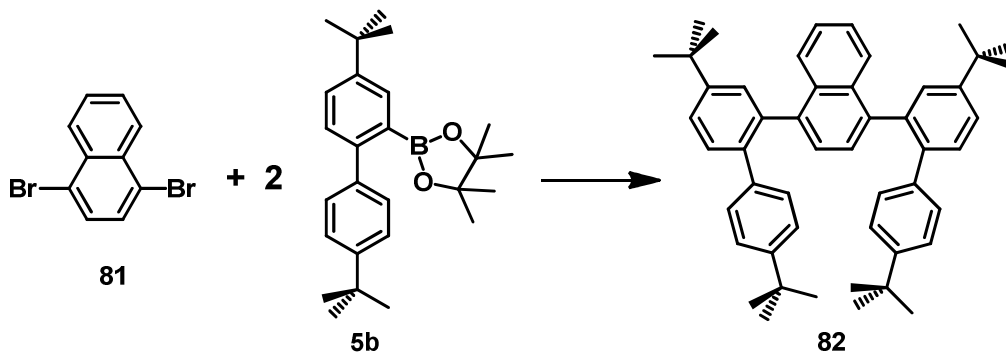


Figure 98. Synthesis of flexible precursor **82**: $Pd(PPh_3)_4$, Na_2CO_3 in Toluene/EtOH/ H_2O , $90^\circ C$, 48h, 90%.

The purification of compound **82** by column chromatography was nevertheless a little confusing because two distinct luminescent spots could clearly be seen on TLC but they were impossible to separate by this technique. In addition, the 1H -NMR spectrum of the mixture of these two products looks like the spectrum of an isomer mixture since several peaks seem doubled (**Figure 99**), but an isomerization reaction is hardly imaginable in such conditions. The only explanation is that compound **82** has two different stable conformers at room temperature and on NMR timescale, that can exchange with each other on a chromatography timescale, which would justify that they are not separable. This hypothesis has been confirmed by a square TLC analysis.

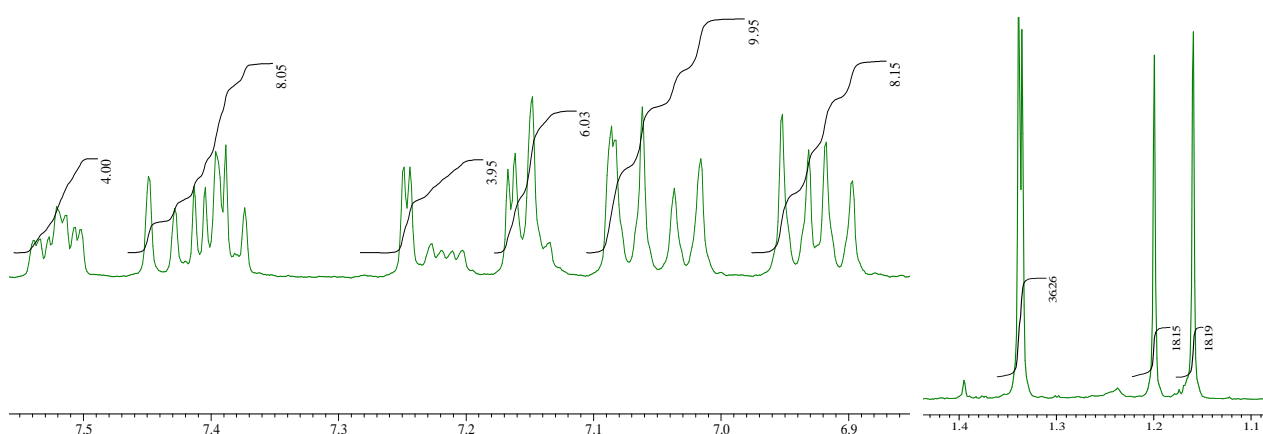


Figure 99. 1H NMR spectrum of compound **82** displaying the peaks in aliphatic (1.4 to 1.1 ppm) and aromatic (7.6 to 6.8 ppm) range.

Explanation of the square TLC technique:

The sample is spotted at one corner of a square TLC plate which is first developed in one direction, air-dried, then rotated by 90° and eluted a second time (**Figure 100**). It is also possible to gently heat the plate after the first elution to accelerate the possible reactions and exchanges happening on silica. Usually, three situations are then possible:

- If there are only spots on the diagonal then the elution is reproducible and no reaction or exchange occurred on silica.
- If there is a spot on one side of the diagonal, corresponding to a spot giving the other one before the 2nd elution, then this first product is probably unstable on silica and the second one is the degradation product.
- If there are spots on both sides of the diagonal, and if the plate is symmetrical according to this diagonal then both compounds are exchanging with each other between the two elutions. This is usually the case of isomerizations or conformational exchanges.

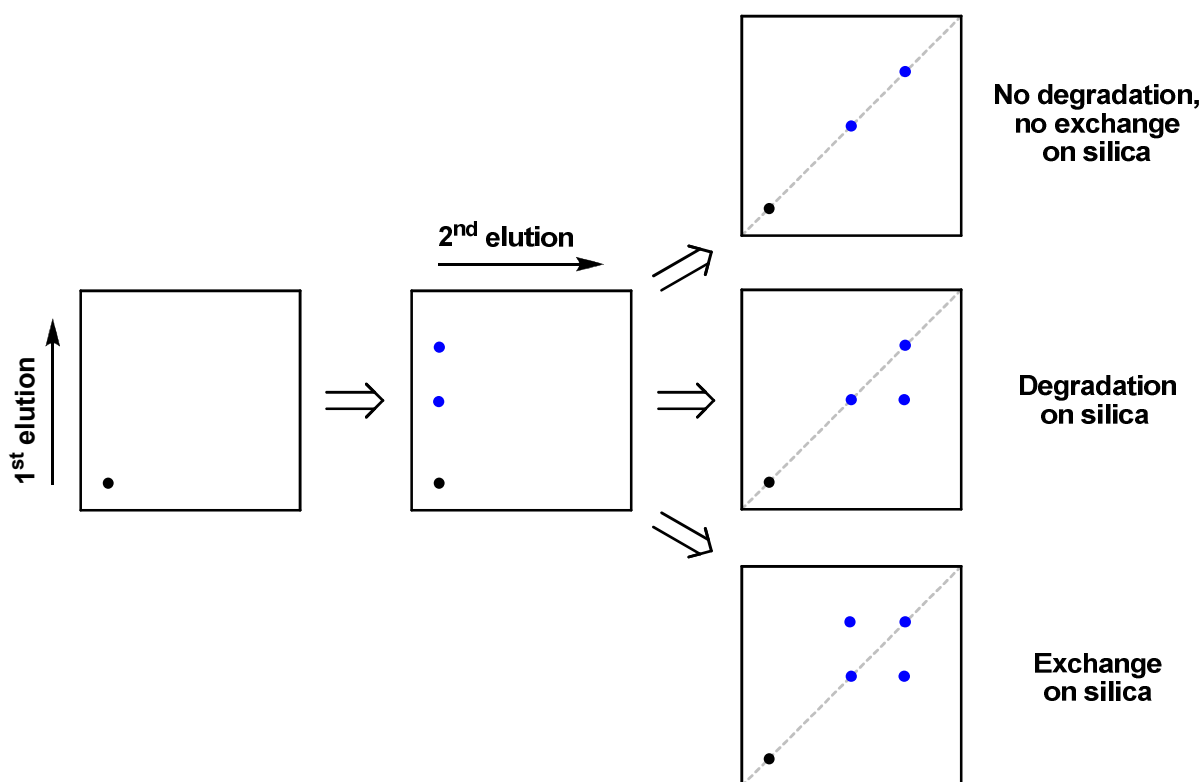


Figure 100. Schematic presentation of the principle of a square TLC.

In the present case, the third situation, corresponding to chemical exchanges on silica, has very clearly been observed (**Figure 101**), confirming that compound **82** presents two stable conformers.

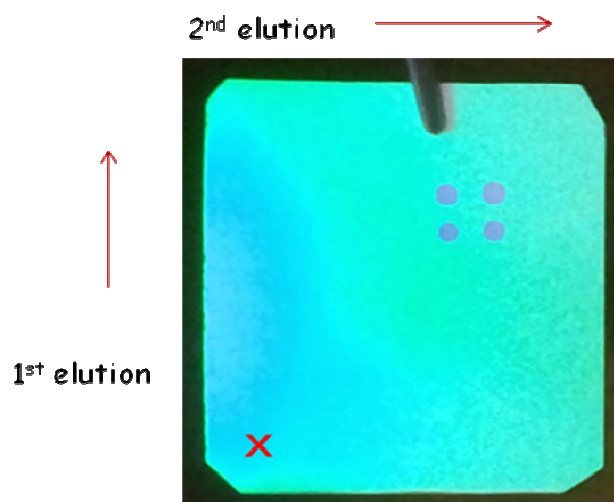


Figure 101. Chemical exchange between two conformers of compound **82** on silica.

Intramolecular Scholl reaction of flexible precursor **82** with FeCl_3 at 0°C (15 minutes) provided very efficiently (95% yield) the single [5]helicene **83**, which can be seen as a monomer of the targeted graphene nanoribbons (**Figure 102**). This compound has been fully characterized by NMR and mass spectrometry.

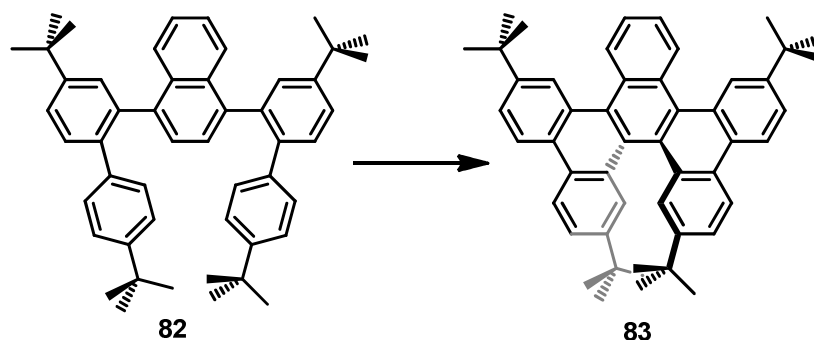


Figure 102. Synthesis of [5]helicene **83**: FeCl_3 , $\text{MeNO}_2 + \text{CH}_2\text{Cl}_2$, Ar bubbling, RT, 15 minutes, EtOH, 95%.

Compound **83** is well soluble in common organic solvents, such as THF, toluene and dichloromethane. The good solubility can be attributed to the introduction of t-butyl groups on the aromatic periphery and to the non planar geometry that avoids π -stacking and reduces aggregation in solution.

In spite of its very good solubility in many solvents, monocrystals of **83** could be obtained as large yellow needles by slow diffusion of methanol in cyclohexane. Analysis by X-ray diffraction of these crystals has been possible and evidenced the distortion of the molecules of **83** in the solid state. Surprisingly, these molecules are not at all symmetrical in this crystal phase. In fact, a biphenyl unit on one side is strongly bent whereas the one on the other side stays straight. This allows the naphthalene part to bend, not to twist, with the two bulky tert-butyl groups on the same side (**Figure 103**).

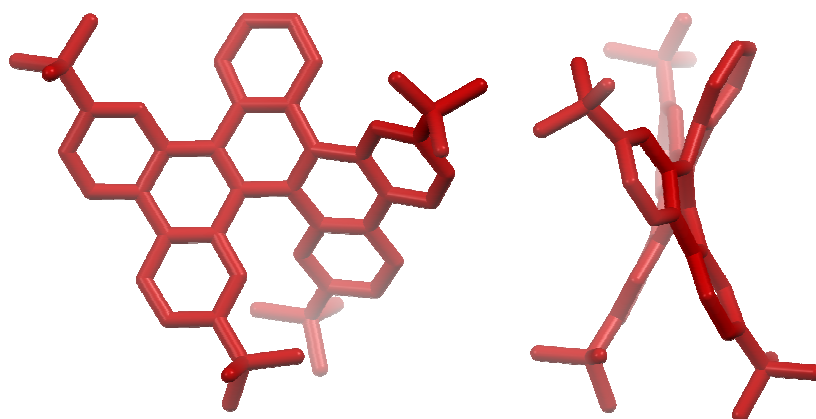


Figure 103. Crystal structure of compound 83 : two different views of a single molecule.

5.3. Synthesis of the dimer.

The first test reaction being a success, a second one was necessary in our opinion to prove that a doubly substituted di-tert-butyl-biphenyl unit reacts correctly –without rearrangements– in Scholl conditions. For this reason, we also decided to synthesize a dimer (**91**) of the twisted nanoribbons, from its flexible precursor **89** incorporating two naphthalene-based monomers and two ending tert-butylphenyl groups.

Two retro-synthetic ways are possible for the synthesis of the flexible precursor **89**. The faster one would rely on a central bifunctional di-tert-butylbiphenyl but we preferred the second strategy, when the central bond is cut and the final step is a true dimerization, because this approach is closer to what would be done for the synthesis of oligomers (**Figure 104**).

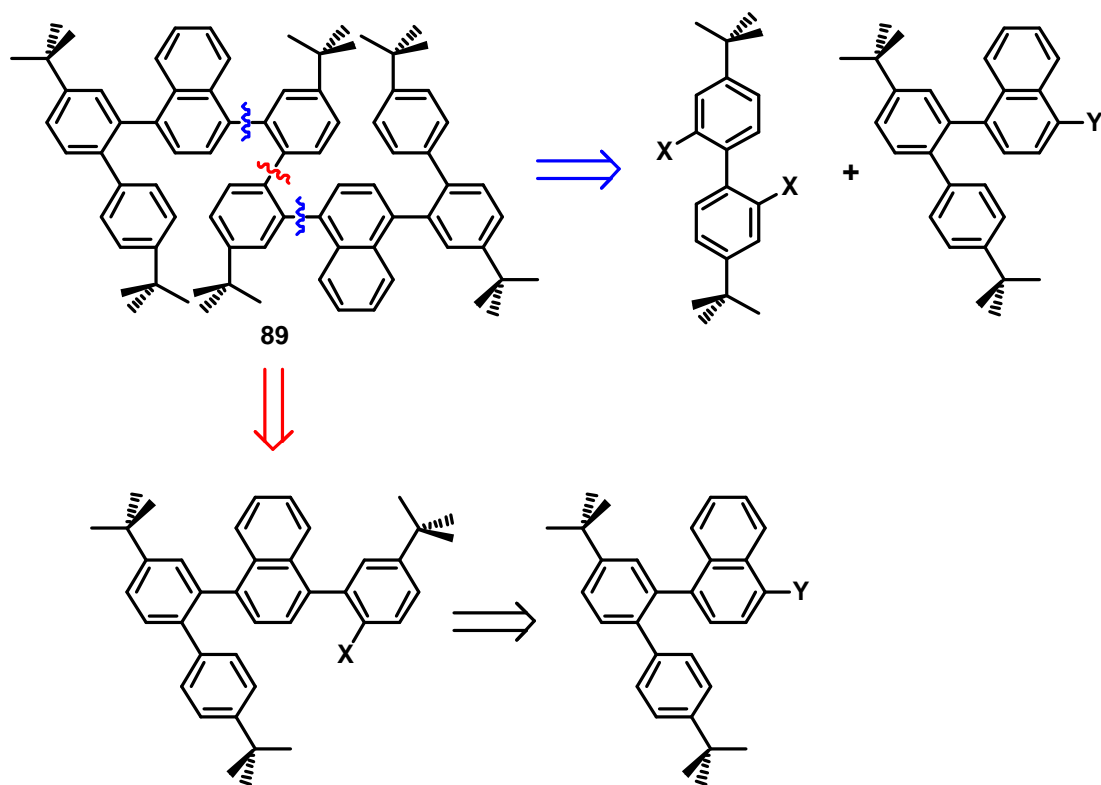


Figure 104. Retro-synthetic strategies for compound **89**.

The formation of the brominated compound **84** relies on a Suzuki coupling mono-reaction of commercially available 1,4-dibromo-naphthalene **81**. As discussed before, the reactivities of the two bromines are not equivalent and this mono-substitution can be done efficiently (75% yield) in classical conditions with the boronic ester **5b**, which was synthesized similarly in two steps following existing procedures (see Chapter II, **Figure 39**). Then another Suzuki coupling of compound **84** with 5-tert-butyl-2-methoxyphenylboronic acid **34** under classical conditions with $\text{Pd}(\text{PPh}_3)_4$ as a catalyst gave the methoxy substituted compound **85** in 95% yield. The methoxy group is then deprotected by action of BBr_3 , leading quantitatively to the phenolic intermediate **86**, whose phenol function is then transformed into a triflate group by action of triflic anhydride in usual conditions to give the precursor **87** in excellent yield (92%). The conversion of the aryl triflate **87** to the boronic ester **88** was carried out by Miyaura coupling reaction of the triflate with bis(pinacolato)diboron using $\text{PdCl}_2(\text{dppf})$ as a catalyst with KOAc as a base (**Figure 105**).

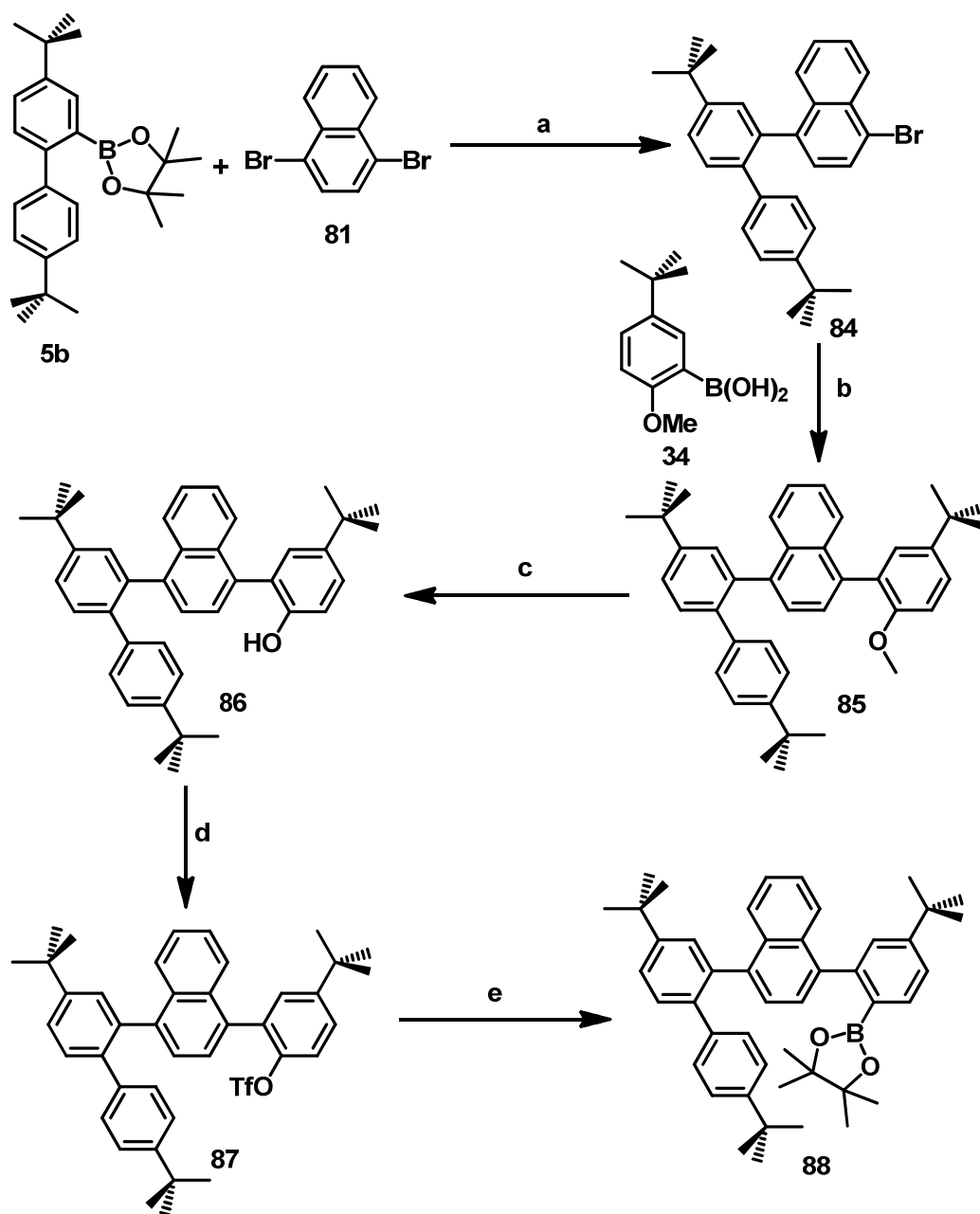


Figure 105. Syntheses of hindered triflate and boronic ester compounds **87** and **88**.

(a) Na_2CO_3 , $\text{Pd}(\text{PPh}_3)_4$ in $\text{PhMe}/\text{H}_2\text{O}/\text{EtOH}$, 90°C , 24h, 75%. (b) Na_2CO_3 , $\text{Pd}(\text{PPh}_3)_4$ in $\text{PhMe}/\text{H}_2\text{O}/\text{EtOH}$, 90°C , 24h, 95%. (c) BBr_3 in CH_2Cl_2 , RT, 16h, 90%. (d) Tf_2O , pyridine in CH_2Cl_2 , RT, 16h, 92%. (e) $\text{Pd}(\text{dppf})\text{Cl}_2$, dppf , Bis(pinacolato)diboron, KOAc in $\text{THF}/\text{H}_2\text{O}$, 67°C , 48h, 70%.

Finally, triflate compound **87** has to couple with boronic ester **88** to form the expected dimeric flexible precursor **89**. We were aware of the disfavored conditions for such a coupling with two sterically hindered compounds, but this was even more difficult than what we expected. Several reaction conditions were tried (**Table 3**) unsuccessfully because of the interfering hydrogenation of both triflate and boronic acid which was much faster than the coupling reaction, leading to inert and useless compound **90** (**Figure 106**). After four attempts with different catalytic systems, developed by Buchwald's group¹ and known to react efficiently on hindered positions, we finally found that Pd(OAc)₂ as a palladium source, SPhos as a ligand, K₃PO₄ as a base in a mixture of THF and water are excellent reaction conditions for this kind of highly hindered coupling. In fact, the result is even beyond our expectations since the coupling of compounds **87** and **88** in these conditions leads to the dimeric flexible precursor **89** with a yield of 80%, and no traces of the difficultly separable hydrogenated compound **90**.

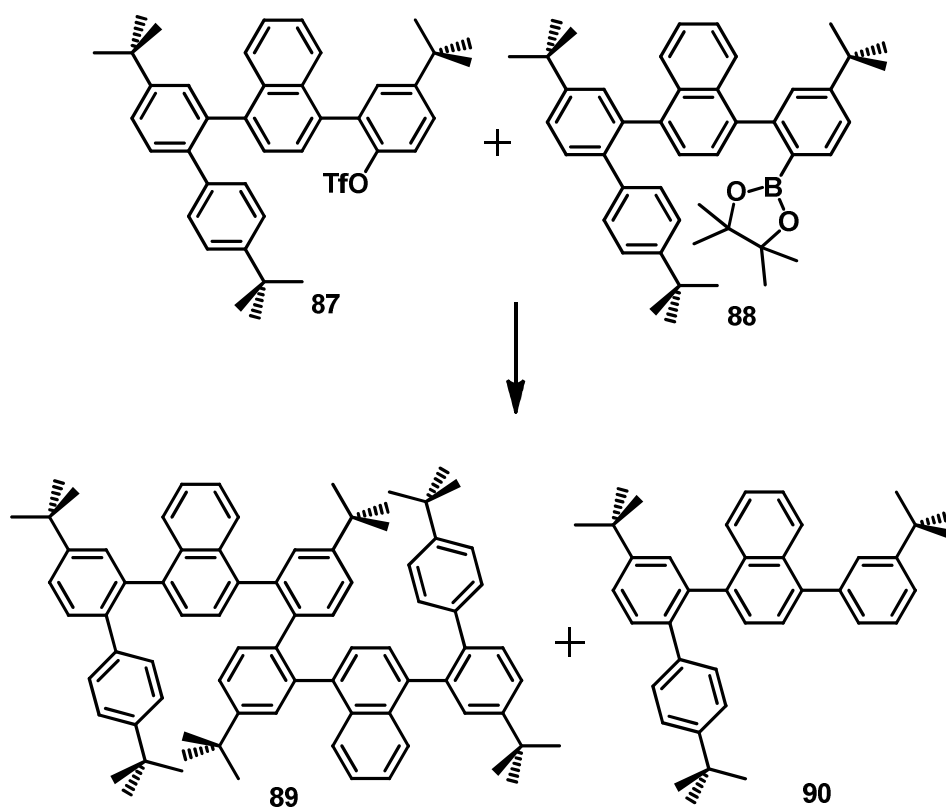
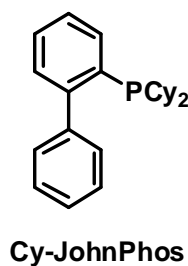
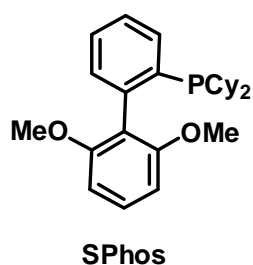


Figure 106. Synthesis of flexible dimer precursor **89**: Pd(OAc)₂, SPhos, K₃PO₄ in THF/H₂O, 67°C, 96h, 80%.

Table 3. Reaction conditions for the synthesis of 89.

Entry	Catalysts & Ligand	Conditions	% 90	% 89
1	Pd(PPh ₃) ₄	Na ₂ CO ₃ , PhMe/H ₂ O/EtOH, 90°C, 96h	85%	/
2	Pd(OAc) ₂ , Cy-JohnPhos	LiOH, THF/H ₂ O, 70°C, 96h	90%	/
3	Pd(OAc) ₂ , Cy-JohnPhos	K ₃ PO ₄ , THF/H ₂ O, 90°C, 96h	80%	/
4	Pd(OAc) ₂ , SPhos	LiOH, THF/H ₂ O, 70°C, 96h	89%	/
5	Pd(OAc) ₂ , SPhos	K ₃ PO ₄ , THF/H ₂ O, 90°C, 96h	/	80%



The conclusion of this is that every detail can be crucial for such difficult reactions. In fact, changing the base or few substituents on the ligand can have drastic effects on the reactivity.

The difficulty when synthesizing the dimer precursor **89** was not only to find the right reaction conditions. In fact, similarly to what was observed on the NMR spectrum of the shortest compound **82**, the very flexible compound **89** presents many stable conformations at room temperature and on the NMR timescale. The result is that **89**'s NMR spectra are absolutely impossible to interpret, except by the measure of the ratio of aromatic versus aliphatic protons. It has been very hard to convince ourselves that the ¹H-NMR spectrum shown on figure 107 was the one of pure compound **89** (as shown on TLC). In addition, usual mass spectrometry techniques (ES, EI, Maldi) are unable to ionize and therefore to analyze cleanly these big and apolar hydrocarbons. Fortunately, the technicians of the analytical platform we are working with (CESAMO, Univ. Bordeaux 1) solved this problem by using an old but very efficient technique of field desorption (FD-MS). With the flexible precursor **89**, only the good signal appeared on its FD-MS spectrum.

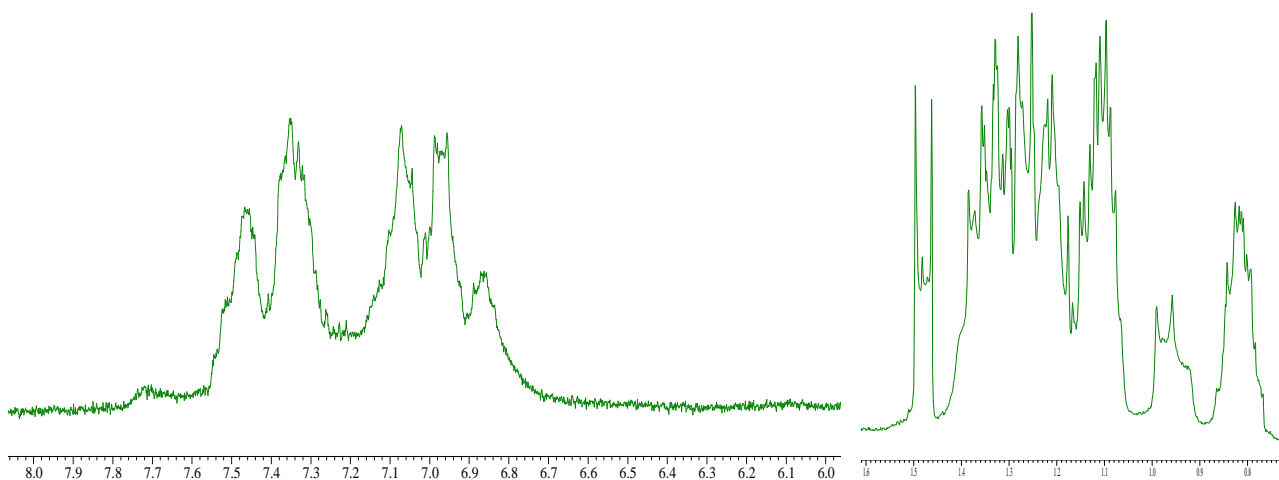


Figure 107. ^1H NMR spectrum of compound **89**; right: aliphatic (0.8 to 1.6 ppm), left: aromatic (6.0 to 8.0 ppm) range.

The flexible precursor **89** was finally submitted to Scholl reaction conditions, with FeCl_3 in dichloromethane and nitromethane at 0°C with argon bubbling for 1 hour. After quenching with methanol, the resulting cyclized products, i.e. dimers of twisted carbon nanoribbons **91** (**Figure 108**), have been obtained in good yield (65%). The purification was done by column chromatography to remove the main impurities which were incompletely reacted compounds, with two missing C-C bonds as shown by mass spectrometry.

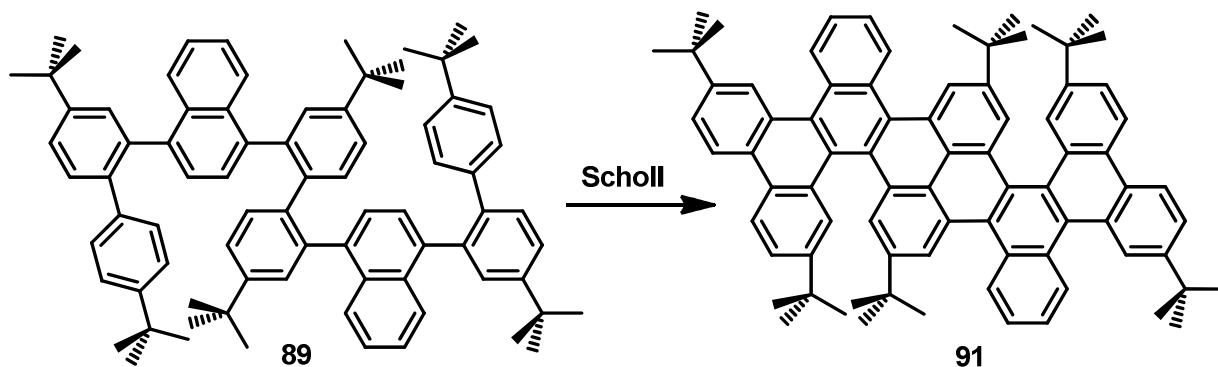


Figure 108. Synthesis of the dimer **91** of twisted GNRs: FeCl_3 , MeNO_2 + CH_2Cl_2 , Ar bubbling, RT, 1h, EtOH, 65%.

Contrary to its flexible precursor **89**, the ^1H -NMR spectrum of the rigidified compound **91** is very simple and can easily be interpreted (**Figure 109**). This is even surprising if we consider-

that compound **91** incorporates two helicenic parts and therefore has three diastereoisomers: the (+ +) and (- -) double helicenes are enantiomers whereas (+ -) and (- +) are the same meso achiral isomer (**Figure 110**) that should have a similar but different NMR spectrum. Yet, the $^1\text{H-NMR}$ spectrum of compound **91** is simple enough to allow us to conclude that the Scholl reaction, in these conditions, has selectively formed either the achiral meso (+ -) compound, or both chiral (+ +) and (- -) enantiomers, but not all of these three stereoisomers.

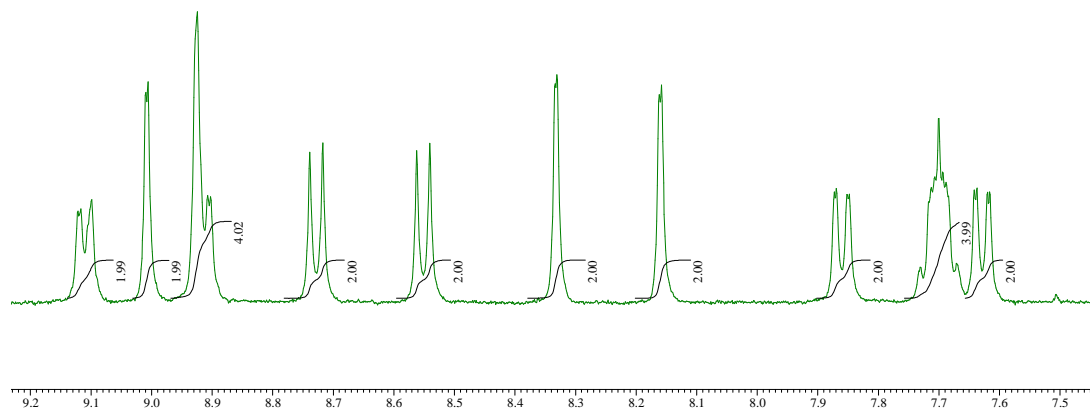


Figure 109. ^1H NMR spectrum of compound **91**.

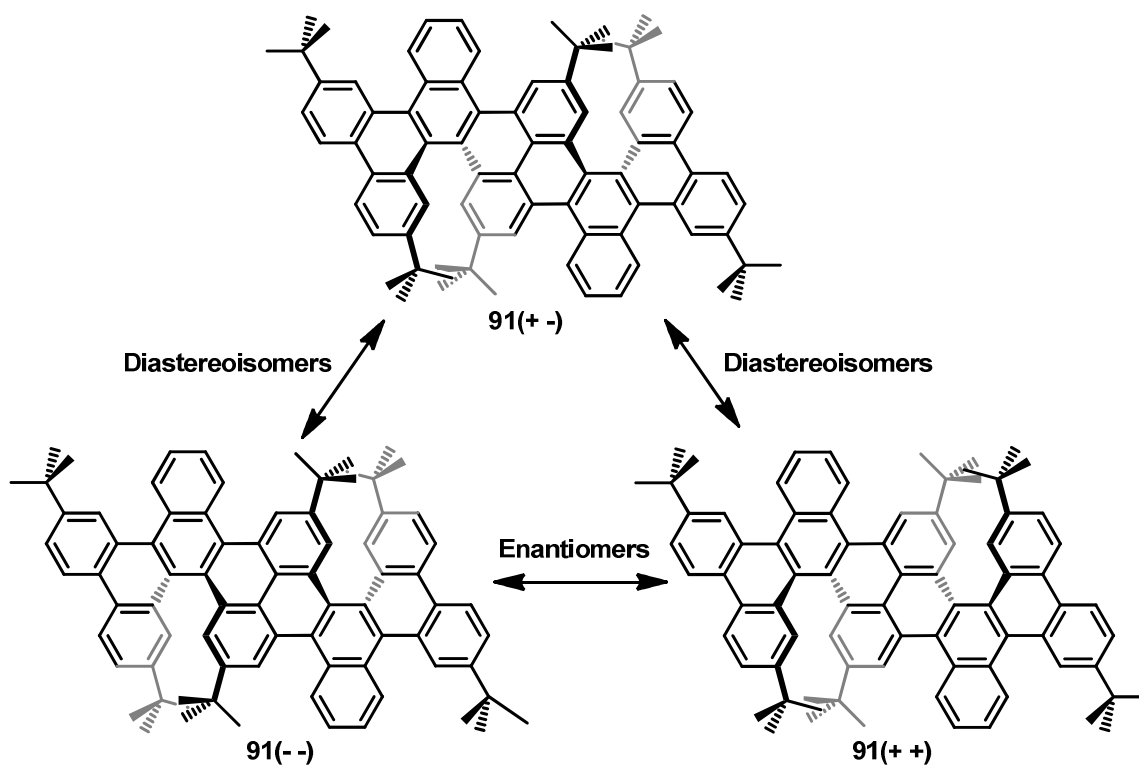


Figure 110. The three different stereoisomers of compound **91**.

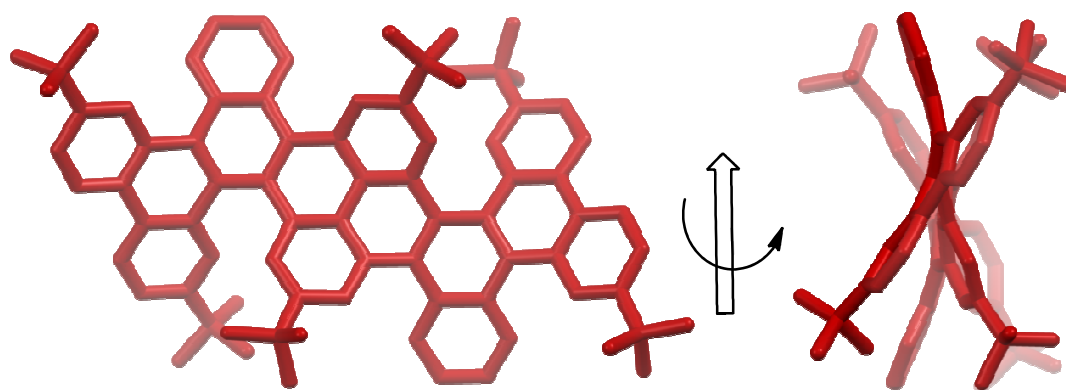
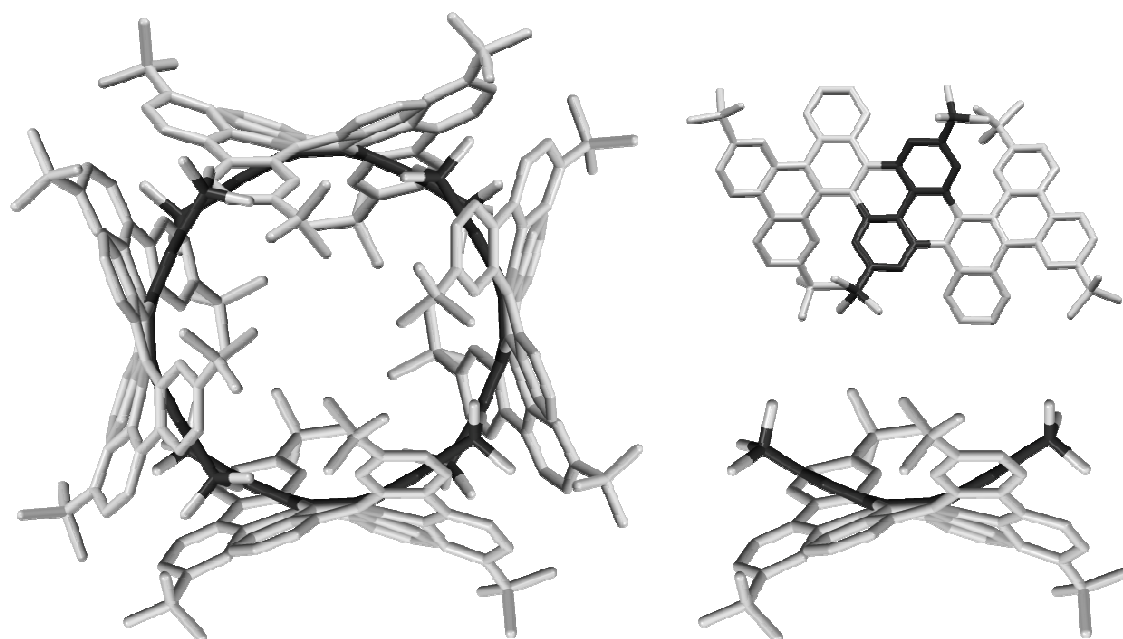


Figure 111. Crystal structure of **91** : two different views of a single molecule.

Even if compound **91** is highly soluble in many organic solvents, monocrystals of it were obtained as yellow needles by slow diffusion of methanol in DCM. Analysis by X-ray diffraction of these crystals has been possible and allowed the determination of the stereochemistry of compound **91**, which appeared to be a racemic mixture of enantiomers (+ +) and (- -) (**Figure 111**).

It is interesting to note that similarly to the monomer's structure, here both naphthalene parts are bent, not twisted, so that for each of them the two close tert-butyl groups are on the same side. In such a configuration, the three biphenyl units have different geometries: The two on the extremities are straight whereas the central one is strongly bent. It is noteworthy that this bending is comparable to the curvature of the phenyl rings in a [8]cyclo-*para*-phenylene (CPP) macrocycle (**Figure 112**).

Apparently, one parameter is important to lower the distortion of the twisted carbon nanoribbons, which may thus influence the nature of their most stable configuration. The naphthalene parts seem to prefer to bend, not to twist, which forces the two close tert-butyl groups to be on the same side of the naphthalene. Each naphthalene facing a helicene part, with two opposite tert-butyl groups, this will automatically force the two biphenyl parts of this helicene to adopt different geometries:



*Figure 112. Similar curvatures in compound **91** and [8]CPP.*

One straight and one strongly bent. Since internal biphenyl units are shared by two helicenes in twisted carbon nanoribbons, having bent instead of twisted naphthalene parts has therefore an important consequence on their global structure: The di-tert-butylbiphenyl units are alternatively straight and strongly bent along the ribbon. We can assume that the more stable configuration of the molecule is certainly the one with the lowest distortion, so the highest number of straight biphenyl units. In the case of short twisted ribbons with an even number of helicenes, there is an odd number of biphenyl units, alternatively straight and bent. Therefore, the most stable configuration should be the one with straight biphenyl parts on the extremities.

This hypothesis concerning the bending of the naphthalene parts, that we cannot completely prove yet, applied to the case of the dimer **91**, brings us to the experimentally confirmed conclusion that the meso (+ -) configuration is more distorted and, as a consequence, less favored than the chiral (+ +) and (- -) molecules.

5.4. Synthesis of the trimer.

In order to prepare a more systematic synthetic strategy for longer flexible precursors of twisted carbon nanoribbons, it was useful to test the reactivity of bifunctional monomers, such as bis-triflate compound **94** or bis-boronic ester **95** (Figure 114). For that purpose, we decided to synthesize the trimer **111** of the twisted carbon nanoribbons, given that a symmetrical strategy for the synthesis of its flexible precursor **110** would imply the use of a bifunctional central monomer (Figure 113).

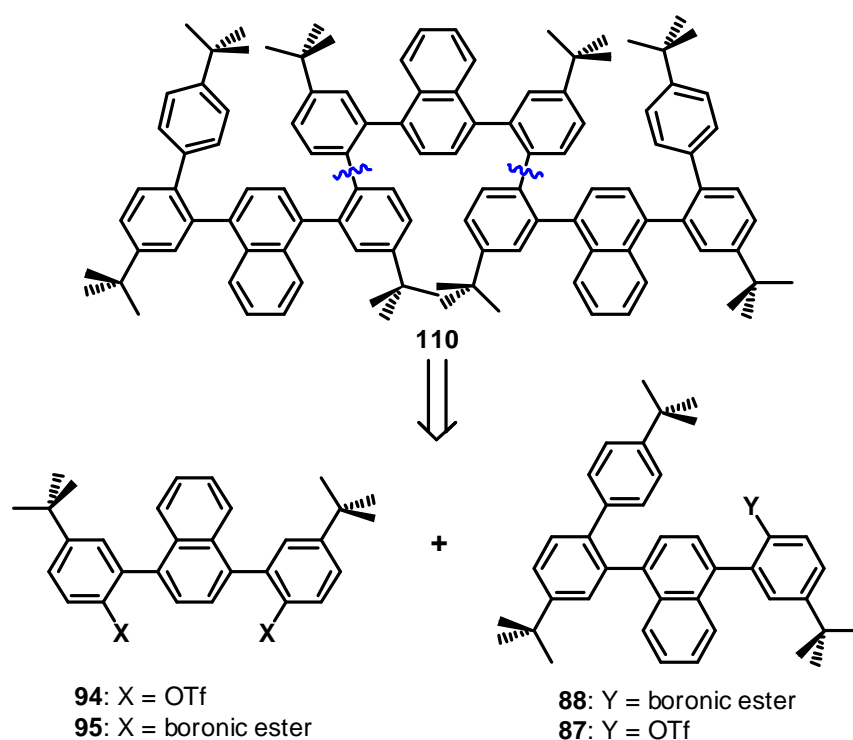


Figure 113. Retro-synthesis of the trimer's flexible precursor 110.

Similarly to what has been done before, commercially available 1,4-dibromo-naphthalene **81** reacts twice with the 5-tert-butyl-2-methoxyphenylboronic acid **34** in usual conditions for Suzuki cross-coupling reactions, with Pd(PPh₃)₄ as a catalyst, which leads efficiently (90% yield) to the dimethoxylated monomer **92**. Both methoxy groups are then deprotected by action of BBr₃, quantitatively giving the phenolic intermediate **93**. These phenol functions are then transformed, by action of triflic anhydride, into triflate groups and the first bifunctional

monomer **94** is obtained in excellent yield (89%). Finally, the double conversion of both triflates functions to boronic ester groups is carried out by Miyaura coupling of **94** with bis(pinacolato)diboron, using PdCl₂(dppf) as catalyst and KOAc as a base, which leads efficiently (80% yield) to the second interesting bifunctional monomer **95**, substituted by two boronic esters (**Figure 114**).

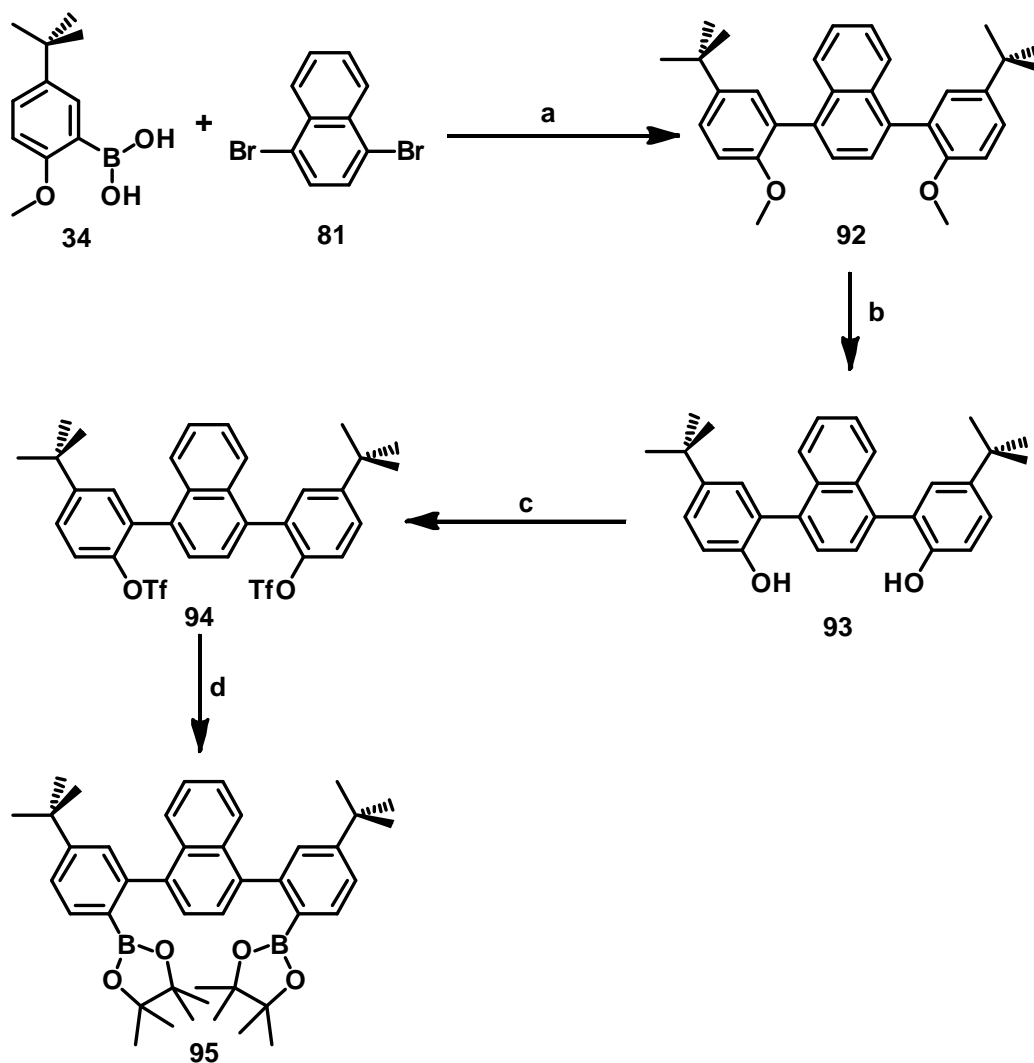


Figure 114. Synthesis of bifunctional monomers **94** and **95**: (a) Na₂CO₃, Pd(PPh₃)₄ in PhMe/H₂O/EtOH, 90°C, 24h, 90%. (b) BBr₃ in CH₂Cl₂, RT, 16h, 99%. (c) Tf₂O, pyridine in CH₂Cl₂, RT, 16h, 89%. (d) Pd(dppf)Cl₂, dppf, Bis(pinacolato)diboron, KOAc in THF/H₂O, 67°C, 48h, 80%.

The first attempt for the synthesis of the flexible precursor **110** of the trimer twisted nanoribbon implied a double Suzuki cross-coupling reaction between one central bis-triflate monomer **94** and two identical monomers **88** functionalized by one boronic ester (**Figure 115**) and one tert-butylphenyl ending group. The reaction has been carried on using the efficient “Buchwald conditions”, specifically for hindered substrates, with Pd(OAc)₂ as a palladium source, SPhos as a ligand, K₃PO₄ as a base in a mixture of THF and water, at reflux during several days. Unfortunately, the first coupling reaction seems to work well since the mono-reacted product **96** can be observed, but the second one, leading then to the desired compound, seems to be a lot more difficult. In fact, hydrogenated compound **90** and **97** could be isolated in large quantities, showing that these conditions are not adapted to this double reaction.

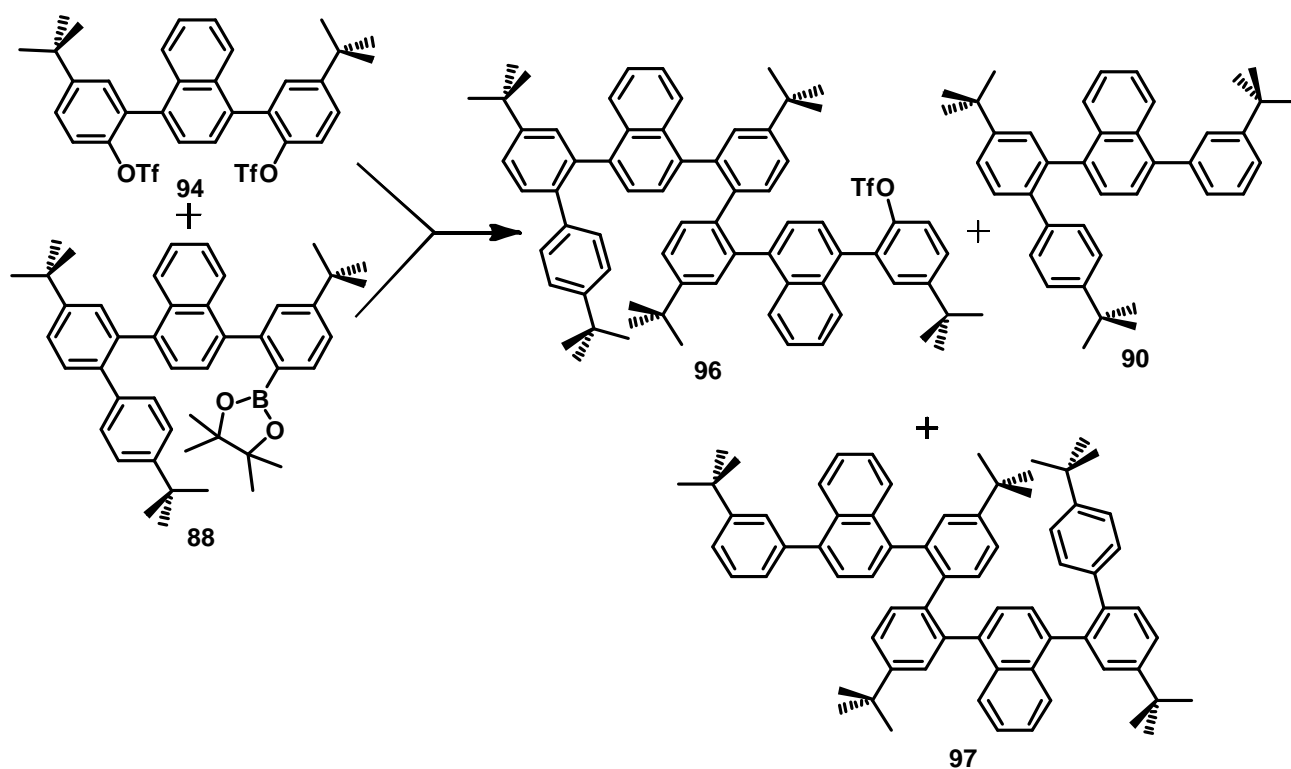


Figure 115. First attempt of synthesis of the trimer precursor **110**: Pd(OAc)₂, SPhos, K₃PO₄ in THF/H₂O, 67°C, 6 days.

The next attempt for the synthesis of the flexible precursor **110** of the trimer twisted nanoribbon implied the opposite double Suzuki cross-coupling reaction between one central bis-boronic ester monomer **95** and two identical monomers **87** functionalized by one triflate and one tert-butylphenyl ending group. The reaction has been carried on using the same “Buchwald conditions” ($\text{Pd}(\text{OAc})_2$ / *SPhos* / K_3PO_4 / $\text{THF} + \text{H}_2\text{O}$) during several days. Unfortunately again, the same observations can be done since only hydrogenated compound **90** and **97** were isolated (**Figure 116**).

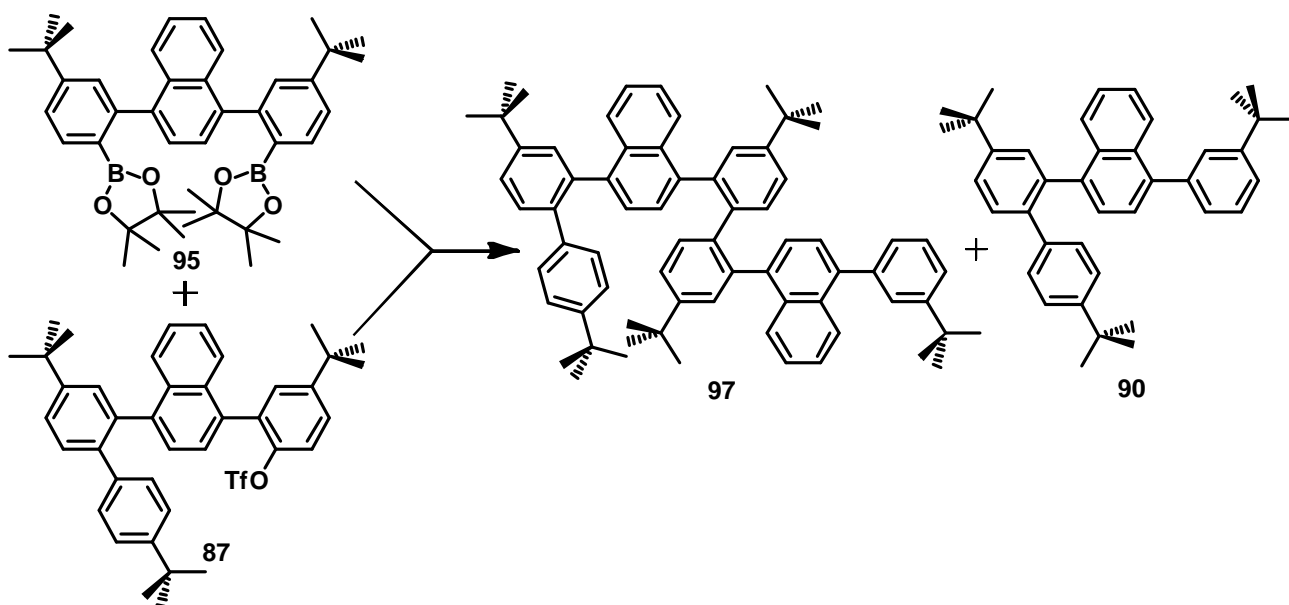


Figure 116. Second attempt of synthesis of the trimer precursor **110**: $\text{Pd}(\text{OAc})_2$, *SPhos*, K_3PO_4 in $\text{THF}/\text{H}_2\text{O}$, 67°C , 6 days.

Thinking that these interfering hydrogenation reactions are due to the presence of water in the reaction mixture, we decided to find new reaction conditions involving only dry organic solvents. Nevertheless, boronic esters need to be hydrolyzed before reacting with Suzuki coupling catalysts and therefore need the presence of water, which is not the case of boronic acids. For this reason, we then tried to hydrolyze beforehand the two boronic esters **88** and **95** to form boronic acids (**Figure 117**). Unfortunately, several unsuccessful attempts were performed, using oxidative, acidic or basic conditions, but the starting compounds were always fully recovered.

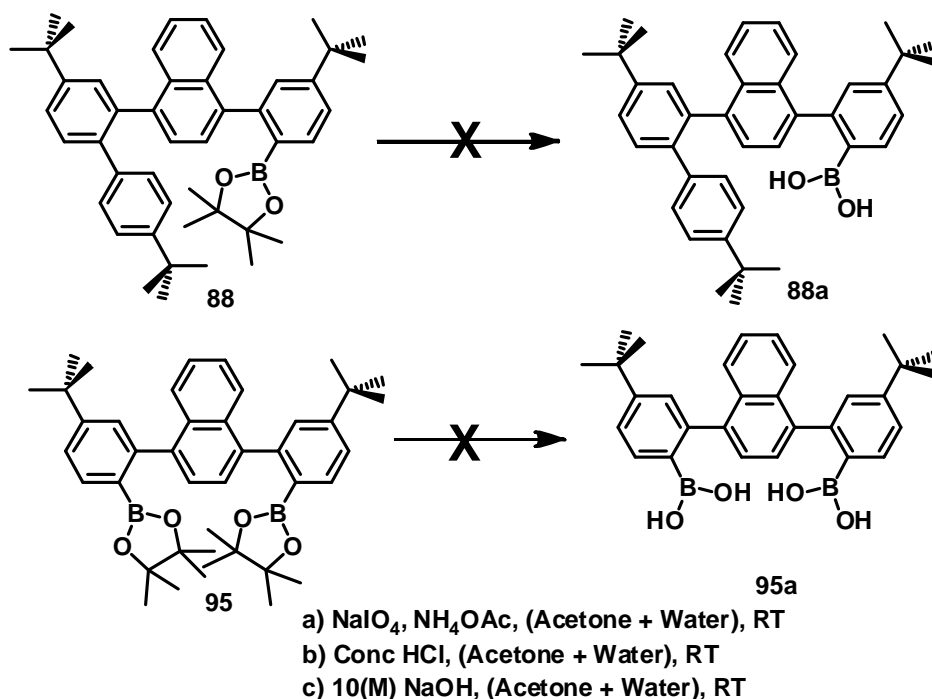


Figure 117. Attempts of hydrolysis of boronic esters **88** and **95**.

At that point, we decided to change our synthetic strategy in order to reduce the global steric hindrance of the coupling precursors. For that purpose, we developed the synthesis of monomer compounds substituted by a methoxy group on one side and an active function, either triflate (**101**) or boronic ester (**102**), on the other side (**Figure 118**). In addition to being less hindering than tert-butylphenyl groups, the methoxy substituents have other advantages. They induce some polarity in the molecules, which will be very helpful during the purifications by column chromatographies, and they are versatile substituents that can easily be deprotected into phenols, which can then be changed into triflates and even boronic esters.

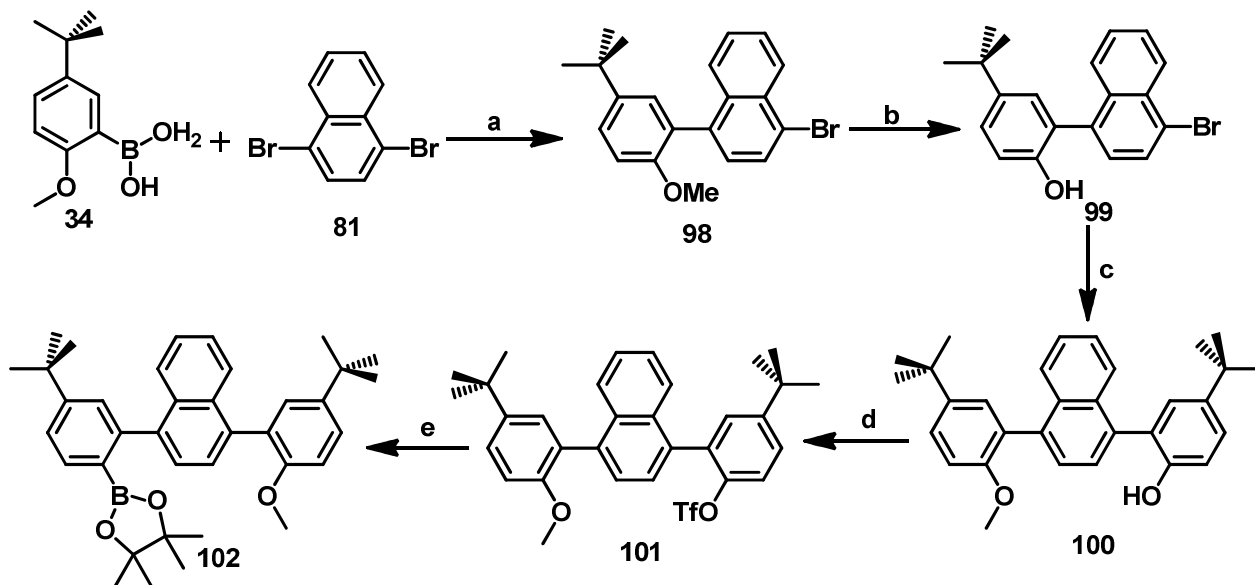


Figure 118. Synthesis of methoxy-substituted monomers **101** and **102**: (a) Na_2CO_3 , $\text{Pd}(\text{PPh}_3)_4$ in $\text{PhMe}/\text{H}_2\text{O}/\text{EtOH}$, 90°C , 24h, 80%. (b) BBr_3 in CH_2Cl_2 , RT, 16h, 99%. (c) Na_2CO_3 , $\text{Pd}(\text{PPh}_3)_4$ in $\text{PhMe}/\text{H}_2\text{O}/\text{EtOH}$, 90°C , 24h, 94%. (d) Tf_2O , pyridine in CH_2Cl_2 , RT, 16h, 91%. (e) $\text{Pd}(\text{dppf})\text{Cl}_2$, *dppf*, Bis(pinacolato)diboron, KOAc in $\text{THF}/\text{H}_2\text{O}$, 67°C , 48h, 71%.

These new key intermediates **101** and **102** were respectively prepared in four and five steps (**Figure 118**). Similarly to the syntheses of compounds **87** and **88**, we first take advantage of the different reactivities of the two bromides on commercially available 1,4-dibromonaphthalene **81**, and perform on it a Suzuki cross-coupling mono-reaction. Compound **98** is efficiently (80% yield) formed by such a reaction with the 5-tert-butyl-2-methoxyphenylboronic acid **34**, in classical conditions. Then follows a demethylation, by action of BBr_3 in usual conditions, which quantitatively affords the corresponding phenol **99**. It then undergoes a second Suzuki cross-coupling reaction with 5-tert-butyl-2-methoxyphenylboronic acid **34**, in the same conditions, which yields the desired mono-protected bis-phenolic compound **100** in 94% yield. The unprotected phenol is transformed into a triflate function, under standard conditions using triflic anhydride, to give the desired product **101** in 91% yield. The conversion of the aryl triflate **101** to the boronic ester **102** was finally carried out by Miyaura coupling reaction with bis(pinacolato)diboron using $\text{PdCl}_2(\text{dppf})$ as a catalyst with KOAc as a base. The overall yield over 5 steps for the formation of the key-compound **102** is excellent: 48%.

The first approach for the synthesis of the flexible trimer precursor **110**, involving the bis-triflate monomer **94**, has been reproduced but this time with the less sterically hindering boronic ester **102** (**Figure 119**). In fact, by using the very efficient catalytic system developed by Buchwald and coworkers ($\text{Pd}(\text{OAc})_2$ / SPhos / K_3PO_4 / THF + H_2O) the double Suzuki cross-coupling reaction worked well and the dimethoxy flexible trimer **103** was formed and easily isolated with a very good yield (70%) given the previous attempts. Double demethylation with BBr_3 afforded then quantitatively the corresponding bis-phenol product **104**, which was then changed into bis-triflate compound **105** under standard conditions using triflic anhydride, with a good yield (80%).

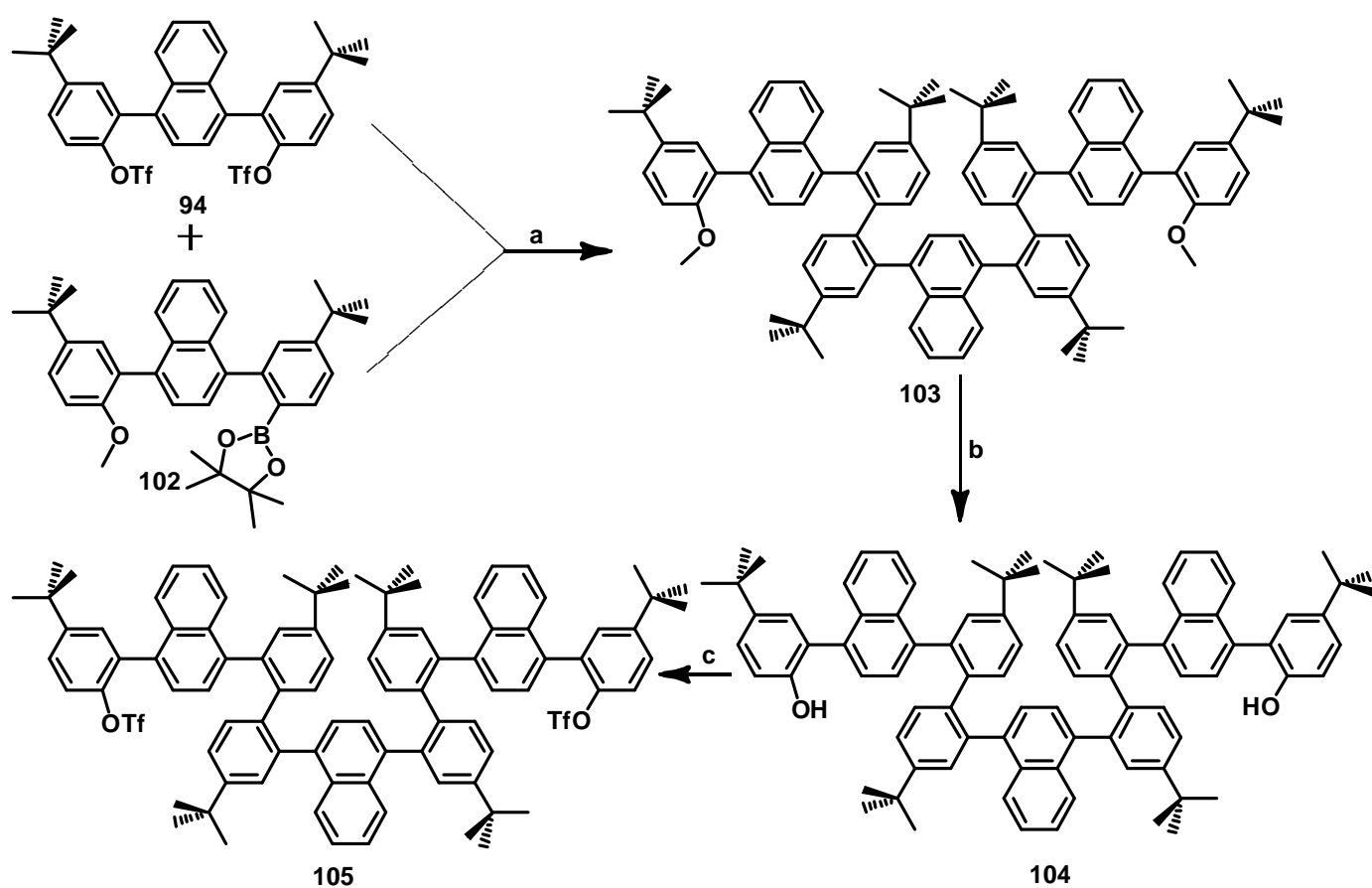


Figure 119. Synthesis of bis-triflate flexible trimer **105**.

(a) $\text{Pd}(\text{OAc})_2$, SPhos, K_3PO_4 in THF/ H_2O , 67°C , 48h, 70%. (b) BBr_3 in CH_2Cl_2 , RT, 16h, 99%. (d) Tf_2O , pyridine in CH_2Cl_2 , RT, 16h, 91%. a) $\text{Pd}(\text{OAc})_2$, SPhos, K_3PO_4 in THF/ H_2O , 67°C , 48h, 80%.

The final step towards the flexible trimer precursor **110** is another double Suzuki cross-coupling reaction implying the bis-triflate trimer **105** and two equivalents of 4-tert-butylphenylboronic acid **9**. Unfortunately, even with the very efficient Buchwald's catalytic system ($\text{Pd}(\text{OAc})_2 / \text{SPhos} / \text{K}_3\text{PO}_4 / \text{THF} + \text{H}_2\text{O}$), the same problem than before occurred, the first coupling reaction working well but the second being much slower, letting the second triflate function being hydrogenated to give an inseparable mixture of the partially reacted triflate product **106** and the hydrogenated incomplete flexible trimer **107** (Figure 120).

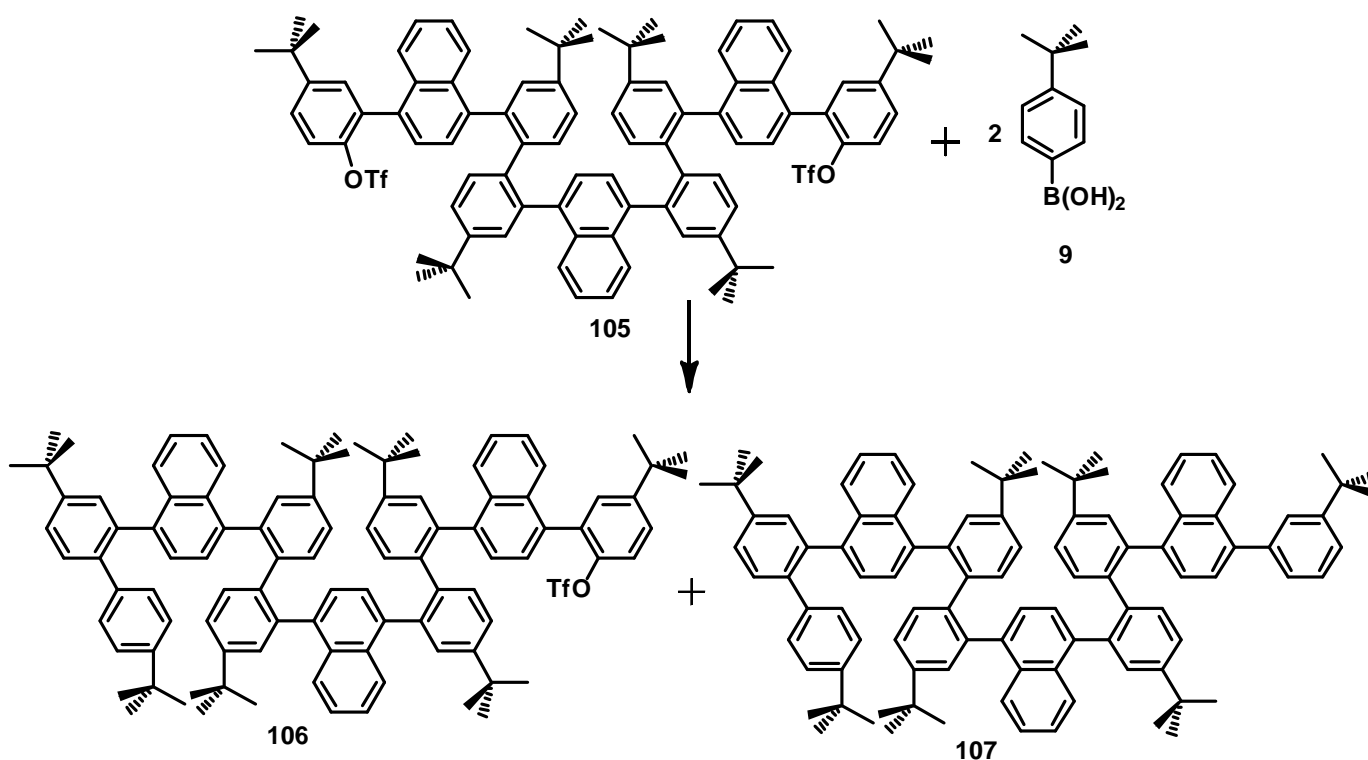


Figure 120. Third attempt of synthesis of the trimer precursor **106**.

$\text{Pd}(\text{OAc})_2$, *SPhos*, K_3PO_4 in *THF*/ H_2O , 67°C , 48h (complex mixture).

Single Suzuki cross coupling reactions on highly hindered substrates having already work well (compound **89**, Figure 106), we decided to modify again the global synthetic strategy for the formation of the flexible trimer precursor **110** by only performing single, therefore faster than double, coupling reactions. Nevertheless, such a stepwise strategy has a major drawback: the step sequence is logically much longer than before since the length of the oligomer has to be incremented one monomer by one monomer.

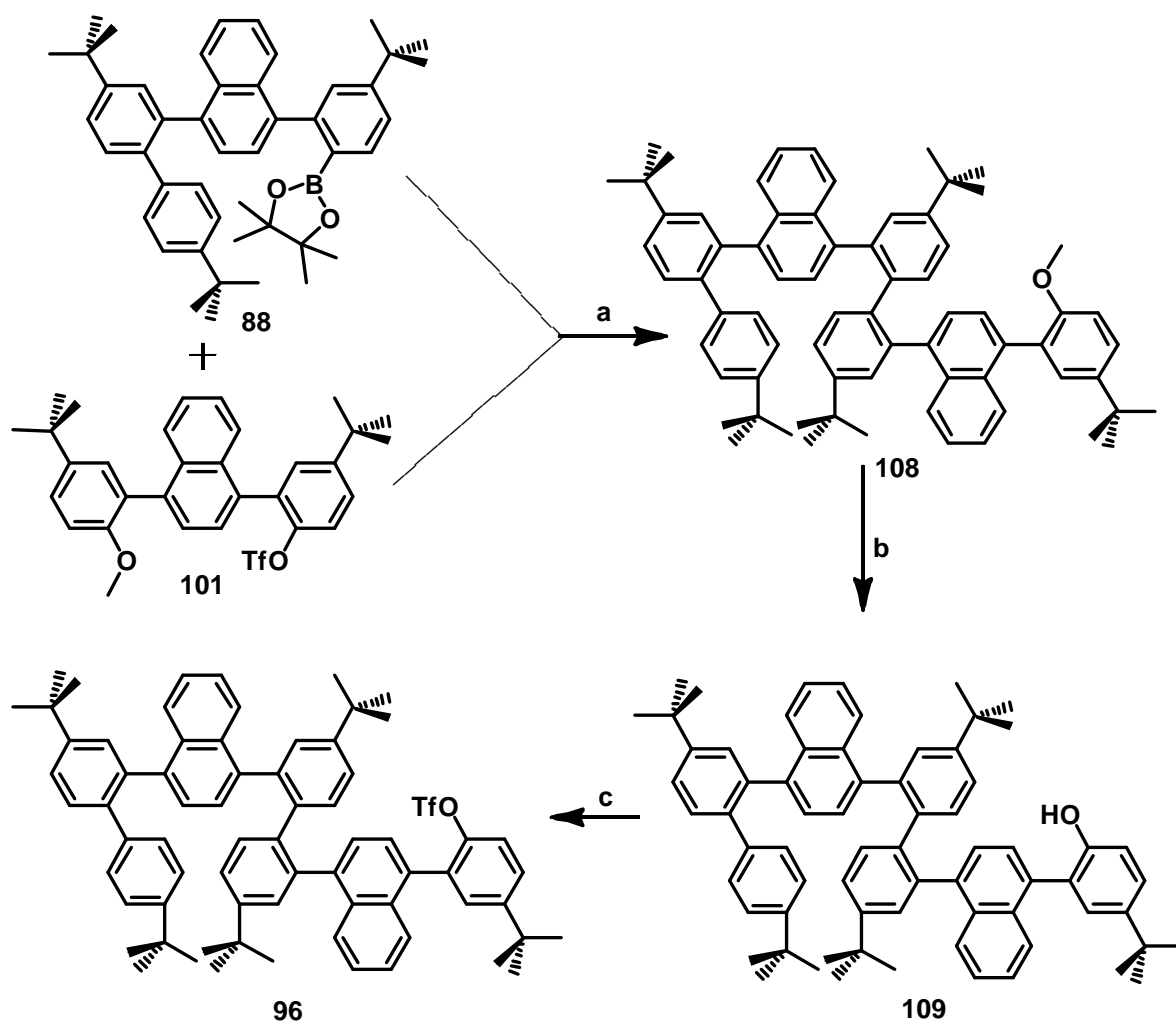


Figure 121. Synthesis of the mono-triflate flexible dimer **96**: (a) $\text{Pd}(\text{OAc})_2$, SPhos, K_3PO_4 in $\text{THF}/\text{H}_2\text{O}$, 67°C , 48h, 75%. (b) BBr_3 in CH_2Cl_2 , RT, 16h, 95%. (c) Tf_2O , pyridine in CH_2Cl_2 , RT, 16h, 96%.

Starting the chain formation from an end, the first Suzuki coupling reaction implies the monofunctional monomer **88** as a boronic ester and the methoxy-triflate-monomer **101**. Because of the steric hindrance of the reacting site on substrate **88**, the optimized catalytic conditions ($\text{Pd}(\text{OAc})_2$ / SPhos / K_3PO_4 / $\text{THF} + \text{H}_2\text{O}$) are used and the methoxy-substituted flexible dimer **108** is obtained with a very good yield (75%). Then, as usual, demethylation is performed with BBr_3 to give the corresponding phenolic product **109** (95% yield), which is then changed into the mono-triflate flexible dimer **96** under standard conditions using triflic anhydride, with an excellent yield (96%) (**Figure 121**).

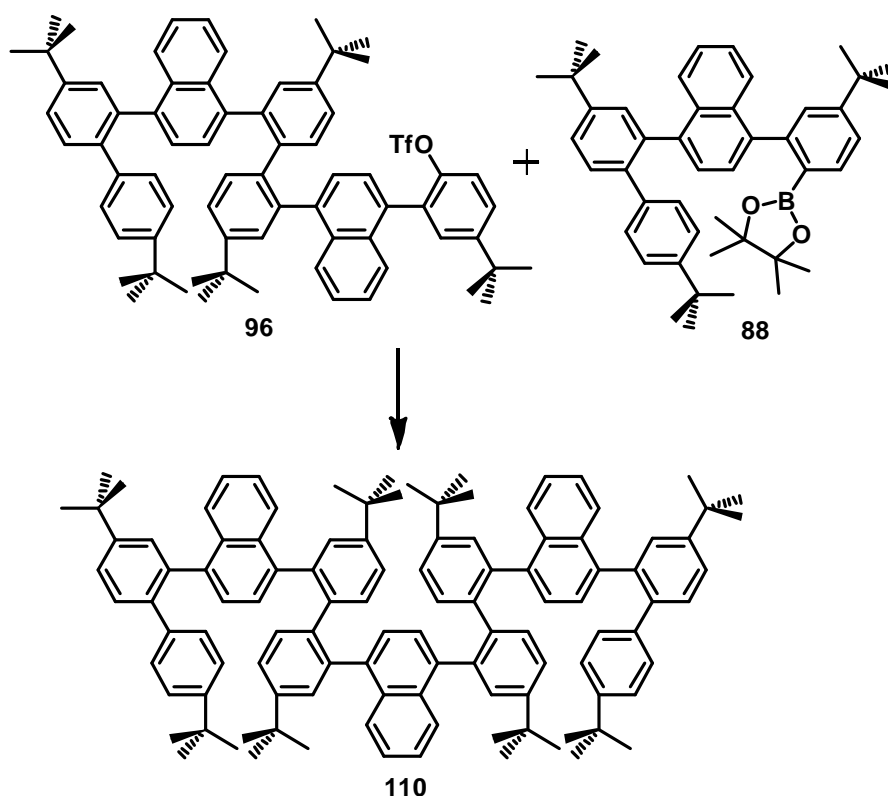


Figure 122. Successful fourth attempt of synthesis of flexible trimer precursor **110**: $Pd(OAc)_2$, *SPhos*, K_3PO_4 in THF/ H_2O , $67^\circ C$, 96h, 74%.

For the final critical step, the same boronic acid **88** is used again but this time with the mono-triflate flexible dimer **96**, in the same optimized catalytic conditions. Fortunately, the expected product, the flexible trimer precursor **110**, is finally formed with an excellent yield (74%) (**Figure 122**).

It is important to point out that, again, all flexible compounds constituted of at least two monomer units were impossible to fully characterize by 1H -NMR because of all the stable conformers. In fact, only mass spectrometry (FD-MS) was satisfying for a reasonable identification of these compounds. ^{19}F -NMR was also used as a fluoride sensor in order to check the appearance or the disappearance of triflate substituents. In the case of flexible hydrocarbons with at least four degrees of liberty (disubstituted ortho-phenylene fragments) such as the flexible dimer or trimer, NMR was even absolutely useless and field desorption mass spectrometry was the only reliable analysis.

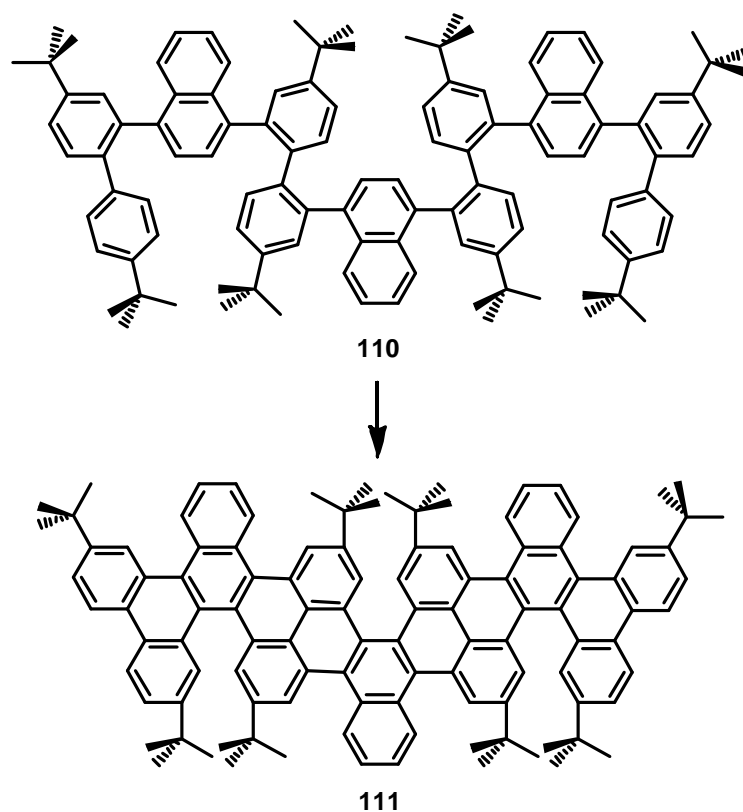


Figure 123. Formation of the trimer twisted carbon nanoribbon **111**: FeCl_3 , MeNO_2 + CH_2Cl_2 , Ar bubbling, RT, 1.5h, MeOH, 40%.

Scholl reaction on flexible precursor **110** (**Figure 123**) was finally carried out in usual conditions, with FeCl_3 in dichloromethane and nitromethane, at 0°C with constant argon bubbling for 1.5 hour. After quenching with methanol the crude product was analyzed by TLC and several closely migrating spots were observed. After partial purification of all these apolar compounds, it appeared that the main one is the correctly graphitized twisted trimer **111**, obtained in about 40% yield, the second one being a partially reacted product, with 2 C-C bonds missing (so 4 more hydrogen atoms detected by FD-MS). Making it reacting again in the same conditions for two more hours did not lead to a satisfying result since what has then been observed by mass spectrometry is a product with two less hydrogens than expected, meaning one more C-C bond. In addition, the $^1\text{H-NMR}$ spectrum is not simple even for this rigidified molecule. The mass spectrometry is not a quantitative technique and therefore it is difficult for us to know if the product containing the twisted trimer **111** is impure or if the complexity of the NMR spectrum is due to a mixture of several stereoisomers. In fact, due to

its three helicene parts, the twisted trimer **111** presents 6 different stereoisomers, with 3 pairs of enantiomers (+++ and ---, +-+ and -+-, ++- and --+) which means three possibly different NMR spectra.

Having not succeed yet in growing analyzable single crystals of trimer **111**, we have to be careful when announcing the result of this important synthetic work: The fully graphitized twisted trimer **111** has been formed (confirmed by FD-MS) and we could separate a reasonable fraction of the crude mixture which is containing it in majority. Nevertheless, the too complicated NMR does not allow us to determine if that compound is pure, with different stable stereoisomers, or not.

This conclusion is not really satisfying but focusing on the synthesis of a trimer, in second thought, was not really relevant. In fact, if we consider the “bent naphthalene rule” that we assumed after getting the structure of the dimer **91**, the only conclusion on the trimer **111** is that stereoisomers +-+ and -+- should be disfavored, letting 4 other favored configurations. On the other hand, the tetramer of such twisted nanoribbons has an even number of helicenes, therefore an odd number of biphenyl units, two of them being bent and shared by helicenes having the same helicity. So only three configurations should be favored: ++++ and ---- which are symmetrical enantiomers and +++- which is an achiral meso compound. As a consequence, the analysis and structural study of such a tetramer should be easier and we decided to focus on its synthesis.

5.5. Synthesis of the tetramer.

Keeping in mind that only strategies involving mono-coupling reactions seem to be efficient, and given the already obtained compounds for the previous syntheses, the retro-synthetic study of the twisted tetramer **117** and its flexible precursor **115** has two possible ways (**Figure 124**). First, dimer triflate **96** can be coupled with its boronic ester counterpart, or a more systematic but longer stepwise approach can be developed from it via the monofunctional trimer triflate **114**.

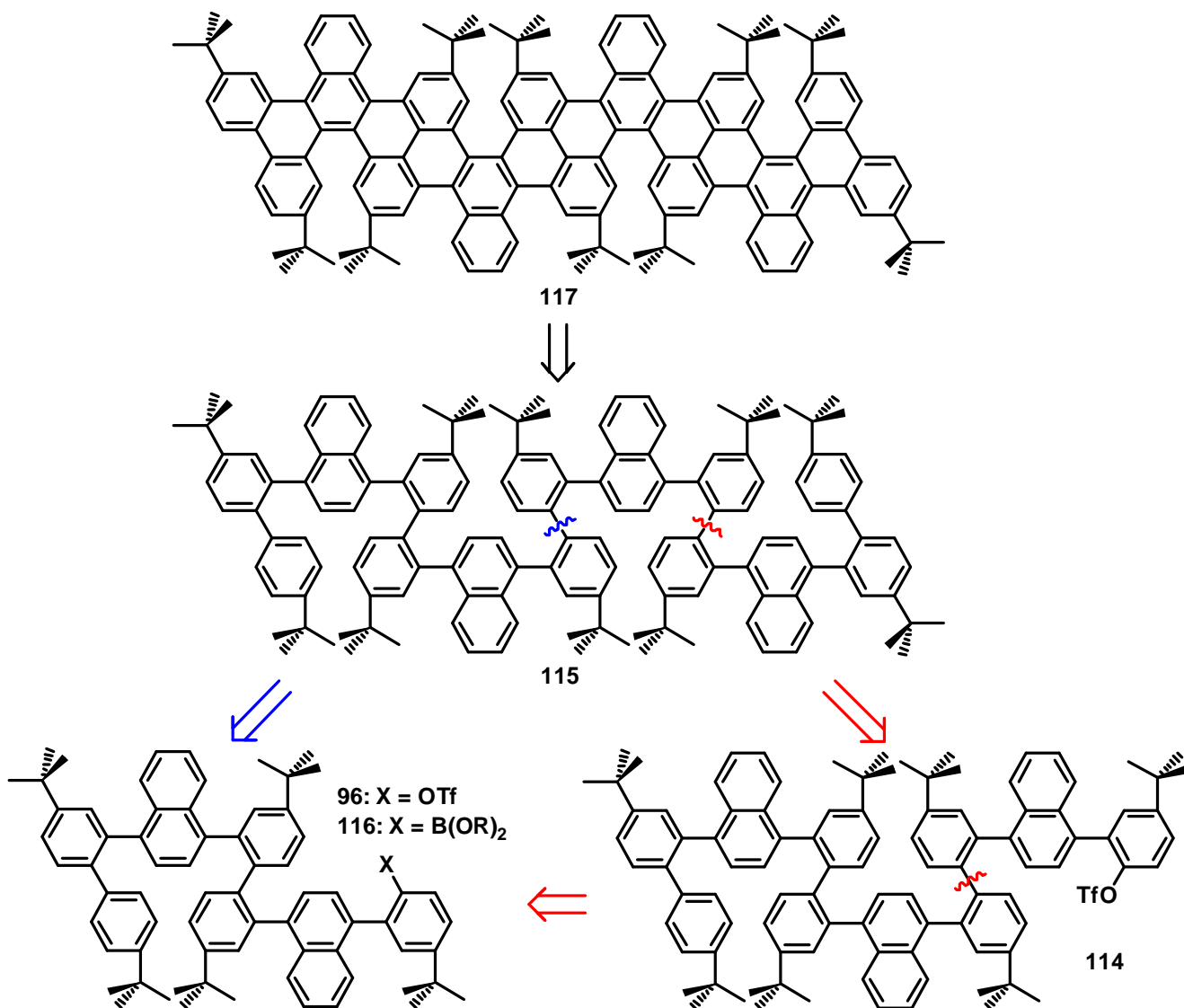


Figure 124. Retro-synthetic study of tetramer **117**. Blue way: Homocoupling. Red way: systematic and stepwise approach.

In order to demonstrate a proof of principle for the global stepwise syntheses of longer oligomers, we decided to develop the second approach (**Figure 125**).

First a Suzuki coupling reaction implying the monofunctional triflate dimer **96** and the methoxy-boronic ester monomer **102** has been carried out. Because of the steric hindrance of the reacting site on substrate **96**, the optimized catalytic conditions ($\text{Pd}(\text{OAc})_2$ / SPhos / K_3PO_4 / THF + H_2O) are used and the methoxy-substituted flexible trimer **112** is obtained with a very good yield (72%). Then, as usual, demethylation is performed with BBr_3 to give the corresponding phenolic product **113** (90% yield), which is then changed into the mono-

triflate flexible trimer **114** under standard conditions using triflic anhydride, with a good yield (83%) (**Figure 125**).

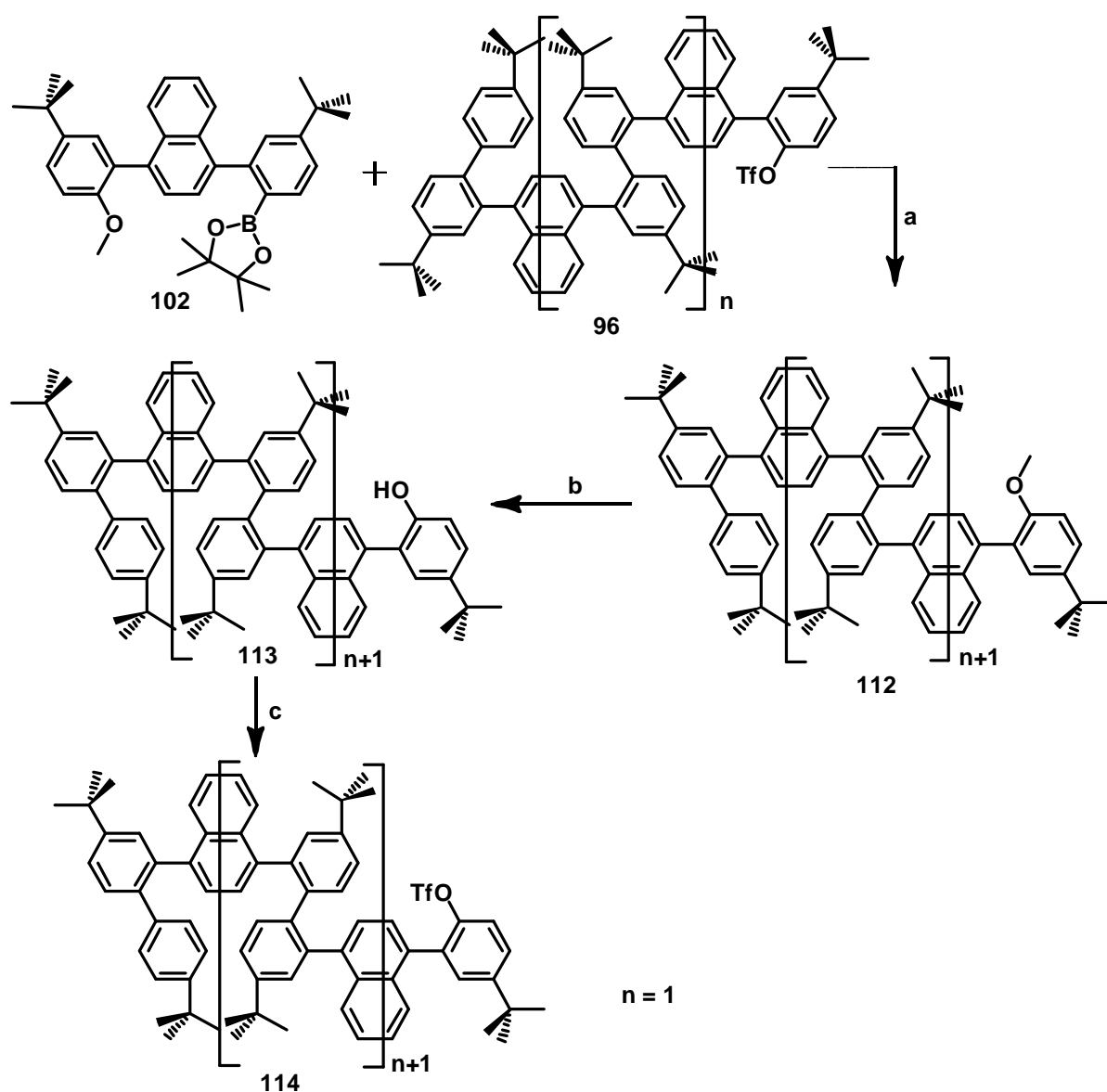


Figure 125. Systematic and stepwise synthesis of flexible oligomers, application to triflate trimer **114**; (a) $\text{Pd}(\text{OAc})_2$, *SPhos*, K_3PO_4 in $\text{THF}/\text{H}_2\text{O}$, 67°C , 48h, 72% for $n=1$. (b) BBr_3 in CH_2Cl_2 , RT, 16h, 90% for $n=1$. (c) $\text{ Tf}_2\text{O}$, pyridine in CH_2Cl_2 , RT, 16h, 83% for $n=1$.

Since this sequence starts with a triflate compound and ends with another, one monomer longer, triflate compound, it is noteworthy that this strategy could be generalized as a systematic procedure for the lengthening of the oligomer chain, one monomer by one monomer.

For the final step, boronic ester **88** is coupled by Suzuki reaction with the mono-triflate flexible trimer **114**, in the same optimized catalytic conditions. The expected product, the flexible tetramer precursor **115**, is partially formed but unfortunately an important amount of triflate trimer **114** stayed unreacted in the crude mixture (**Figure 126**). Since these 2 products are of comparable size and apolar, they are unseparable by chromatography. In addition, they have similar non interpretable $^1\text{H-NMR}$ spectra, and $^{19}\text{F-NMR}$ can only confirm the presence of the triflate substrate. Therefore, this problem could be solved by following the progression of the reaction by $^{19}\text{F-NMR}$ but hydrogenation of the triflate compound giving hydrocarbon **107** is also observed by FD-MS.

We think that the too important size similarity between trimer compounds **111** and **107**, and tetramer precursor **115** is making the purification even more difficult so we decided to try the other synthetic strategy described in figure 127. In fact, in this approach the main impurity to fear is the hydrogenated dimer **97**, which size is half the one of the desired flexible tetramer. We hope that this size and structural difference would allow an easier purification.

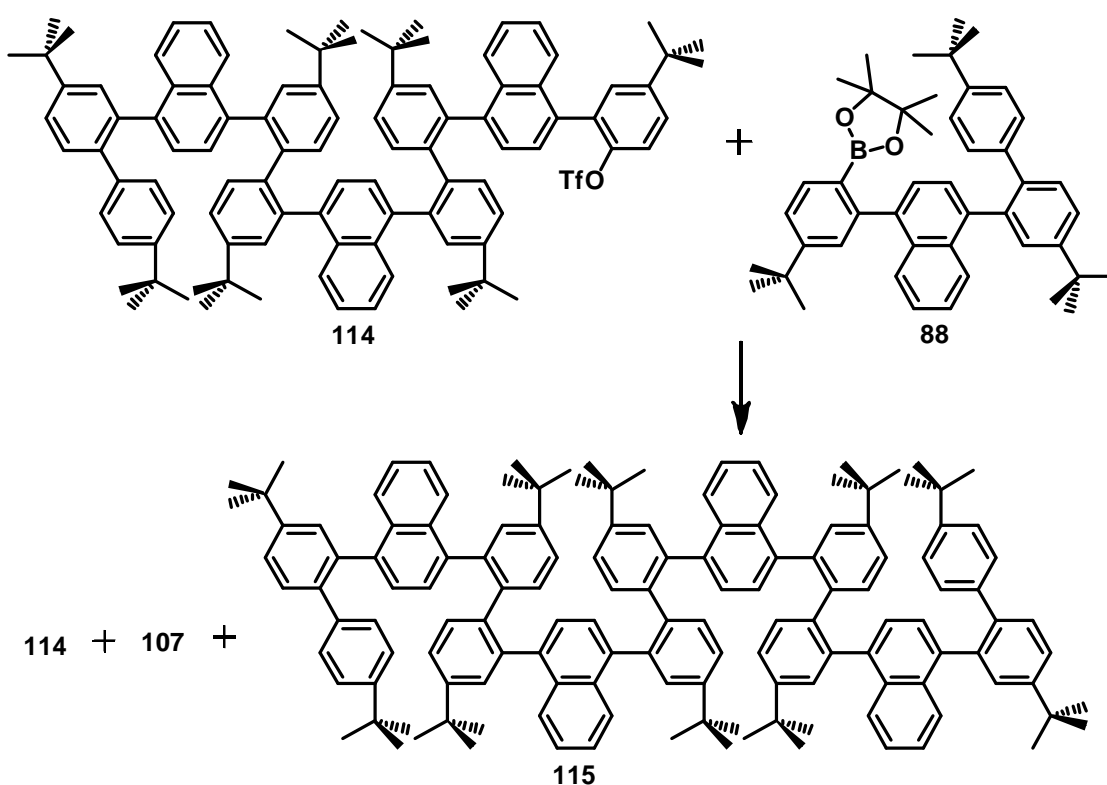


Figure 126. Attempt of synthesis of flexible tetramer **115**

$\text{Pd}(\text{OAc})_2$, *SPhos*, K_3PO_4 in $\text{THF}/\text{H}_2\text{O}$, 67°C , 96h.

First the conversion of the dimer triflate **96** to the corresponding boronic ester **116** is carried out by Miyaura coupling reaction with bis(pinacolato)diboron using $\text{PdCl}_2(\text{dppf})$ as a catalyst and KOAc as a base, with a good yield (80%) (**Figure 127**). It is finally coupled with dimer triflate **96** under optimized catalytic conditions ($\text{Pd}(\text{OAc})_2$ / SPhos / K_3PO_4 / THF + H_2O) for 2 days. Fortunately, this time the crude product can be purified and the flexible tetramer **115** is obtained pure (as confirmed by FD-MS) with a very good yield.

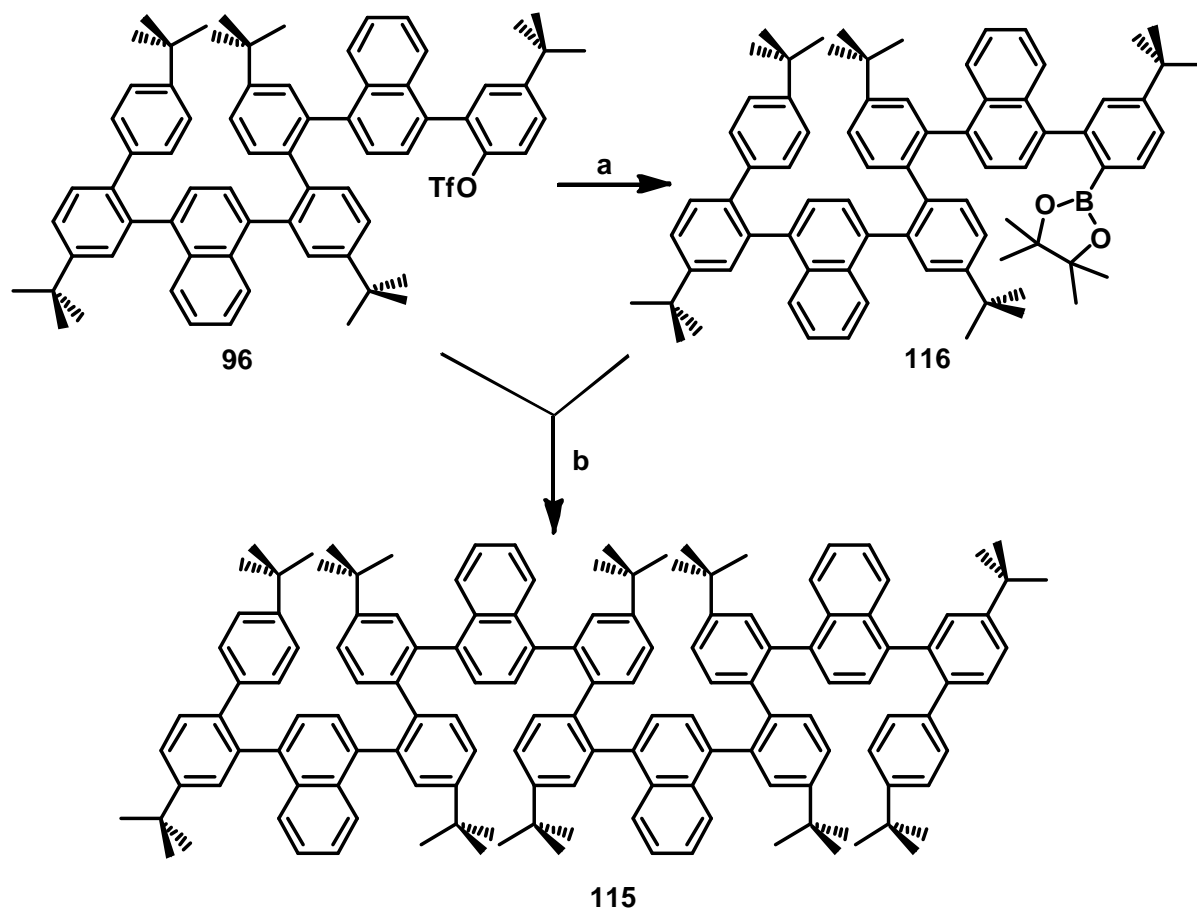


Figure 127. Synthesis of tetramer flexible precursor **115**: (a) $\text{Pd}(\text{dppf})\text{Cl}_2$, *dppf*, Bis(pinacolato)diboron, KOAc in THF/ H_2O , 67°C, 48h, 80%. (b) $\text{Pd}(\text{OAc})_2$, SPhos, K_3PO_4 in THF/ H_2O , 67°C, 48h, 82%.

Scholl reaction on flexible precursor **115** was finally carried out in usual conditions, with FeCl_3 in dichloromethane and nitromethane, at 0°C with constant argon bubbling for 2.5 hour. After quenching with methanol the crude product was analyzed by TLC and only two closely migrating spots were observed. After purification by column chromatography twisted

nanoribbons tetramer **117** was obtained in about 30% yield (**Figure 128**), the second compound (as shown by FD-MS) being an over-reacted product, with 2 hydrogens missing so one supplementary C-C bond. This points out a new difficulty in the synthesis of such twisted nanoribbons: The reaction conditions have to be optimized for the last Scholl reaction which advancement cannot be simply followed and which substrate is extremely expensive.

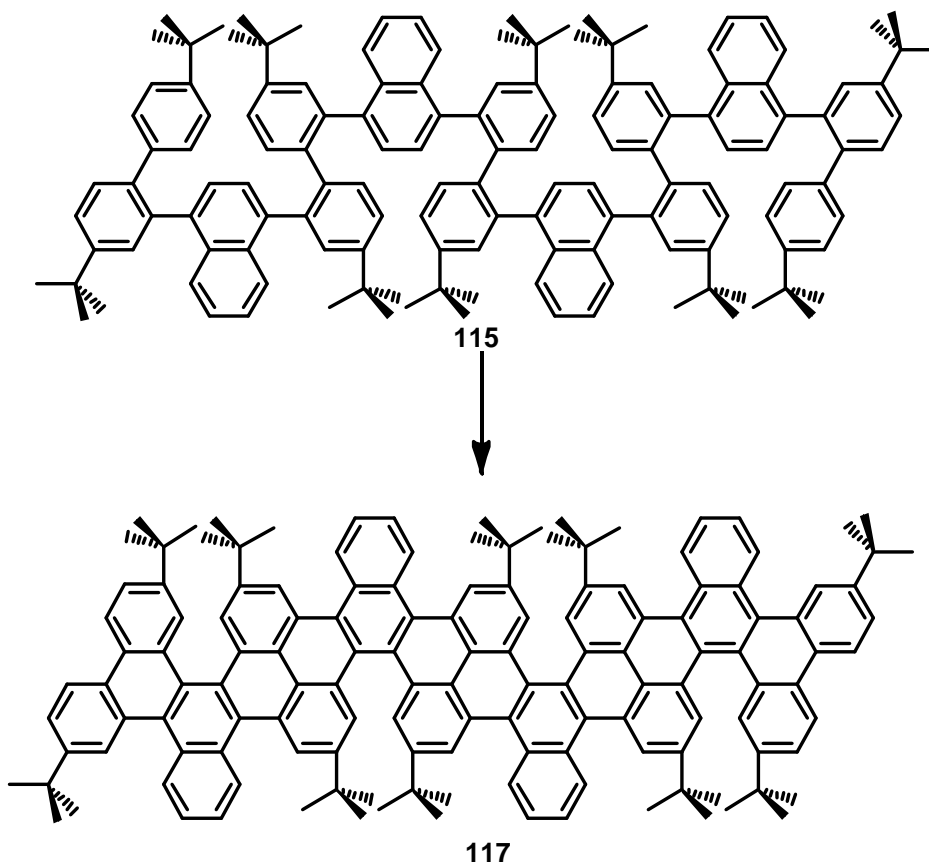


Figure 128. Synthesis of the tetramer of twisted GNRs **117**: FeCl_3 , $\text{MeNO}_2 + \text{CH}_2\text{Cl}_2$, Ar bubbling, RT, 2.5 h, MeOH, 30%.

To conclude this part, the results of test reactions were successful and the studies of the monomer and dimer crystal structures gave some interesting, yet incomplete, information about the general configuration of the targeted twisted carbon nanoribbons. Unfortunately, they also taught us that the organic synthesis of such flexible precursors become more and more difficult when their size is extended. In fact, NMR of the monomer flexible precursor was not trivial whereas the NMR of the dimer flexible precursor was already non interpretable and almost useless, making very specific analytical techniques (FD-MS) absolutely necessary. In addition, it appears that long stepwise strategies are necessary therefore polymerization of

bifunctional monomers is compromised. Added to the highly complicated purifications, due to the non polarity of the mixed compounds, the development of long flexible oligomeric precursors of twisted carbon nanoribbons is therefore an extremely difficult project. Finally, the Scholl reactions on the trimer and tetramer precursors are promising but the reaction conditions are not optimized enough for the moment to lead to clear conclusions. It is then very likely, to our disappointment, that this project will not be continued.

5.6 Reference.

1. S. D. Walker, T. E. Barder, J. R. Martinelli, S. L. Buchwald, *Angew. Chem. Int. Ed.* **2004**, *43*, 1871.

Conclusion

The initial project of this PhD thesis was the controlled organic synthesis of well defined graphene nanoribbons, involving the graphitization of flexible polyaryl precursors by Scholl reaction as a last step. The first approach relied on the formation and rigidification of substituted poly-*ortho*-phenylene chains but some test reactions convinced us that this geometry was not adapted.

The project has then evolved and we focused on geometrically different flexible poly-phenylene precursors, with alternating *ortho*- and *para*- connections. Nevertheless, when doing test reactions on small molecules, we discovered an unexpected and counter-intuitive regioselectivity of the Scholl reaction. In fact, twisted helicenic structures were obtained preferentially to the desired less crowded isomers, showing that the steric hindrance has a poor impact on this reaction. Attempts of protection were unsuccessful.

We then decided to take advantage of this serendipitous discovery to develop the synthesis of highly distorted poly-helicenic species. Hexabenzotriphenylene (HBTP) has first been obtained, following a very simple and efficient procedure, and its structure could even be determined by X-ray crystallography.

Hexabenzotriphenylene being seen as the 2nd generation dendrimer of the triphenylene series, we then aimed at the formation of the 3rd generation dendrimer, which is the hexaphenanthrotriphenylene (HPTP), an extremely distorted aromatic polycyclic compound including three [5]helicenic and three [7]helicenic parts. Unfortunately four different approaches, some of them implying many steps, were tried for the formation of flexible precursors but not any was successful. Nevertheless, one last strategy remains conceivable but it involves about 12 synthetic steps.

Willing to explore the Scholl reactivity and especially to check if higher order than [5]helicenes can be made by this reaction, we synthesized a family of C₃-symmetrical flexible precursors by a versatile synthetic strategy based on the formation of a common tris-triflate precursor. Synthesis of [6]helicenes did not succeed since we observed unpredicted rearrangements leading to the formation of hexa[7]circulene species. Nevertheless, such

rearrangements did not occur when synthesizing TMS-containing HBTP or distorted and soluble hexabenzocoronene (HBC) when ^tBu groups are in the bay regions.

If [6]helicenes may not be synthesizable by Scholl reaction, it appears that [5]helicenes are highly favored since even rearrangement occur to form them. We finally designed twisted carbon nanoribbons incorporating this [5]helicene as a repeated motif. The synthesis of the monomer was easy but analytical difficulties were already felt when making the dimer. Nevertheless, X-ray structures of both compounds provided interesting information about the global structure of the twisted carbon nanoribbons. Syntheses of the trimer and tetramer flexible precursors were exceptionally long and tedious, mainly because of purification and analysis problems. The Scholl reaction on these two compounds gave promising results but the reaction conditions still have to be optimized.

The electrochemical properties of all these new polyaromatic molecules are currently studied.

Perspectives

In spite of the changes in the initial project, we kept in mind that our first goal was the organic synthesis of flat carbon nanoribbons. Having developed an efficient, though difficult, synthesis for flexible precursors of twisted carbon nanoribbons, we decided to use these results and keep the same aromatic part for the design of fully graphitized nanoribbons. The incomplete Scholl reaction leading to helicenic parts is due to the steric hindrance between the too close tert-butyl groups. Removing these bulky groups and adding other solubilizing substituents somewhere else on the molecule would therefore certainly give fully cyclized and flat ribbons (**Figure 129**).

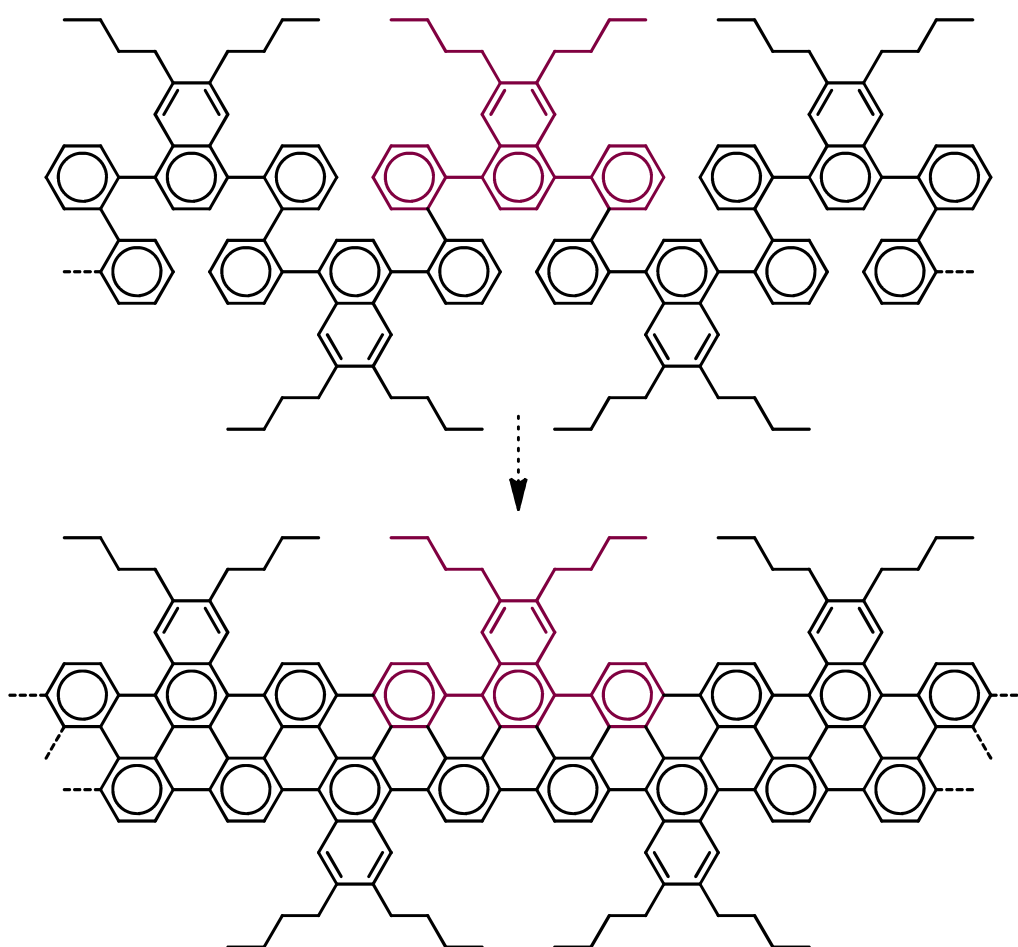


Figure 129. New design of flat nanoribbons.

The external positions on the naphthalene parts are ideally located for solubilizing aliphatic chains but such substituted naphthalene compounds are unfortunately not easily accessible. A few steps synthesis is now being developed (**Figure 130**) to form new bifunctional monomers, with linear chains on the naphthalene unit only, and with the same functions than before (methoxy and boronic ester) in order to apply the same synthetic strategy to the formation of flexible oligomers.

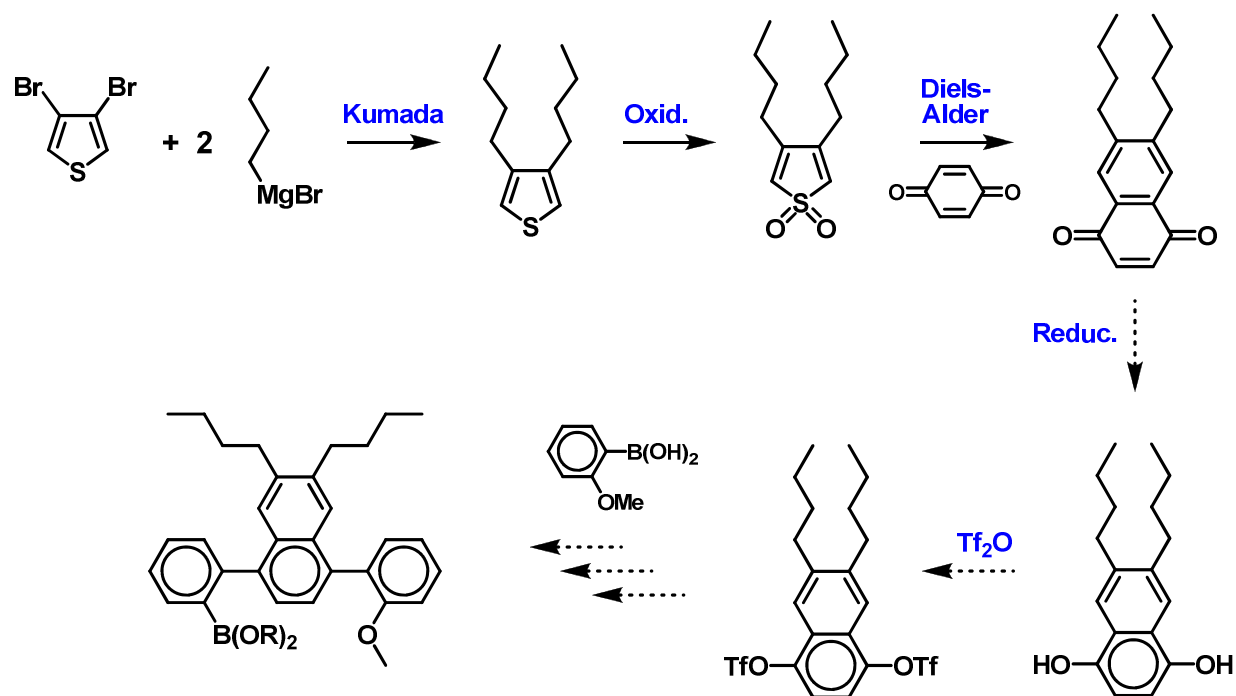


Figure 130. Synthetic strategy for the formation of bifunctional monomers of flat carbon nanoribbons.

Parallely, another apparently easier approach has been explored, involving pyrene-based monomers (**Figure 131**). In fact, in the previous project depicted in figure 44 (chapter II), if the para-phenylene linkers are replaced by a 1,6-pyrenylene fragments then there is only one possibility for the Scholl reaction and no interfering regioselectivity would occur.

One test reaction has been done to verify that this is true and that no rearrangement is interfering with the expected reactivity (**Figure 132**). The short symmetrical precursor **119** has been first obtained by a double Suzuki cross coupling reaction with the commercially available 1,6-dibromopyrene **118** and the boronic ester **5b**.

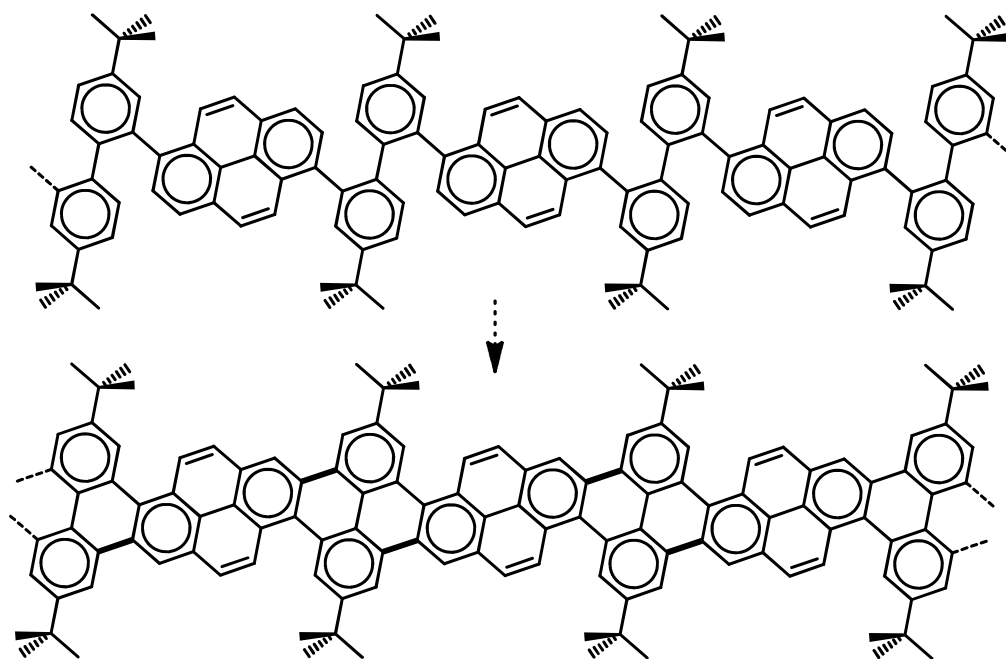


Figure 131. Design of pyrene-based nanoribbons.

It then reacted by intramolecular Scholl reaction to efficiently give the expected aromatic polycyclic compound **120**, proving that this strategy is a reasonable approach for the formation of carbon nanoribbons.

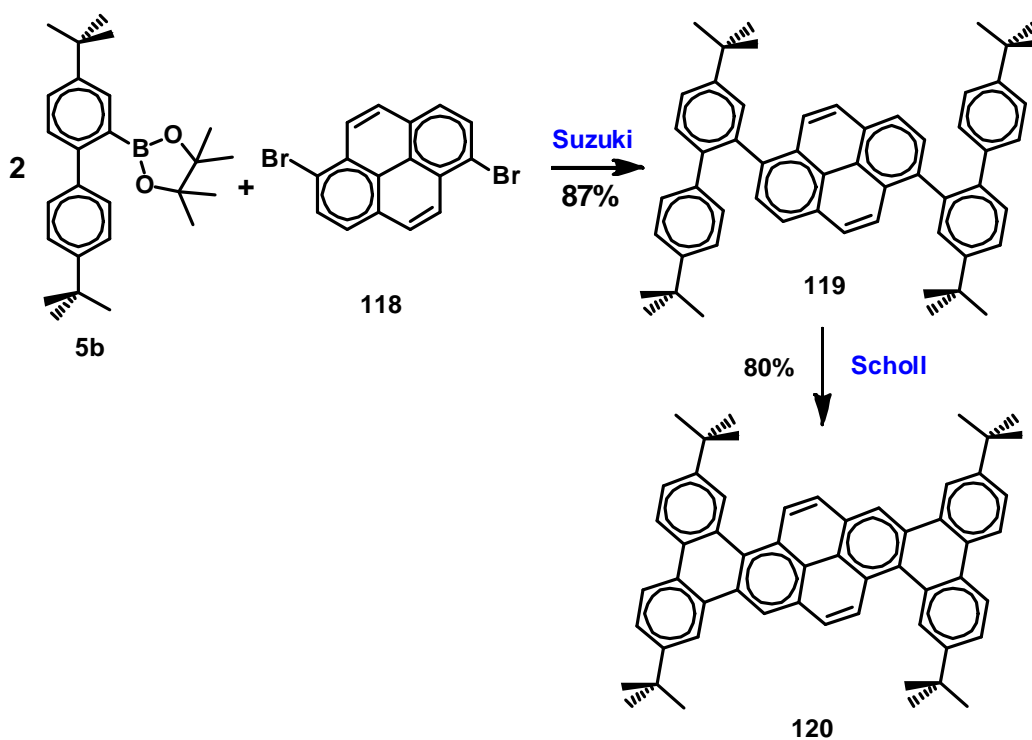


Figure 132. Test reaction for the pyrene-based approach to carbon nanoribbons.

Experimental section

Instrumentation

Proton Nuclear Magnetic Resonance (^1H NMR) and Carbon Nuclear Magnetic Resonance (^{13}C NMR) spectra were acquired at room temperature on a **JEOL ECS400** (400 MHz) spectrometer. The spectra were referenced to residual proton-solvent references (^1H : CD_2Cl_2 : 5.32 ppm, CDCl_3 : 7.26 ppm, DMSO-d_6 : 2.50 ppm; ^{13}C : CD_2Cl_2 : 54.0 ppm, CDCl_3 : 77.23 ppm). For the most complex molecules, NOESY and COSY experiments were performed to complete the assignments. In the assignments, the chemical shift (δ in ppm) is given first, followed, in brackets, by the multiplicity of the signal (s: singlet, d: doublet, t: triplet, q: quadruplet, dd: double doublet, m: multiplet), the number of protons involved, the value of the coupling constants (in Hertz) if applicable.

ESI mass spectra were performed by the CESAMO (Bordeaux, France) on a **QStar Elite** mass spectrometer (Applied Biosystems). The instrument is equipped with an ESI source and spectra were recorded in the positive mode. The electrospray needle was maintained at 4500 V and operated at room temperature. Samples were introduced by injection through a 10 μL sample loop into a 200 $\mu\text{L}/\text{min}$ flow of methanol from the LC pump.

MALDI mass spectra were performed by the CESAMO (Bordeaux, France) on a **Voyager** mass spectrometer (Applied Biosystems). The instrument is equipped with a pulsed N_2 laser (337 nm) and a time-delayed extracted ion source. Spectra were recorded in the positive-ion mode using the reflectron and with an accelerating voltage of 20 kV. Samples were dissolved in CH_2Cl_2 at 10 mg/ml. The dithranol matrix (1,8-dihydroxyanthrone) solution was prepared by dissolving 10 mg in 1 ml of CH_2Cl_2 . A MeOH solution of cationisation agent (NaI, 10 mg/ml) was also prepared. The solutions were combined in a 10:1:1 volume ratio of matrix to sample to cationisation agent. One to two microliters of the obtained solution was deposited onto the sample target and vacuum-dried.

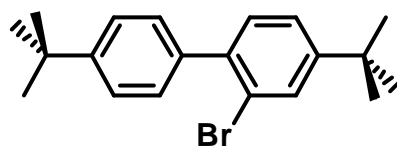
Field Desorption High Resolution Mass Spectra (**FD-HRMS**) were performed by the CESAMO (Bordeaux, France). The measurements were carried out on a TOF mass spectrometer AccuTOF GCv using an FD emitter with an emitter voltage of 10 kV. One to two microliters solution of the compound is deposited on a 13 m emitter wire.

Chromatographic supports

Thin-layer chromatographies were performed using aluminum sheets coated with silica. They were examined under the UV lamp (luminescent compounds) or after oxidation with iodine. Column chromatography was carried out on silica gel (Carlo Erba, 35-70 μm).

The crystallographic data were collected with a Bruker APEX II diffractometer, equipped with a graphite monochromator centred on the path of MoK_α . Single crystals were coated with Paratone N-oil and mounted on a fiber loop followed by data collection at 120 K. The program SAINT was used to integrate the data, which was thereafter corrected for absorption using SADABS. All structures were solved by direct methods and refined by a full-matrix least-squares method on F^2 using SHELXL-97. Non-hydrogen atoms were refined with anisotropic displacement parameters. Hydrogen atoms were placed at calculated positions using suitable riding models. Their positions were constrained relative to their parent atom using the appropriate HFIX command in SHELXL-97

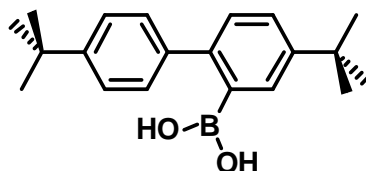
Preparation of 2-bromo-4,4'-di-tert-butylbiphenyl (4)



4,4'-Di-tert-butylbiphenyl (10.64 g, 40.0 mmol) **3** was dissolved in chloroform (80 mL). A solution of bromine (4.53 mL, 88.0 mmol) in chloroform (20 mL) was added very slowly over 1 h. The solution was heated at 70 °C for overnight. After cooling to room temperature water was added to the reaction mixture. The organic layer was then decanted and the aqueous layer was extracted 2 times with diethyl ether. The combine organic layer was washed with brine solution, dried (Na₂SO₄), and evaporated in *vacuo*. The residue was purified by recrystallization from ethanol. (white solid, 9.50 g, 69%).

Mp 97-98 °C; ¹H NMR (400 MHz, CD₂Cl₂): δ 7.64 (d, 1H, *J* = 1.6 Hz), 7.42 (d, 2H, *J* = 8.4 Hz), 7.36 (dd, 1H, *J* = 2, 8 Hz), 7.32 (d, 2H, *J* = 8.4 Hz), 7.23 (d, 1H, *J* = 7.6 Hz), 1.34 (s, 9H), 1.31 (s, 9H). ¹³C NMR (100 MHz, CDCl₃): δ 152.0, 150.3, 139.5, 138.1, 131.1, 130.2, 129.2, 124.9, 124.6, 122.5, 34.7, 31.5, 31.3. ESI HRMS calcd (M⁺) 345.11, found 345.10.

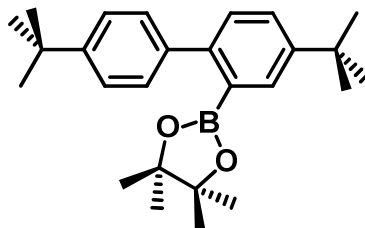
Compound 5a



2-Bromo-4,4'-di-tert-butylbiphenyl **4** (10.0 g, 28.98 mmol) in THF (100 mL) at -80 °C was added a solution of *n*-butyllithium in hexanes (6.71 mL, 18.10 mmol) After stirring for 5-15 min at -80 °C, trimethyl borate (11.80 mL, 31.89 mmol) was added, the reaction was allowed to 1h. Upon reaching room temperature the reaction was quenched by the addition of water and few drops of concentrated HCL (Upto pH 1), then extracted with ethyl acetate. The extract was washed with water, dried with sodium sulfate, filtered and concentrated *in vacuo*. The crude product was purified by chromatography on silicagel by using pet. ether / EtOAc (20%) as the eluent to give the title compound **5a** (white solid, 7.20 g, 80%).

¹H NMR (400 MHz, CDCl₃): δ 7.95 (d, 1H, *J* = 2.0 Hz), 7.50 (dd, 1H, *J* = 2.0, 8.0 Hz), 7.45 (d, 2H, *J* = 8.8 Hz), 7.33(d, 2H, *J* = 8.8 Hz), 7.25 (d, 1H, *J* = 8.4 Hz), 1.37 (s, 9H), 1.35 (s, 9H).

Compound 5b

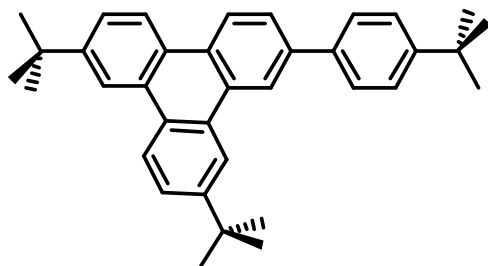


2-Bromo-4,4'-di-tert-butylbiphenyl **4** (3.0 g, 8.7 mmol) in THF (50 mL) at -80 °C was added a solution of *n*-butyllithium in hexanes (3.6 mL, 9.7 mmol) After stirring for 5-15 min at -80 °C, 2-Methoxy-4,4,5,5-tetramethyl-1,3,2-dioxaborolane (1.57 mL, 9.7 mmol) was added, the

reaction was allowed to 1h. Upon reaching room temperature the reaction was quenched by the addition of water, then extracted with ethyl acetate. The extract was washed with water, dried with sodium sulfate, filtered and concentrated *in vacuo*. The crude product was purified by chromatography on silicagel by using pet. ether / EtOAc (5%) as the eluent to give the title compound **5b** (white solid, 2.54 g, 74.5%).

Mp 94-95 °C; ¹H NMR (400 MHz, CD₂Cl₂): δ 7.64 (d, 1H, *J* = 2.0 Hz), 7.46 (dd, 1H, *J* = 2.4, 8.4 Hz), 7.37 (d, 2H, *J* = 8.4 Hz), 7.29 (d, 1H, *J* = 8.4 Hz), 7.26 (d, 2H, *J* = 8.4 Hz), 1.33 (s, 9H), 1.32 (s, 9H), 1.18 (s, 12H). ¹³C NMR (100 MHz, CD₂Cl₂): δ 149.8, 148.8, 144.4, 140.1, 131.1, 128.6, 128.5, 127.1, 124.8, 83.6, 34.4, 34.3, 31.2, 31.1, 24.4. ESI HRMS calcd (M+Na⁺) 415.2778, found 415.2772.

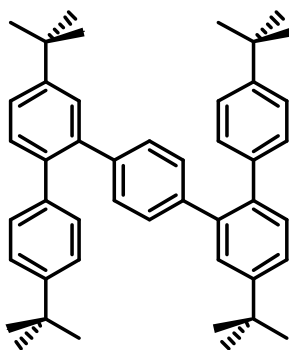
2,6-di-tert-butyl-11-(4-tert-butylphenyl)triphenylene (12)



Compound **10** (300 mg, 0.344 mmol) was dissolved in 50 mL of unstabilized dichloromethane and degassed with an argon stream for 15 minutes. Then a solution of 1.12 g FeCl₃ (6.88 mmol) in 10 mL nitromethane was added dropwise while continuously degassing with an argon stream. After 1 h the reaction was stopped by adding 100 mL of ethanol. Then the organic phase was extracted with water two times and dried with anhydrous sodium sulfate. The solvent was removed *in vacuo* and The crude product was purified by chromatography on silicagel by using pet. ether / CH₂Cl₂ (1%) as the eluent to give the title compound **12** (yellow solid, 122 mg, 75%) .

Mp 380-381 °C; ¹H NMR (400 MHz, CDCl₃): δ 8.82 (d, 1H, *J* = 2.0 Hz), 8.70 (d, 1H, *J* = 2.0 Hz), 8.65 (d, 1H, *J* = 8.0 Hz), 8.62 (d, 1H, *J* = 8.4 Hz), 8.61 (s, 1H), 8.56 (d, 1H, *J* = 8.8 Hz), 7.85 (dd, 1H, *J* = 1.6, 8.4 Hz), 7.75 (d, 2H, *J* = 8.4 Hz), 7.74-7.72 (m, 1H), 7.70 (dd, 1H, *J* = 2.0, 8.4 Hz), 7.57 (d, 2H, *J* = 8.0 Hz), 1.50 (s, 9H), 1.49 (s, 9H), 1.41 (s, 9H). ESI HRMS calcd (M⁺) 472.21015, found 472.21104.

Compound 16

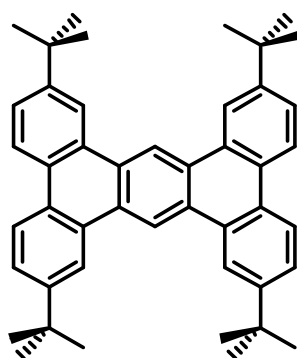


2-Bromo-4,4'-di-tert-butylbiphenyl **4** (3.80 g, 11.0 mmol), 1,4-Phenylenebisboronic acid **15** (829 mg, 5.0 mmol) and Na₂CO₃ (10.60 g, 100 mmol) were dissolved in toluene (150 mL),

water (50 mL) and ethanol (30 mL). The solution was degassed three times, Pd(PPh₃)₄ (577.70 mg, 0.5 mmol) was added under an Ar stream and the mixture was degassed three times again. The solution was heated at 90 °C for overnight. The organic layer was then decanted and the aqueous layer was extracted 2 times with CH₂Cl₂. The combine organic layer was washed with water and evaporated. The crude product was purified by chromatography on silicagel by using pet. ether / CH₂Cl₂ (2%) as the eluent to give the title compound **16** (white solid, 2.43 g, 80%).

Mp 311-312 °C; ¹H NMR (400 MHz, CD₂Cl₂): δ 8.41 (d, 1H, *J* = 2 Hz), 7.39 (d, 1H, *J* = 2 Hz), 7.37 (d, 2H, *J* = 2 Hz), 7.31 (d, 2H, *J* = 8 Hz), 7.24 (d, 4H, *J* = 8.4 Hz), 7.02 (d, 4H, *J* = 8.0 Hz), 6.98 (s, 4H), 1.34 (s, 18H), 1.27 (s, 18H). ¹³C NMR (100 MHz, CD₂Cl₂): δ 150.3, 149.3, 140.3, 139.9, 138.5, 137.6, 130.2, 129.5, 129.4, 127.5, 124.6, 124.5, 34.5, 34.3, 31.1. Maldi-MS calcd (M+Na⁺) 629.41, found 629.40.

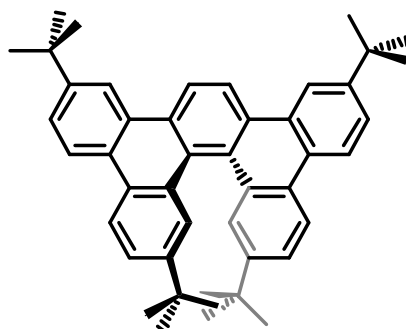
2,7,11,16-tetra-tert-butyltribenzo[f,k,m]tetraphene (17)...



Compound **16** (100 mg, 0.165 mmol) were dissolved in 30 mL of unstabilized dichloromethane and degassed with an argon stream for 15 minutes. Then a solution of 535.20 mg FeCl₃ (3.3 mmol) in 5 mL nitromethane was added dropwise while continuously degassing with an argon stream. Throughout the whole reaction, a constant stream of argon was bubbled through the mixture to remove HCl formed in situ. The reaction was stirred for 25 min and then quenched by adding methanol (50 mL). The precipitate was collected by filtration, washed with methanol. The crude product was recrystallised by Toluene. White solid (10 mg, 10% yield).

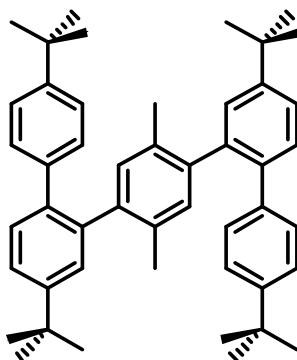
Mp >400 °C; ¹H NMR (400 MHz, CDCl₃): δ 9.96 (s, 2H), 8.94 (s, 4H), 8.57 (d, 4H, *J* = 4.4 Hz), 7.75 (d, 4H, *J* = 3.6 Hz) 1.58 (s, 36H). ¹³C NMR (100 MHz, CDCl₃): δ 149.7, 129.3, 129.1, 127.9, 125.6, 123.3, 119.2, 117.5, 35.2, 31.5. Maldi-MS calcd (M⁺) 602.39, found 602.20.

... and 2,7,10,15-tetra-tert-butyl dibenzo[f,j]picene (18)



The mother liquor was recrystallised in n-pentane. White solid (79 mg, 80% yield).
 Mp 392-393 °C; ¹H NMR (400 MHz, CDCl₃): δ 8.68 (s, 2H), 8.65 (d, 2H, *J* = 1.6 Hz), 8.60 (d, 2H, *J* = 8.8 Hz), 8.17 (d, 2H, *J* = 1.6 Hz), 7.78 (dd, 2H, *J* = 1.6, 8.8 Hz), 7.52 (dd, 2H, *J* = 2, 8.8 Hz), 1.53 (s, 18H), 1.05 (s, 18H). ¹³C NMR (100 MHz, CDCl₃): δ 149.8, 147.2, 130.7, 130.4, 129.1, 128.5, 128.2, 127.5, 127.4, 125.2, 124.8, 123.2, 123.0, 121.3, 119.6, 35.2, 34.5, 31.6, 30.9 (18C). Maldi-MS calcd (M⁺) 602.39, found 602.20.

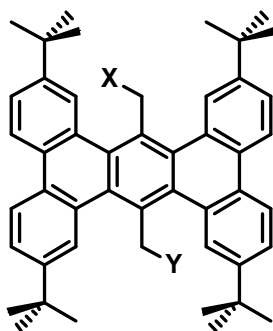
Compound 20



1,4-Dibromo-2,5-dimethylbenzene **19** (500 mg, 1.89 mmol), 2-(4,4'-di-tert-butylbiphenyl-2-yl)-4,4,5,5-tetramethyl-1,3,2-dioxaborolane **5b** (1.57 g, 4.0 mmol) and Na₂CO₃ (2.0 g, 18.9 mmol) were dissolved in toluene (30 mL), water (10 mL) and ethanol (5 mL). The solution was degassed three times, Pd(PPh₃)₄ (218.2 mg, 0.189 mmol) was added under an Ar stream and the mixture was degassed three times again. The solution was heated at 90 °C for 48h. The organic layer was then decanted and the aqueous layer was extracted 2 times with CH₂Cl₂. The combine organic layer was washed with water and evaporated. The crude product was purified by chromatography on silicagel by using pet. ether / CH₂Cl₂ (5%) as the eluent to give the title compound **20** (white solid, 981mg, 84%).

Mp 180-181 °C; ¹H NMR (400 MHz, CD₂Cl₂): δ 7.42-7.40 (m, 2H), 7.38-7.29 (m, 4H), 7.24-7.20 (m, 4H), 7.07-7.05 (m, 4H), 6.85-6.79 (m, 2H), 1.76-1.68 (m, 6H), 1.33 (s, 18H), 1.29-1.26 (m, 18H). ¹³C NMR (100 MHz, CD₂Cl₂): δ 149.9, 149.7, 149.4, 149.2, 140.7, 139.8, 139.6, 138.7, 138.5, 138.0, 137.7, 132.9, 132.6, 132.3, 131.9, 129.6, 129.5, 129.1, 128.2, 128.0, 124.5, 124.3, 34.5, 34.3, 31.2, 19.3, 19.1. ESI HRMS calcd (M⁺) 634.45385, found 634.45482.

Compound 21

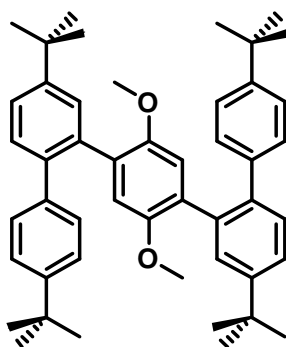


Compound **20** (100 mg, 0.157 mmol) were dissolved in 50 mL of unstabilized dichloromethane and degassed with an argon stream for 15 minutes. Then a solution of 585.7

mg FeCl₃ (3.61 mmol) in 5 mL nitromethane was added dropwise while continuously degassing with an argon stream. After 1 h the reaction was stopped by adding 100 mL of ethanol. Then the organic phase was extracted with water two times and dried with anhydrous sodium sulfate. The solvent was removed in *vacuo* and the crude product was purified by chromatography on silicagel by using pet. ether / CH₂Cl₂ (1%) as the eluent to give the title compound **21** (yellow solid, 62 mg, 63%)

¹H NMR (400 MHz, CDCl₃): δ 9.00 (d, 2H, *J* = 1.6 Hz), 8.68 (d, 2H, *J* = 9.2 Hz), 8.66 (d, 2H, *J* = 8.8 Hz), 8.42 (d, 2H, *J* = 2.0 Hz), 7.76-7.70 (m, 4H), 6.12 (s, 2H), 2.35 (s, 1H), 1.72-1.71 (m, 3H), 1.56 (s, 18H), 1.53 (s, 18H).

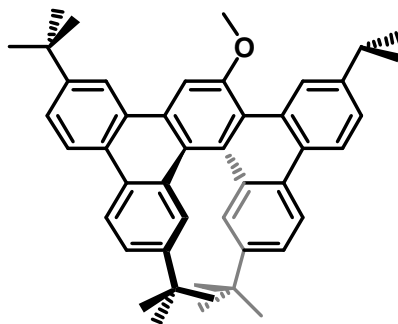
1,4-bis(4,4'-di-*tert*-butylbiphenyl-2-yl)-2,5-dimethoxybenzene (**23**)



Commercially available 1,4-dibromo-2,5-dimethoxybenzene **21** (296 mg, 1.0 mmol), 2-(4,4'-di-*tert*-butylbiphenyl-2-yl)-4,4,5,5-tetramethyl-1,3,2-dioxaborolane **5b** (823 mg, 2.1 mmol) and Na₂CO₃ (1.06 g, 10 mmol) were dissolved in toluene (24 mL), water (8 mL) and ethanol (4 mL). The solution was degassed, Pd(PPh₃)₄ (115 mg, 0.1 mmol) was added under an Ar stream and the mixture was degassed again. The solution was heated at 90°C overnight. The organic layer was separated and the aqueous layer was extracted with CH₂Cl₂. The combined organic layer was washed with water and evaporated. The crude product was purified by chromatography on silica gel by using petroleum ether / CH₂Cl₂ (20%) as the eluent to give the title compound **23** (white solid, 547 mg, 82%).

Mp 172-173°C; ¹H NMR (400 MHz, CD₂Cl₂): δ 7.41 (dd, 2H, *J* = 2.2, 8.2 Hz), 7.34 (d, 2H, *J* = 7.2 Hz), 7.33 (d, 2H, *J* = 2.4 Hz), 7.30 (d, 4H, *J* = 8.4 Hz), 7.07 (d, 4H, *J* = 8.4 Hz), 6.55 (s, 2H), 3.07 (s, 6H), 1.34 (s, 18H), 1.27 (s, 18H); ¹³C NMR (100 MHz, CD₂Cl₂): δ 150.2, 150.0, 149.3, 139.0, 138.6, 136.8, 130.6, 129.2, 128.6, 127.9, 124.7, 124.3, 115.2, 55.5, 34.5, 34.3, 31.1; FD-HRMS Calcd (M⁺) 666.44368, found 666.44045.

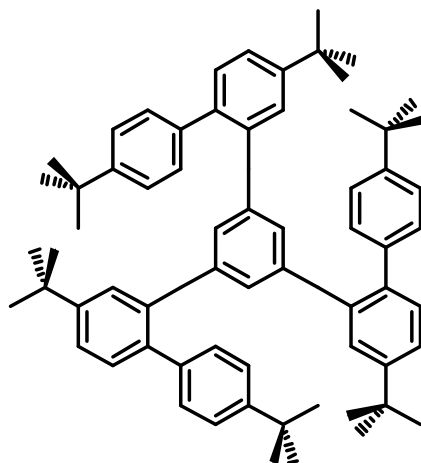
2,7,10,15-tetra-*tert*-butyl-17-methoxydibenzo[*f,j*]picene (**24**)



Compound **23** (100 mg, 0.15 mmol) was dissolved in 30 mL of unstabilized dichloromethane and degassed with an Ar stream for 15 minutes. A solution of FeCl₃ (145 mg, 0.89 mmol) in 5 mL of nitromethane was added drop wise while continuously degassing with an Ar stream. After 30 minutes the reaction was stopped by adding 100 mL of methanol. The organic phase was then washed twice with water and dried over anhydrous Na₂SO₄. The solvent was removed *in vacuo* and the crude product was purified by chromatography on silica gel by using petroleum ether / CH₂Cl₂ (8%) as the eluent to give the title compound **24** (yellow solid, 84 mg, 89%).

Mp 314-315°C; ¹H NMR (400 MHz, CD₂Cl₂): δ 9.56 (d, 1H, *J* = 2.0 Hz), 8.60 (d, 1H, *J* = 8.8 Hz), 8.58 (s, 1H), 8.57 (d, 1H, *J* = 9.2 Hz), 8.44 (d, 1H, *J* = 8.4 Hz), 8.41 (d, 1H, *J* = 8.8 Hz), 8.09 (s, 1H), 8.03 (d, 1H, *J* = 2.4 Hz), 8.00 (d, 1H, *J* = 2.0 Hz), 7.79 (dd, 1H, *J* = 2.0, 8.8 Hz), 7.75 (dd, 1H, *J* = 2.2, 8.8 Hz), 7.52 (dd, 1H, *J* = 1.6, 8.8 Hz), 7.47 (dd, 1H, *J* = 2.2, 8.6 Hz), 4.31 (s, 3H), 1.54 (s, 9H), 1.50 (s, 9H), 1.02 (s, 18H); ¹³C NMR (100 MHz, CD₂Cl₂): δ 157.0, 149.6, 149.1, 147.3, 147.2, 131.9, 130.7, 130.6, 130.2, 128.7, 128.4, 128.3, 128.1, 127.7, 127.4, 126.9, 126.3, 125.2, 124.9, 124.8, 124.5, 123.7, 122.9, 122.8, 122.2, 122.0, 119.2, 102.4, 56.3, 35.0, 34.9, 34.2, 31.3, 31.2, 30.6; FD-HRMS Calcd (M⁺) 632.40181, found 632.40384.

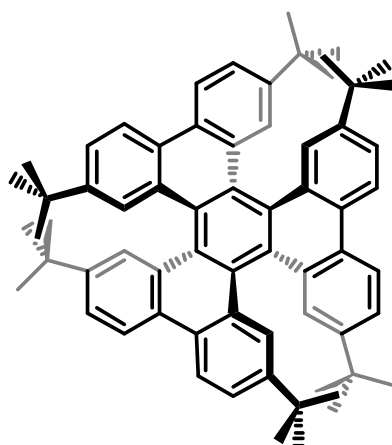
Compound 27



1,3,5-tribromobenzene **26** (500 mg, 1.59 mmol), 2-(4,4'-di-tert-butylbiphenyl-2-yl)-4,4,5,5-tetramethyl-1,3,2-dioxaborolane **5b** (2.49 g, 6.35 mmol) and Na₂CO₃ (3.36 g, 31.8 mmol) were dissolved in toluene (30 mL), water (10 mL) and ethanol (5 mL). The solution was degassed three times, Pd(PPh₃)₄ (183.7 mg, 0.159 mmol) was added under an Ar stream and the mixture was degassed three times again. The solution was heated at 90 °C for 48h. The organic layer was then decanted and the aqueous layer was extracted 2 times with CH₂Cl₂. The combine organic layer was washed with water and evaporated. The crude product was purified by chromatography on silicagel by using pet. ether / CH₂Cl₂ (4%) as the eluent to give the title compound **27** (white solid, 1.05 g, 76%).

Mp 277-278 °C; ¹H NMR (400 MHz, CD₂Cl₂): δ 7.39 (d, 6H, *J* = 8.4 Hz), 7.37 (dd, 3H, *J* = 2, 8.6 Hz), 7.26 (d, 3H, *J* = 8.4 Hz), 7.16 (d, 3H, *J* = 2Hz), 6.94 (d, 6H, *J* = 8.8 Hz), 6.82 (s, 3H), 1.28 (s, 27H), 1.26 (s, 27H). ¹³C NMR (100 MHz, CD₂Cl₂): δ 150.2, 149.2, 142.6, 139.9, 138.1, 137.3, 130.3, 129.9, 129.48, 128.0, 124.7, 124.6, 34.4, 34.3, 31.2, 31.1. ESI HRMS calcd (M+Na⁺) 893.5995, found 893.6007.

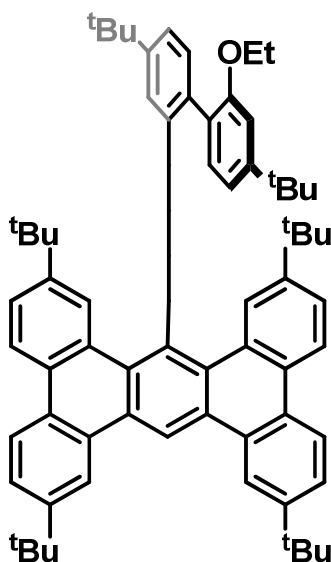
Hexa-tert-butyl-hexabenzotriphenylene 28



Compound **27** (300 mg, 0.344 mmol) were dissolved in 50 mL of unstabilized dichloromethane and degassed with an argon stream for 15 minutes. Then a solution of 1.12 g FeCl_3 (6.88 mmol) in 10 mL nitromethane was added dropwise while continuously degassing with an argon stream. After 1 h the reaction was stopped by adding 100 mL of ethanol. Then the organic phase was extracted with water two times and dried with anhydrous sodium sulfate. The solvent was removed in *vacuo* and The crude product was purified by chromatography on silicagel by using pet. ether / CH_2Cl_2 (1%) as the eluent to give the title compound **28** (yellow solid, 187 mg, 63%).

Mp >400 °C; ^1H NMR (400 MHz, CD_2Cl_2): δ 8.33 (d, 6H, $J = 8$ Hz), 7.95 (d, 6H, $J = 2$ Hz), 7.43 (dd, 6H, $J = 2, 8.4$ Hz), 0.91 (s, 54H). ^{13}C NMR (100 MHz, CD_2Cl_2): δ 147.5, 131.3, 128.7, 127.6, 127.2, 124.6, 122.8, 34.5, 30.8. ESI HRMS calcd (M+) 865.28, found 865.2. TOF MS calcd (M+Na) 887.5526, found 887.5490.

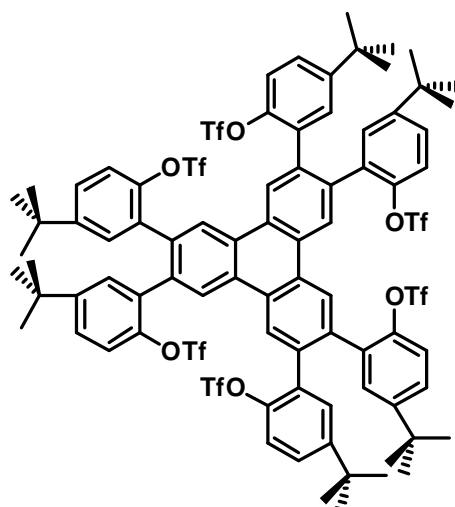
Compound 29



^1H NMR (400 MHz, CD_2Cl_2): δ 8.92 (d, 2H, $J = 1.6$ Hz), 8.51 (d, 2H, $J = 8.8$ Hz), 8.41 (d, 2H, $J = 9.2$ Hz), 8.02 (d, 1H, $J = 1.2$ Hz), 7.99 (d, 1H, $J = 8.0$ Hz), 7.87 (d, 1H, $J = 7.6$ Hz), 7.76 (s, 1H), 7.74 (d, 1H, $J = 2.0$ Hz), 7.72 (d, 1H, $J = 1.6$ Hz), 7.49 (dd, 1H, $J = 1.8, 8.2$ Hz), 7.46 (d, 2H, $J = 1.6$ Hz), 7.31 (dd, 2H, $J = 1.8, 8.6$ Hz), 7.22 (dd, 1H, $J = 1.6, 8.0$ Hz), 6.25 (d,

1H, $J = 1.6$ Hz), 3.72 (q, 2H, $J = 7.2$ Hz), 3.38-3.39 (m, 3H), 1.58 (s, 18H), 1.13 (s, 9H), 1.0 (s, 18H), 0.70 (s, 9H).

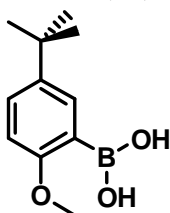
Compound 33



To the compound **38** (278 mg, 0.25 mmol) dissolved in 10 mL of anhydrous CH_2Cl_2 were added 5 mL of pyridine and the solution was cooled to 0°C . Trifluoromethanesulfonic anhydride (0.50 mL, 2.98 mmol) was added drop wise and the mixture was warmed to room temperature and stirred overnight. The solvent was removed under vacuum. The crude product was purified by chromatography on silica gel by using petroleum ether / CH_2Cl_2 (40%) as the eluent to give the title compound **33** (white solid, 454 mg, 95%).

Mp $180\text{-}181^\circ\text{C}$; ^1H NMR (400 MHz, DMSO): δ 9.06-8.78 (br, 6H), 7.81-7.39 (br, 12H), 7.29-7.02 (br, 6H), 1.39-1.01 (br, 54H); ^{19}F NMR (376 MHz, DMSO): δ -74.46, -75.78; ^{13}C NMR (100 MHz, CD_2Cl_2): δ 151.9-151.6(br), 144.7-144.5 (br), 135.5-135.0 (br), 133.3-132.9 (br), 131.2-131.0 (br), 129.5, 127.0-126.2 (br), 121.2-120.6 (br), 119.9, 116.8-116.6 (br), 34.6, 30.8; FD-HRMS Calcd (M+) 1908.32249, found 1908.32776.

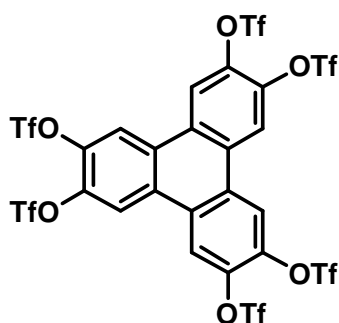
5-tert-butyl-2-methoxyphenylboronic acid (**34**)



2-bromo-4-tert-butyl-1-methoxybenzene **69** (4.0 g, 16.45 mmol) in THF (50 mL) at -80°C was added a solution of *n*-butyllithium in hexanes(6.71 mL, 18.10 mmol) After stirring for 5-15 min at -80°C , trimethyl borate (2.05 mL, 18.10 mmol) was added, the reaction was allowed to 1h. Upon reaching room temperature the reaction was quenched by the addition of water and few drops of concentrated HCL (Upto pH 1), then extracted with ethyl acetate. The extract was washed with water, dried with sodium sulfate, filtered and concentrated *in vacuo*. The crude product was purified by chromatography on silicagel by using pet. ether / EtOAc (8%) as the eluent to give the title compound **34** (white solid, 3.08 g, 90%).

^1H NMR (400 MHz, CD_2Cl_2): δ 7.79 (d, 1H, $J = 2.8$ Hz), 7.45 (dd, 1H, $J = 2.8, 8.8$ Hz), 6.86 (d, 1H, $J = 8.4$ Hz), 5.97-5.84 (br, 2H), 3.86 (s, 3H), 1.28 (s, 9H).

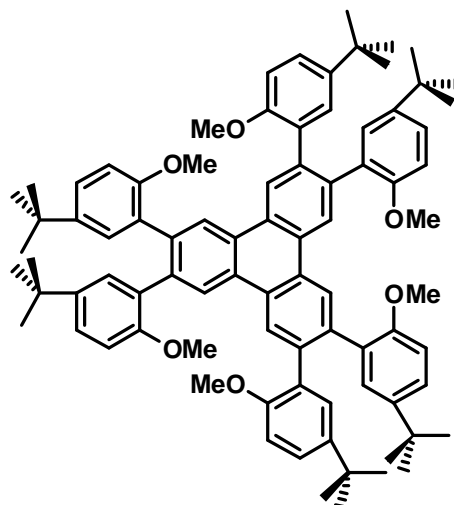
Compound 35



To the compound 2,3,6,7,10,11-hexahydroxy triphenylene compound **36** (200 mg, 0.62 mmol) dissolved in 5 mL of anhydrous CH_2Cl_2 were added 5.0 mL of pyridine and the solution was cooled to 0°C . Trifluoromethanesulfonic anhydride (1.25 mL, 7.40 mmol) was added drop wise and the mixture was warmed to room temperature and stirred overnight. The solvent was removed under vacuum. The crude product was purified by chromatography on silica gel by using petroleum ether / CH_2Cl_2 (15%) as the eluent to give the title compound **35** (white solid, 527 mg, 85%).

Mp $167\text{--}168^\circ\text{C}$; ^1H NMR (400 MHz, CD_2Cl_2): δ 8.57(s, 6H); ^{19}F NMR (400 MHz, CD_2Cl_2): δ -72.80; ^{13}C NMR (100 MHz, CD_2Cl_2): δ 140.9, 129.1, 119.7; FD-HRMS Calcd (M+) 1115.75909, found 1115.76078.

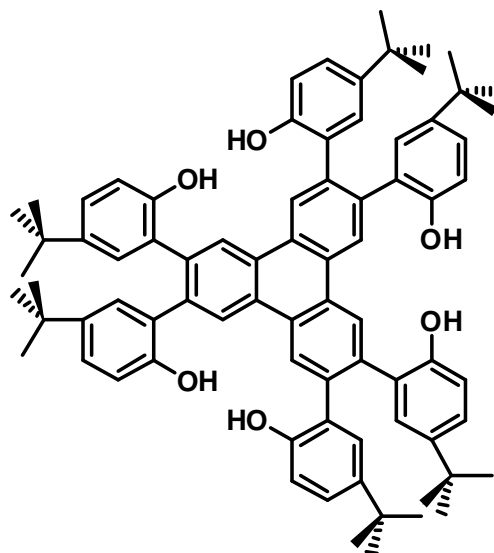
Compound 37



To the compound 2,3,6,7,10,11-hexa(trifluoromethanesulfonate) triphenylene **35** (480 mg, 0.43 mmol), 5-*tert*-butyl-2-methoxyphenylboronic acid **34** (804.92 mg, 3.87 mmol) and K_3PO_4 (2.73 g, 12.87 mmol) were dissolved in a mixture of THF (10 mL) and water (2 mL). The solution was degassed, $\text{Pd}(\text{OAc})_2$ (28.90 mg, 0.129 mmol) and 2-dicyclohexylphosphino-2',6'-dimethoxybiphenyl SPhos (63.40 mg, 0.154 mmol) were added under an Ar stream and the mixture was degassed again. The solution was heated at 70°C for 96h. The organic layer was then decanted and the aqueous layer was extracted twice with CH_2Cl_2 . The combine organic layer was washed with water and evaporated. The crude product was purified by chromatography on silica gel by using petroleum ether / CH_2Cl_2 (50%) as the eluent to give the title compound **37** (white solid, 388 mg, 75%).

Mp 200-201 °C; ¹H NMR (400 MHz, CDCl₃): δ 8.72 (s, 6H), 7.16-7.14 (m, 12H), 6.70 (d, 6H, *J* = 8.0 Hz), 3.50 (s, 18H), 1.16 (s, 54H); ¹³C NMR (100 MHz, CD₂Cl₂): δ 154.4, 142.5, 137.4, 130.5, 129.2, 129.1, 125.9, 124.6, 110.0, 55.4, 34.0, 31.7; FD-HRMS Calcd (M+) 1201.72851, found 1201.72339.

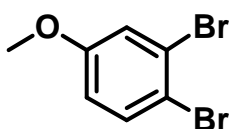
Compound 38



To the compound **37** (300 mg, 0.25 mmol) was dissolved in 10 mL of dry CH₂Cl₂ under N₂ and brought to -20 °C. BBr₃ (1 M in CH₂Cl₂, 10.0 equiv, 2.49 mmol, 2.49 mL) was added dropwise with stirring and the reaction mixture stirred overnight, warming to room temperature. The reaction mixture was then poured into ice water, organic layer was then decanted and the aqueous layer was extracted 2 times with CH₂Cl₂. The combine organic layer was washed with water and dried over anhydrous Na₂SO₄. The solvent was removed under vacuum, yielding **38** (275 mg, 99%) as a brown-red solid, which was judged pure enough by TLC to be used in subsequent steps without further purification.

Mp 274-275 °C; ¹H NMR (400 MHz, CDCl₃): δ 8.79 (s, 6H), 7.12 (d, 6H, *J* = 10.4 Hz), 7.02 (s, 6H), 6.73 (d, 6H, *J* = 7.2 Hz), 1.12 (s, 54H). ¹³C NMR (100 MHz, CD₂Cl₂): δ 150.3, 143.2, 137.4, 129.4, 128.4, 126.6, 126.3, 125.9, 115.2, 34.0, 31.5. FD-HRMS calcd (M+) 1116.62679, found 1116.62828.

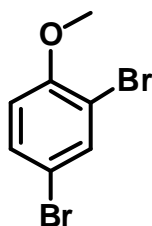
3,4-dibromo-1-methoxybenzene (41)



To a solution of 3,4-dibromophenol **42** (10.0 g, 39.69 mmol) in 100 mL of acetone was added potassium carbonate (13 g, 94.1 mmol) and iodomethane (4.90 mL, 79.34 mmol). The reaction mixture was stirred at 56 °C for overnight. The reaction mixture was concentrated, and then it was diluted with DCM and water. The organic layer was then decanted and the aqueous layer was extracted 2 times DCM. The combine organic layer was washed with brine solution, dried (Na₂SO₄), and evaporated in *vacuo*, yielding **41** without further purification (Colorless liquid, 10.34 g, 100%).

^1H NMR (400 MHz, CDCl_3): δ 7.52 (d, 1H, $J = 8.8$ Hz), 7.18 (d, 1H, $J = 2.8$ Hz), 6.75 (d, 1H, $J = 8.8$ Hz), 3.81 (s, 3H).

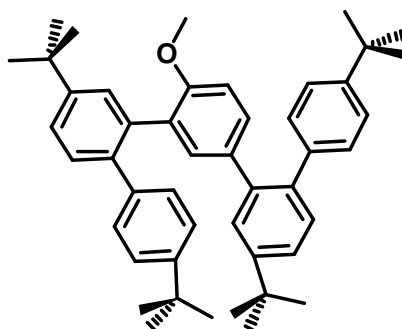
2,4-dibromo-1-methoxybenzene (**45**)



To a solution of 2,4-dibromophenol **44** (15.0 g, 59.54 mmol) in 100 mL of acetone was added potassium carbonate (19.5 g, 141.2 mmol) and iodomethane (7.34 mL, 119 mmol). The reaction mixture was stirred at 56 °C for overnight. The reaction mixture was concentrated, and then it was diluted with DCM and water. The organic layer was then decanted and the aqueous layer was extracted 2 times DCM. The combined organic layer was washed with brine solution, dried (Na_2SO_4), and evaporated *in vacuo*, yielding **45** without further purification (Colourless liquid, 15.5 g, 99%).

^1H NMR (400 MHz, CD_2Cl_2): δ 7.64 (d, 1H, $J = 2.4$ Hz), 7.38 (dd, 1H, $J = 2.6, 9.0$ Hz), 6.79 (d, 1H, $J = 8.8$ Hz), 3.84 (s, 3H).

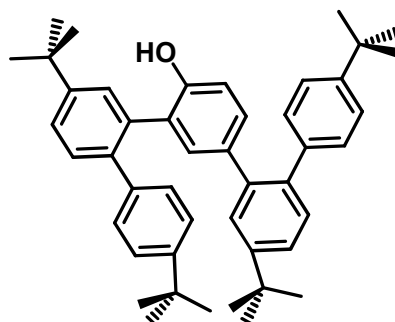
Compound **46**



2,4-dibromo-1-methoxybenzene **45** (1.0 g, 3.76 mmol), 4,4'-di-tert-butylbiphenyl-2-ylboronic acid **5** (2.57 mg, 8.27 mmol) and Na_2CO_3 (7.97 g, 75.2 mmol) were dissolved in toluene (60 mL), water (20 mL) and ethanol (10 mL). The solution was degassed three times, $\text{Pd}(\text{PPh}_3)_4$ (434.06 mg, 0.376 mmol) was added under an Ar stream and the mixture was degassed three times again. The solution was heated at 90 °C for 48h. The organic layer was then decanted and the aqueous layer was extracted 2 times with CH_2Cl_2 . The combined organic layer was washed with water and evaporated. The crude product was purified by chromatography on silicagel by using pet. ether / CH_2Cl_2 (22%) as the eluent to give the title compound **46** (white solid, 1.92 g, 80%).

Mp 140-141 °C; ^1H NMR (400 MHz, CD_2Cl_2): δ 7.41-7.38 (m, 2H), 7.36 (d, 1H, $J = 2.0$ Hz), 7.30-7.27 (m, 4H), 7.22 (s, 1H), 7.21 (s, 2H), 7.10 (d, 2H, $J = 8.4$ Hz), 7.03-7.02 (m, 1H), 7.00 (dd, 1H, $J = 2.2, 8.2$ Hz), 6.95 (d, 2H, $J = 8.0$ Hz), 6.55 (d, 1H, $J = 8.4$ Hz), 3.16 (s, 3H), 1.35 (s, 9H), 1.31 (s, 9H), 1.26 (s, 9H), 1.24 (s, 9H). ^{13}C NMR (100 MHz, CD_2Cl_2): 155.0, 150.2, 149.9, 149.2, 149.0, 139.7, 139.1, 138.7, 138.6, 137.5, 136.7, 134.8, 132.9, 131.0, 130.4, 129.9, 129.6, 129.2, 128.5, 128.2, 127.9, 124.8, 124.6, 124.3, 110.5, 54.9, 34.5, 34.4, 34.3, 31.2. FD-HRMS Calcd (M^+) 636.43311, found 636.43618.

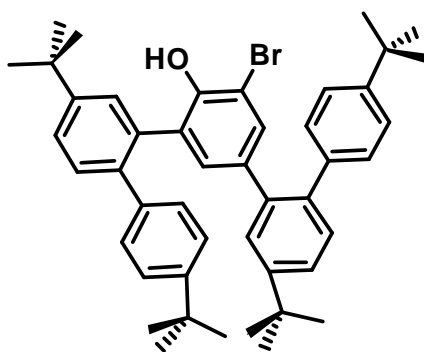
Compound 47



Compound **46** (1.775 g, 2.79 mmol) was dissolved in 40 mL of dry CH_2Cl_2 under N_2 and brought to $-20\text{ }^\circ\text{C}$. BBr_3 (1 M in CH_2Cl_2 , 3.0 equiv, 4.18 mmol, 4.18 mL) was added dropwise with stirring and the reaction mixture stirred overnight, warming to room temperature. The reaction mixture was then poured into ice water, organic layer was then decanted and the aqueous layer was extracted 2 times with CH_2Cl_2 . The combine organic layer was washed with water and dried over anhydrous Na_2SO_4 . The solvent was removed under vacuum, yielding **47** (1.622 g, 93.4%) as a brown-red solid, which was judged pure enough by TLC to be used in subsequent steps without further purification.

Mp $133\text{-}134\text{ }^\circ\text{C}$; $^1\text{H NMR}$ (400 MHz, CD_2Cl_2): δ 7.47 (dd, 1H, $J = 2.2, 8.2$ Hz), 7.38 (d, 1H, $J = 8.0$ Hz), 7.37 (dd, 1H, $J = 2.4, 8.4$ Hz), 7.29-7.26 (m, 7H), 7.06 (d, 2H, $J = 8.8$ Hz), 7.03 (d, 2H, $J = 8.0$ Hz), 6.99 (d, 1H, $J = 2.4$ Hz), 6.85 (dd, 1H, $J = 2.2, 8.2$ Hz), 6.57 (d, 1H, $J = 8.0$ Hz), 1.33 (s, 18H), 1.27 (s, 9H), 1.25 (s, 9H). $^{13}\text{C NMR}$ (100 MHz, CD_2Cl_2): δ 151.2, 151.0, 150.3, 149.9, 149.2, 139.5, 138.5, 138.3, 137.4, 134.7, 134.3, 132.3, 130.6, 130.5, 130.4, 129.6, 128.8, 127.8, 125.8, 125.0, 124.8, 124.3, 114.9, 34.6, 34.5, 34.4, 34.3, 31.2, 31.1. FD-HRMS Calcd (M^+) 622.41746, found 622.41444.

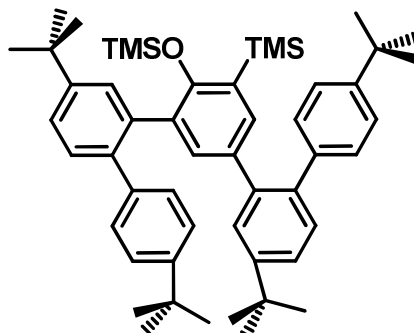
Compound 48



A solution of NBS (331.70 mg, 1.86 mmol) in CH_2Cl_2 (45 mL) was added dropwise over 30 min to a solution of Compound **47** (1.16 g, 1.86 mmol) and $i\text{-Pr}_2\text{-NH}$ (0.03 mL, 0.187 mmol) in CH_2Cl_2 . After addition was complete, the mixture was stirred at room temperature for 1 h, poured on H_2O (80 mL), and acidified to pH 1 by careful addition of concentrated H_2SO_4 . The resulting mixture was extracted with CH_2Cl_2 , and the combined organic layers were dried over anhydrous Na_2SO_4 , filtered, and concentrated under reduced pressure. Column chromatography of the residue (SiO_2 , 1:5 AcOEt/hexane) afforded **48** as a white solid (1.064 g, 84%).

Mp 114-115 °C; ¹H NMR (400 MHz, CD₂Cl₂): δ 7.45 (dd, 1H, *J* = 2.4, 8.4 Hz), 7.39-7.35 (m, 2H), 7.29-7.25 (m, 7H), 7.03-6.99 (m, 5H), 6.88 (d, 1H, *J* = 2.0 Hz), 5.22 (s, 1H), 1.32 (s, 18H), 1.26 (s, 9H), 1.25 (s, 9H). ¹³C NMR (100 MHz, CD₂Cl₂): δ 150.5, 150.4, 149.7, 149.5, 148.1, 138.4, 138.2, 138.1, 137.7, 137.5, 135.6, 134.7, 132.9, 132.3, 130.3, 130.1, 129.8, 129.6, 128.8, 128.2, 127.4, 125.7, 124.9, 124.7, 109.5, 34.5, 34.4, 34.3, 31.1, 29.7. FD-HRMS Calcd (M⁺) 700.32798, found 700.33147.

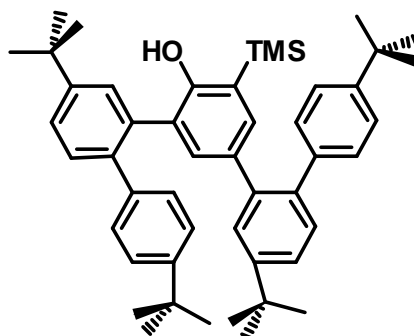
Compound 49



n-BuLi (2.28 mL, 2.5 M, 6.1 mmol) was added dropwise to a solution of **48** (2.87 g, 4.1 mmol) in THF (40 mL) cooled to -78 °C. After stirring at -78 °C for 15 min, TMSCl (0.83 mL, 6.5 mmol) was added, the cooling bath was removed, and stirring was kept for 10 min at room temperature. The mixture was again cooled to -78 °C, *n*-BuLi (1.5 mL, 2.5 M, 4.1 mmol) was added dropwise, stirring was kept up at -78 °C for 15 min, and TMSCl (0.83 mL, 6.5 mmol) was added. Stirring at room temperature was kept up overnight, H₂O (15 mL) was added, and the resulting mixture was extracted with Et₂O. The combined organic layers were dried over anhydrous Na₂SO₄, filtered, and concentrated under reduced pressure. The crude product was purified by chromatography on silica gel by using petroleum ether / CH₂Cl₂ (20%) as the eluent to give the title compound **49** (white solid, 2.51 g, 90%).

Mp 120-121 °C; ¹H NMR (400 MHz, CD₂Cl₂): δ 7.45 (d, 1H, *J* = 2.4 Hz), 7.40-7.37 (m, 3H), 7.31 (d, 1H, *J* = 8.0 Hz), 7.30-7.23 (m, 4H), 7.18 (d, 2H, *J* = 8.4 Hz), 7.04 (d, 2H, *J* = 8.4 Hz), 6.97 (d, 2H, *J* = 8.8 Hz), 6.79 (d, 1H, *J* = 2.4 Hz), 1.36 (s, 18H), 1.25 (s, 18H), -0.21 (s, 9H), -0.32 (s, 9H). ¹³C NMR (100 MHz, CD₂Cl₂): δ 156.1, 150.3, 149.9, 148.9, 148.7, 139.9, 139.1, 138.8, 138.7, 138.4, 137.7, 137.0, 134.5, 133.9, 132.9, 130.2, 129.8, 129.6, 128.7, 127.1, 124.7, 124.2, 124.1, 34.4, 34.2, 31.2, 0.2, -0.7. FD-HRMS Calcd (M⁺) 766.49652, found 766.49823.

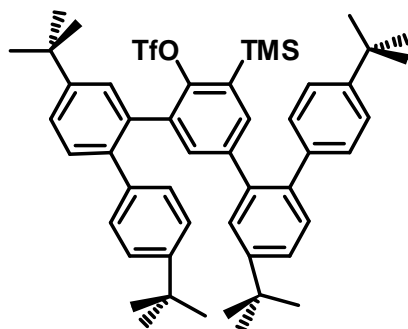
Compound 50



To a solution of compound **49** (2.0 g, 2.6 mmol) in 15 mL of THF was added 20ml 1(M) NaOH (8equivalent) solution. The reaction mixture was stirred at room temperature. The reaction mixture was concentrated, and then it was diluted with Et₂O and water. The organic layer was then decanted and the aqueous layer was extracted 2 times Et₂O. The combine organic layer was washed with brine solution, dried (Na₂SO₄), and evaporated in *vacuo*. (White solid, 1.80 g, 99%).

Mp 140-141 °C; ¹H NMR (400 MHz, CD₂Cl₂): δ 7.50 (dd, 1H, *J* = 2.0, 8.0 Hz), 7.43-7.36 (m, 4H), 7.30 (d, 1H, *J* = 8.0 Hz), 7.27 (d, 4H, *J* = 8.0 Hz), 7.17 (d, 1H, *J* = 2.4 Hz), 7.08 (d, 2H, *J* = 8.4 Hz), 7.02 (d, 2H, *J* = 8.4 Hz), 6.76 (d, 1H, *J* = 2.4 Hz), 4.86 (s, 1H), 1.36 (s, 9H), 1.34 (s, 9H), 1.26 (s, 18H), -0.15 (s, 9H). ¹³C NMR (100 MHz, CD₂Cl₂): δ 155.5, 151.2, 150.4, 150.1, 149.1, 139.8, 138.8, 138.1, 137.5, 137.1, 137.0, 134.8, 133.6, 133.0, 130.3, 129.7, 128.7, 128.6, 127.5, 127.3, 125.9, 125.0, 124.8, 124.7, 124.1, 34.6, 34.5, 34.4, 34.3, 31.2, 31.1, -1.7. FD-HRMS Calcd (M⁺) 694.45699, found 694.45919.

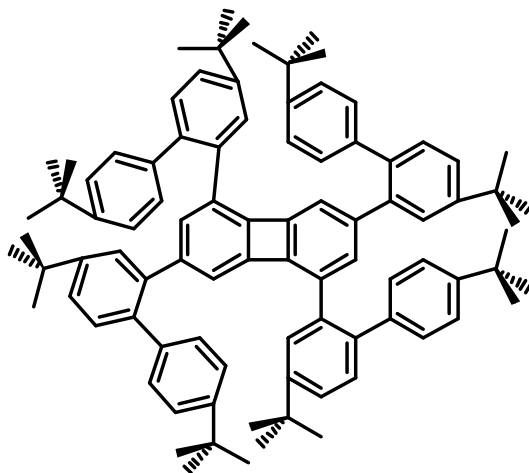
Compound 51



n-BuLi (0.46 mL, 2.5 M, 1.25 mmol) was added dropwise to a solution of **50** (728 mg, 1.05 mmol) in THF (20 mL) cooled to -78 °C. After stirring at -78 °C for 15 min, Trifluoromethanesulfonic anhydride (0.35 mL, 2.09 mmol) was added, the reaction was allowed to 1h. Upon reaching room temperature the reaction was quenched by the addition of water, then extracted with ethyl acetate. The extract was washed with water, dried with sodium sulfate, filtered and concentrated *in vacuo*. The crude product was purified by chromatography on silicagel by using pet. ether / DCM (20%) as the eluent to give the title compound **51** (white solid, 690 mg, 80%).

Mp 86-87 °C; ¹H NMR (400 MHz, CD₂Cl₂): δ 7.45-7.44 (m, 4H), 7.35 (d, 1H, *J* = 8.4 Hz), 7.31 (d, 4H, *J* = 8.0 Hz), 7.21 (d, 2H, *J* = 8.4 Hz), 7.10 (d, 2H, *J* = 8.0 Hz), 7.07 (d, 1H, *J* = 2.8 Hz), 6.87 (d, 2H, *J* = 8.4 Hz), 1.38 (s, 9H), 1.34 (s, 9H), 1.26 (s, 9H), 1.25 (s, 9H), -0.15 (s, 9H). ¹³C NMR (100 MHz, CD₂Cl₂): δ 150.6, 150.2, 149.6, 149.4, 148.5, 141.8, 138.6, 138.3, 138.1, 137.9, 137.8, 135.8, 134.9, 134.5, 134.3, 134.3, 130.7, 129.8, 129.7, 129.5, 129.0, 128.8, 128.7, 128.6, 127.6, 125.6, 125.2, 125.1, 125.0, 124.8, 124.7, 34.6, 34.5, 34.3, 31.2, 31.0, 29.8, -0.59. FD-HRMS Calcd (M⁺) 826.40628, found 826.40930.

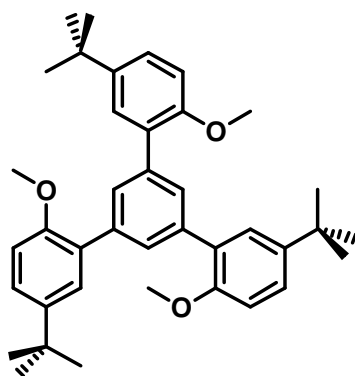
Compound 53



Finely powdered anhydrous CsF (314 mg, 2.1 mmol) was added to a solution of **51** (570 mg, 0.69 mmol), and [Pd₂(dba)₃] (63.10 mg, 0.069 mmol) in CH₃CN/CH₂Cl₂ 3:1 (20 mL), and the mixture was stirred at 40°C for 96 h. After this time, the solvent was removed under reduced pressure and the residue was purified by column chromatography (silica gel; ether/CH₂Cl₂ 4:1), affording **53** (270 mg, 65%) as a white solid.

Mp 115-116 °C; ¹H NMR (400 MHz, CD₂Cl₂): δ 7.82 (d, 2H, *J* = 1.2 Hz), 7.75 (d, 2H, *J* = 7.6 Hz), 7.49(d, 2H, *J* = 2.0 Hz), 7.45 (dd, 2H, *J* = 2.0, 8.0 Hz), 7.41 (dd, 2H, *J* = 2.0, 8.0 Hz), 7.39 (d, 2H, *J* = 1.2 Hz), 7.32 (d, 2H, *J* = 8.4 Hz), 7.14 (d, 4H, *J* = 8.4 Hz), 7.01 (d, 4H, *J* = 8.4 Hz), 6.85 (s, 2H), 6.81 (d, 4H, *J* = 6.4 Hz), 6.75 (d, 4H, *J* = 6.4 Hz), 1.50 (s, 18H), 1.41 (s, 18H), 1.34 (s, 18H), 1.21 (s, 18H). ¹³C NMR (100 MHz, CD₂Cl₂): δ 158.4, 151.5, 150.3, 149.1, 144.1, 143.3, 143.2, 143.1, 139.5, 138.7, 138.5, 137.8, 132.4, 130.3, 129.4, 128.1, 126.4, 124.8, 124.7, 124.3, 124.2, 118.4, 116.3, 66.4, 62.5, 34.9, 34.5, 34.2, 32.0, 31.9, 31.4, 31.2, 31.1, 29.7. FD-HRMS Calcd (M⁺) 1208.81, found 1208.80.

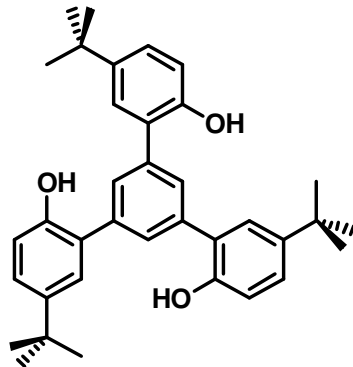
1,3,5-tris(5-*tert*-butyl-2-methoxyphenyl)benzene (**55**)



1,3,5-Tribromobenzene **26** (1.0 g, 3.2 mmol), 5-*tert*-butyl-2-methoxyphenylboronic acid **34** (2.4 g, 11.5 mmol) and Na₂CO₃ (3.4 g, 32 mmol) were dissolved in toluene (30 mL), water (10 mL) and ethanol (5mL). The solution was degassed, Pd(PPh₃)₄ (369 mg, 0.32 mmol) was added under an Ar stream and the mixture was degassed again, then heated at 90°C for 48h. The organic layer was decanted and the aqueous layer was extracted twice with CH₂Cl₂. The combine organic layer was washed with water and evaporated. The crude product was purified by chromatography on silica gel by using petroleum ether / CH₂Cl₂ (20%) as the eluent to give the title compound **55** (white solid, 1.67 g, 95%).

Mp 119-120°C; ¹H NMR (400 MHz, CD₂Cl₂): δ 7.55 (s, 3H), 7.39 (d, 3H, *J* = 2.8 Hz), 7.33 (dd, 3H, *J* = 2.8, 8.8 Hz), 6.93 (d, 3H, *J* = 8.4 Hz), 3.79 (s, 9H), 1.30 (s, 27H); ¹³C NMR (100 MHz, CD₂Cl₂): δ 154.4, 143.5, 138.5, 130.0, 129.4, 128.3, 125.3, 110.6, 55.5, 34.1, 31.3; FD-HRMS Calcd (M⁺) 564.36034, found 564.35856.

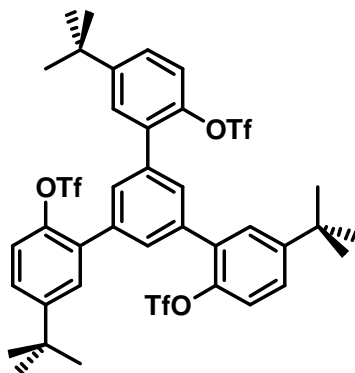
1,3,5-tris(5-*tert*-butyl-2-hydroxyphenyl)benzene (**56**)



Compound **55** (1.72 g, 3.05 mmol) was dissolved in 50 mL of dry CH₂Cl₂ under Ar and brought to -20°C. BBr₃ (1 M in CH₂Cl₂, 12.2 mmol, 12.2 mL) was added drop-wise with vigorous stirring, the reaction mixture was stirred overnight and finally warmed to room temperature. The reaction mixture was then poured on crushed ice, the organic layer was decanted and the aqueous layer was extracted twice with CH₂Cl₂. The combine organic layer was washed with water and dried over anhydrous Na₂SO₄. The solvent was removed under vacuum, yielding **56** without further purification (1.57 g, 99%) as a white solid.

Mp 247-248°C; ¹H NMR (400 MHz, CD₂Cl₂): δ 7.63 (s, 3H), 7.34 (d, 3H, *J* = 2.4 Hz), 7.28 (dd, 3H, *J* = 2.6, 8.2 Hz), 6.88 (d, 3H, *J* = 8.8 Hz), 5.24 (s, 3H), 1.29 (s, 27H); ¹³C NMR (100 MHz, CD₂Cl₂): δ 150.3, 143.9, 139.4, 128.9, 127.5, 126.9, 126.3, 115.5, 34.1, 31.3; FD-HRMS Calcd (M⁺) 522.31339, found 522.31410.

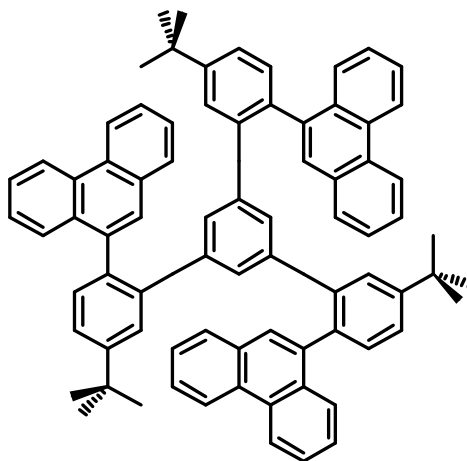
1,3,5-tris(5-*tert*-butyl-2-trifluoromethylsulfonyloxyphenyl)benzene (**57**)



To compound **56** (1.50 g, 2.87 mmol) dissolved in 100 mL of anhydrous CH₂Cl₂ were added 5 mL of pyridine and the solution was cooled to 0°C. Trifluoromethanesulfonic anhydride (1.9 mL, 11 mmol) was added drop wise and the mixture was warmed to room temperature and stirred overnight. The solvent was removed under vacuum. The crude product was purified by chromatography on silica gel by using petroleum ether / CH₂Cl₂ (15%) as the eluent to give the title compound **57** (white solid, 2.53 g, 96%).

Mp 173-174°C; ¹H NMR (400 MHz, CD₂Cl₂): δ 7.65(s, 3H), 7.64 (d, 3H, *J* = 2.8 Hz), 7.48 (dd, 3H, *J* = 2.6, 9.0 Hz), 7.31 (d, 3H, *J* = 8.8 Hz), 1.36 (s, 27H); ¹⁹F NMR (400 MHz, CD₂Cl₂): δ -74.21; ¹³C NMR (100 MHz, CD₂Cl₂): δ 152.3, 144.7, 136.9, 133.8, 130.1, 129.4, 126.7, 121.4, 34.8, 30.9; FD-HRMS Calcd (M⁺) 918.16125, found 918.16261.

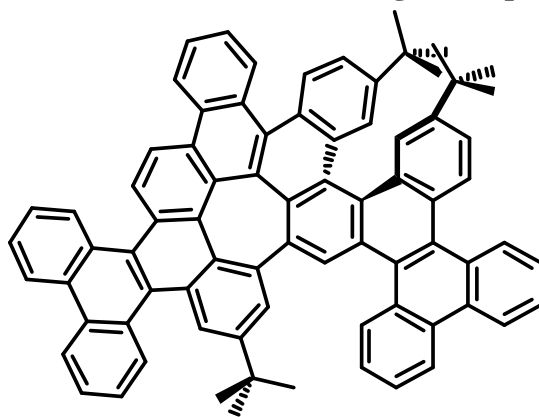
1,3,5-tris(5-*tert*-butyl-2-phenanthren-9-ylphenyl)benzene (**59**)



Compound **57** (400 mg, 0.435 mmol) and phenanthrene-9-boronic acid **58** (386 mg, 1.74 mmol) and K₃PO₄ (1.11 g, 5.22 mmol) were dissolved in a mixture of THF (10 mL) and water (2 mL). The solution was degassed, Pd(OAc)₂ (14.6 mg, 0.065 mmol) and 2-dicyclohexylphosphino-2',6'-dimethoxybiphenyl SPhos (32 mg, 0.078 mmol) were added under an Ar stream and the mixture was degassed again. The solution was heated at 70 °C for 72h. The organic layer was then decanted and the aqueous layer extracted twice with CH₂Cl₂. The combine organic layer was washed with water and evaporated. The crude product was purified by chromatography on silica gel by using petroleum ether / CH₂Cl₂ (12%) as the eluent to give the title compound **59** (white solid, 414 mg, 95%).

Mp 214-215°C; ¹H NMR (400 MHz, DMSO, 150 °C): δ 8.67-8.63 (m, 6H), 7.58-7.43 (m, 9H), 7.42 (d, 3H, *J* = 8.0 Hz), 7.31 (d, 3H, *J* = 8.0 Hz), 7.25-7.21 (m, 6H), 7.01 (d, 3H, *J* = 8.4 Hz), 6.96 (s, 3H), 6.68 (s, 3H), 6.49 (s, 3H), 1.05 (s, 27H); ¹³C NMR (100 MHz, CD₂Cl₂): δ 150.5, 150.4, 140.8, 140.3, 138.1, 137.9, 135.4, 131.9, 131.4, 130.2, 129.5, 128.7, 128.6, 128.2, 127.1, 126.6, 126.4, 126.1, 126.0, 123.4, 122.8, 122.5, 34.2, 34.1, 31.0, 30.9; FD-HRMS Calcd (M⁺) 1002.51645, found 1002.52118.

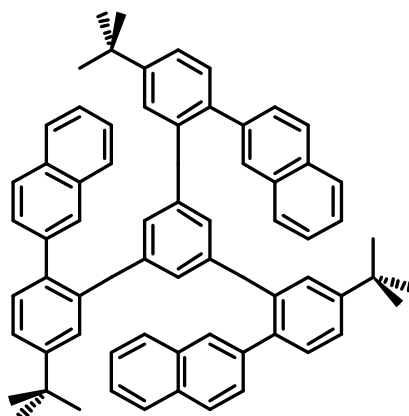
Hexa[7]circulene- and [5]helicene-based rearranged compound (**60**)



Compound **59** (300 mg, 0.3 mmol) was dissolved in 50 mL of unstabilized dichloromethane and degassed with an Ar stream for 15 minutes. Then a solution of FeCl₃ (970 mg, 6.0 mmol) in 10 mL of nitromethane was added drop wise while continuously degassing with an Ar stream. After 1h the reaction was stopped by adding 100 mL of ethanol. The organic phase was then washed twice with water and dried over anhydrous Na₂SO₄. The solvent was removed *in vacuo* and the crude product was purified by chromatography on silica gel by using petroleum ether / CH₂Cl₂ (4%) as the eluent to give the title compound **60** (greenish yellow solid, 218 mg, 73%).

Mp > 400°C; ¹H NMR (400 MHz, CD₂Cl₂): δ 9.10-9.07 (m, 1H), 8.95-8.91 (m, 1H), 8.76-8.72 (m, 1H), 8.67-8.63 (m, 2H), 8.54 (d, 1H, *J* = 8.4 Hz), 8.52 (d, 1H, *J* = 8.4 Hz), 8.43 (d, 1H, *J* = 8.0 Hz), 8.15 (dd, 2H, *J* = 2.2, 7.8 Hz), 7.87 (d, 1H, *J* = 8.0 Hz), 7.75 (d, 1H, *J* = 8.0 Hz), 7.72-7.68 (m, 5H), 7.59 (dd, 1H, *J* = 2.0, 8.4 Hz), 7.50 (t, 1H, *J* = 8.4 Hz), 7.45-7.42 (m, 2H), 7.31 (t, 1H, *J* = 7.6 Hz), 7.17 (t, 1H, *J* = 7.2 Hz), 7.14-7.7.05 (m, 4H), 6.98 (d, 1H, *J* = 7.6 Hz), 6.71 (t, 1H, *J* = 7.0 Hz), 6.44 (d, 1H, *J* = 7.6 Hz), 6.43 (d, 1H, *J* = 7.6 Hz), 1.18 (s, 9H), 1.02 (s, 9H), 0.63 (s, 9H); ¹³C NMR (100 MHz, CD₂Cl₂): δ 148.1, 147.7, 147.4, 142.3, 138.2, 136.8, 136.2, 136.1, 134.9, 134.8, 133.5, 133.0, 132.4, 131.6, 131.4, 131.3, 131.1, 130.7, 130.6, 129.8, 129.7, 129.6, 129.5, 129.4, 128.8, 128.7, 128.6, 128.5, 128.4, 128.3, 128.2, 128.1, 128.0, 127.8, 127.7, 127.4, 127.3, 127.2, 126.8, 126.7, 126.6, 126.0, 125.8, 125.6, 125.5, 125.2, 125.1, 124.9, 124.7, 124.5, 124.4, 124.3, 123.9, 123.6, 123.5, 122.5, 122.2, 121.3, 121.1, 35.9, 34.7, 34.4, 32.3, 30.9, 30.5; FD-HRMS Calcd (M⁺) 994.45385, found 994.45604.

1,3,5-tris(5-*tert*-butyl-2-naphthalen-2-ylphenyl)benzene (**62**)



Compound **57** (600 mg, 0.65 mmol), naphthalene-2-boronic acid **61** (448 mg, 2.6 mmol) and K₃PO₄ (1.67 g, 7.82 mmol) were dissolved in a mixture of THF (10 mL) and water (2 mL). The solution was degassed, Pd(OAc)₂ (22 mg, 0.1 mmol) and 2-dicyclohexylphosphino-2',6'-dimethoxybiphenyl SPhos (48 mg, 0.12 mmol) were added under an Ar stream and the mixture was degassed again. The solution was heated at 70°C for 48h. The organic layer was then decanted and the aqueous layer was extracted twice with CH₂Cl₂. The combine organic layer was washed with water and evaporated. The crude product was purified by chromatography on silica gel by using petroleum ether / CH₂Cl₂ (10%) as the eluent to give the title compound **62** (white solid, 511 mg, 92%).

Mp 186-187°C; ¹H NMR (400 MHz, CD₂Cl₂): δ 7.81-7.77 (m, 6H), 7.76 (s, 3H), 7.64 (d, 3H, *J* = 8.8 Hz), 7.47-7.40 (m, 6H), 7.31 (d, 3H, *J* = 8.0 Hz), 7.29 (d, 3H, *J* = 8.4 Hz), 6.89 (s, 3H), 6.84 (dd, 3H, *J* = 2.0, 8.8 Hz), 6.69 (s, 3H), 1.01 (s, 27H); ¹³C NMR (100 MHz, CD₂Cl₂):

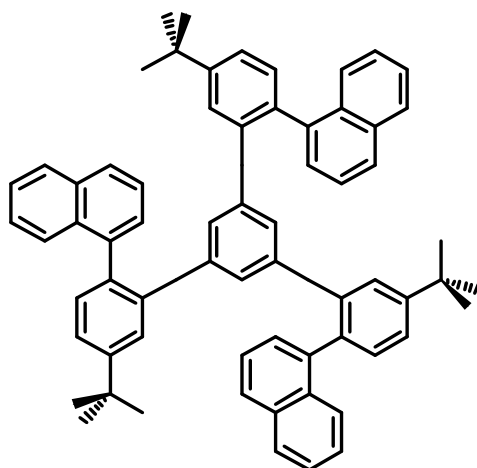
δ 150.6, 141.6, 139.8, 139.3, 137.3, 133.6, 132.0, 130.6, 129.8, 128.9, 128.1, 128.0, 127.8, 126.6, 126.1, 125.9, 124.4, 34.1, 30.8; FD-HRMS Calcd (M⁺) 852.46950, found 852.47021.

Unidentified rearranged compound (63).

Compound **62** (200 mg, 0.24 mmol) was dissolved in 50 mL of unstabilized dichloromethane and degassed with an Ar stream for 15 minutes. Then a solution of FeCl₃ (760 mg, 4.7 mmol) in 10 mL of nitromethane was added drop wise while continuously degassing with an Ar stream. After 1.5h the reaction was stopped by adding 100 mL of ethanol. The organic phase was then washed twice with water and dried over anhydrous Na₂SO₄. The solvent was removed *in vacuo* and the crude product was purified by chromatography on silica gel by using petroleum ether / CH₂Cl₂ (4%) as the eluent to give the title compound **63** (greenish yellow solid, 178 mg, 90%).

Mp > 400°C; ¹H NMR (400 MHz, CD₂Cl₂): δ 9.17 (s, 1H), 9.13 (d, 1H, *J* = 8.4 Hz), 9.03 (d, 1H, *J* = 8.4 Hz), 8.78 (d, 1H, *J* = 9.2 Hz), 8.66 (d, 1H, *J* = 8.0 Hz), 8.59 (d, 1H, *J* = 8.8 Hz), 8.49 (d, 1H, *J* = 8.4 Hz), 8.45 (d, 1H, *J* = 8.4 Hz), 8.30 (d, 1H, *J* = 8.4 Hz), 8.17 (d, 1H, *J* = 8.4 Hz), 8.14 (d, 1H, *J* = 8.8 Hz), 7.87 (d, 1H, *J* = 8.4 Hz), 7.83 (d, 1H, *J* = 7.6 Hz), 7.68-7.57 (m, 6H), 7.43-7.40 (m, 2H), 7.23 (t, 1H, *J* = 7.4 Hz), 7.17 (t, 1H, *J* = 7.2 Hz), 6.80 (t, 1H, *J* = 7.6 Hz), 6.62 (t, 1H, *J* = 8.2 Hz), 1.04 (s, 9H), 0.79 (s, 9H), 0.76 (s, 9H); ¹³C NMR (100 MHz, CD₂Cl₂): δ 149.3, 149.0, 148.8, 132.9, 132.8, 132.7, 132.0, 132.6, 131.0, 130.8, 130.7, 130.4, 129.4, 128.8, 128.7, 128.4, 128.2, 128.0, 127.9, 127.8, 127.7, 127.5, 127.4, 127.2, 126.9, 126.8, 126.2, 125.9, 125.8, 125.6, 125.5, 125.3, 125.2, 125.0, 124.6, 124.5, 124.4, 124.2, 124.0, 123.7, 122.9, 122.4, 121.4, 121.0, 120.8, 120.0, 118.3, 39.3, 34.1, 34.0, 32.6, 30.5, 30.4; FD-HRMS found 844.40311.

1,3,5-tris(5-*tert*-butyl-1-naphthalen-2-ylphenyl)benzene (65)

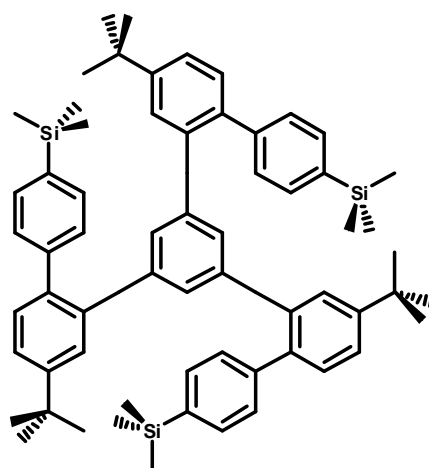


Compound **57** (600 mg, 0.65 mmol), naphthalene-1-boronic acid **64** (673.80 mg, 3.9 mmol) and K₃PO₄ (1.67 g, 7.82 mmol) were dissolved in a mixture of THF (10 mL) and water (2 mL). The solution was degassed, Pd(OAc)₂ (22 mg, 0.1 mmol) and 2-dicyclohexylphosphino-2',6'-dimethoxybiphenyl SPhos (48 mg, 0.12 mmol) were added under an Ar stream and the mixture was degassed again. The solution was heated at 70°C for 48h. The organic layer was then decanted and the aqueous layer was extracted twice with CH₂Cl₂. The combine organic layer was washed with water and evaporated. The crude product was purified by

chromatography on silica gel by using petroleum ether / CH₂Cl₂ (10%) as the eluent to give the title compound **58** (white solid, 505 mg, 90%).

Mp 214-215 °C; ¹H NMR (400 MHz, CD₂Cl₂): δ 7.83-7.76 (m, 3H), 7.75-7.67 (m, 3H), 7.60-7.52 (m, 3H), 7.42-7.32 (m, 5H), 7.29-7.21 (m, 7H), 7.14-7.08 (m, 4H), 6.63-6.57 (m, 3H), 6.51-6.47 (m, 5H), 1.20 (s, 14H), 1.15 (s, 13H); ¹³C NMR (100 MHz, CD₂Cl₂): δ 150.4, 150.3, 141.0, 140.7, 139.3, 135.6, 133.6, 133.5, 133.4, 132.2, 131.5, 131.2, 128.5, 128.4, 128.3, 128.1, 127.2, 127.0, 126.9, 126.8, 126.2, 125.8, 125.7, 125.6, 125.5, 125.0, 123.4, 34.4, 34.3, 31.2, 31.1; FD-HRMS Calcd (M⁺) 852.46950, found 852.47021.

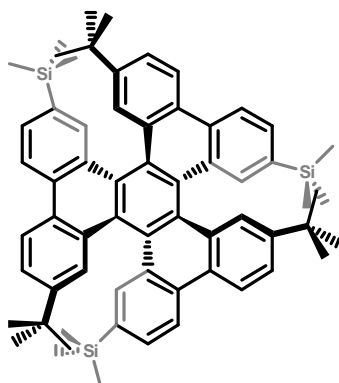
1,3,5-tris(5-*tert*-butyl-2-(4-trimethylsilylphenyl)phenyl)benzene (**67**)



Compound **57** (400 mg, 0.44 mmol), 4-(trimethylsilyl)phenylboronic acid **66** (338 mg, 1.7 mmol) and K₃PO₄ (1.1 g, 5.2 mmol) were dissolved in a mixture of THF (10 mL) and water (2 mL). The solution was degassed, Pd(OAc)₂ (14.7 mg, 0.065 mmol) and 2-dicyclohexylphosphino-2',6'-dimethoxybiphenyl SPhos (32 mg, 0.078 mmol) were added under an Ar stream and the mixture was degassed again. The solution was heated at 70°C for 48h. The organic layer was then decanted and the aqueous layer was extracted twice with CH₂Cl₂. The combine organic layer was washed with water and evaporated. The crude product was purified by chromatography on silica gel by using petroleum ether / CH₂Cl₂ (12%) as the eluent to give the title compound **67** (white solid, 384 mg, 96%).

Mp 254-255°C; ¹H NMR (400 MHz, CD₂Cl₂): δ 7.53 (d, 6H, *J* = 7.6 Hz), 7.39 (dd, 3H, *J* = 2.0, 8.4 Hz), 7.28 (d, 3H, *J* = 8.4 Hz), 7.14 (d, 3H, *J* = 1.6 Hz), 6.98 (d, 6H, *J* = 7.6 Hz), 6.82 (s, 3H), 1.28 (s, 27H), 0.20 (s, 27H); ¹³C NMR (100 MHz, CD₂Cl₂): δ 150.5, 142.5, 141.5, 139.9, 138.1, 137.4, 132.9, 130.4, 129.6, 128.0, 124.8, 34.5, 31.1, -1.2; FD-HRMS Calcd (M⁺) 918.54113, found 918.54367.

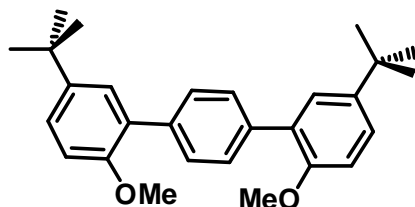
3,11,19-tri-*tert*-butyl-6,14,22-tris(trimethylsilyl)hexabenzotriphenylene (68)



Compound **67** (200 mg, 0.22 mmol) was dissolved in 50 mL of unstabilized dichloromethane and degassed with an Ar stream for 15 minutes. Then a solution of FeCl₃ (700 mg, 4.3 mmol) in 10 mL of nitromethane was added drop wise while continuously degassing with an Ar stream. After 1.5h the reaction was stopped by adding 100 mL of ethanol. The organic phase was then washed twice with water and dried over anhydrous Na₂SO₄. The solvent was removed *in vacuo* and the crude product was purified by chromatography on silica gel by using petroleum ether / CH₂Cl₂ (2%) as the eluent to give the title compound **68** (yellow solid, 129 mg, 65%).

Mp > 300°C (decomposes at 300°C); ¹H NMR (400 MHz, CD₂Cl₂): δ 8.55 (d, 3H, *J* = 8.4 Hz), 8.53 (d, 3H, *J* = 8.4 Hz), 8.29 (s, 3H), 8.14 (d, 3H, *J* = 2.0 Hz), 7.65 (dd, 3H, *J* = 1.8, 8.4 Hz), 7.60 (dd, 3H, *J* = 1.8, 8.4 Hz), 1.05 (s, 27H), -0.02 (s, 27H); ¹³C NMR (100 MHz, CD₂Cl₂): δ 148.1, 136.6, 136.5, 131.7, 130.9, 130.6, 130.2, 128.5, 128.4, 127.6, 124.5, 122.9, 122.2, 34.5, 30.8, -1.7; FD-HRMS Calcd (M⁺) 912.49418, found 912.49536.

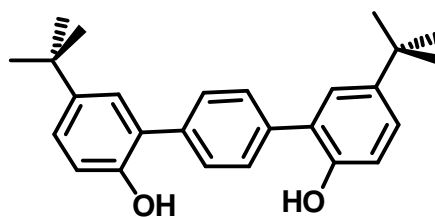
1,4-bis(5-*tert*-butyl-2-methoxyphenyl)benzene (70)



1,4-Phenylenediboronic acid **15** (1.0 g, 6.0 mmol), 5-*tert*-butyl-2-methoxyphenylbromide **69** (3.2 g, 13.1 mmol) and Na₂CO₃ (6.30 g, 59.5 mmol) were dissolved in toluene (48 mL), water (16 mL) and ethanol (8mL). The solution was degassed, Pd(PPh₃)₄ (690 mg, 0.60 mmol) was added under an Ar stream and the mixture was degassed again. The solution was heated at 90°C for 48h. The organic layer was then decanted and the aqueous layer was extracted twice with CH₂Cl₂. The combine organic layer was washed with water and evaporated. The crude product was purified by chromatography on silica gel by using petroleum ether / CH₂Cl₂ (20%) as the eluent to give the title compound **70** (white solid, 2.15 g, 90%).

Mp 165-166°C; ¹H NMR (400 MHz, CD₂Cl₂): δ 7.50 (s, 4H), 7.35 (d, 2H, *J* = 2.8 Hz), 7.32 (dd, 2H, *J* = 2.6, 8.6 Hz), 6.93 (d, 2H, *J* = 8.4 Hz), 3.79 (s, 6H), 1.31 (s, 18H); ¹³C NMR (100 MHz, CD₂Cl₂): δ 154.4, 143.5, 137.7, 129.8, 129.1, 128.0, 125.3, 110.7, 55.5, 34.0, 31.3; FD-HRMS Calcd (M⁺) 402.25588, found 402.25699.

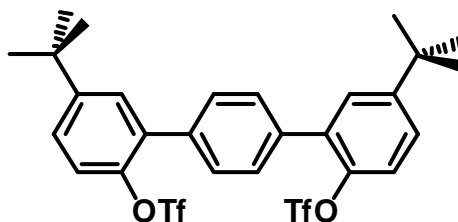
1,4-bis(5-*tert*-butyl-2-hydroxyphenyl)benzene (**71**)



Compound **70** (1.86 g, 4.6 mmol) was dissolved in 50 mL of dry CH₂Cl₂ under Ar and brought to -20°C. BBr₃ (1 M in CH₂Cl₂, 11.6 mmol, 11.6 mL) was added drop-wise with vigorous stirring, the reaction mixture was stirred overnight and finally warmed to room temperature. The reaction mixture was then poured onto crushed ice, organic layer was then decanted and the aqueous layer was extracted twice with CH₂Cl₂. The combine organic layer was washed with water and dried over anhydrous Na₂SO₄. The solvent was removed under vacuum, yielding **71** (1.71 g, 99%) as a white solid.

Mp 161-162°C; ¹H NMR (400 MHz, CD₂Cl₂): δ 7.59 (s, 4H), 7.29 (d, 2H, *J* = 2.8 Hz), 7.27 (dd, 2H, *J* = 2.6, 7.8 Hz), 6.87 (d, 2H, *J* = 8.4 Hz), 5.10 (s, 2H), 1.31 (s, 18H); ¹³C NMR (100 MHz, CD₂Cl₂): δ 150.3, 143.8, 137.2, 129.8, 127.3, 127.1, 126.1, 115.4, 34.1, 31.3; FD-HRMS Calcd (M⁺) 374.22458, found 374.22408.

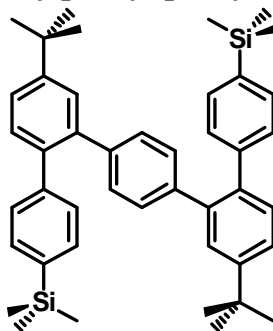
1,4-bis(5-*tert*-butyl-2-trifluoromethylsulfonyloxyphenyl)benzene (**72**)



To compound **71** (1.50 g, 4.0 mmol) in 100 mL of anhydrous CH₂Cl₂ were added 3.5 mL of pyridine and the solution was cooled to 0°C. Trifluoromethanesulfonic anhydride (1.7 mL, 10 mmol) was added drop wise and the mixture was warmed to room temperature and stirred overnight. The solvent was removed under vacuum. The crude product was purified by chromatography on silica gel by using petroleum ether / CH₂Cl₂ (15%) as the eluent to give the title compound **72** (white solid, 2.43 g, 95%).

Mp 180-181°C; ¹H NMR (400 MHz, CD₂Cl₂): δ 7.56 (s, 4H), 7.50 (d, 2H, *J* = 2.4 Hz), 7.47 (dd, 2H, *J* = 2.0, 8.8 Hz), 7.32 (d, 2H, *J* = 8.4 Hz), 1.35 (s, 18H); ¹⁹F NMR (400 MHz, CD₂Cl₂): δ -74.24; ¹³C NMR (100 MHz, CD₂Cl₂): δ 152.1, 144.6, 136.2, 134.0, 129.5, 129.2, 126.4, 121.6, 34.8, 31.0; FD-HRMS Calcd (M⁺) 638.12315, found 638.12510.

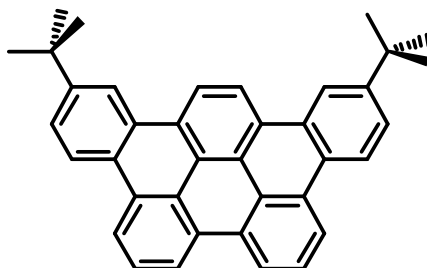
1,4-bis(5-*tert*-butyl-2-(4-trimethylsilylphenyl)phenyl)benzene (**73**)



Compound **72** (600 mg, 0.94 mmol), 4-(trimethylsilyl)phenylboronic acid **66** (460 mg, 2.4 mmol) and K_3PO_4 (1.6 g, 7.5 mmol) were dissolved in a mixture of THF (10 mL) and water (2 mL). The solution was degassed, $Pd(OAc)_2$ (21 mg, 0.09 mmol) and 2-dicyclohexylphosphino-2',6'-dimethoxybiphenyl SPhos (46 mg, 0.11 mmol) were added under an Ar stream and the mixture was degassed again. The solution was heated at 70°C for 48h. The organic layer was then decanted and the aqueous layer was extracted twice with CH_2Cl_2 . The combine organic layer was washed with water and evaporated. The crude product was purified by chromatography on silica gel by using petroleum ether / CH_2Cl_2 (10%) as the eluent to give the title compound **73** (white solid, 540 mg, 90%).

Mp 305-306°C; 1H NMR (400 MHz, CD_2Cl_2): δ 7.58 (d, 1H, $J = 2.4$ Hz), 7.41 (d, 1H, $J = 2.0$ Hz), 7.39 (d, 2H, $J = 1.6$ Hz), 7.38 (d, 4H, $J = 7.6$ Hz), 7.32 (d, 2H, $J = 8.4$ Hz), 7.10 (d, 4H, $J = 8.0$ Hz), 6.99 (s, 4H), 1.35 (s, 18H), 0.22 (s, 18H); ^{13}C NMR (100 MHz, CD_2Cl_2): δ 150.6, 141.9, 140.2, 139.9, 138.2, 137.6, 132.8, 130.3, 129.5, 129.2, 127.6, 124.6, 34.5, 31.1, -1.4; FD-HRMS Calcd (M⁺) 638.37640, found 638.37464.

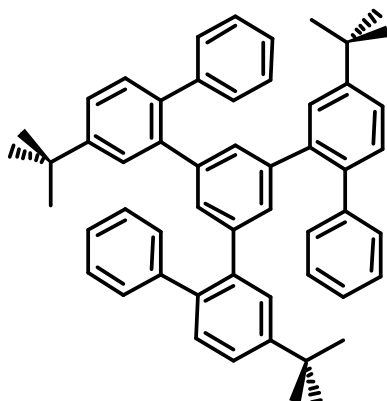
2,13-di-*tert*-butyltribenzo[fg,ij,rst]pentaphene (**74**)



Compound **73** (200 mg, 0.31 mmol) was dissolved in 50 mL of unstabilized dichloromethane and degassed with an Ar stream for 15 minutes. Then a solution of $FeCl_3$ (610 mg, 3.8 mmol) in 5 mL of nitromethane was added drop wise while continuously degassing with an Ar stream. After 1h the reaction was stopped by adding 100 mL of methanol. The organic phase was then washed twice with water and dried over anhydrous Na_2SO_4 . The solvent was removed *in vacuo* and the crude product was purified by chromatography on silica gel by using petroleum ether / CH_2Cl_2 (4%) as the eluent to give the title compound **74** (yellow solid, 139 mg, 91%).

Mp 276-277°C; 1H NMR (400 MHz, CD_2Cl_2): δ 9.06 (s, 2H), 8.87 (d, 2H, $J = 7.6$ Hz), 8.84 (d, 2H, $J = 1.6$ Hz), 8.78 (d, 2H, $J = 8.0$ Hz), 8.68 (d, 2H, $J = 8.8$ Hz), 8.95 (t, 2H, $J = 8.0$ Hz), 7.82 (dd, 2H, $J = 1.6, 8.8$ Hz), 1.60 (s, 18H); ^{13}C NMR (100 MHz, CD_2Cl_2): δ 150.4, 129.9, 129.7, 129.5, 127.6, 127.5, 126.4, 125.6, 124.1, 123.4, 121.3, 121.2, 120.7, 119.6, 35.2, 31.3; FD-HRMS Calcd (M⁺) 488.25040, found 488.25075.

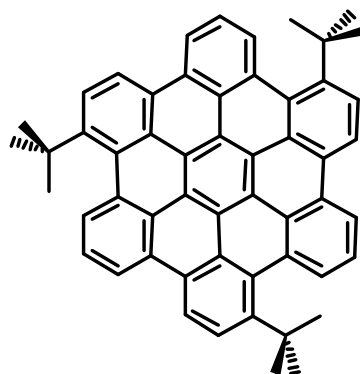
1,3,5-tris(4-*tert*-butylbiphenyl-2-yl)benzene (**76**)



Compound **57** (430 mg, 0.47 mmol), phenylboronic acid **75** (230 mg, 1.9 mmol) and K_3PO_4 (1.2 g, 5.7 mmol) were dissolved in a mixture of THF (10 mL) and water (2 mL). The solution was degassed, $Pd(OAc)_2$ (15.8 mg, 0.070 mmol) and 2-dicyclohexylphosphino-2',6'-dimethoxybiphenyl SPhos (35 mg, 0.084 mmol) were added under an Ar stream and the mixture was degassed again. The solution was heated at 70°C for 48h. The organic layer was then decanted and the aqueous layer was extracted 2 times with CH_2Cl_2 . The combine organic layer was washed with water and evaporated. The crude product was purified by chromatography on silica gel by using petroleum ether / CH_2Cl_2 (10%) as the eluent to give the title compound **76** (white solid, 322 mg, 98%).

Mp 263-264°C; 1H NMR (400 MHz, CD_2Cl_2): δ 7.36 (dd, 3H, $J = 2.0, 8.0$ Hz), 7.31-7.21 (m, 12H), 7.00 (d, 6H, $J = 7.2$ Hz), 6.91 (d, 3H, $J = 2.0$ Hz), 6.77 (s, 3H), 1.28 (s, 27H); ^{13}C NMR (100 MHz, CD_2Cl_2): δ 150.4, 141.6, 141.5, 139.9, 137.7, 130.2, 130.1, 129.7, 127.8, 127.7, 126.5, 124.4, 34.5, 31.2; FD-HRMS Calcd (M+) 702.42255, found 702.42535.

1,7,13-tri-*tert*-butyl-hexa-peri-hexabenzocoronene (**77**)

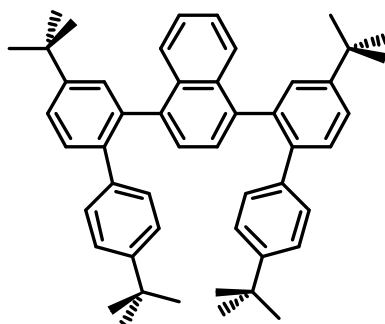


Compound **76** (150 mg, 0.21 mmol) was dissolved in 50 mL of unstabilized dichloromethane and degassed with an Ar stream for 15 minutes. Then a solution of $FeCl_3$ (690 mg, 4.3 mmol) in 10 mL of nitromethane was added drop wise while continuously degassing with an Ar stream. After 1h the reaction was stopped by adding 100 mL of ethanol. The organic phase was then washed twice with water and dried over anhydrous Na_2SO_4 . The solvent was removed *in vacuo* and the crude product was purified by chromatography on silica gel by

using petroleum ether / CH₂Cl₂ (5%) as the eluent to give the title compound **77** (yellow solid, 106 mg, 72%).

Mp > 400 °C; ¹H NMR (400 MHz, CD₂Cl₂): δ 8.94 (d, 3H, *J* = 8.0 Hz), 8.92 (d, 3H, *J* = 8.8 Hz), 8.46 (d, 3H, *J* = 8.0 Hz), 8.39 (d, 3H, *J* = 8.8 Hz), 7.92 (t, 3H, *J* = 8.0 Hz), 1.61 (s, 27H); ¹³C NMR (100 MHz, CD₂Cl₂): δ 147.2, 131.7, 130.5, 130.3, 129.5, 128.3, 123.8, 121.6, 120.7, 120.3, 120.0, 38.5, 34.4; FD-HRMS Calcd (M+) 690.32865, found 690.32689.

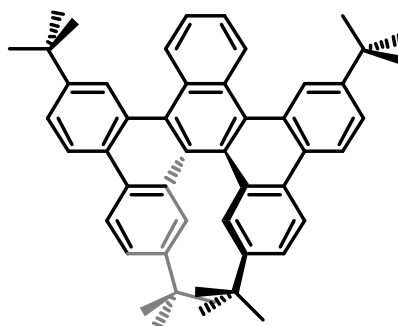
1,4-bis(4,4'-di-tert-butylbiphenyl-2-yl)naphthalene (**82**)



1,4-dibromonaphthalene **81** (571.94 mg, 2.0 mmol), 2-(4,4'-di-tert-butylbiphenyl-2-yl)-4,4,5,5-tetramethyl-1,3,2-dioxaborolane **5b** (1.65 g, 4.2 mmol) and Na₂CO₃ (4.24g, 40.0 mmol) were dissolved in toluene (30 mL), water (10 mL) and ethanol (5 mL). The solution was degassed three times, Pd(PPh₃)₄ (230.8 mg, 0.20 mmol) was added under an Ar stream and the mixture was degassed three times again. The solution was heated at 90 °C for 24h. The organic layer was then decanted and the aqueous layer was extracted 2 times with CH₂Cl₂. The combine organic layer was washed with water and evaporated. The crude product was purified by chromatography on silicagel by using pet. ether / CH₂Cl₂ (5%) as the eluent to give the title compound **82** (white solid, 1.20 g, 91%).

Mp 145-146 °C; ¹H NMR (400 MHz, CD₂Cl₂): δ 7.60-7.58(m, 1H), 7.56-7.50 (m, 3H), 7.49-7.46 (m, 4H), 7.47 (d, 1H, *J* = 8.0 Hz), 7.42 (d, 1H, *J* = 7.6 Hz), 7.33 (d, 1H, *J* = 2.0 Hz), 7.24-7.22 (m, 1H), 7.16 (s, 1H), 7.14-7.06 (m, 6H), 7.00-6.98 (m, 4H), 1.35 (s, 18H), 1.21 (s, 9H), 1.17 (s, 9H). ¹H NMR (400 MHz, CDCl₃, 50 °C): δ 7.64-7.62 (m, 1H), 7.56-7.53 (m, 1H), 7.49-7.46 (m, 4H), 7.44 (s, 1H), 7.35 (d, 1H, *J* = 2.4 Hz), 7.23-7.20 (m, 1H), 7.16 (s, 1H), 7.12-7.07 (m, 4H), 7.03-6.95 (m, 6H), 1.38 (s, 7H), 1.37 (s, 11H), 1.21 (s, 11H), 1.17 (s, 7H). ¹H NMR (400 MHz, DMSO): δ 7.54-7.51 (m, 2H), 7.45-7.37 (m, 4H), 7.25 (d, 1H, *J* = 2.0 Hz), 7.23-7.20 (m, 1H), 7.17-7.13 (m, 3H), 7.09-7.06(m, 3H), 7.03 (d, 2H, *J* = 8.4 Hz), 6.94 (d, 2H, *J* = 8.4 Hz), 6.91 (d, 2H, *J* = 8.4 Hz), 1.35 (s, 9H), 1.28 (s, 9H), 1.14 (s, 9H), 1.09 (s, 9H). ¹³C NMR (100 MHz, CD₂Cl₂): δ 149.8, 149.7, 149.2, 149.1, 139.4, 139.3, 138.9, 138.6, 138.5, 138.4, 132.4, 132.0, 129.9, 129.2, 128.9, 128.8, 127.6, 127.3, 126.5, 126.4, 125.3, 125.1, 124.9, 124.8, 124.5, 124.4, 34.5, 34.3, 34.2, 31.2, 31.1, 31.0, 27.0. ESI HRMS calcd (M+) 656.40, found 656.20.

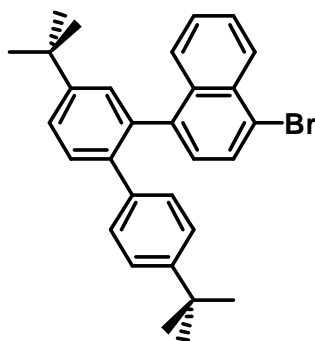
2,7,10,15-tetra-tert-butyltribenzo[f,j,s]picene (**83**)



Compound **82** (100 mg, 0.152 mmol) was dissolved in 50 mL of unstabilized dichloromethane and degassed with an argon stream for 15 minutes. Then a solution of 567.85 mg FeCl₃ (3.50 mmol) in 5 mL nitromethane was added dropwise while continuously degassing with an argon stream. After 1 h the reaction was stopped by adding 100 mL of ethanol. Then the organic phase was extracted with water two times and dried with anhydrous sodium sulfate. The solvent was removed in *vacuo* and The crude product was purified by chromatography on silicagel by using pet. ether / CH₂Cl₂ (1%) as the eluent to give the title compound **83** (yellow solid, 95 mg, 96%).

Mp >400 °C; ¹H NMR (400 MHz, CD₂Cl₂): δ 8.91 (d, 2H, *J* = 1.6 Hz), 8.89 (q, 2H, *J* = 3.2 Hz), 8.67 (d, 2H, *J* = 8.8 Hz), 8.51 (d, 2H, *J* = 8.8 Hz), 7.91 (d, 2H, *J* = 2.0 Hz), 7.79 (dd, 2H, *J* = 2.0, 8.8 Hz), 7.59 (q, 2H, *J* = 3.2 Hz), 7.55 (dd, 2H, *J* = 2.2, 8.6 Hz), 1.53 (s, 18H), 1.05 (s, 18H). ¹³C NMR (100 MHz, CD₂Cl₂): δ 148.5, 147.1, 130.9, 130.0, 129.4, 129.3, 129.1, 128.6, 128.4, 128.3, 127.7, 127.0, 126.7, 125.9, 125.5, 124.8, 124.6, 122.8, 35.2, 34.6, 31.6, 31.0. ESI HRMS calcd (M⁺) 652.40, found 652.20.

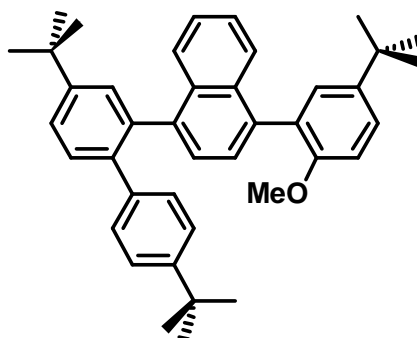
1-bromo-4-(4,4'-di-tert-butylbiphenyl-2-yl)naphthalene (**84**)



1,4-dibromonaphthalene **81** (1.46 g, 5.11 mmol), 2-(4,4'-di-tert-butylbiphenyl-2-yl)-4,4,5,5-tetramethyl-1,3,2-dioxaborolane (**5b**, 1.0 g, 2.55 mmol) and Na₂CO₃ (2.70 g, 25.5 mmol) were dissolved in toluene (30 mL), water (10 mL) and ethanol (5 mL). The solution was degassed three times, Pd(PPh₃)₄ (295.53 mg, 0.256 mmol) was added under an Ar stream and the mixture was degassed three times again. The solution was heated at 90 °C for 24h. The organic layer was then decanted and the aqueous layer was extracted 2 times with CH₂Cl₂. The combine organic layer was washed with water and evaporated. The crude product was purified by chromatography on silicagel by using pet. ether / CH₂Cl₂ (4%) as the eluent to give the title compound **84** (white solid, 902 mg, 75%).

Mp 152-153 °C; ¹H NMR (400 MHz, CD₂Cl₂): δ 8.20 (d, 1H, *J* = 8.8 Hz), 7.65 (d, 1H, *J* = 7.2 Hz), 7.64 (d, 1H, *J* = 8.0 Hz), 7.53-7.50 (m, 2H), 7.42 (d, 1H, *J* = 8.4 Hz), 7.39-7.35 (m, 1H), 7.33 (d, 1H, *J* = 2.0 Hz), 7.06 (d, 1H, *J* = 7.6 Hz), 7.04 (d, 2H, *J* = 8.0 Hz), 6.95 (d, 2H, *J* = 8.8 Hz), 1.34 (s, 9H), 1.15 (s, 9H), 1.18. ¹³C NMR (100 MHz, CD₂Cl₂): δ 149.8, 149.3, 140.6, 138.7, 138.1, 137.4, 133.7, 131.8, 130.1, 129.2, 128.8, 128.7, 128.6, 128.5, 127.1, 127.0, 126.6, 125.1, 124.7, 121.4, 34.5, 34.2, 31.1, 30.9. FD-HRMS calcd (M⁺) 470.16091, found 470.16022.

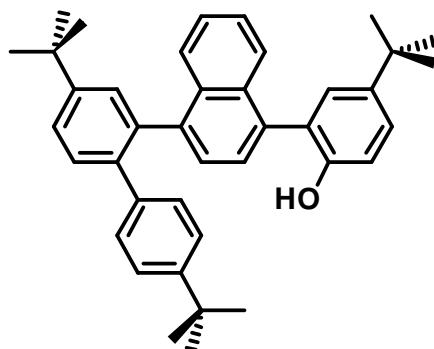
Compound 85



1-bromo-4-(4,4'-di-tert-butylbiphenyl-2-yl)naphthalene **84** (650 mg, 1.38 mmol), 2-(5-tert-butyl-2-methoxyphenyl)boronic acid **34** (316.36 mg, 1.52 mmol) and Na₂CO₃ (1.46 g, 13.8 mmol) were dissolved in toluene (30 mL), water (10 mL) and ethanol (5 mL). The solution was degassed three times, Pd(PPh₃)₄ (159.31 mg, 0.138 mmol) was added under an Ar stream and the mixture was degassed three times again. The solution was heated at 90 °C for 48h. The organic layer was then decanted and the aqueous layer was extracted 2 times with CH₂Cl₂. The combine organic layer was washed with water and evaporated. The crude product was purified by chromatography on silicagel by using pet. ether / CH₂Cl₂ (10%) as the eluent to give the title compound **85** (white solid, 737 mg, 95%).

Mp 90-91 °C; ¹H NMR (400 MHz, CD₂Cl₂): δ 7.69-7.67 (m, 1H), 7.56-7.51 (m, 2H), 7.46-7.39 (m, 3H), 7.32-7.28 (m, 2H), 7.26-7.21 (m, 3H), 7.09 (d, 2H, *J* = 8.0 Hz), 7.06-7.02 (m, 2H), 6.97 (d, 1H, *J* = 8.8 Hz), 3.67 (s, 2.01H), 3.60 (s, 0.99H), 1.37 (s, 9H), 1.30 (s, 9H), 1.18 (s, 9H). ¹³C NMR (100 MHz, CD₂Cl₂): δ 155.0, 149.7, 149.2, 143.3, 139.7, 138.9, 138.7, 138.6, 138.4, 136.8, 132.5, 132.4, 132.3, 132.1, 130.1, 129.2, 129.1, 128.8, 127.7, 127.6, 126.7, 126.5, 125.6, 125.5, 125.3, 124.6, 113.2, 111.2, 110.3, 55.9, 34.6, 34.2, 34.1, 31.3, 31.2, 31.0. ESI HRMS calcd (M⁺) 554.35, found 554.40.

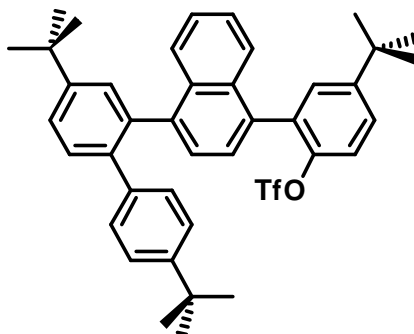
Compound 86



1-(5-tert-butyl-2-methoxyphenyl)-4-(4,4'-di-tert-butylbiphenyl-2-yl)naphthalene **85** (680 mg, 1.23 mmol) was dissolved in 40 mL of dry CH_2Cl_2 under N_2 and brought to -20°C . BBr_3 (1 M in CH_2Cl_2 , 1.5 equiv, 1.84 mmol, 1.84 mL) was added dropwise with stirring and the reaction mixture stirred overnight, warming to room temperature. The reaction mixture was then poured into ice water, organic layer was then decanted and the aqueous layer was extracted 2 times with CH_2Cl_2 . The combine organic layer was washed with water and dried over anhydrous Na_2SO_4 . The solvent was removed under vacuum, yielding 4-tert-butyl-2-(4-(4,4'-di-tert-butylbiphenyl-2-yl)naphthalen-1-yl)phenol **86** (598.67 mg, 90%) as a brown-red solid, which was judged pure enough by TLC to be used in subsequent steps without further purification.

Mp $94\text{--}95^\circ\text{C}$; ^1H NMR (400 MHz, CD_2Cl_2): δ 7.73-7.69 (m, 1H), 7.62-7.58 (m, 1H), 7.55-7.53 (m, 1H), 7.46-7.40 (m, 2H), 7.37-7.33 (m, 4H), 7.31-7.29 (m, 1H), 7.25-7.24 (m, 1H), 7.10 (d, 1H, $J = 8.4$ Hz), 7.04 (d, 2H, $J = 9.6$ Hz), 6.98 (d, 1H, $J = 8.0$ Hz), 6.93 (dd, 1H, $J = 1.8, 8.6$ Hz), 4.77 (s, 0.40H), 4.66 (s, 0.35H), 1.37 (s, 4.65H), 1.36 (s, 4.35H), 1.30 (s, 9H), 1.18 (s, 4.75H), 1.14 (s, 4.25H). ^{13}C NMR (100 MHz, CD_2Cl_2): δ 151.0, 150.8, 149.9, 149.8, 149.3, 149.2, 143.4, 143.3, 141.0, 140.9, 138.9, 138.8, 138.5, 138.4, 138.2, 138.1, 133.9, 133.5, 133.0, 133.0, 131.9, 131.8, 130.2, 129.9, 128.9, 128.8, 128.6, 128.3, 128.1, 128.0, 127.4, 127.1, 126.4, 126.3, 126.2, 126.1, 125.8, 125.0, 124.9, 124.7, 124.5, 114.8, 114.6, 34.5, 34.2, 34.2, 34.1, 31.3, 31.2, 31.0. ESI HRMS calcd (M^+) 540.34, found 540.30.

Compound 87

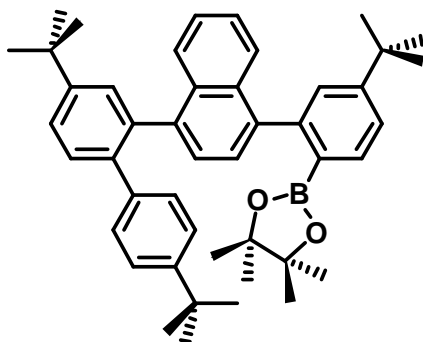


Compound **86** (600 mg, 1.11 mmol) dissolved in 25 mL of anhydrous CH_2Cl_2 was added pyridine (0.89 mL, 11.10 mmol). The solution was cooled to 0°C and Trifluoromethanesulfonic anhydride (0.375 mL, 2.22 mmol) was added drop-wise and the mixture was warmed to room temperature and stirred overnight. The solvent was removed under vacuum. The crude product was purified by chromatography on silica gel by using

petroleum ether / CH₂Cl₂ (15%) as the eluent to give the title compound **87** (white solid, 690 mg, 92%).

Mp 103-104 °C; ¹H NMR (400 MHz, CD₂Cl₂): δ 7.75-7.68(m, 1H), 7.55-7.42(m, 5H), 7.38-7.31(m, 5H), 7.29-7.25(m, 1H), 7.09-6.99(m, 4H), 1.36 (s, 9H), 1.33 (s, 9H), 1.17 (s, 2.64H) 1.13 (s, 6.36H); ¹⁹F NMR (400 MHz, CD₂Cl₂): δ -74.58; ¹³C NMR (100 MHz, CD₂Cl₂): δ 152.3, 144.7, 136.9, 133.8, 130.1, 129.4, 126.7, 121.4, 34.8, 30.9; FD-HRMS Calcd (M+) 672.29, found 672.30.

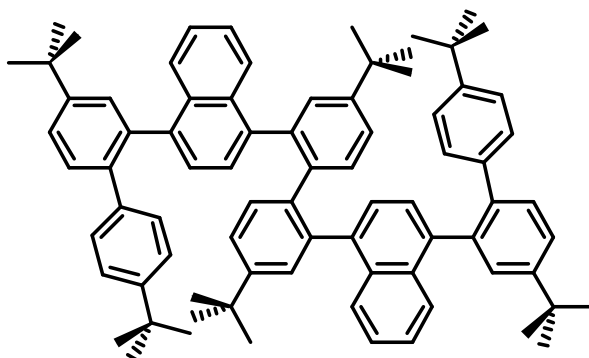
Compound 88



Compound **87** (300 mg, 0.446 mmol), dppf (24.7 mg, 0.045 mmol), bis(pinacolato)diboron (226.63 mg, 0.893 mmol), potassium acetate (262.65 mg, 2.67 mmol) and Pd(dppf)Cl₂,CH₂Cl₂ (36.42 mg, 0.045 mmol) were dissolved in dry dioxane (10 mL). The mixture was heated at reflux and stirred under Ar overnight. After the solution was cooled down at room temperature, 20 mL of water and 20 mL of CH₂Cl₂ were added. The organic layer was then decanted and the aqueous layer was extracted 3 times with CH₂Cl₂. After drying (Na₂SO₄) the solvent was evaporated and the residue was purified by column chromatography on silica gel using petroleum ether or mixtures of petroleum ether and CH₂Cl₂ as eluent to give the title compound **88** (white solid, 204 mg, 70%).

Mp 105-106 °C; ¹H NMR (400 MHz, CD₂Cl₂): δ 7.73-7.66 (m, 2H), 7.59-7.57 (m, 1H), 7.53-7.49 (m, 1H), 7.44-7.41 (m, 3H), 7.34-7.27 (m, 3H), 7.24(s, 1H), 7.20 (s, 1H), 7.16-7.08 (m, 4H), 1.34 (s, 18H), 1.19 (s, 9H), 0.98 (s, 6H), 0.94-0.78 (m, 6H). ¹³C NMR (100 MHz, CD₂Cl₂): δ 153.5, 149.5, 149.2, 148.9, 145.9, 145.8, 141.1, 139.4, 139.3, 138.7, 138.4, 134.5, 134.4, 134.2, 133.1, 133.0, 132.6, 132.5, 130.7, 130.6, 129.8, 129.6, 129.0, 128.9, 128.8, 128.1, 127.2, 127.1, 126.6, 126.4, 125.9, 125.3, 124.8, 124.7, 123.5, 83.6, 83.1, 34.8, 34.5, 34.3, 31.1, 31.0, 24.7, 24.4, 24.3, 24.2. FD-HRMS calcd (M+) 649.43314, found 649.43444.

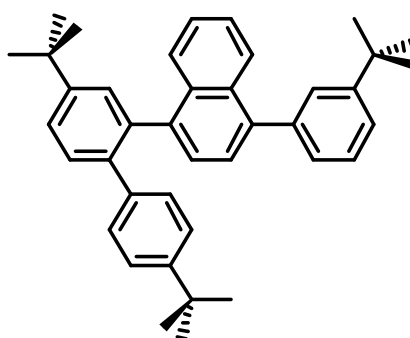
Compound 89



To the compound **87** (196 mg, 0.29 mmol), 2-(4-tert-butyl-2-(4-(4,4'-di-tert-butylbiphenyl-2-yl)naphthalen-1-yl)phenyl)-4,4,5,5-tetramethyl-1,3,2-dioxaborolane **88** (190 mg, 0.29 mmol) and K_3PO_4 (124 mg, 0.58 mmol) were dissolved in a mixture of THF (2 mL) and water (0.5 mL). The solution was degassed, $Pd(OAc)_2$ (6.5 mg, 0.03 mmol) and 2-dicyclohexylphosphino-2',6'-dimethoxybiphenyl SPhos (14.4 mg, 0.035 mmol) were added under an Ar stream and the mixture was degassed again. The solution was heated at 70°C for 72h. The organic layer was then decanted and the aqueous layer was extracted twice with CH_2Cl_2 . The combine organic layer was washed with water and evaporated. The crude product was purified by chromatography on silica gel by using petroleum ether / CH_2Cl_2 (10%) as the eluent to give the title compound **89** (white solid, 246 mg, 81%).

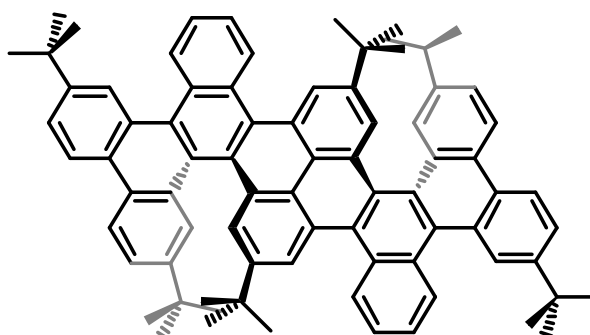
Mp 319-320 °C; 1H NMR (400 MHz, CD_2Cl_2): δ 7.55-6.77 (m, 32H), 1.41-0.78 (m, 54H); FD-HRMS Calcd (M+) 1042.64165, found 1042.63854.

Compound 90



Mp 180-181 °C; 1H NMR (400 MHz, CD_2Cl_2): δ 7.91-7.89 (m, 1H), 7.72-7.70 (m, 1H), 7.53 (dd, 1H, $J = 2.0, 8.0$ Hz), 7.51 (s, 1H), 7.44 (d, 2H, $J = 8.0$ Hz), 7.42-7.38 (m, 2H), 7.36-7.32 (m, 2H), 7.30-7.25 (m, 3H), 7.10 (d, 2H, $J = 8.8$ Hz), 7.05 (d, 2H, $J = 8.8$ Hz), 1.36 (s, 9H), 1.35 (s, 9H), 1.18 (s, 9H); ^{13}C NMR (100 MHz, CD_2Cl_2): δ 151.3, 149.8, 149.2, 140.4, 139.8, 139.7, 138.8, 138.6, 138.3, 132.8, 131.7, 130.2, 129.1, 128.8, 127.9, 127.7, 127.4, 127.3, 126.8, 126.2, 125.6, 124.9, 124.7, 124.2, 34.7, 34.5, 34.2, 31.2, 31.0. ESI HRMS calcd (M+) 524.34, found 524.30.

Compound 91

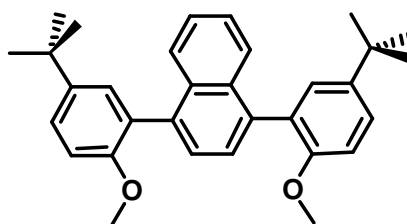


To the compound 4,4'-(4,4'-di-tert-butylbiphenyl-2,2'-diyl)bis(1-(4,4'-di-tert-butylbiphenyl-2-yl)naphthalene) **89** (121 mg, 0.115 mmol) were dissolved in 40 mL of unstabilized dichloromethane and degassed with an argon stream for 15 minutes. Then a solution of 374 mg $FeCl_3$ (2.31 mmol) in 5 mL nitromethane was added dropwise while continuously degassing with an argon stream. After 1 h the reaction was stopped by adding 100 mL of ethanol. Then the organic phase was extracted with water two times and dried with anhydrous

sodium sulfate. The solvent was removed *in vacuo* and The crude product was purified by chromatography on silicagel by using pet. ether / CH₂Cl₂ (1%) as eluent to give the title compound **91** (yellow solid, 76.50 mg, 65%).

Mp >400 °C; ¹H NMR (400 MHz, CD₂Cl₂): δ 9.09 (d, 2H, *J* = 8.4 Hz), 8.99 (s, 2H), 8.90-8.88 (m, 4H), 8.73 (d, 2H, *J* = 8.8 Hz), 8.57 (d, 2H, *J* = 8.8 Hz), 8.31 (s, 2H), 8.13 (s, 2H), 7.87 (d, 2H, *J* = 8.0 Hz), 7.74-7.70 (m, 4H), 7.65 (dd, 2H, *J* = 1.2, 8.8 Hz), 1.54 (s, 18H), 1.17 (s, 36H). ¹³C NMR (100 MHz, CD₂Cl₂): δ 149.2, 147.6, 146.3, 131.7, 131.2, 130.7, 130.2, 129.4, 129.2, 128.5, 128.0, 127.9, 127.3, 127.2, 127.1, 127.0, 126.6, 126.5, 126.1, 125.9, 125.7, 125.2, 125.0, 124.8, 124.6, 123.3, 123.1, 35.1, 34.9, 34.6, 31.3, 31.0, 30.8. FD-HRMS Calcd (M⁺) 1038.61035, found 1038.61579.

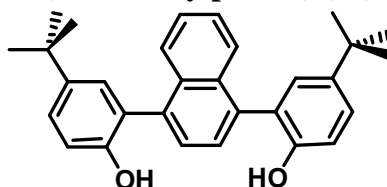
1,4-bis(5-tert-butyl-2-methoxyphenyl)naphthalene (**92**)



1,4-dibromonaphthalene **81** (500 mg, 1.75 mmol), 2-(5-tert-butyl-2-methoxyphenyl) boronic acid **34** (801.57 mg, 3.85 mmol) and Na₂CO₃ (1.85 g, 17.5 mmol) were dissolved in toluene (30 mL), water (10 mL) and ethanol (5 mL). The solution was degassed three times, Pd(PPh₃)₄ (202.02 mg, 0.175 mmol) was added under an Ar stream and the mixture was degassed three times again. The solution was heated at 90 °C for 48h. The organic layer was then decanted and the aqueous layer was extracted 2 times with CH₂Cl₂. The combine organic layer was washed with water and evaporated. The crude product was purified by chromatography on silicagel by using pet. ether / CH₂Cl₂ (15%) as eluent to give the title compound **92** (white solid, 713 mg, 90%).

Mp 102-103 °C; ¹H NMR (400 MHz, CD₂Cl₂): δ 7.58-7.55 (m, 2H), 7.45 (t, 1H, *J* = 2.6 Hz), 7.43 (t, 1H, *J* = 2.4 Hz), 7.41 (s, 1H), 7.40 (s, 1H), 7.36 (d, 1H, *J* = 2.8 Hz), 7.34-7.32 (m, 2H), 7.30 (d, 1H, *J* = 2.8 Hz), 7.00 (d, 1H, *J* = 8.0 Hz), 6.99 (d, 1H, *J* = 8.8 Hz), 3.72 (s, 3H), 3.68 (s, 3H), 1.32 (s, 18H); ¹H NMR (400 MHz, CDCl₃): δ 7.66-7.63 (m, 2H), 7.47 (s, 2H), 7.44 (d, 1H, *J* = 2.8 Hz), 7.42 (d, 1H, *J* = 2.4 Hz), 7.40 (d, 1H, *J* = 2.4 Hz), 7.36-7.33 (m, 3H), 6.99 (d, 2H, *J* = 8.4 Hz), 3.72 (s, 3H), 3.71 (s, 3H), 1.34 (s, 18H). ¹³C NMR (100 MHz, CD₂Cl₂): δ 155.1, 143.4, 143.3, 137.2, 137.1, 132.1, 129.3, 129.1, 128.8, 128.8, 126.9, 126.7, 126.6, 125.6, 125.5, 125.4, 125.3, 110.4, 110.3, 55.5, 34.1, 31.4. ESI HRMS calcd (M⁺) 452.27, found 452.20.

2,2'-(naphthalene-1,4-diyl)bis(4-tert-butylphenol) (**93**)

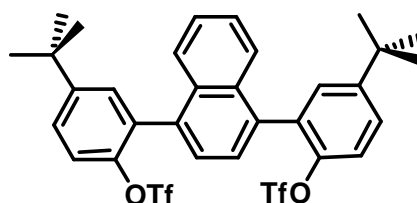


Compound **92** (1.0 g, 2.21 mmol) was dissolved in 50 mL of dry CH₂Cl₂ under N₂ and brought to -20 °C. BBr₃ (1 M in CH₂Cl₂, 2.7 equiv, 5.96 mmol, 5.96 mL) was added dropwise with stirring and the reaction mixture stirred overnight, warming to room temperature. The

reaction mixture was then poured into ice water, organic layer was then decanted and the aqueous layer was extracted 2 times with CH_2Cl_2 . The combine organic layer was washed with water and dried over anhydrous Na_2SO_4 . The solvent was removed under vacuum, yielding **93** (928.50 mg, 99%) as a brown-red solid, which was judged pure enough by TLC to be used in subsequent steps without further purification.

Mp 126-127 °C; ^1H NMR (400 MHz, CDCl_3): δ 7.79-7.76 (m, 2H), 7.60 (s, 1H), 7.59 (s, 1H), 7.51-7.49 (m, 2H), 7.43-7.42 (m, 1H), 7.40-7.39 (m, 1H), 7.32 (d, 1H, $J = 2.4$ Hz), 7.30 (d, 1H, $J = 2.4$ Hz), 7.01 (d, 2H, $J = 8.4$ Hz), 1.33 (s, 18H). ^{13}C NMR (100 MHz, CD_2Cl_2): δ 150.9, 150.8, 143.5, 143.4, 135.7, 135.6, 135.5, 132.4, 128.3, 128.2, 128.1, 128.0, 127.9, 126.9, 126.8, 126.6, 126.5, 126.4, 126.3, 125.6, 125.5, 125.4, 115.1, 115.0, 114.9, 34.1, 34.0, 31.4, 31.32. ESI HRMS calcd (M+) 424.24, found 424.10.

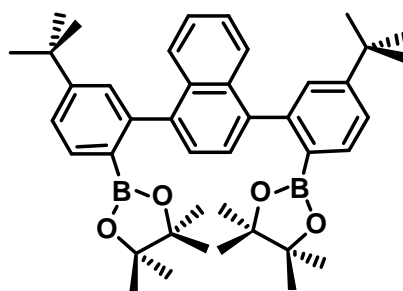
Compound 94



To the 2,2'-(naphthalene-1,4-diyl)bis(4-tert-butylphenol) **93** (900 mg, 2.12 mmol) in anhydrous CH_2Cl_2 was added pyridine (1.707 mL, 21.20 mmol) and the solution was cooled to 0 °C. Trifluoromethanesulfonic anhydride (0.897 mL, 5.30 mmol) was added dropwise and the mixture was warmed to room temperature and stirred overnight. The solvent was removed under vacuum. The crude product was purified by chromatography on silica gel by using petroleum ether / CH_2Cl_2 (20%) as eluent to give the title compound **94** (white solid, 1.40 g, 96%).

Mp 152-153 °C; ^1H NMR (400 MHz, CDCl_3): δ 7.63-7.58 (m, 2H), 7.55-7.54 (m, 1H), 7.53 (s, 2H), 7.51 (d, 2H, $J = 2.8$ Hz), 7.48 (d, 1H, $J = 2.4$ Hz), 7.47-7.42 (m, 3H), 7.37 (d, 1H, $J = 8.4$ Hz) 1.38 (s, 9H), 1.36 (s, 9H). ^{13}C NMR (100 MHz, CD_2Cl_2): δ 152.0, 151.7, 145.4, 145.2, 134.7, 134.6, 133.1, 132.8, 132.0, 131.9, 130.5, 130.4, 127.5, 126.8, 126.4, 126.0, 125.9, 121.2, 121.1, 34.8, 34.7, 31.1. ESI HRMS calcd (M+) 688.14, found 688.10.

Compound 95

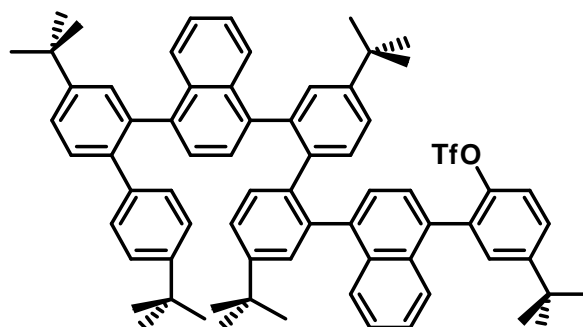


Compound **94** (1.1 g, 1.60 mmol), dppf (88.54 mg, 0.159 mmol), bis(pinacolato)diboron (1.62 g, 6.39 mmol), potassium acetate (940 mg, 9.58 mmol) and $\text{Pd}(\text{dppf})\text{Cl}_2$, CH_2Cl_2 (130.42 mg, 0.159 mmol) were dissolved in dry dioxane (10 mL). The mixture was heated at reflux and stirred under Ar overnight. After the solution was cooled down at room temperature, 20 mL of water and 20 mL of CH_2Cl_2 were added. The organic layer was then decanted and the aqueous layer was extracted 3 times with CH_2Cl_2 . After drying (Na_2SO_4) the solvent was evaporated and the residue was purified by column chromatography on silica gel using petroleum ether or

mixtures of petroleum ether and CH₂Cl₂ as eluent to give the title compound **95** (white solid, 825mg, 80%).

Mp 93-94 °C; ¹H NMR (400 MHz, CD₂Cl₂): δ 7.72 (d, 2H, *J* = 7.2 Hz), 7.65-7.62 (m, 2H), 7.45-7.43 (m, 4H), 7.31-7.28 (m, 4H), 1.34 (s, 18H), 0.97 (s, 12H), 0.84 (s, 12H). ¹³C NMR (100 MHz, CD₂Cl₂): δ 153.3, 146.2, 141.1, 134.3, 132.9, 127.5, 126.4, 126.1, 125.1, 123.4, 83.2, 34.7, 31.0, 24.9, 24.2, 24.1. FD- HRMS calcd (M⁺) 642.42808, found 642.42644.

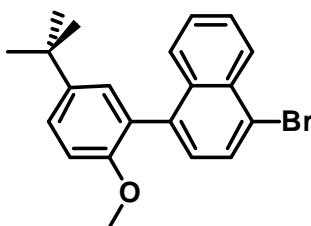
Compound 96



To the compound 4-tert-butyl-2-(4-(4,4'-di-tert-butyl-2'-(4-(4,4'-di-tert-butylbiphenyl-2-yl)naphthalen-1-yl) biphenyl-2-yl)naphthalen-1-yl)phenol **109** (440 mg, 0.47 mmol) dissolved in 20 mL of anhydrous CH₂Cl₂ were added 0.5 mL of pyridine and the solution was cooled to 0°C. Trifluoromethanesulfonic anhydride (0.12 mL, 0.714 mmol) was added drop wise and the mixture was warmed to room temperature and stirred overnight. The solvent was removed under vacuum. The crude product was purified by chromatography on silica gel by using petroleum ether / CH₂Cl₂ (15%) as the eluent to give the title compound **96** (white solid, 478 mg, 96%).

Mp 160-161 °C; ¹H NMR (400 MHz, CD₂Cl₂): δ 7.66-6.71(br, 28H), 1.45-1.01 (m, 45H); ¹⁹F NMR (400 MHz, CD₂Cl₂): δ -74.58; FD-HRMS Calcd (M⁺) 1062.52325, found 1062.52773.

1-bromo-4-(5-tert-butyl-2-methoxyphenyl)naphthalene (**98**)

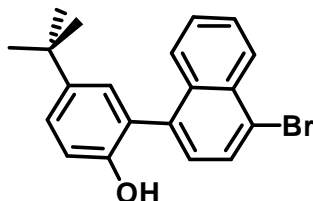


1,4-dibromonaphthalene **81** (4.27 g, 14.9 mmol), 5-tert-butyl-2-methoxyphenylboronic acid **34** (2.8 g, 13.57 mmol) and Na₂CO₃ (7.2 g, 74.6 mmol) were dissolved in toluene (54 mL), water (18 mL) and ethanol (9 mL). The solution was degassed three times, Pd(PPh₃)₄ (626.5 mg, 0.59 mmol) was added under an Ar stream and the mixture was degassed three times again. The solution was heated at 90 °C for overnight. The organic layer was then decanted and the aqueous layer was extracted 2 times with CH₂Cl₂. The combine organic layer was washed with water and evaporated. The crude product was purified by chromatography on silicagel by using pet. ether / CH₂Cl₂ (20%) as the eluent to give the title compound **98** (white solid, 4.40 g, 80%).

Mp 95-96 °C; ¹H NMR (400 MHz, CD₂Cl₂): δ 8.26 (d, 1H, *J* = 8.4 Hz), 7.81 (d, 1H, *J* = 7.2 Hz), 7.59-7.53 (m, 2H), 7.45-7.40 (m, 2H), 7.24 (s, 1H), 8.23 (d, 1H, *J* = 8.0 Hz), 6.97 (d, 1H,

$J = 8.8$ Hz), 3.64 (s, 3H), 1.30 (s, 9H). ^{13}C NMR (100 MHz, CD_2Cl_2): δ 154.9, 143.6, 138.0, 137.8, 129.5, 128.9, 127.8, 127.2, 126.5, 126.0, 121.9, 113.3, 110.6, 55.5, 34.1, 31.4. FD-HRMS Calcd (M⁺) 368.07758, found 368.07656.

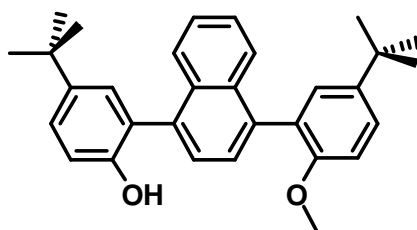
2-(4-bromonaphthalen-1-yl)-4-tert-butylphenol (**99**)



1-bromo-4-(5-tert-butyl-2-methoxyphenyl)naphthalene **98** (1.0 g, 2.71 mmol) was dissolved in 50 mL of dry CH_2Cl_2 under N_2 and brought to -20 °C. BBr_3 (1 M in CH_2Cl_2 , 1.5 equiv, 4.06 mmol, 4.06 mL) was added dropwise with stirring and the reaction mixture stirred overnight, warming to room temperature. The reaction mixture was then poured into ice water, organic layer was then decanted and the aqueous layer was extracted 2 times with CH_2Cl_2 . The combine organic layer was washed with water and dried over anhydrous Na_2SO_4 . The solvent was removed under vacuum, yielding **99** (950.0 mg, 99%) as a brown-red solid, which was judged pure enough by TLC to be used in subsequent steps without further purification.

Mp 89-90 °C; ^1H NMR (400 MHz, CD_2Cl_2): δ 8.31 (d, 1H, $J = 8.0$ Hz), 7.87 (d, 1H, $J = 7.2$ Hz), 7.64 (s, 1H), 7.63-7.61 (m, 1H), 7.51-7.48 (m, 1H), 7.37 (dd, 1H, $J = 2.4, 8.4$ Hz), 7.32 (d, 1H, $J = 7.6$ Hz), 7.22 (d, 1H, $J = 2.4$ Hz), 6.93 (d, 1H, $J = 8.0$ Hz), 4.64 (s, 1H), 1.30 (s, 9H). ^{13}C NMR (100 MHz, CD_2Cl_2): δ 150.8, 143.5, 135.4, 133.2, 132.3, 129.9, 128.5, 128.1, 127.7, 127.5, 127.4, 126.7, 126.5, 125.0, 123.1, 115.1, 34.1, 31.3. FD-HRMS Calcd (M⁺) 354.06193, found 354.06186.

Compound 100

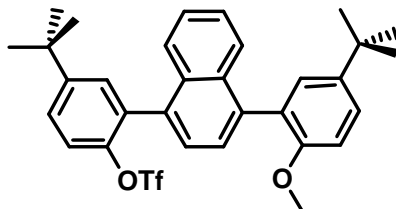


Compound 2-(4-bromonaphthalen-1-yl)-4-tert-butylphenol **99** (1.0 g, 2.82 mmol), 5-tert-butyl-2-methoxyphenylboronic acid (702.6 mg, 3.38 mmol) and Na_2CO_3 (1.2 g, 11.26 mmol) were dissolved in toluene (24 mL), water (8 mL) and ethanol (4 mL). The solution was degassed three times, $\text{Pd}(\text{PPh}_3)_4$ (162.42 mg, 0.141 mmol) was added under an Ar stream and the mixture was degassed three times again. The solution was heated at 90 °C for 48h. The organic layer was then decanted and the aqueous layer was extracted 2 times with CH_2Cl_2 . The combine organic layer was washed with water and evaporated. The crude product was purified by chromatography on silicagel by using pet. ether / CH_2Cl_2 (50%) as eluent to give the title compound **100** (white solid, 1.16 g, 94%).

Mp 97-98 °C; ^1H NMR (400 MHz, CD_2Cl_2): δ 7.68-7.62 (m, 2H), 7.51 (dd, 1H, $J = 2.0, 7.2$ Hz), 7.48-7.44 (m, 2H), 7.42-7.37 (m, 3H), 7.34 (dd, 1H, $J = 2.4, 9.2$ Hz), 7.29 (dd, 1H, $J = 2.4, 9.0$ Hz), 7.00 (d, 1H, $J = 9.0$ Hz), 6.96 (dd, 1H, $J = 4.0, 8.0$ Hz), 4.92 (s, 0.4H), 4.88 (s,

0.6H), 3.69 (s, 3H), 1.32 (s, 18H). ^{13}C NMR (100 MHz, CD_2Cl_2): δ 155.0, 151.0, 143.4, 138.3, 134.4, 134.2, 132.7, 131.9, 129.1, 129.0, 128.4, 127.7, 127.3, 127.1, 126.4, 126.3, 126.2, 126.0, 125.9, 125.8, 115.0, 114.9, 110.5, 55.6, 34.1, 34.0, 31.4, 31.3. FD-HRMS Calcd (M+) 438.25588, found 438.25491.

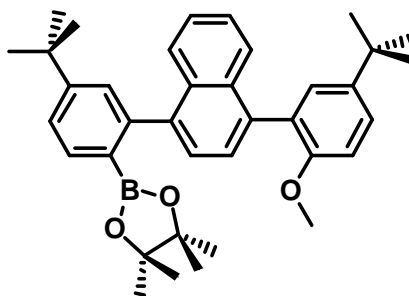
Compound 101



To the compound 4-tert-butyl-2-(4-(5-tert-butyl-2-methoxyphenyl)naphthalen-1-yl)phenol **100** (12.70 g, 28.96 mmol) dissolved in 100 mL of anhydrous CH_2Cl_2 were added 23.40 mL of pyridine and the solution was cooled to 0°C . Trifluoromethanesulfonic anhydride (9.80 mL, 57.93 mmol) was added drop wise and the mixture was warmed to room temperature and stirred overnight. The solvent was removed under vacuum. The crude product was purified by chromatography on silica gel by using petroleum ether / CH_2Cl_2 (40%) as eluent to give the title compound **101** (white solid, 15.0 g, 91%).

Mp $75-76^\circ\text{C}$; ^1H NMR (400 MHz, CD_2Cl_2): δ 7.64-7.60(m, 2H), 7.58-7.54(m, 2H), 7.51-7.44(m, 3H), 7.41-7.38(m, 3H), 7.31 (dd, 1H, $J = 2.8, 8.4$ Hz), 7.00 (d, 1H, $J = 8.4$ Hz), 3.68 (s, 2H), 3.64 (s, 1H), 1.37 (s, 9H), 1.34 (s, 5H), 1.33 (s, 4H); ^{19}F NMR (400 MHz, CD_2Cl_2): δ -74.70; ^{13}C NMR (100 MHz, CD_2Cl_2): δ 155.3, 155.0, 151.8, 145.5, 143.5, 143.4, 138.7, 133.5, 133.0, 133.0, 132.5, 132.4, 130.7, 130.4, 129.1, 128.9, 128.8, 128.6, 127.8, 127.7, 126.9, 126.6, 126.0, 125.9, 125.6, 121.2, 121.0, 111.1, 110.5, 55.8, 55.5, 34.8, 34.1, 31.4, 31.1; FD-HRMS Calcd (M+) 570.20516, found 570.20274.

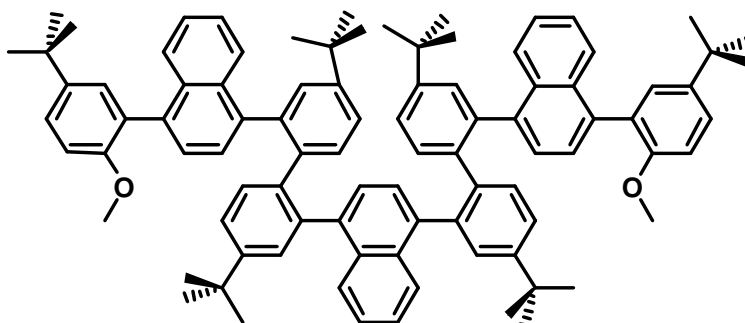
Compound 102



Compound 4-tert-butyl-2-(4-(5-tert-butyl-2-methoxyphenyl)naphthalen-1-yl)phenyl trifluoromethane sulfonate **101** (3.0 g, 5.26 mmol), dppf (291.44 mg, 0.53 mmol), bis(pinacolato)diboron (2.67 g, 10.51 mmol), potassium acetate (3.1 g, 31.54 mmol) and $\text{Pd}(\text{dppf})\text{Cl}_2 \cdot \text{CH}_2\text{Cl}_2$ (429.30 mg, 0.53 mmol) were dissolved in dry dioxane (20 mL). The mixture was heated at reflux and stirred under Ar overnight. After the solution was cooled down at room temperature, 20 mL of water and 20 mL of CH_2Cl_2 were added. The organic layer was then decanted and the aqueous layer was extracted 3 times with CH_2Cl_2 . After drying (Na_2SO_4) the solvent was evaporated and the residue was purified by column chromatography on silica gel using petroleum ether or mixtures of petroleum ether and CH_2Cl_2 as eluent to give the title compound **102** (white solid, 2.0 g, 71%).

Mp 115-116 °C; ^1H NMR (400 MHz, CD_2Cl_2): δ 7.74-7.71 (m, 1H), 7.66-7.60 (m, 1H), 7.58-7.53 (m, 1H), 7.47-7.42 (m, 3H), 7.38-7.37 (m, 2H), 7.35-7.27 (m, 3H), 7.0 (dd, 1H, $J = 2.0$, 8.4 Hz), 3.71-3.65 (m, 3H), 1.36 (s, 9H), 1.33-1.32 (m, 9H), 0.97-0.96 (m, 6H), 0.82-0.78 (m, 6H). ^{13}C NMR (100 MHz, CD_2Cl_2): δ 155.2, 155.1, 153.5, 153.4, 146.1, 146.0, 143.3, 143.2, 141.4, 136.8, 136.7, 134.3, 134.1, 132.9, 132.8, 132.2, 132.1, 129.3, 129.1, 127.4, 127.2, 126.7, 126.6, 126.5, 126.4, 126.3, 126.1, 125.5, 125.4, 125.3, 125.2, 125.1, 125.0, 123.5, 83.1, 55.6, 55.5, 34.8, 34.1, 31.4, 31.3, 31.1, 24.2, 24.1, 24.0, 23.9. ESI HRMS calcd (M^+) 548.35, found 548.30.

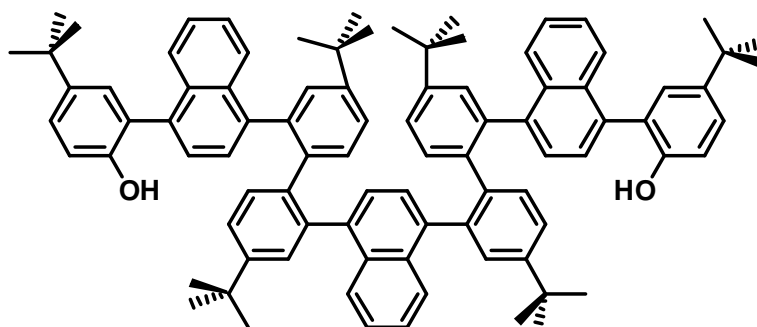
Compound 103



Compound **94** (1.5 g, 2.18 mmol), boronicester **102** (3.30 g, 6.0 mmol) and K_3PO_4 (2.78 g, 13.10 mmol) were dissolved in a mixture of THF (15 mL) and water (3 mL). The solution was degassed, $\text{Pd}(\text{OAc})_2$ (48.90 mg, 0.218 mmol) and 2-dicyclohexylphosphino-2',6'-dimethoxybiphenyl SPhos (107.29 mg, 0.26 mmol) were added under an Ar stream and the mixture was degassed again. The solution was heated at 70°C for 96h. The organic layer was then decanted and the aqueous layer was extracted twice with CH_2Cl_2 . The combine organic layer was washed with water and evaporated. The crude product was purified by chromatography on silica gel by using petroleum ether / CH_2Cl_2 (40%) as eluent to give the title compound **103** (white solid, 2.0 g, 75%).

Mp 215-216 °C; ^1H NMR (400 MHz, CD_2Cl_2): δ 7.96-7.90 (m, 2H), 7.78-6.84 (m, 34H), 3.70-3.68 (m, 6H), 1.32-1.12 (m, 54H); FD-HRMS Calcd (M^+) 1232.74209, found 1232.74103.

Compound 104

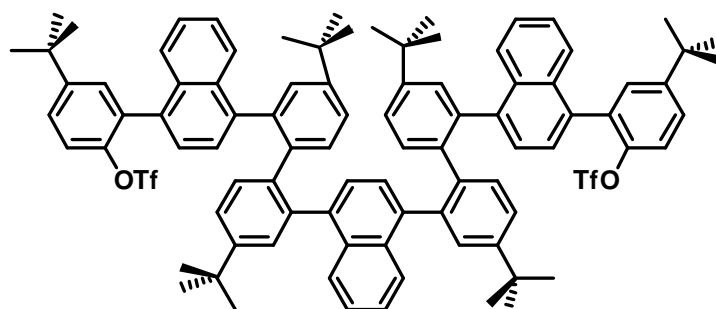


Compound **103** (2.2 g, 1.79 mmol) was dissolved in 50 mL of dry CH_2Cl_2 under N_2 and brought to -20 °C. BBr_3 (1 M in CH_2Cl_2 , 2.5 equiv, 4.47 mmol, 4.47 mL) was added dropwise with stirring and the reaction mixture stirred overnight, warming to room temperature. The reaction mixture was then poured into ice water, organic layer was then decanted and the

aqueous layer was extracted 2 times with CH_2Cl_2 . The combine organic layer was washed with water and dried over anhydrous Na_2SO_4 . The solvent was removed under vacuum, yielding **104** (2.1 g, 99%) as a brown-red solid, which was judged pure enough by TLC to be used in subsequent steps without further purification.

Mp 175-176 °C; ^1H NMR (400 MHz, CD_2Cl_2): δ 7.96-7.94 (m, 2H), 7.69-7.68 (m, 2H), 7.55-7.29 (m, 30H), 6.96-6.94 (m, 2H), 4.81-4.71 (br, 2H), 1.42-1.18 (m, 54H). FD-HRMS Calcd (M+) 1204.70973, found 1204.70555.

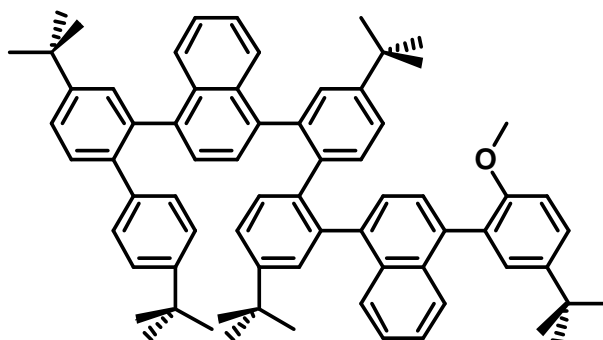
Compound 105



Compound **104** (2.2 g, 1.83 mmol) was dissolved in 30 mL of anhydrous CH_2Cl_2 were added 1.5 mL of pyridine and the solution was cooled to 0°C. Trifluoromethanesulfonic anhydride (0.80 mL, 4.58 mmol) was added drop wise and the mixture was warmed to room temperature and stirred overnight. The solvent was removed under vacuum. The crude product was purified by chromatography on silica gel by using petroleum ether / CH_2Cl_2 (15%) as eluent to give the title compound **105** (white solid, 2.55 g, 95%).

Mp 190-191 °C; ^1H NMR (400 MHz, CD_2Cl_2): δ 7.62-7.35(m, 36H), 1.40-1.17 (m, 54H; ^{19}F NMR (376 MHz, CD_2Cl_2): δ -74.46; FD-HRMS Calcd (M+) 1469.63021, found 1469.63232.

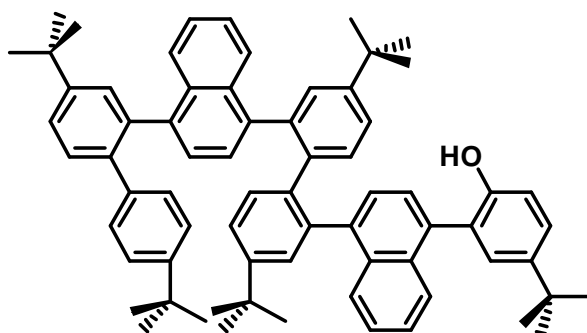
Compound 108



Compound **101** (600 mg, 1.05 mmol), and boronic ester compound **88** (821.0 mg, 1.26 mmol) and K_3PO_4 (891.53 g, 4.20 mmol) were dissolved in a mixture of THF (12 mL) and water (1.5 mL). The solution was degassed, $\text{Pd}(\text{OAc})_2$ (23.57 mg, 0.13 mmol) and 2-dicyclohexylphosphino-2',6'-dimethoxybiphenyl SPhos (51.72 mg, 0.15 mmol) were added under an Ar stream and the mixture was degassed again. The solution was heated at 70°C for 48h. The organic layer was then decanted and the aqueous layer was extracted twice with CH_2Cl_2 . The combine organic layer was washed with water and evaporated. The crude product was purified by chromatography on silica gel by using petroleum ether / CH_2Cl_2 (20%) as eluent to give the title compound **108** (white solid, 724 mg, 73%).

Mp 177-178 °C; ^1H NMR (400 MHz, CD_2Cl_2): δ 7.62-6.79 (m, 28H), 3.70-3.52 (m, 3H), 1.42-1.04 (m, 45H); FD-HRMS Calcd (M+) 944.58961, found 944.58711.

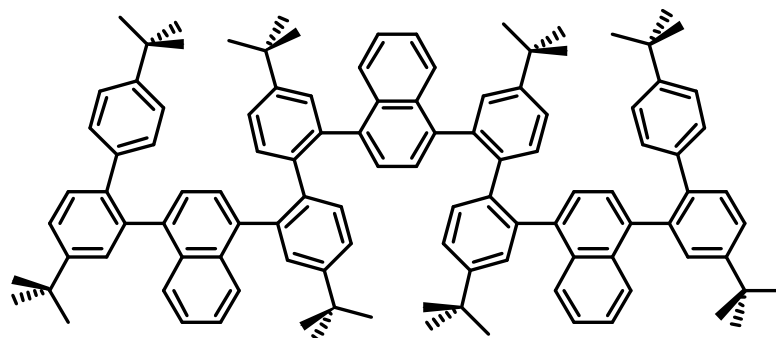
Compound 109



Compound **108** (450 mg, 0.476 mmol) was dissolved in 20 mL of dry CH_2Cl_2 under N_2 and brought to $-20\text{ }^\circ\text{C}$. BBr_3 (1 M in CH_2Cl_2 , 1.5 equiv, 0.714 mmol, 0.72 mL) was added dropwise with stirring and the reaction mixture stirred overnight, warming to room temperature. The reaction mixture was then poured into ice water, organic layer was then decanted and the aqueous layer was extracted 2 times with CH_2Cl_2 . The combine organic layer was washed with water and dried over anhydrous Na_2SO_4 . The solvent was removed under vacuum, yielding **109** (420.80 mg, 95%) as a brown-red solid, which was judged pure enough by TLC to be used in subsequent steps without further purification.

Mp $167\text{-}168\text{ }^\circ\text{C}$; $^1\text{H NMR}$ (400 MHz, CD_2Cl_2): δ 7.63-6.76 (m, 28H), 4.72-4.56 (m, 1H), 1.44-1.06 (m, 45H); FD-HRMS Calcd (M^+) 930.57396, found 930.57278.

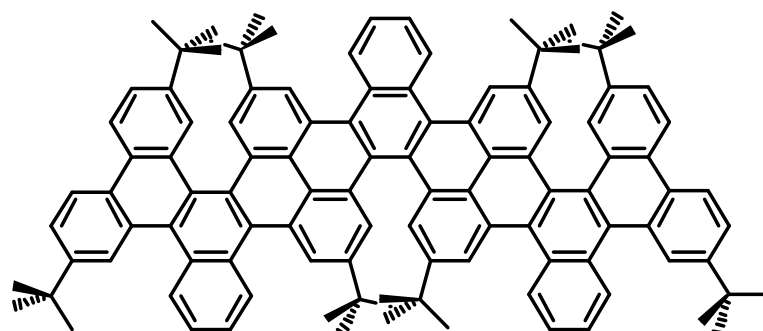
Compound 110



Compound **96** (450 mg, 0.42 mmol), boronic ester **88** (358 mg, 0.55 mmol) and K_3PO_4 (359 mg, 1.70 mmol) were dissolved in a mixture of THF (10 mL) and water (0.5 mL). The solution was degassed, $\text{Pd}(\text{OAc})_2$ (9.50 mg, 0.042 mmol) and 2-dicyclohexylphosphino-2',6'-dimethoxybiphenyl SPhos (20.80 mg, 0.051 mmol) were added under an Ar stream and the mixture was degassed again. The solution was heated at $70\text{ }^\circ\text{C}$ for 96h. The organic layer was then decanted and the aqueous layer was extracted twice with CH_2Cl_2 . The combine organic layer was washed with water and evaporated. The crude product was purified by chromatography on silica gel by using petroleum ether / CH_2Cl_2 (10%) as eluent to give the title compound **110** (white solid, 446 mg, 74%).

Mp $260\text{-}261\text{ }^\circ\text{C}$; $^1\text{H NMR}$ (400 MHz, CD_2Cl_2): δ 7.57-6.75(m, 44H), 1.44-0.94(m, 72H); FD-HRMS Calcd (M^+) 1436.90770, found 1436.91285.

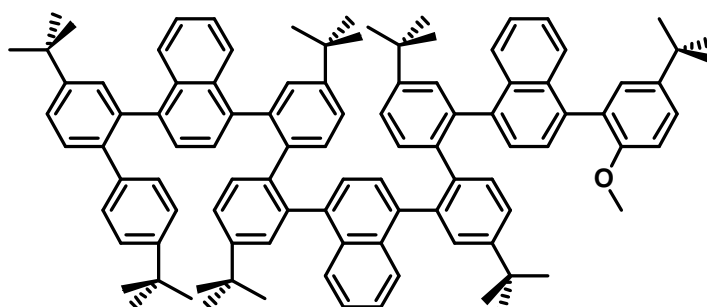
Compound 111



Compound **110** (100 mg, 0.07 mmol) was dissolved in 50 mL of unstabilized dichloromethane and degassed with an Ar stream for 15 minutes. Then a solution of FeCl_3 (406.37 mg, 2.5 mmol) in 5 mL of nitromethane was added drop wise while continuously degassing with an Ar stream. After 1.5h the reaction was stopped by adding 100 mL of methanol. The organic phase was then washed twice with water and dried over anhydrous Na_2SO_4 . The solvent was removed *in vacuo* and the crude product was purified by chromatography on silica gel by using petroleum ether / CH_2Cl_2 (4%) as the eluent to give the title compound **111** (yellow solid, 39 mg, 40%).

Mp >400 °C; ^1H NMR complex NMR spectra, FD-HRMS Calcd (M+) 1424.81, found 1424.70.

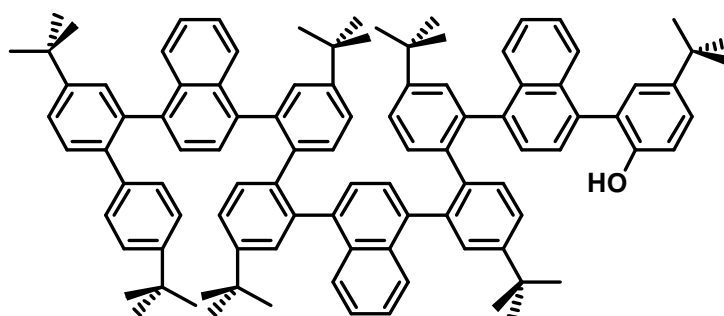
Compound 112



Compound **96** (200 mg, 0.19 mmol), boronic-ester **102** (206.30 mg, 0.37 mmol) and K_3PO_4 (159.60 mg, 0.75 mmol) were dissolved in a mixture of THF (6 mL) and water (0.5 mL). The solution was degassed, $\text{Pd}(\text{OAc})_2$ (4.22 mg, 0.019 mmol) and 2-dicyclohexylphosphino-2',6'-dimethoxybiphenyl SPhos (9.3 mg, 0.023 mmol) were added under an Ar stream and the mixture was degassed again. The solution was heated at 70°C for 72h. The organic layer was then decanted and the aqueous layer was extracted twice with CH_2Cl_2 . The combine organic layer was washed with water and evaporated. The crude product was purified by chromatography on silica gel by using petroleum ether / CH_2Cl_2 (20%) as the eluent to give the title compound **112** (white solid, 164 mg, 65%).

Mp 180-181 °C; ^1H NMR (400 MHz, CD_2Cl_2): δ 7.95-7.88 (m, 1H), 7.67-6.71 (m, 39H), 3.69 (s, 3H), 1.44-1.04 (m, 63H); ESI-MS Calcd (M+) 1334.82, found 1334.80.

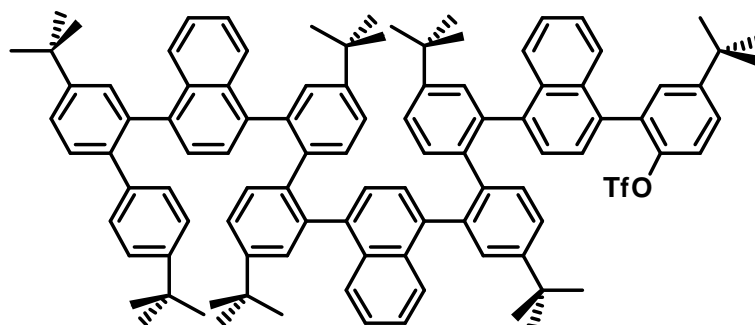
Compound 113



Compound **112** (250 mg, 0.19 mmol) was dissolved in 10 mL of dry CH_2Cl_2 under N_2 and brought to -20°C . BBr_3 (1 M in CH_2Cl_2 , 2.0 equiv, 0.376 mmol, 0.38 mL) was added dropwise with stirring and the reaction mixture stirred overnight, warming to room temperature. The reaction mixture was then poured into ice water, organic layer was then decanted and the aqueous layer was extracted 2 times with CH_2Cl_2 . The combine organic layer was washed with water and dried over anhydrous Na_2SO_4 . The solvent was removed under vacuum, yielding **113** (220 mg, 90%) as a brown-red solid, which was judged pure enough by TLC to be used in subsequent steps without further purification.

Mp $195\text{-}196^\circ\text{C}$; $^1\text{H NMR}$ (400 MHz, CD_2Cl_2): δ 7.97-7.95 (m, 1H), 7.74-6.74 (m, 39H), 4.78-4.72 (m, 1H), 1.44-1.13 (m, 63H); ESI-MS calcd (M+) 1320.81, found 1320.80.

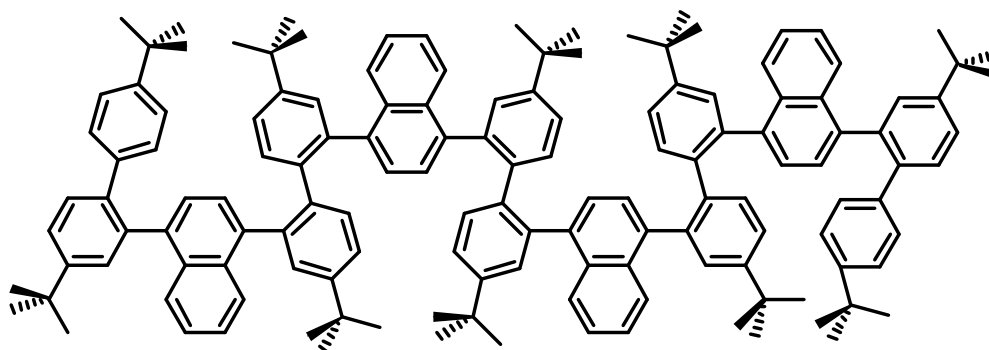
Compound 114



Compound **113** (248 mg, 0.19 mmol) dissolved in 10 mL of anhydrous CH_2Cl_2 was added 0.3 mL of pyridine and the solution was cooled to 0°C . Trifluoromethanesulfonic anhydride (0.07 mL, 1.67 mmol) was added drop wise and the mixture was warmed to room temperature and stirred overnight. The solvent was removed under vacuum. The crude product was purified by chromatography on silica gel by using petroleum ether / CH_2Cl_2 (15%) as the eluent to give the title compound **114** (white solid, 241 mg, 83%).

Mp $170\text{-}171^\circ\text{C}$; $^1\text{H NMR}$ (400 MHz, CD_2Cl_2): δ 7.98-7.94(m, 1H), 7.74-6.75 (m, 39H), 1.37-1.11(m, 63H); $^{19}\text{F NMR}$ (376 MHz, CD_2Cl_2): δ -74.70; ESI-MS Calcd (M+) 1452.76, found 1452.70.

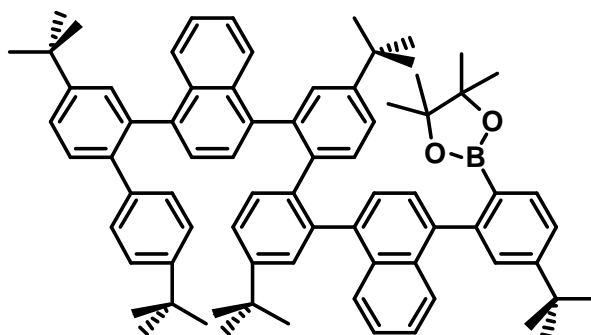
Compound 115



Compound **92** (354.10 mg, 0.33 mmol), dimer boronic ester **113** (520 mg, 0.50 mmol) and K_3PO_4 (425 mg, 2.0 mmol) were dissolved in a mixture of THF (10 mL) and water (1 mL). The solution was degassed, $Pd(OAc)_2$ (7.45 mg, 0.033 mmol) and 2-dicyclohexylphosphino-2',6'-dimethoxybiphenyl SPhos (16.26 mg, 0.040 mmol) were added under an Ar stream and the mixture was degassed again. The solution was heated at 70°C for 120h. The organic layer was then decanted and the aqueous layer was extracted twice with CH_2Cl_2 . The combine organic layer was washed with water and evaporated. The crude product was purified by chromatography on silica gel by using petroleum ether / CH_2Cl_2 (10%) as eluent to give the title compound **112** (white solid, 510 mg, 82%).

Mp 240-241 °C; 1H NMR (400 MHz, CD_2Cl_2): δ 7.87-6.24(m, 56H), 1.42-1.0 (m, 90H); ESI-HRMS Calcd (M⁺) 1827.14, found 1827.20 and ESI-HRMS Calcd (M+SiO₂) 1888.14, found 1888.10.

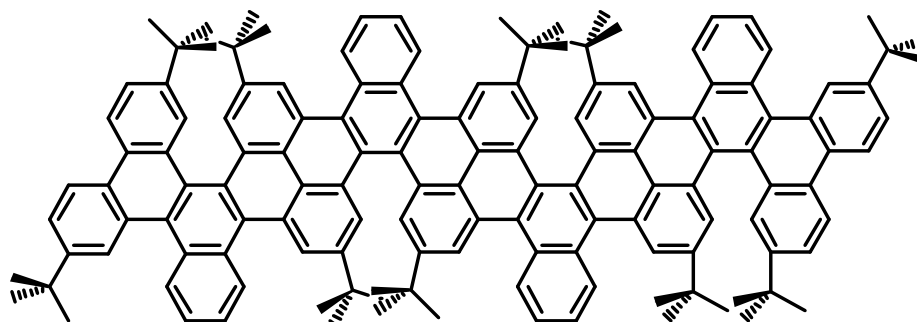
Compound 116



Compound **96** (400 mg, 0.38 mmol), dppf (20.8 mg, 0.038 mmol), bis(pinacolato)diboron (190.9 mg, 0.75 mmol), potassium acetate (221.4 mg, 2.26 mmol) and $Pd(dppf)Cl_2 \cdot CH_2Cl_2$ (28.0 mg, 0.038 mmol) were dissolved in dry dioxane (10 mL). The mixture was heated at reflux and stirred under Ar 48 hours. After the solution was cooled down at room temperature, 20 mL of water and 20 mL of CH_2Cl_2 were added. The organic layer was then decanted and the aqueous layer was extracted 3 times with CH_2Cl_2 . After drying (Na_2SO_4) the solvent was evaporated and the residue was purified by column chromatography on silica gel using petroleum ether or mixtures of petroleum ether and CH_2Cl_2 as eluent to give the title compound **116** (white solid, 315 mg, 80%).

Mp 214-215 °C; ¹H NMR (400 MHz, CD₂Cl₂): δ 7.73-6.71(m, 28H), 1.43-1.10 (m, 45H), 1.03-0.72 (m, 12H); FD-HRMS Calcd (M⁺) 1039.66789, found 1039.66497.

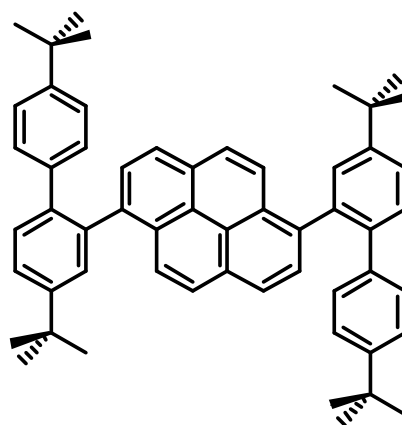
Compound 117



Compound **115** (113 mg, 0.06 mmol) was dissolved in 50 mL of unstabilized dichloromethane and degassed with an Ar stream for 15 minutes. Then a solution of FeCl₃ (501.0 mg, 3.09 mmol) in 5 mL of nitromethane was added drop wise while continuously degassing with an Ar stream. After 2h the reaction was stopped by adding 100 mL of methanol. The organic phase was then washed twice with water and dried over anhydrous Na₂SO₄. The solvent was removed *in vacuo* and the crude product was purified by chromatography on silica gel by using petroleum ether / CH₂Cl₂ (4%) as the eluent to give the title compound **117** (yellow solid, 30 mg, 30%).

¹H NMR (400 MHz, CD₂Cl₂): Complex NMR spectra, FD-HRMS Calcd (M⁺) 1811.02, found 1811.10.

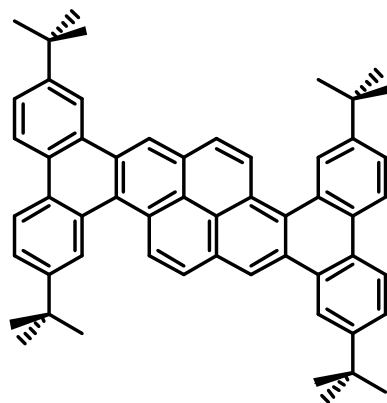
1,6-bis(4,4'-di-tert-butylbiphenyl-2-yl)pyrene (119)



1,6-dibromopyrene **118** (994 mg, 2.76 mmol), 2-(4,4'-di-tert-butylbiphenyl-2-yl)-4,4,5,5-tetramethyl-1,3,2-dioxaborolane **5b** (2.28 g, 5.80 mmol) and Na₂CO₃ (5.85 g, 55.20 mmol) were dissolved in toluene (48 mL), water (16 mL) and ethanol (8 mL). The solution was degassed three times, Pd(PPh₃)₄ (318.62 mg, 0.276 mmol) was added under an Ar stream and the mixture was degassed three times again. The solution was heated at 90 °C for 48h. The organic layer was then decanted and the aqueous layer was extracted 2 times with CH₂Cl₂. The combine organic layer was washed with water and evaporated. The crude product was purified by chromatography on silicagel by using pet. ether / CH₂Cl₂ (8%) as eluent to give the title compound **119** (white solid, 1.75 g, 87%).

Mp 358-359 °C; ¹H NMR (400 MHz, CD₂Cl₂): δ 8.01 (dd, 2H, *J* = 2.4, 9.2 Hz), 7.96-7.89 (m, 4H), 7.67 (s, 1H), 7.64 (d, 1H, *J* = 2.4 Hz), 7.55-7.54 (m, 4H), 7.52-7.51 (m, 2H), 7.04 (s, 1H), 7.03 (s, 1H), 6.99-6.95 (m, 6H), 1.39 (s, 18H), 1.11 (s, 18H). ¹³C NMR (100 MHz, CD₂Cl₂): δ 149.8, 149.7, 149.2, 149.1, 139.0, 138.9, 138.8, 138.7, 138.4, 138.3, 138.2, 138.1, 130.3, 130.2, 130.0, 129.7, 129.6, 129.6, 129.5, 129.1, 129.0, 128.9, 128.8, 127.3, 125.4, 125.0, 124.9, 124.8, 124.7, 124.6, 124.0, 123.9, 34.5, 34.2, 34.1, 31.2, 31.0, 30.9. FD-HRMS calcd (M⁺) 730.45385, found 730.45721.

2,7,13,18-tetra-tert-butyl-dibenzo[j,tuv]phenanthro[9,10-b]picene (120)



1,6-bis(4,4'-di-tert-butylbiphenyl-2-yl)pyrene (100 mg, 0.137 mmol) **119** was dissolved in 50 mL of unstabilized dichloromethane and degassed with an argon stream for 15 minutes. Then a solution of 511 mg FeCl₃ (3.15 mmol) in 5 mL nitromethane was added dropwise while continuously degassing with an argon stream. After 1 h the reaction was stopped by adding 100 mL of ethanol. Then the organic phase was extracted with water two times and dried with anhydrous sodium sulfate. The solvent was removed in *vacuo* and crude product was purified by chromatography on silicagel by using pet. ether / CH₂Cl₂ (1%) as eluent to give the title compound **120** (yellow solid, 79.70 mg, 80%).

Mp >400 °C; ¹H NMR (400 MHz, CD₂Cl₂): δ 9.37 (s, 2H), 9.19 (d, 2H, *J* = 9.2 Hz), 8.93 (d, 2H, *J* = 1.6 Hz), 8.89 (d, 2H, *J* = 1.6 Hz), 8.63 (d, 2H, *J* = 8.8 Hz), 8.62 (d, 2H, *J* = 8.8 Hz), 8.47 (d, 2H, *J* = 9.2 Hz), 7.8-7.76 (m, 4H), 1.57 (s, 9H), 1.54 (s, 18H), 1.53 (s, 9H). ¹³C NMR (100 MHz, CD₂Cl₂): δ 150.1, 148.6, 129.6, 128.9, 127.9, 127.6, 127.2, 125.8, 125.6, 124.8, 123.4, 123.2, 123.0, 120.2, 118.3, 35.3, 35.2, 31.7, 31.6. FD-HRMS calcd (M⁺) 726.4209, found 726.4210.

Table 4. Crystallographic data of **28** · 3CH₂Cl₂ and **28** · C₄H₈O₂ · 2H₂O at **120 K**.

	28 · 3CH ₂ Cl ₂	28 · C ₄ H ₈ O ₂ · 2H ₂ O
Empirical formula	C ₆₆ H ₇₂ , 3(C H ₂ Cl ₂)	C ₆₆ H ₇₂ , 2(H ₂ O), C ₄ H ₈ O ₂
Formula weight	1120.01	989.37
Crystal system	Hexagonal	Monoclinic
Space group	P-3C1	C2/c
Wavelength, Å	0.71073	0.71073
a, Å	15.6720(6)	38.0928(10)
b, Å	15.6720(6)	14.9095(4)
c, Å	14.3279(8)	27.1064(6)
α, °	90	90
β, °	90	128.1180(10)
γ, °	120	90
V, Å ³	3047.6(2)	12111.8(5)
Z	2	8
ρ _{calcd} , Mg/m ³	1.221	1.160
M, 1/mm	0.322	0.065
Reflections collected	16549	49747
Independent reflections	2324	13868
R ₁ ^a	0.0856	0.1159
wR ₂ ^a	0.2218	0.3406
GoF ^a	1.208	1.313

^a $I > 2\sigma(I)$, $R_1 = \Sigma(|F_o| - |F_c|)/\Sigma|F_o|$, $wR_2 = \{\Sigma[w(F_o^2 - F_c^2)^2]/\Sigma[w(F_o^2)^2]\}^{1/2}$. GoF (goodness of fit on F^2) = $\{\Sigma[w(F_o^2 - F_c^2)^2]/(n-p)\}^{1/2}$

Table 11. Crystallographic data of **33** at **120K**.

Empirical formula	C84 H78 F18 O18 S6
Formula weight	1909.82
Crystal system	Monoclinic
Space group	P21/c
Wavelength, Å	0.71073
a, Å	15.630(5)
b, Å	18.879(6)
c, Å	32.000(9)
α , °	90
β , °	106.211(16)
γ , °	90
V, Å ³	9067(5)
Z	4
ρ_{calcd} , Mg/m ³	1.399
M, 1/mm	0.252
Reflections collected	140976
Independent reflections	7158
R_1^a	0.1342
wR_2^a	0.3681
GoF ^a	1.676

^a $R_1 = \Sigma||F_0| - |F_C||/\Sigma|F_0|$ and ^b $wR_2 = [\Sigma w(F_0^2 - F_C^2)^2/\Sigma w(F_0^2)^2]^{1/2}$

Table 5. Crystallographic data of **60** · C₆H₁₄O at **120K**.

Formula	C ₇₈ H ₅₈ , C ₆ H ₁₄ O
FW (g·mol ⁻¹)	1097.42
Crystal color	yellow
Crystal size (mm)	0.16 x 0.09 x 0.07
Crystal system	triclinic
Space group	P-1
Temperature	120 K
<i>a</i> (Å)	11.102(3)
<i>b</i> (Å)	13.823(3)
<i>c</i> (Å)	21.704(6)
α (°)	78.067(9)
β (°)	83.121(9)
γ (°)	69.937(8)
<i>V</i> (Å ³)	3056.8(13)
<i>Z</i>	2
<i>d</i> _{calc}	1.192
μ (mm ⁻¹)	0.068
Absorp. correction	SADABS
θ_{\min} - θ_{\max}	1.59° - 25.52°
Refl. coll. / unique	59514 / 11221
Completeness to 2 θ	0.983
<i>R</i> _{int}	0.0619
Refined param./restr.	841 / 1
^a <i>R</i> ₁ (<i>I</i> > 2 σ (<i>I</i>))	0.0636
^b <i>wR</i> ₂ (all data)	0.1993
Goodness of fit	1.075

$$^a R_1 = \sum ||F_o| - |F_c|| / \sum |F_o| \text{ and } ^b wR_2 = [\sum w(F_o^2 - F_c^2)^2 / \sum w(F_o^2)^2]^{1/2}$$

Table 12. Crystallographic data of **63a** at **120K**.

Empirical formula	C67 H57 Cl O2
Formula weight	929.58
Crystal system	Monoclinic
Space group	P21/c
Wavelength, Å	0.71073
a, Å	15.9372(13)
b, Å	15.5116(12)
c, Å	25.1760(19)
α , °	90
β , °	126.374(3)
γ , °	90
V, Å ³	5011.2(7)
Z	4
ρ_{calcd} , Mg/m ³	1.232
M, 1/mm	0.124
Reflections collected	138040
Independent reflections	9178
R_1^a	0.0807
wR_2^a	0.2285
GoF ^a	1.040

$$^a R_1 = \frac{\sum ||F_0| - |F_C||}{\sum |F_0|} \text{ and } ^b wR_2 = [\frac{\sum w(F_0^2 - F_C^2)^2}{\sum w(F_0^2)^2}]^{1/2}$$

Table 6. Crystallographic data of **68** at **120K**.

Formula	(C ₆₃ H ₇₂ Si ₃) ₄ , (CH ₂ Cl ₂) _{2.5}
FW (g·mol ⁻¹)	3866.22
Crystal color	yellow
Crystal size (mm)	0.20 x 0.10 x 0.07
Crystal system	triclinic
Space group	P-1
Temperature	120 K
<i>a</i> (Å)	15.6315(37)
<i>b</i> (Å)	15.9006(37)
<i>c</i> (Å)	26.6120(63)
α (°)	91.090(15)
β (°)	105.275(15)
γ (°)	111.548(14)
<i>V</i> (Å ³)	5885(2)
<i>Z</i>	1
<i>d</i> _{calc}	1.091
μ (mm ⁻¹)	0.174
Absorp. correction	SADABS
θ_{\min} - θ_{\max}	0.80° - 25.55°
Refl. coll. / unique	79712 / 21230
Completeness to 2 θ	0.964
<i>R</i> _{int}	0.0940
Refined param./restr.	1273 / 28
^a <i>R</i> ₁ (<i>I</i> > 2 σ (<i>I</i>))	0.0924
^b w <i>R</i> ₂ (all data)	0.3041
Goodness of fit	1.047

$$^aR_1 = \Sigma||F_0| - |F_C||/\Sigma|F_0| \text{ and } ^b wR_2 = [\Sigma w(F_0^2 - F_C^2)^2/\Sigma w(F_0^2)]^{1/2}$$

Table 7. Crystallographic data of **74** at **120K**.

Formula	C ₃₈ H ₃₂
FW (g·mol ⁻¹)	488.64
Crystal color	colourless
Crystal size (mm)	0.26 x 0.05 x 0.04
Crystal system	monoclinic
Space group	C2
Temperature	120 K
<i>a</i> (Å)	55.846(12)
<i>b</i> (Å)	6.9266(14)
<i>c</i> (Å)	44.338(10)
α (°)	90
β (°)	95.087(17)
γ (°)	90
<i>V</i> (Å ³)	17083(6)
<i>Z</i>	24
<i>d</i> _{calc}	1.140
μ (mm ⁻¹)	0.064
Absorp. correction	SADABS
θ_{\min} - θ_{\max}	1.13° - 19.97°
Refl. coll. / unique	85695 / 15455
Completeness to 2 θ	0.97
<i>R</i> _{int}	0.0808
Refined param./restr.	2008 / 171
^a <i>R</i> ₁ (<i>I</i> > 2 σ (<i>I</i>))	0.1536
^b w <i>R</i> ₂ (all data)	0.4437
Goodness of fit	1.708

$$^aR_1 = \Sigma||F_0| - |F_C||/\Sigma|F_0| \text{ and } ^b wR_2 = [\Sigma w(F_0^2 - F_C^2)^2/\Sigma w(F_0^2)^2]^{1/2}$$

Table 8. Crystallographic data of **79-80** at **120K**.

Formula	(C ₅₀ H ₃₅ Cl) _{0.4} , (C ₅₀ H ₃₆ O ₂) _{0.6}
FW (g·mol ⁻¹)	670.01
Crystal color	orange
Crystal size (mm)	0.19 x 0.09 x 0.06
Crystal system	monoclinic
Space group	P2 ₁ /c
Temperature	120 K
<i>a</i> (Å)	15.4016(5)
<i>b</i> (Å)	8.3054(2)
<i>c</i> (Å)	25.6869(7)
α (°)	90
β (°)	99.9220(10)
γ (°)	90
<i>V</i> (Å ³)	3236.63(16)
<i>Z</i>	4
<i>d</i> _{calc}	1.383
μ (mm ⁻¹)	0.112
Absorp. correction	SADABS
θ_{\min} - θ_{\max}	1.34° - 25.39°
Refl. coll. / unique	73668 / 5927
Completeness to 2 θ	0.996
<i>R</i> _{int}	0.0320
Refined param./restr.	509 / 2
^a <i>R</i> ₁ (<i>I</i> > 2 σ (<i>I</i>))	0.0630
^b w <i>R</i> ₂ (all data)	0.2124
Goodness of fit	1.136

$$^aR_1 = \Sigma||F_0| - |F_C||/\Sigma|F_0| \text{ and } ^b wR_2 = [\Sigma w(F_0^2 - F_C^2)^2/\Sigma w(F_0^2)^2]^{1/2}$$

Table 10. Crystallographic data of **83** at **100K**.

Empirical formula	C56 H64
Formula weight	737.07
Crystal system	Monoclinic
Space group	P21/c
Wavelength, Å	0.71073
a, Å	28.914(3)
b, Å	24.744(3)
c, Å	12.3709(14)
α , °	90
β , °	94.195(6)
γ , °	90
V, Å ³	8827.1(18)
Z	8
ρ_{calcd} , Mg/m ³	1.109
M, 1/mm	0.062
Reflections collected	217950
Independent reflections	16221
R_1^a	0.0923
wR_2^a	0.2532
GoF ^a	1.022

$$^a R_1 = \Sigma||F_0| - |F_C||/\Sigma|F_0| \text{ and } ^b wR_2 = [\Sigma w(F_0^2 - F_C^2)^2/\Sigma w(F_0^2)^2]^{1/2}$$

Table 9. Crystallographic data of **91** at **120K**.

	91 · CH ₂ Cl ₂
Empirical formula	C ₈₁ H ₈₀ Cl ₂
Formula weight	1124.35
Crystal system	Monoclinic
Space group	Cc
Wavelength, Å	0.71073
a, Å	14.8956(6)
b, Å	30.3740(11)
c, Å	14.6293(6)
α, °	90
β, °	106.204(2)
γ, °	90
V, Å ³	6355.9(4)
Z	4
ρ _{calcd} , Mg/m ³	1.175
M, 1/mm	0.147
Reflections collected	52490
Independent reflections	11699
R ₁ ^a	0.0625
wR ₂ ^a	0.1485
GoF ^a	1.017

^aR₁ = $\sum||F_0| - |F_C||/\sum|F_0|$ and ^bwR₂ = $[\sum w(F_0^2 - F_C^2)^2/\sum w(F_0^2)^2]^{1/2}$

Communications

Articles

Highly Twisted Arenes by Scholl Cyclizations with Unexpected Regioselectivity.

A. Pradhan, P. Dechambenoit, H. Bock, F. Durola, *Angew. Chem.* **2011**, *50*, 12582.

Twisted polycyclic arenes by intramolecular Scholl reactions of C₃-symmetric precursors.

A. Pradhan, P. Dechambenoit, H. Bock, F. Durola, *J. Org. Chem.* **2013**, *78*, 2266.

(Highlighted in *Synfacts*. **2013**, *9*(6), 0617.)

Oral presentation:

Strongly twisted arenes by Scholl cyclizations with unexpected regioselectivity.

A. Pradhan, P. Dechambenoit, H. Bock, F. Durola

SECO-49 summer school, Annecy, France, May 21-26th, **2012**.

Strongly twisted arenes by Scholl cyclizations with unexpected regioselectivity.

A. Pradhan, P. Dechambenoit, H. Bock, F. Durola.

GSO2012, ENSCPB, Bordeaux, France, November 30th, **2012**.

Strongly twisted arenes by Scholl cyclizations towards soluble carbon nanoribbons.

A. Pradhan, P. Dechambenoit, H. Bock, F. Durola.

14th Journée de l'école doctorale des sciences chimiques de Bordeaux, April 25th, **2013**.

Posters:

Strongly twisted arenes by Scholl cyclizations towards soluble carbon nanoribbons.

A. Pradhan, P. Dechambenoit, H. Bock, F. Durola.

13th Journée de l'école doctorale des sciences chimiques de Bordeaux, April 7th, **2012**.

Strongly twisted arenes by Scholl cyclizations with unexpected regioselectivity.

A. Pradhan, P. Dechambenoit, H. Bock, F. Durola.

21st IUPAC International Conference on Physical Organic Chemistry (ICPOC-21), Durham, UK, September 9-13th, **2012** (selected poster for a **flash oral presentation**).

Distorted arenes by Scholl cyclizations, towards twisted carbon nanoribbons.

A. Pradhan, P. Dechambenoit, H. Bock, F. Durola.

15th International Symposium on Novel Aromatic Compounds (ISNA-15), Taipei, Taiwan, July 28th – August 2nd, **2013**.

